Función de Dot1 en el *checkpoint* de recombinación meiótica y en la tolerancia al daño en el DNA

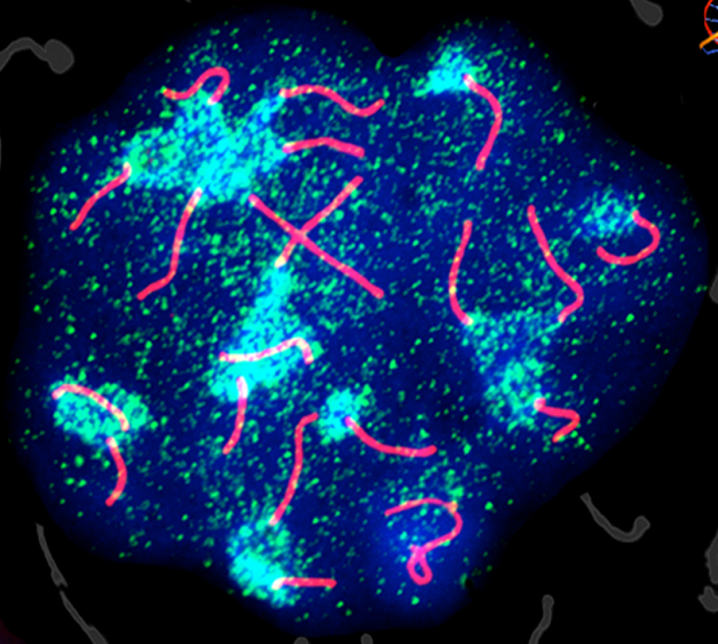

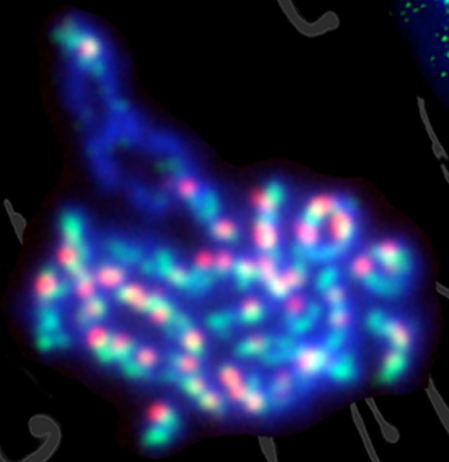

David Ontoso Picón

Salamanca, 2013

VNiVERSiDAD D SALAMANCA

Departamento de Microbiología y Genética

Instituto de Biología Funcional y Genómica

VNiVERSiDAD D SALAMANCA

CAMPUS DE EXCELENCIA INTERNACIONAL

CSIC

CONSEJO SUPERIOR DE INVESTIGACIONES CIENTÍFICAS

ibfg

Departamento de Microbiología y Genética

Universidad de Salamanca

Instituto de Biología Funcional y Genómica

(CSIC / USAL)

TESIS DOCTORAL

Función de Dot1 en el *checkpoint* de recombinación meiótica y en la tolerancia al daño en el DNA

Role of Dot1 in the meiotic recombination checkpoint and in DNA damage tolerance

David Ontoso Picón

Salamanca, 2013

VNiVERSiDAD D SALAMANCA
CAMPUS DE EXCELENCIA INTERNACIONAL
CSIC
Consejo Superior de Investigaciones Científicas
ibfg
Instituto de Biología Funcional y Genómica
Departamento de Microbiología y Genética

La presente memoria, titulada "Función de Dot1 en el *checkpoint* de recombinación meiótica y en la tolerancia al daño en el DNA", elaborada por el licenciado David Ontoso Picón y que constituye su Tesis Doctoral para optar al grado de Doctor en Biología con Mención Europea, ha sido redactada en el formato de compendio de artículos originales de investigación publicados en revistas científicas de prestigio internacional e indexadas en la edición científica del *Journal Citation Reports*.

Y para que así conste se recogen a continuación los tres artículos originales de investigación, su título, autores y afiliación de los mismos, junto la referencia completa de la revista científica donde fueron publicados:

"Dot1-dependent histone H3K79 methylation promotes activation of the Mek1 meiotic checkpoint effector kinase by regulating the Hop1 adaptor"

David Ontoso[1], Isabel Acosta[1], Fred van Leeuwen[2], Raimundo Freire[3], Pedro A. San-Segundo[1]

[1]Instituto de Biología Funcional y Genómica, Consejo Superior de Investigaciones Científicas y Universidad de Salamanca, Salamanca, España.

[2]Division of Gene Regulation, Netherlands Cancer Institute, Amsterdam, The Netherlands.

[3]Unidad de Investigación, Hospital Universitario de Canarias, Tenerife, España.

PLOS Genetics, volumen 9, número 1, e1003262. Enero 2013.

DOI: 10.1371/journal.pgen.1003262

ISSN versión impresa: 1553-7390; ISSN versión electrónica: 1553-7404.

http://dx.plos.org/10.1371/journal.pgen.1003262

VNiVERSiDAD D SALAMANCA
CAMPUS DE EXCELENCIA INTERNACIONAL
CSIC
Consejo Superior de Investigaciones Científicas
ibfg
Instituto de Biología Funcional y Genómica
Departamento de Microbiología y Genética

"Dynamics of DOT1L localization and H3K79 methylation during meiotic prophase I in mouse spermatocytes"

David Ontoso[1], Liisa Kauppi[2,3], Scott Keeney[2], Pedro A. San-Segundo[1]

[1]Instituto de Biología Funcional y Genómica, Consejo Superior de Investigaciones Científicas y Universidad de Salamanca, 37007 Salamanca, España.

[2]Molecular Biology Program, Memorial Sloan-Kettering Cancer Center, 1275 York Avenue, New York, NY 10065, USA.

[3]present address: Research Programs Unit (Genome-Scale Biology) and Institute of Biomedicine (Biochemistry and Developmental Biology), University of Helsinki, Haartmaninkatu 8, Helsinki, FIN-00014, Finland.

Chromosoma (publicado en línea), Octubre 2013.

DOI: 10.1007/s00412-013-0438-5

ISSN versión impresa: 0009-5915; ISSN versión electrónica: 1432-0886.

http://dx.doi.org/10.1007/s00412-013-0438-5

"Regulation of tolerance to DNA alkylating damage by Dot1 and Rad53 in *Saccharomyces cerevisiae*"

Francisco Conde[1], **David Ontoso**[1], Isabel Acosta[1], Alfonso Gallego-Sánchez[2], Avelino Bueno[2], Pedro A. San-Segundo[1]

[1]Instituto de Microbiología Bioquímica, Consejo Superior de Investigaciones Científicas y Universidad de Salamanca, 37007 Salamanca, España.

[2]Instituto de Biología Celular y Molecular del Cáncer, Consejo Superior de Investigaciones Científicas y Universidad de Salamanca, 37007 Salamanca, España.

DNA Repair, volumen 9, número 10, pp. 1038–1049. Julio 2010.

DOI: 10.1016/j.dnarep.2010.07.003

ISSN: 1568-7864.

http://dx.doi.org/10.1016/j.dnarep.2010.07.003

VNiVERSiDAD D SALAMANCA
CAMPUS DE EXCELENCIA INTERNACIONAL
Departamento de Microbiología y Genética

DR. LUIS ROMÁN FERNÁNDEZ LAGO, PROFESOR TITULAR de la UNIVERSIDAD DE SALAMANCA y DIRECTOR del DEPARTAMENTO DE MICROBIOLOGÍA Y GENÉTICA de la UNIVERSIDAD DE SALAMANCA,

CERTIFICA:

Que la memoria titulada "Función de Dot1 en el *checkpoint* de recombinación meiótica y en la tolerancia al daño en el DNA", presentada por el licenciado David Ontoso Picón, ha sido realizada bajo la dirección del Dr. Pedro A. San Segundo Nieto, en el Instituto de Biología Funcional y Genómica (IBFG), centro mixto de la Universidad de Salamanca y del Consejo Superior de Investigaciones Científicas (CSIC).

Y para autorizar su presentación y evaluación por el tribunal correspondiente, expide el presente certificado en Salamanca, a 13 de Noviembre de 2013.

Dr. Luis Román Fernández Lago

CSIC
CONSEJO SUPERIOR DE INVESTIGACIONES CIENTÍFICAS

ibfg Instituto de Biología Funcional y Genómica

DR. PEDRO ANTONIO SAN SEGUNDO NIETO, CIENTÍFICO TITULAR del CONSEJO SUPERIOR DE INVESTIGACIONES CIENTÍFICAS en el INSTITUTO DE BIOLOGÍA FUNCIONAL Y GENÓMICA,

CERTIFICA:

Que el licenciado David Ontoso Picón ha realizado el trabajo titulado "Función de Dot1 en el *checkpoint* de recombinación meiótica y en la tolerancia al daño en el DNA" bajo mi dirección, en el Instituto de Biología Funcional y Genómica (IBFG), centro mixto de la Universidad de Salamanca y del Consejo Superior de Investigaciones Científicas (CSIC), para optar al grado de Doctor en Biología con Mención de Doctorado Europeo.

Que autorizo a la presentación de dicho trabajo en la modalidad de compendio de artículos científicos.

Y para autorizar su presentación y evaluación por el tribunal correspondiente, expide el presente certificado en Salamanca, a 13 de Noviembre de 2013.

Dr. Pedro Antonio San Segundo Nieto

VNiVERSiDAD D SALAMANCA
CAMPUS DE EXCELENCIA INTERNACIONAL
Departamento de Microbiología y Genética

CSIC
Consejo Superior de Investigaciones Científicas

ibfg
Instituto de Biología Funcional y Genómica

DR. FERNANDO LEAL SÁNCHEZ, PROFESOR TITULAR del DEPARTAMENTO DE MICROBIOLOGÍA Y GENÉTICA de la UNIVERSIDAD DE SALAMANCA,

CERTIFICA:

Que la memoria titulada "Función de Dot1 en el *checkpoint* de recombinación meiótica y en la tolerancia al daño en el DNA" presentada por el licenciado David Ontoso Picón, ha sido realizada con mi tutoría y bajo la dirección del Dr. Pedro A. San Segundo Nieto, en el Instituto de Biología Funcional y Genómica (IBFG), centro mixto de la Universidad de Salamanca y del Consejo Superior de Investigaciones Científicas (CSIC).

Que autorizo a la presentación de dicho trabajo en la modalidad de compendio de artículos científicos.

Y para autorizar su presentación y evaluación por el tribunal correspondiente, expide el presente certificado en Salamanca, a 13 de Noviembre de 2013.

Dr. Fernando Leal Sánchez

VNiVERSiDAD D SALAMANCA
CAMPUS DE EXCELENCIA INTERNACIONAL

Evaluación anual del Plan de Investigación

Programa de Doctorado: Microbiología y Genética moleculares (R.D. 778/1998)

Doctorando/a: David Ontoso Picón

Anualidad: 1ª ☐ 2ª ☐ 3ª ☐ 4ª ☐ 5ª ☑

Fecha de evaluación: 7/10/2013

Comisión Académica que emite el informe: Departamento de Microbiología y Genética

Composición:

Director del Departamento: Dr. Luis Román Fernández Lago

Coordinador/a del programa: Dr. Pedro F. Mateos González

RESOLUCIÓN DE EVALUACIÓN:

Positiva: ☑ **Negativa:** ☐

MOTIVACIÓN:

(En caso de evaluación negativa)

Autorización para la presentación de la tesis doctoral en el formato de compendio de artículos

La Comisión Académica (Consejo de Departamento/Instituto) reunida en sesión el día 7 de Octubre de 2013 acordó autorizar al doctorando para que elabore y presente su tesis en el formato de compendio de artículos.

En Salamanca, a 7 de 10 de 2013

El Presidente de la Comisión Académica:
(Director del Departamento)

DEPARTAMENTO DE MICROBIOLOGIA Y GENETICA - UNIVERSIDAD DE SALAMANCA

Fdo: Dr. Luis Román Fernández Lago

El coordinador del Programa de Doctorado:

Fdo: Dr. Pedro F. Mateos González

VNiVERSiDAD D SALAMANCA
CAMPUS DE EXCELENCIA INTERNACIONAL

VICERRECTORADO DE INVESTIGACIÓN
Patio de Escuelas nº 1
37008 Salamanca

En relación con la petición de **D. DAVID ONTOSO PICÓN,** solicitando autorización para la presentación de la Tesis Doctoral en el formato de compendio de artículos/publicaciones,

Este Vicerrectorado, teniendo en cuenta el visto bueno del director de la tesis y del tutor y según lo establecido en el "Procedimiento para la presentación de la tesis doctoral en la Universidad de Salamanca en el formato de compendio de artículos/publicaciones" aprobado por la Comisión de Doctorado y Posgrado el día 15 de febrero de 2013,

HA RESUELTO autorizar lo solicitado.

Salamanca, 07 de octubre de 2013
LA VICERRECTORA DE INVESTIGACIÓN

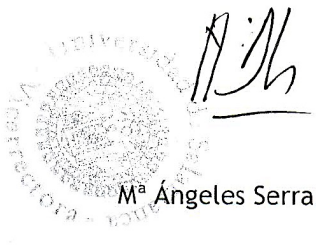

Mª Ángeles Serrano García

SR. DIRECTOR
DPTO. DE MICROBIOLOGÍA Y GENÉTICA
Edificio Departamental
Campus Miguel de Unamuno

El presente trabajo es el fruto de cinco años de trabajo, un tiempo que se ha pasado volando, como los ya diez años que llevo en Salamanca. Parece que no fue hace tanto cuando llegué a la RU San Bartolomé, a la facultad de Biología y a la capital charra, desde mi querida Aranda de Duero natal. Ha sido una década de grandes cambios, me he hecho *viejuno*, tengo muchas más canas, pero también mucha más experiencia y estoy muy satisfecho de esta increíble época universitaria-predoctoral. En este periodo he conocido a muchísima gente, a grandes amigos y a excepcionales compañeros, a todos ellos tengo que agradecerles que este trabajo haya resultado así, sin olvidarme de todos los que ya conocía de antes y que siguen siendo muy importantes.

En primer lugar es menester agradecérselo al que más ha tenido que ver en el desarrollo del presente trabajo, al que más pendiente ha estado todo el rato, a Pedro San Segundo. Increíble su tenacidad, meticulosidad, capacidad memorística y entrega al trabajo. Ha habido momentos mejores y peores, pero creo que el balance global que nos llevamos los dos es bastante positivo. Y a continuación agradecérselo a los compañeros de laboratorio con los que tantísimo tiempo he pasado y sin los que nada hubiese sido lo mismo: a Paco, el primero en doctorarse, un trocito de pan y perfecto maestro; a Esther, mi profe y amiga con la que más tiempo compartí la poyata, hasta que decidió alejarse para tomar sus nuevos rumbos; a Isa, genial tenerte codo con codo, siempre atenta y trabajadora incansable, graciosa hasta cuando refunfuña; a Santi, todo lo que tiene de grande lo tiene de bueno, siempre dispuesto a echar una mano; a Sara, tan callada como buena y trabajadora. También gracias a los compañeros que estuvieron menos tiempo, pero a los que fue genial conocer: a Bradley Woliter, que gran *wingman*, el perfecto *gentleman-gambitero*; a Marina, esa brillante *scout*-científica-artista de la capi; a Natalia y Vanessa, a las que conocí menos, pero igualmente buenas compañeras.

Después de los compañeros del propio laboratorio, los siguientes con los que más tiempo, inquietudes, bueno y malos momentos he compartido es con los compañeros del centro, primero IMB y ahora IBFG. Muchísima gente a la que agradecerle su amistad, sus ánimos, su compañía durante las larguísimas sesiones de microscopio o micromanipulador. A esos compañeros-amigos que compartan su sabiduría y alegría, y que saben estar ahí, dentro y fuera del laboratorio. Así que muchísimas gracias a: Alicia, un ejemplo en todo, con ese puntito castellano que mola; Camilla, cómo se puede ser siempre tan maja con todo el mundo y tan buena; Esther, qué *curranta*, siempre dispuesta a animar y ver el lado positivo; Rebeca, esa alegría extremeña, nunca sabes cuando la va a soltar; Sofía, super buena, inteligente y simpática, como Maru; Susana, otra gran trabajadora y mejor persona, como David; Nacho y Civi, grandes compañeros, *gambiteros* y amigos; Nagore, esa tipa dura tan buena; Cris, esa asturiana siempre con una sonrisa y tan buen corazón; Sónia, esa portuguesa única e irrepetible; a José Luis, grandísima persona; Sara G., Luisa, Marta, Mari, Ana J., Julia, Laura D., Mónica, Vero, Mariona, Rosana, Sara O., Sara V., Prakhar, Carlos, el pibe Alejandro, Elsa, Grazia, Ana Yepes, Jorge, Alberto, Laura Marín… y al resto de compañero pasados y presentes.

Siguiendo con la IBFG *people*, agradecerles su ayuda también a los jefes y profesores, especialmente a Fernando Leal, Marga, Ramón Santamaría y Bea. A Noelia y Mari Carmen, por su simpatía, paciencia y saber

estar, siempre anima tener a alguien tan agradable al llegar. A Carmen Castro por estar siempre dispuesta a ayudar con una sonrisa y paciencia infinita. A Alegría, Paco Soriano, Paco Alonso y Encarna porque sin ellos esto no funcionaría.

Many thanks to the host laboratories where I carried out my short-term stays. Firstly, thank you very much to Fred van Leeuwen for giving me the opportunity to visit his lab in The Netherlands Cancer Institute and for his support over these years, and to all the members of the B4 yeast lab, especially to Tibor van Welsem. That summer in Amsterdam was great, my first experience alone abroad, new country, new people and new lab. Dankjewel! I would also like to thank Scott Keeney for giving me the chance to visit his lab in the Memorial Sloan-Kettering Cancer Center. I had an awesome experience in the Big Apple, in a big lab and using a new model organism. My thanks go also to all the members of Keeney's lab, especially to Liisa, Megan, Julian, Isabel, Ryan, Mariko and Jodie.

A Direna, esa canaria que llegó de improviso y que es una de las personas que más me ha impresionado, tan inteligente, como buena persona. Siempre es genial estar contigo y espero compartir muchos más ratos en la nueva etapa.

Saliendo ya del laboratorio, pero quedándonos en Salamanca, agradecerles su amistad y compañía a mi gente de la ciudad del Tormes. Empezando por los *Bartolos*, vaya tres años épicos en la residencia. A Daniel Pinto, José-Shane, Javier Trujillo y Álvaro Gil por estar siempre ahí, menudos *gambiteros*, cuántas aventuras juntos. A Carmen, María, Lucía T., Lola, Silvia, Vanesa, Imanol y David Benito por haber compartido tantos buenos momentos juntos. A Ana Gleeson, la pequeña *sister* rubita a la que hemos visto crecer y hacerse toda una neurocirujana. A Ana Mora, por su inagotable simpatía y ser tan buena.

¡Y no me puedo olvidar de todos mis arandinos! Desde aquellos tiempos del Sandoval seguimos juntos, lo ratos que hemos pasado en la Bodega y en la Huerta. A Eva, eres la mejor, una persona increíble, siempre con ganas de hacer cosas y al gran fichaje de Ferrer; a Carlos, gran químico y siguiente doctor; Clara, Dani, Lucía, Óscar, Andrés, Víctor, Esther, David, Elena, Lara, Diego y Sandra; un grupo excepcional de amigos dispuestos para lo que quieras, ir a pescar, de excursión, de claretes, a pasar un buen rato donde sea… sin vosotros la Villa que alegra Castilla, corazón de la Ribera del Duero, no sería lo mismo. ¡Moláis 1000!

A mi familia, sin la que nada de esto hubiese sido posible. A mi madre Fabiola, a la que debo todo lo que soy y mi gran ejemplo en la vida. A mis tíos Antonio, Gabriel, Cani, Nuria y José Antonio, y a mi abuelo Antonino. Por supuesto a los que ya no están pero siempre recordaremos José Benito, Encarna, Ana y Baudilia. Y a todas mis primas, que son geniales y que se están haciendo mayores: Laura, Cristina, Nerea, Silvia y Leticia.

Y por último, a la persona que pese haber llegado hace no mucho se ha convertido en alguien muy especial, con la que siempre quiero estar y con la que me gustaría compartir muchísimo tiempo más. Muchas gracias Laura por ser como eres, por esa sonrisa, tu cariño y complicidad, por ser tan bonica.

SINOPSIS GENERAL

Función de Dot1 en el *checkpoint* de recombinación meiótica y en la tolerancia al daño en el DNA

GENERAL SYNOPSIS

Role of Dot1 in the meiotic recombination checkpoint and in DNA damage tolerance

SINOPSIS GENERAL

RESUMEN

Las modificaciones post-traduccionales de las histonas repercuten en numerosas funciones biológicas, regulando procesos esenciales como la transcripción, la replicación, la reparación del DNA, la recombinación o el control del ciclo celular. En la presente tesis doctoral se ha estudiado la influencia de la metilación de la lisina 79 de la histona H3 (H3K79me), mediada en exclusiva por la singular enzima Dot1, en mecanismos celulares implicados en el mantenimiento de la integridad genómica. Así, hemos dilucidado las bases moleculares de la función de Dot1 en el *checkpoint* de recombinación meiótica en *Saccharomyces cerevisiae*, un mecanismo de vigilancia que asegura la correcta distribución del material genético a los gametos. La metilación de H3K79me es necesaria para la apropiada localización y activación de proteínas adaptadoras y efectoras del *checkpoint*, que consiguen disparar este mecanismo de supervivencia celular. Además, hemos expandido nuestra investigación a la meiosis en mamíferos analizando la distribución de DOT1L y de la metilación de H3K79me en espermatocitos de ratón. Los patrones diferenciales de localización de las distintas formas de H3K79me, apuntan a funciones específicas para cada marca epigenética durante la espermatogénesis. Por otro lado, puesto que Dot1 también actúa durante el ciclo mitótico, hemos determinado la relevancia funcional de la metilación de H3K79 en la tolerancia al daño por alquilación en el DNA mediado por síntesis a través de lesión (TLS) en la levadura de gemación. En conclusión, las modificaciones epigenéticas catalizadas por la proteína conservada evolutivamente Dot1 participan en múltiples procesos cruciales para la estabilidad del genoma tanto durante el ciclo de división meiótico, como mitótico.

1. ANTECEDENTES

El DNA eucariota se condensa dentro del núcleo celular gracias a la asociación de aproximadamente 147 pares de bases alrededor de un octámero de histonas (un heterotetrámero H3/H4 y dos dímeros H2A/H2B) para formar el nucleosoma, la unidad fundamental y repetitiva de la cromatina (Kornberg and Lorch 1999). Las histonas poseen un dominio globular que constituye el núcleo del nucleosoma, y unas colas terminales sin estructurar que sobresalen del mismo. Estas proteínas, y particularmente sus colas, son susceptibles de experimentar numerosas modificaciones covalentes post-traduccionales, siendo las mejor conocidas la acetilación, metilación, fosforilación, ubiquitilación y sumoilación, siempre en unos residuos concretos y con diferentes grados de reversibilidad. Estas modificaciones alteran el grado de compactación de la cromatina, modificando su accesibilidad, y la capacidad de otras proteínas para interaccionar con

el DNA. Además, existen chaperonas, variantes de histonas, otras proteínas estructurales y complejos remodeladores de la cromatina, que también influyen en la estructura de la cromatina. De esta forma se regulan numerosos procesos biológicos, como la actividad transcripcional, el establecimiento de regiones de heterocromatina, la replicación o la reparación del DNA (Kouzarides 2007; Luger et al. 2012; Becker and Workman 2013)

Un proceso esencial para todos los organismos con reproducción sexual, y del que cada vez se conocen más aspectos de su regulación por factores que afectan a la dinámica de la cromatina, es la división celular meiótica. Esta división reduccional consigue generar productos meióticos haploides (esporas en levaduras o gametos en metazoos) desde una célula diploide, ya que se suceden dos rondas de segregación cromosómica precedidas por una única ronda de replicación del DNA. La etapa más característica de la meiosis es una particularmente prolongada profase I, en la que se lleva a cabo el apareamiento, la sinapsis y la recombinación entre los cromosomas homólogos (Cohen et al. 2006). El correcto desarrollo y finalización de estos eventos es supervisado por un mecanismo de vigilancia específico, el *checkpoint* de recombinación meiótica o *checkpoint* de paquitene. En caso de detectar defectos en dichos procesos, este *checkpoint* meiótico bloquea o retrasa la progresión de la meiosis para evitar la segregación aberrante de los cromosomas y la consiguiente formación de gametos portadores de alteraciones genómicas (Roeder and Bailis 2000; Macqueen and Hochwagen 2011).

Precisamente, en un escrutinio genético para descubrir mutantes defectivos en este *checkpoint* en *Saccharomyces cerevisiae* se aisló *dot1*, ya que eliminaba el bloqueo de la progresión meiótica que sufre un mutante defectivo en sinapsis como *zip1*. Así se comprobó que la proteína codificada por *DOT1*, cuya actividad catalítica se desconocía en ese momento, es necesaria para inducir el *checkpoint* tanto en mutantes con defectos en sinapsis (*zip1*), como con defectos en la recombinación meiótica (*dmc1*) (San-Segundo and Roeder 2000). *DOT1* también había sido aislado en un escrutinio genético independiente dirigido a identificar genes cuya sobreexpresión alterase el silenciamiento telomérico, de donde proviene su nombre "*Disruptor Of Telomeric silencing 1*" (Singer et al. 1998). Poco después, varios grupos, también de forma independiente y con diferentes aproximaciones, demostraron que la proteína Dot1 de *S. cerevisiae* y su homóloga en mamíferos DOT1L (*Dot1-Like*) catalizan la metilación la lisina 79 de la histona H3 (H3K79me). Esta metilación en H3K79 sólo ocurre con el nucleosoma como sustrato y es el único sitio de metilación descubierto dentro del dominio globular de las histonas (Figura 1A; Feng et al. 2002; Lacoste et al. 2002; van Leeuwen et al. 2002; Ng et al. 2002).

Desde el descubrimiento de su actividad enzimática como N-metiltransferasa de lisina en histonas (EC 2.1.1.43), se ha seguido profundizando en su caracterización funcional. Dot1

es la única metiltransferasa que tiene por residuo diana la H3K79, ya que su eliminación en levadura, mosca y ratón conlleva la pérdida total de metilación en esta lisina (van Leeuwen et al. 2002; Shanower et al. 2005; Jones et al. 2008). Dot1 cataliza la mono-, di- y trimetilación de la H3K79 (H3K79me1, -me2 y –me3) mediante un mecanismo distributivo, lo que la diferencia de otras metil-transferasas de histonas, englobadas en la familia SET y que poseen un mecanismo de acción procesivo (Figura 1B; Frederiks et al. 2008). Hasta el momento, no se conoce ninguna demetilasa que revierta la acción de Dot1.

Así mismo, también se han conseguido grandes avances en el esclarecimiento de las numerosas funciones biológicas de Dot1/DOT1L (Figura 2; Nguyen and Zhang 2011). Comenzando con los papeles de Dot1 en *Saccharomyces cerevisiae*, se ha establecido que la función de Dot1 inicialmente descrita en el silenciamiento telomérico se debe a la competencia con la proteína de silenciamiento Sir3 por el mismo sitio de unión en los nucleosomas, y a la imposibilidad de Sir3 de unirse a nucleosomas portadores de H3K79me (van Welsem et al. 2008). Por otro lado, se ha encontrado que Dot1 interviene en numerosos aspectos de la respuesta al daño en el DNA durante el ciclo vegetativo. Así, Dot1 es necesario para la activación de Rad53 mediada por Rad9 en los *checkpoints* de daño en DNA G_1/S e intra-S (Giannattasio et al. 2005; Wysocki et al. 2005). Además, Dot1 modula distintas vías de reparación del DNA ante radiación ionizante o ultravioleta (Game et al. 2006; Toh et al. 2006; Bostelman et al. 2007).

En nuestro grupo, también se ha estudiado el papel de Dot1 en la respuesta al daño en el DNA generado por el agente alquilante metil-metano-sulfonato (MMS) y en la reparación de las roturas de doble cadena por recombinación con la cromátida hermana (Conde and San-Segundo 2008; Conde et al. 2009). Sorprendentemente, el mutante *dot1* presenta una mayor resistencia al tratamiento crónico con MMS que la cepa silvestre. Estos estudios demostraron que Dot1 regula negativamente la ruta de tolerancia al daño en el DNA mediante síntesis a través de lesión (TLS), y que la mayor resistencia a MMS de *dot1*Δ se debe a una actividad TLS aumentada, aunque a expensas de una mayor tasa de mutagénesis (Conde and San-Segundo 2008). Pero quisimos profundizar en este mecanismo y conocer mejor los detalles de cómo Dot1 estaba regulando este proceso. Para ello, llevamos a cabo los experimentos publicados en el tercer artículo que compone esta tesis doctoral: "Regulation of tolerance to DNA alkylating damage by Dot1 and Rad53 in *Saccharomyces cerevisiae*" (Conde et al. 2010), en el que he contribuido determinando que el papel de Dot1 en TLS está mediado por su actividad catalítica metil-transferasa sobre H3K79.

Retomando el estudio de la función de Dot1 en la meiosis, como se ha comentado anteriormente, se sabía que es esencial para el funcionamiento del *checkpoint* de recombinación meiótica en *S. cerevisiae* (San-Segundo and

Roeder 2000). pero se desconocían los mecanismos moleculares responsables. Así que éste fue el principal objetivo de esta tesis, siendo el trabajo resultante publicado en el primer artículo que se presenta en esta memoria: "Dot1-dependent histone H3K79 methylation promotes activation of the Mek1 meiotic checkpoint effector kinase by regulating the Hop1 adaptor" (Ontoso et al. 2013a).

La proteína Dot1 está conservada a lo largo de la evolución, y progresivamente se han ido describiendo más funciones de sus homólogos en distintos organismos como: *Dictyostelium*, *Trypanosoma*, *Caenorhabditis*, *Drosophila*, ratón y humano (Feng et al. 2002; Shanower et al. 2005; Jones et al. 2008; Müller-Taubenberger et al. 2011; Cecere et al. 2013). Sin embargo, una de las pocas excepciones de organismos que no poseen ni Dot1, ni H3K79me es *Schizosaccharomyces pombe*.

En mamíferos, DOT1L participa en múltiples procesos biológicos (Nguyen and Zhang 2011). Así, desempeña importante papeles en la regulación de la transcripción (Steger et al. 2008; Kim et al. 2012a), es esencial durante el desarrollo embrionario y la diferenciación (Jones et al. 2008; Barry et al. 2009; Ooga et al. 2013), necesaria para la función cardíaca (Nguyen et al. 2011), la hematopoyesis (Feng et al. 2010; Jo et al. 2011), la proliferación celular y el envejecimiento (Kim et al. 2012b) y la condrogénesis (Castaño Betancourt et al. 2012). Alteraciones de la función de DOT1L están relacionadas con algunos tipos de leucemia de linaje mixto (Okada et al. 2005; Krivtsov et al. 2008; Bernt et al. 2011), la aparición de defectos en la formación del tubo neural (Zhang et al. 2013) y osteoartritis (Castaño Betancourt et al. 2012). Esta asociación entre disfunciones de DOT1L y patologías ha convertido a esta proteína en un prometedora diana terapéutica (Daigle et al. 2011; Yao et al. 2011; Anglin et al. 2012; Helin and Dhanak 2013). A pesar de lo relevante de la función de Dot1 durante la meiosis en levadura, se sabe muy poco del papel de DOT1L en la meiosis de mamíferos, existiendo un único artículo al respecto en oocitos de ratón (Ooga et al. 2008). Por tanto, un segundo objetivo de esta tesis fue la caracterización citológica inicial de DOT1L y la H3K79me durante la profase meiótica I en espermatocitos de ratón. Los resultados obtenidos han sido publicados en el segundo artículo de la tesis: "Dynamics of DOT1L localization and H3K79 methylation during meiotic prophase I in mouse spermatocytes" (Ontoso et al. 2013b).

Así, la presente memoria de tesis doctoral titulada "Función de Dot1 en el *checkpoint* de recombinación meiótica y en la tolerancia al daño en el DNA", elaborada por compendio de artículos, queda estructurada en tres apartados, cada uno de los cuales corresponde a una publicación:

ARTÍCULO 1: "Dot1-dependent histone H3K79 methylation promotes activation of the Mek1 meiotic checkpoint effector kinase by regulating the Hop1 adaptor"
http://dx.plos.org/10.1371/journal.pgen.1003262

ARTÍCULO 2: "Dynamics of DOT1L localization and H3K79 methylation during meiotic prophase I in mouse spermatocytes"
http://dx.doi.org/10.1007/s00412-013-0438-5

ARTÍCULO 3: "Regulation of tolerance to DNA alkylating damage by Dot1 and Rad53 in *Saccharomyces cerevisiae*"
http://dx.doi.org/10.1016/j.dnarep.2010.07.003

2. HIPÓTESIS DE TRABAJO

Las modificaciones post-traduccionales de las histonas configuran la estructura y dinámica de la cromatina, regulando así los numerosos procesos biológicos que ocurren asociados a ella. La metilación de H3K79, mediada por Dot1, es un marca epigenética abundante, presente durante todo el ciclo celular, tanto en el proceso de división mitótico como meiótico, y que se sabe que interviene en numerosos procesos biológicos. Así, cabía esperar un papel relevante para H3K79me en mecanismos que regulan el mantenimiento de la integridad genómica tanto en meiosis como en mitosis.

3. OBJETIVOS GENERALES

- Estudiar la función de la metilación de H3K79, mediada por Dot1, en un mecanismo de vigilancia de la meiosis como es el *checkpoint* de recombinación meiótica.

- Determinar la contribución funcional de H3K79me a la regulación de la tolerancia al daño alquilante en el DNA mediada por TLS durante el ciclo mitótico.

4. CONCLUSIONES GENERALES

1- Dot1 es crucial para el funcionamiento del *checkpoint* de recombinación meiótica en *S. cerevisiae*, ya que la metilación de H3K79 es necesaria para permitir la correcta localización y activación de proteínas adaptadoras y efectoras del *checkpoint* (Hop1 y Mek1, respectivamente), y así activar este mecanismo de supervivencia.

2- DOT1L y los diferentes estados de metilación de H3K79me presentan dinámicas de localización espacio-temporal diferenciales a lo largo de la profase meiótica I en espermatocitos de ratón, lo que sugiere funciones específicas para cada estado de metilación.

3- La metilación de H3K79, catalizada por Dot1, regula la tolerancia al daño por alquilación en el DNA modulando la actividad de la quinasa efectora del *checkpoint* de daño en DNA Rad53 y la unión a la cromatina del factor de TLS Rev1.

GENERAL SYNOPSIS

SUMMARY

Histone posttranslational modifications affect multiple biological functions, regulating essential processes such as transcription, replication, DNA repair, recombination or cell cycle control. During this thesis work, we have studied the role of methylation of histone H3 at lysine 79 (H3K79me) solely mediated by the enzyme Dot1, in cellular mechanisms involved in the maintenance of genomic integrity. Thus, we have uncovered the molecular basis of Dot1 function in the meiotic recombination checkpoint in *Saccharomyces cerevisiae*, a surveillance mechanism that monitors the correct distribution of genetic material to gametes. H3K79me is required for proper localization and activation of adaptor and effector checkpoint proteins in order to trigger this quality control mechanism. Moreover, we have expanded our studies to mammalian meiosis, analyzing DOT1L and H3K79me distribution in mouse spermatocytes. We found that each H3K79 methylation state exhibits differential localization patterns, suggesting specific functions for each epigenetic mark during mouse spermatogenesis. On the other hand, since Dot1 is also active during the mitotic cell cycle, we determined the functional relevance of H3K79me in the tolerance to alkylating DNA damage mediated by translesion synthesis (TLS) in budding yeast. In conclusion, epigenetic modifications catalyzed by the evolutionarily conserved Dot1 protein are involved in a variety of crucial biological processes to ensure genomic stability, during both meiotic and mitotic cell divisions.

1. BACKGROUND

Eukaryotic DNA is condensed in the cell nucleus through the interaction of roughly 147 base pairs wrapped around each histone octamer (an H3/H4 heterotetramer and two H2A/H2B dimers) to form the nucleosome, the basic repeating unit of chromatin (Kornberg and Lorch 1999). Histones are composed of a globular domain, which forms the nucleosome core, and unstructured tails that protrude from the core. Histone proteins are subjected to multiple posttranslational modifications (PTMs) especially at the tails. Well-known PTMs include acetylation, methylation, phosphorylation, ubiquitylation and sumoylation, being always residue-specific and with different degree of reversibility. PTMs modify chromatin condensation, thus controlling the accessibility of other DNA-binding proteins. Moreover, there are histone chaperones, histone variants, architectural chromatin proteins and chromatin remodelers that also transform chromatin structure. Many biological processes are regulated in this way; for example, transcription, heterochromatin formation, replication and DNA repair (Kouzarides 2007; Luger et al. 2012; Becker and Workman 2013).

An essential process in all sexually reproducing organisms, influenced by chromatin modifications, is the meiotic cell division. This specialized reductional division generates haploid products (spores in yeast or gametes in Metazoa) from a single diploid cell, because two rounds of chromosome segregation are preceded by a single phase of DNA replication. During meiosis, the unique meiotic prophase I is the most prolonged and elaborate stage, during which pairing, synapsis and recombination between homologous chromosomes occur (Cohen et al. 2006). Progression and completion of meiotic events are specifically monitored by a surveillance mechanism, the meiotic recombination checkpoint or pachytene checkpoint. Thus, in response to meiotic defects this checkpoint is triggered and blocks or delays meiotic progression in order to prevent aberrant chromosome segregation and the ensuing formation of aneuploid meiotic products (Roeder and Bailis 2000; Macqueen and Hochwagen 2011).

Precisely, the *dot1* mutant was isolated in a genetic screen for pachytene-checkpoint defective mutants in *Saccharomyces cerevisiae*. In the absence of *DOT1*, whose enzymatic activity was unknown at that time, the checkpoint-induced meiotic arrest of a synapsis-defective mutant (i.e., *zip1*) or recombination-defective mutant (i.e., *dmc1*) is abolished (San-Segundo and Roeder 2000). *DOT1* had already been independently isolated in a genetic screen for high-copy disruptors of telomeric silencing, hence its name "*Disruptor Of Telomeric silencing 1*" (Singer et al. 1998). A few years later, several groups, independently and using different approaches, discovered that Dot1 in budding yeast, and its mammalian homolog DOT1L (for Dot1-like), are the methyltransferase of lysine 79 on histone H3 (H3K79). This methylation reaction occurs in the context of nucleosomes and H3K79 is the only known methylated residue that lies within a histone globular domain (Figure 1A; Feng et al. 2002; Lacoste et al. 2002; van Leeuwen et al. 2002; Ng et al. 2002).

Since the discovery of Dot1 activity as histone-lysine N-methyltransferase (EC 2.1.1.43), more and more work has been done to improve its characterization. Dot1 is the only methyltransferase that targets H3K79, Dot1-deficient mutants in yeast, flies or mice do not exhibit any methylation at this lysine (van Leeuwen et al. 2002; Shanower et al. 2005; Jones et al. 2008). Dot1 is responsible for catalyzing mono-, di- and trimethylation of H3K79 (H3K79me1, -me2 y –me3, respectively) in a non-processive (or distributive) manner, which differs from the rest of histone methyltransferases, which possess a SET-domain and a processive mechanism of action (Figure 1B; Frederiks et al. 2008). To date, there is no demethylase known capable of reverting H3K79me.

Major advances have been made in uncovering the multiple Dot1/DOT1L biological functions (Figure 2; Nguyen and Zhang 2011). Starting with the roles of Dot1 in *Saccharomyces cerevisiae* and regarding its first described function in telomeric silencing, it is now known that is mediated by Dot1 competing with the silencing

protein Sir3 for same binding site on the nucleosomes and the inability of Sir3 for binding to methylated H3K79 nucleosomes (van Welsem et al. 2008). Furthermore, Dot1 plays numerous roles in the DNA damage response during the vegetative cycle. Thus, Dot1 is needed for Rad9-mediated activation of Rad53 in the G_1/S and intra-S DNA damage checkpoints (Giannattasio et al. 2005; Wysocki et al. 2005). In addition, Dot1 modulates DNA damage repair pathways in response to ionizing or ultraviolet radiation (Game et al. 2006; Toh et al. 2006; Bostelman et al. 2007).

Our laboratory has been interested in studying the role of Dot1 in the response to alkylating DNA damage caused by methyl methanesulfonate (MMS) and in double-strand break (DSB) repair by sister chromatid recombination (Conde and San-Segundo 2008; Conde et al. 2009). Unexpectedly, deletion of *DOT1* results in increased resistance to chronic MMS exposure. Our results indicate that Dot1 negatively regulates the tolerance to DNA alkylating damage response mediated by translesion synthesis (TLS). The MMS resistance observed in *dot1* results from the enhanced TLS activity, but at the expense of elevated mutagenesis frequency (Conde and San-Segundo 2008). We further focused on characterizing in more detail how Dot1 regulates DNA damage tolerance. The results are presented in the third research article that composes this doctoral thesis, entitled "Regulation of tolerance to DNA alkylating damage by Dot1 and Rad53 in *Saccharomyces cerevisiae*" (Conde et al. 2010). My contribution to this work consisted in demonstrating that the role of Dot1 in the TLS pathway relies in its methyltransferase activity on H3K79.

Regarding the research on the meiotic roles of Dot1, it was previously shown to be essential for meiotic recombination checkpoint function in *S. cerevisiae* (San-Segundo and Roeder 2000). However, the molecular mechanisms involved remained largely unknown. Therefore, the main goal of my thesis was to uncover the role of Dot1-dependent H3K79 methylation in meiotic checkpoint activation. The results obtained were published in the first article presented in this thesis report, entitled "Dot1-dependent histone H3K79 methylation promotes activation of the Mek1 meiotic checkpoint effector kinase by regulating the Hop1 adaptor" (Ontoso et al. 2013a).

Dot1 is conserved through evolution and the biological functions of Dot1 homologues in a wide range of organisms, such as *Dictyostelium*, *Trypanosoma*, *Caenorhabditis*, *Drosophila*, mice and humans have been progressively discovered (Feng et al. 2002; Shanower et al. 2005; Jones et al. 2008; Müller-Taubenberger et al. 2011; Cecere et al. 2013). Of note, *Schizosaccharomyces pombe* lacks Dot1 and H3K79me. In mammals, DOT1L-mediated H3K79me participates in multiple biological processes (Nguyen and Zhang 2011). Thus, DOT1L performs important roles in transcriptional regulation (Steger et al. 2008; Kim et al. 2012a), is involved in embryonic development and differentiation (Jones et al. 2008; Barry et al. 2009; Ooga et al. 2013), cardiac function (Nguyen et

al. 2011), hematopoiesis (Feng et al. 2010; Jo et al. 2011), cell proliferation and aging (Kim et al. 2012b) and chondrogenesis (Castaño Betancourt et al. 2012). Alteration of DOT1L function is related with some types of mixed lineage leukemia (Okada et al. 2005; Krivtsov et al. 2008; Bernt et al. 2011), neural tube defects (Zhang et al. 2013) and osteoarthritis (Castaño Betancourt et al. 2012). The discovery of an increasing number of pathologies related with altered DOT1L-mediated H3K79me patterns points to DOT1L as a promising therapeutic target (Daigle et al. 2011; Yao et al. 2011; Anglin et al. 2012; Helin and Dhanak 2013). However, little was known about DOT1L activity in mammalian meiosis; only a study in mouse oocytes has been reported (Ooga et al. 2008). Therefore, another aim of my thesis was the initial cytological characterization of DOT1L and H3K79me during meiotic prophase I in mouse spermatocytes. The findings were published in the second article presented in this report, entitled "Dynamics of DOT1L localization and H3K79 methylation during meiotic prophase I in mouse spermatocytes" (Ontoso et al. 2013b).

Thus, three sections compose the present thesis report entitled "Function of Dot1 in the meiotic recombination checkpoint and in DNA damage tolerance"; each of one is based on a published research article:

ARTICLE 1: "Dot1-dependent histone H3K79 methylation promotes activation of the Mek1 meiotic checkpoint effector kinase by regulating the Hop1 adaptor"
http://dx.plos.org/10.1371/journal.pgen.1003262

ARTICLE 2: "Dynamics of DOT1L localization and H3K79 methylation during meiotic prophase I in mouse spermatocytes"
http://dx.doi.org/10.1007/s00412-013-0438-5

ARTICLE 3: "Regulation of tolerance to DNA alkylating damage by Dot1 and Rad53 in *Saccharomyces cerevisiae*"
http://dx.doi.org/10.1016/j.dnarep.2010.07.003

2. WORKING HYPOTHESIS

Histone posttranslational modifications influence chromatin structure and dynamics, thus controlling multiple biological processes that take place associated to chromatin. Dot1-mediated H3K79 methylation represents an abundant epigenetic mark, which is present during both mitotic and meiotic cell cycles. Previous work has uncovered its function in multiple biological processes. Therefore, an important role for H3K79me in mechanisms contributing to the maintenance of genome integrity during mitosis and meiosis was expected.

3. GENERAL OBJECTIVES

- We aimed to investigate the molecular mechanisms underlying the function of Dot1-mediated H3K79 methylation during meiosis; particularly, in surveillance pathways such as the meiotic recombination checkpoint.

- We aimed to determine the functional contribution of H3K79me to the regulation of

alkylating DNA damage tolerance by TLS during the mitotic cell cycle.

4. GENERAL CONCLUSIONS

1- Dot1 is crucial for meiotic recombination checkpoint function in *S. cerevisiae*, because H3K79me is required to promote the correct localization and activation of adaptor and effector checkpoint proteins (Hop1 and Mek1, respectively), thus sustaining the meiotic checkpoint response.

2- DOT1L and the different H3K79 methylation states exhibit characteristic spatio-temporal localization patterns during meiotic prophase I in mouse spermatocytes, suggesting differential meiotic roles for each methylation state.

3- Dot1-mediated H3K79 methylation regulates alkylating DNA damage tolerance by modulating the activity of the Rad53 DNA damage checkpoint effector kinase and chromatin binding of the Rev1 TLS factor.

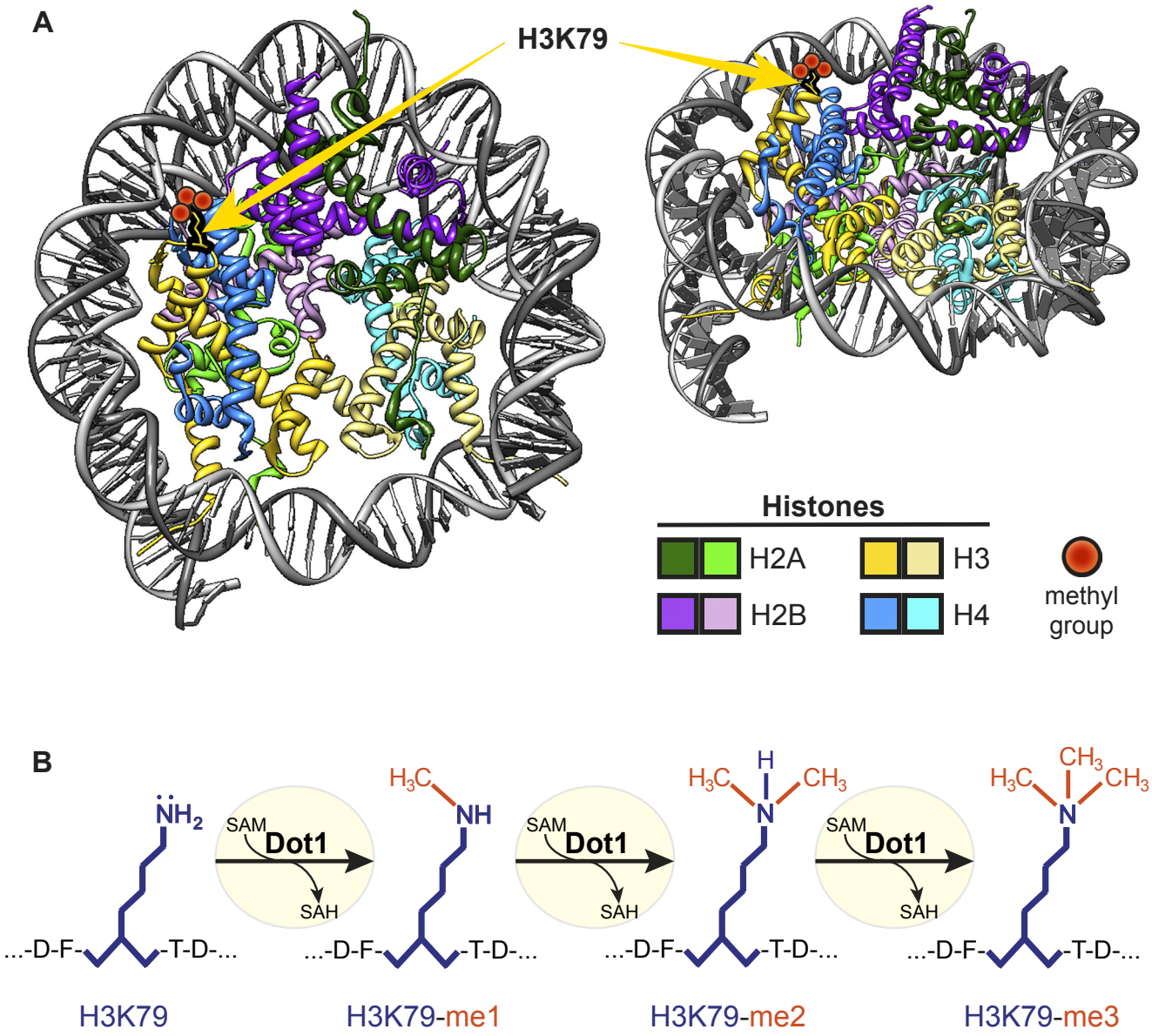

Figure 1. Methylation of histone H3 at lysine 79 is mediated by Dot1/DOT1L. (A) Two views of the nucleosome structure, highlighting the position of H3K79 and its trimethylated state. Lys79 is positioned in a loop region between two α-helixes on the solvent-accessible surface of the nucleosome, without contact with DNA or other histones (Ng et al. 2002). Unlike most other histone PTMs located on histone tails, methylation of H3K79 occurs within the histone globular domain. UCSF Chimera software was used to display PDB ID 3AFA. (B) Dot1/DOT1L catalyzes mono-, di- or trimethylation of H3K79 in a non-processive step-by-step mechanism using S-Adenosyl Methionine (SAM) cosubstrate as the methyl-donor group (Frederiks et al. 2008).

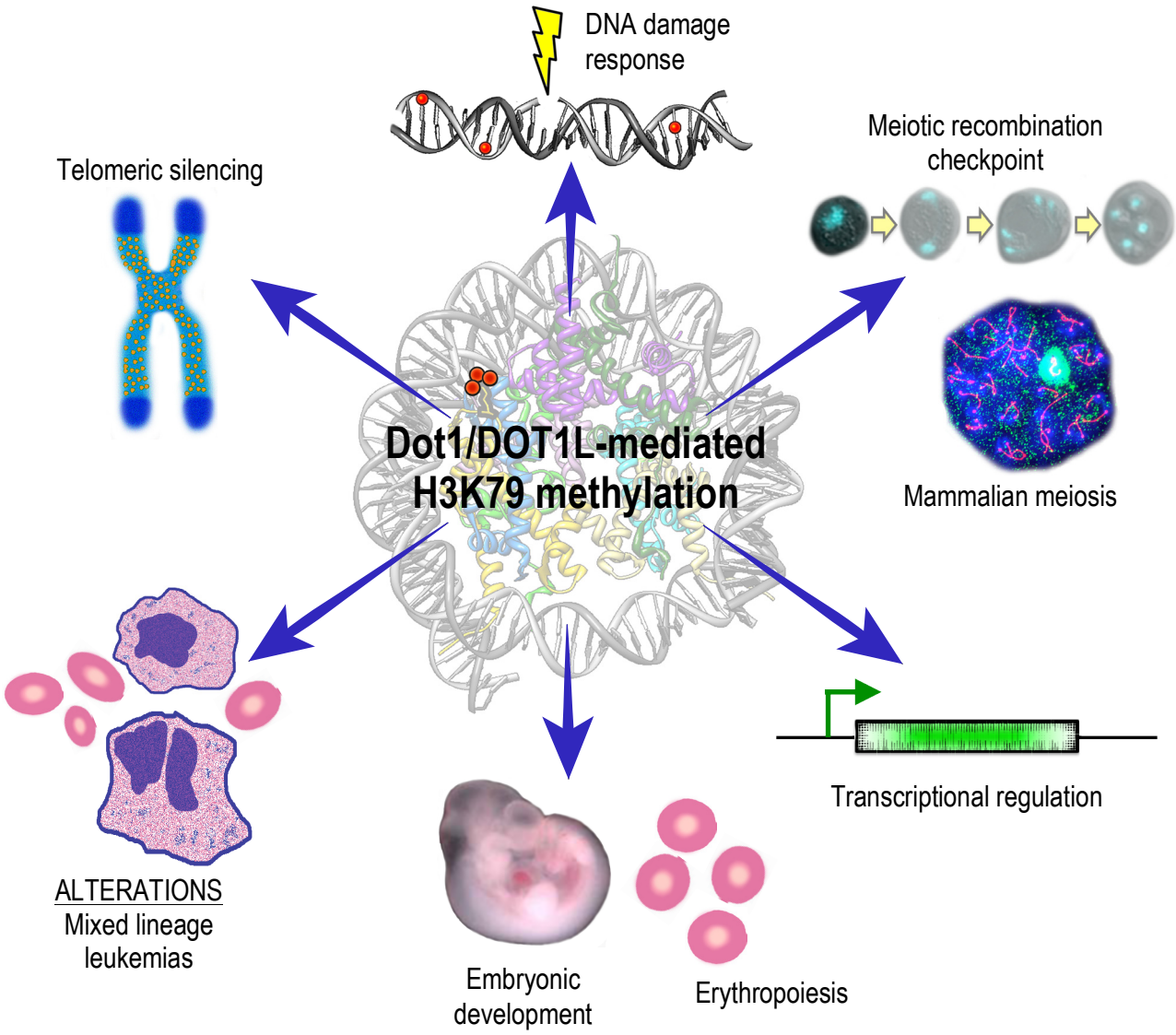

Figure 2. Multiple biological functions of Dot1/DOT1L-mediated H3K79 methylation. The constitutive H3K79 methylation catalyzed by Dot1/DOT1L plays important roles in fundamental biological processes, such as the DNA damage response, meiotic recombination checkpoint, transcriptional regulation, telomeric silencing, embryonic development and erythropoiesis. Misregulation of DOT1L leads to generation of mixed-lineage leukemia (Nguyen and Zhang 2011).

BIBLIOGRAFÍA / BIBLIOGRAPHY

Anglin JL, Deng L, Yao Y, et al. (2012) Synthesis and structure-activity relationship investigation of adenosine-containing inhibitors of histone methyltransferase DOT1L. J Med Chem 55:8066–8074. doi: 10.1021/jm300917h

Barry ER, Krueger W, Jakuba CM, et al. (2009) ES cell cycle progression and differentiation require the action of the histone methyltransferase Dot1L. Stem Cells 27:1538–1547. doi: 10.1002/stem.86

Becker PB, Workman JL (2013) Nucleosome remodeling and epigenetics. Cold Spring Harb Perspect Biol (First published online September 3, 2013). doi: 10.1101/cshperspect.a017905

Bernt KM, Zhu N, Sinha AU, et al. (2011) MLL-rearranged leukemia is dependent on aberrant H3K79 methylation by DOT1L. Cancer Cell 20:66–78. doi: 10.1016/j.ccr.2011.06.010

Bostelman LJ, Keller AM, Albrecht AM, et al. (2007) Methylation of histone H3 lysine-79 by Dot1p plays multiple roles in the response to UV damage in *Saccharomyces cerevisiae*. DNA Repair 6:383–395. doi: 10.1016/j.dnarep.2006.12.010

Castaño Betancourt MC, Cailotto F, Kerkhof HJ, et al. (2012) Genome-wide association and functional studies identify the DOT1L gene to be involved in cartilage thickness and hip osteoarthritis. Proc Natl Acad Sci U S A 109:8218–8223. doi: 10.1073/pnas.1119899109

Cecere G, Hoersch S, Jensen MB, et al. (2013) The ZFP-1(AF10)/DOT-1 complex opposes H2B ubiquitination to reduce Pol II transcription. Mol Cell 50:894–907. doi: 10.1016/j.molcel.2013.06.002

Cohen PE, Pollack SE, Pollard JW (2006) Genetic analysis of chromosome pairing, recombination, and cell cycle control during first meiotic prophase in mammals. Endocr Rev 27:398–426. doi: 10.1210/er.2005-0017

Conde F, Ontoso D, Acosta I, et al. (2010) Regulation of tolerance to DNA alkylating damage by Dot1 and Rad53 in *Saccharomyces cerevisiae*. DNA Repair 9:1038–1049. doi: 10.1016/j.dnarep.2010.07.003

Conde F, Refolio E, Cordón-Preciado V, et al. (2009) The Dot1 histone methyltransferase and the Rad9 checkpoint adaptor contribute to cohesin-dependent double-strand break repair by sister chromatid recombination in *Saccharomyces cerevisiae*. Genetics 182:437–446. doi: 10.1534/genetics.109.101899

Conde F, San-Segundo PA (2008) Role of Dot1 in the response to alkylating DNA damage in *Saccharomyces cerevisiae*: regulation of DNA damage tolerance by the error-prone polymerases Polζ/Rev1. Genetics 179:1197–1210. doi: 10.1534/genetics.108.089003

Daigle SR, Olhava EJ, Therkelsen CA, et al. (2011) Selective killing of mixed lineage leukemia cells by a potent small-molecule DOT1L inhibitor. Cancer Cell 20:53–65. doi: 10.1016/j.ccr.2011.06.009

Feng Q, Wang H, Ng HH, et al. (2002) Methylation of H3-lysine 79 is mediated by a new family of HMTases without a SET domain. Curr Biol 12:1052–1058.

Feng Y, Yang Y, Ortega MM, et al. (2010) Early mammalian erythropoiesis requires the Dot1L methyltransferase. Blood 116:4483–4491. doi: 10.1182/blood-2010-03-276501

Frederiks F, Tzouros M, Oudgenoeg G, et al. (2008) Nonprocessive methylation by Dot1 leads to functional redundancy of histone H3K79 methylation states. Nat Struct Mol Biol 15:550–557. doi: 10.1038/nsmb.1432

Game JC, Williamson MS, Spicakova T, Brown JM (2006) The RAD6/BRE1 histone modification pathway in Saccharomyces confers radiation resistance through a RAD51-dependent process that is independent of RAD18. Genetics 173:1951–1968. doi: 10.1534/genetics.106.057794

Giannattasio M, Lazzaro F, Plevani P, Muzi-Falconi M (2005) The DNA damage checkpoint response requires histone H2B ubiquitination by Rad6-Bre1 and H3 methylation by Dot1. J Biol Chem 280:9879–9886. doi: 10.1074/jbc.M414453200

Helin K, Dhanak D (2013) Chromatin proteins and modifications as drug targets. Nature 502:480–488. doi: 10.1038/nature12751

Hochwagen A, Amon A (2006) Checking your breaks: surveillance mechanisms of meiotic recombination. Curr Biol 16:R217–28. doi: 10.1016/j.cub.2006.03.009

Jo SY, Granowicz EM, Maillard I, et al. (2011) Requirement for Dot1l in murine postnatal hematopoiesis and leukemogenesis by MLL translocation. Blood 117:4759–4768. doi: 10.1182/blood-2010-12-327668

Jones B, Su H, Bhat A, et al. (2008) The histone H3K79 methyltransferase Dot1L is essential for mammalian development and heterochromatin structure. PLOS Genet 4:e1000190. doi: 10.1371/journal.pgen.1000190

Keeney S (2008) Spo11 and the formation of DNA double-strand breaks in meiosis. Genome Dyn Stab 2:81–123. doi: 10.1007/7050_2007_026

Kim S-K, Jung I, Lee H, et al. (2012a) Human histone H3K79 methyltransferase DOT1L binds actively transcribing RNA polymerase II to regulate gene expression. J Biol Chem 287:39698–39709. doi: 10.1074/jbc.M112.384057

Kim W, Kim R, Park G, et al. (2012b) Deficiency of H3K79 histone methyltransferase Dot1-like protein (DOT1L) inhibits cell proliferation. J Biol Chem 287:5588–5599. doi: 10.1074/jbc.M111.328138

Kornberg RD, Lorch Y (1999) Twenty-five years of the nucleosome, fundamental particle of the eukaryote chromosome. Cell 98:285–294.

Kouzarides T (2007) Chromatin modifications and their function. Cell 128:693–705. doi:10.1016/j.cell.2007.02.005

Krivtsov A V, Feng Z, Lemieux ME, et al. (2008) H3K79 methylation profiles define murine and human MLL-AF4 leukemias. Cancer Cell 14:355–368. doi: 10.1016/j.ccr.2008.10.001

Lacoste N, Utley RT, Hunter JM, et al. (2002) Disruptor of telomeric silencing-1 is a chromatin-specific histone H3 methyltransferase. J Biol Chem 277:30421–30424. doi: 10.1074/jbc.C200366200

van Leeuwen F, Gafken PR, Gottschling DE (2002) Dot1p modulates silencing in yeast by methylation of the nucleosome core. Cell 109:745–756.

Luger K, Dechassa ML, Tremethick DJ (2012) New insights into nucleosome and chromatin structure: an ordered state or a disordered affair? Nat Rev Mol Cell Biol 13:436–447. doi: 10.1038/nrm3382

Macqueen AJ, Hochwagen A (2011) Checkpoint mechanisms: the puppet masters of meiotic prophase. Trends Cell Biol 21:393–400. doi: 10.1016/j.tcb.2011.03.004

Müller-Taubenberger A, Bönisch C, Fürbringer M, et al. (2011) The histone methyltransferase Dot1 is required for DNA damage repair and proper development in Dictyostelium. Biochem Biophys Res Commun 404:1016–1022. doi: 10.1016/j.bbrc.2010.12.101

Ng HH, Feng Q, Wang H, et al. (2002) Lysine methylation within the globular domain of histone H3 by Dot1 is important for telomeric silencing and Sir protein association. Genes Dev 16:1518–1527. doi: 10.1101/gad.1001502

Nguyen AT, Xiao B, Neppl RL, et al. (2011) DOT1L regulates dystrophin expression and is critical for cardiac function. Genes Dev 25:263–274. doi: 10.1101/gad.2018511

Nguyen AT, Zhang Y (2011) The diverse functions of Dot1 and H3K79 methylation. Genes Dev 25:1345–1358. doi: 10.1101/gad.2057811

Okada Y, Feng Q, Lin Y, et al. (2005) hDOT1L links histone methylation to leukemogenesis. Cell 121:167–178. doi: 10.1016/j.cell.2005.02.020

Ontoso D, Acosta I, van Leeuwen F, et al. (2013a) Dot1-dependent histone H3K79 methylation promotes activation of the Mek1 meiotic checkpoint effector kinase by regulating the Hop1 adaptor. PLOS Genet 9:e1003262. doi: 10.1371/journal.pgen.1003262

Ontoso D, Kauppi L, Keeney S, San-Segundo PA (2013b) Dynamics of DOT1L localization and H3K79 methylation during meiotic prophase I in mouse spermatocytes. Chromosoma (First published online October 9, 2013). doi: 10.1007/s00412-013-0438-5

Ooga M, Inoue A, Kageyama S, et al. (2008) Changes in H3K79 methylation during preimplantation development in mice. Biol Reprod 78:413–24. doi: 10.1095/biolreprod.107.063453

Ooga M, Suzuki MG, Aoki F (2013) Involvement of DOT1L in the remodeling of heterochromatin configuration during early preimplantation development in mice. Biol Reprod (First published online October 16, 2013). doi: 10.1095/biolreprod.113.113258

Pawlowski WP, Cande WZ (2005) Coordinating the events of the meiotic prophase. Trends Cell Biol 15:674–681. doi: 10.1016/j.tcb.2005.10.005

Roeder GS, Bailis JM (2000) The pachytene checkpoint. Trends Genet 16:395–403. doi: 10.1038/hdy.2008.84

San-Segundo PA, Roeder GS (2000) Role for the silencing protein Dot1 in meiotic checkpoint control. Mol Biol Cell 11:3601–3615.

Shanower GA, Muller M, Blanton JL, et al. (2005) Characterization of the *grappa* gene, the Drosophila histone H3 lysine 79 methyltransferase. Genetics 169:173–184. doi: 10.1534/genetics.104.033191

Singer MS, Kahana A, Wolf AJ, et al. (1998) Identification of high-copy disruptors of telomeric silencing in *Saccharomyces cerevisiae*. Genetics 150:613–632.

Steger DJ, Lefterova MI, Ying L, et al. (2008) DOT1L/KMT4 recruitment and H3K79 methylation are ubiquitously coupled with gene transcription in

mammalian cells. Mol Cell Biol 28:2825–39. doi: 10.1128/MCB.02076-07

Toh GW-L, O'Shaughnessy AM, Jimeno S, et al. (2006) Histone H2A phosphorylation and H3 methylation are required for a novel Rad9 DSB repair function following checkpoint activation. DNA Repair 5:693–703. doi: 10.1016/j.dnarep.2006.03.005

van Welsem T, Frederiks F, Verzijlbergen KF, et al. (2008) Synthetic lethal screens identify gene silencing processes in yeast and implicate the acetylated amino terminus of Sir3 in recognition of the nucleosome core. Mol Cell Biol 28:3861–3872. doi: 10.1128/MCB.02050-07

Wysocki R, Javaheri A, Allard S, et al. (2005) Role of Dot1-dependent histone H3 methylation in G_1 and S phase DNA damage checkpoint functions of Rad9. Mol Cell Biol 25:8430–8443. doi: 10.1128/MCB.25.19.8430-8443.2005

Yao Y, Chen P, Diao J, et al. (2011) Selective inhibitors of histone methyltransferase DOT1L: design, synthesis, and crystallographic studies. J Am Chem Soc 133: 16746–16749. doi: 10.1021/ja206312b

Zhang Q, Xue P, Li H, et al. (2013) Histone modification mapping in human brain reveals aberrant expression of histone H3 lysine 79 dimethylation in neural tube defects. Neurobiol Dis 54:404–413. doi: 10.1016/j.nbd.2013.01.014

ARTÍCULO 1

Dot1-dependent histone H3K79 methylation promotes activation of the Mek1 meiotic checkpoint effector kinase by regulating the Hop1 adaptor

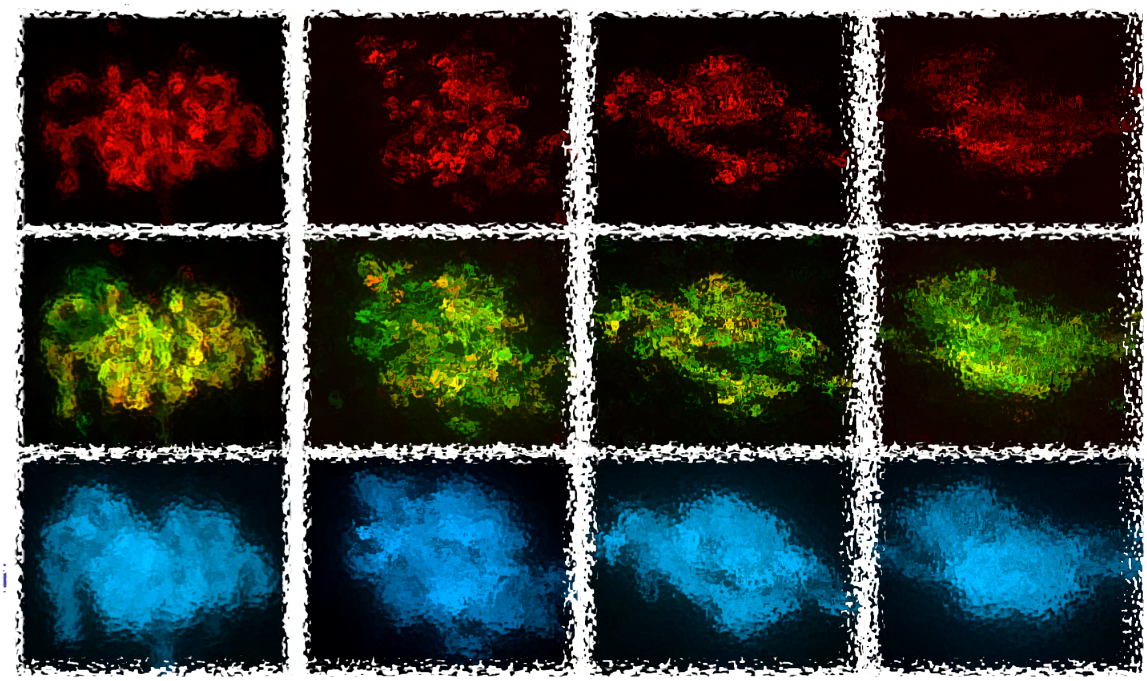

La metilación de la lisina 79 de la histona H3 dependiente de Dot1 promueve la activación de la quinasa efectora del checkpoint meiótico Mek1, mediante la regulación del adaptador Hop1

RESUMEN

Durante la meiosis, la segregación correcta de los cromosomas depende de la interacción apropiada entre los homólogos mediante la sinapsis y recombinación. El *checkpoint* de recombinación meiótica es un mecanismo de control de calidad que supervisa estos eventos cruciales. En respuesta a defectos en sinapsis y/o recombinación, este *checkpoint* bloquea o retrasa la progresión de la meiosis, evitando la formación de gametos aberrantes. La recombinación meiótica ocurre en el contexto de la cromatina y, de hecho, las modificaciones post-traduccionales de las histonas tienen un papel fundamental en el mantenimiento de la integridad genómica. En este trabajo, describimos la función de Dot1 en el *checkpoint* de recombinación meiótica en *Saccharomyces cerevisiae*. Dot1 es una proteína conservada evolutivamente que lleva a cabo la metilación de la lisina 79 en la histona H3 (H3K79me). Demostramos que la función de Dot1 en el *checkpoint* meiótico se debe exclusivamente a la metilación de H3K79, ya que las mutaciones *H3-K79A* o *H3K79R* recapitulan todos los fenotipos meióticos de la deleción de *DOT1*. Además, manipulando genéticamente la actividad catalítica de Dot1, encontramos que el grado de metilación de H3K79 modula la respuesta del *checkpoint* meiótico. También, mediante ensayos de *western blot* con Phos-tag, definimos los eventos secuenciales de fosforilación involucrados en la activación del la quinasa efectora Mek1. La actividad catalítica de Dot1 es necesaria para la autofosforilación de Mek1, pero no para su fosforilación inicial dependiente de Mec1/Tel1. Mediante inmunofluorescencia de extensiones de cromosomas y microscopía de fluorescencia en células vivas, observamos que Dot1 también promueve la activación de Hop1 y su adecuada distribución a lo largo de los cromosomas meióticos en el mutante *zip1* defectivo en sinapsis. Es más, la sobreexpresión de *HOP1* suprime el requerimiento de Dot1 para la activación del checkpoint. También hemos encontrado que la regulación de la distribución cromosómica de Hop1 llevada a cabo por Dot1 se ejerce, al menos en parte, mediante la exclusión de la cromatina de la proteína del *checkpoint* Pch2. Proponemos que la remodelación de la cromatina resultante de las roturas de doble cadena meióticas sin reparar y/o de interacciones defectivas entre los homólogos, conlleva la exposición de H3K79 metilada por Dot1 que, a su vez, excluye a Pch2 de los cromosomas. Puesto que Pch2 regula negativamente la abundancia de Hop1 en los cromosomas, la exclusión de Pch2 permite la localización continua del adaptador Hop1 a lo largo de los ejes cromosómicos lo que, a su vez, promueve la plena activación de Mek1 para disparar las respuestas correspondientes, como el bloqueo meiótico.

GRAPHICAL ABSTRACT

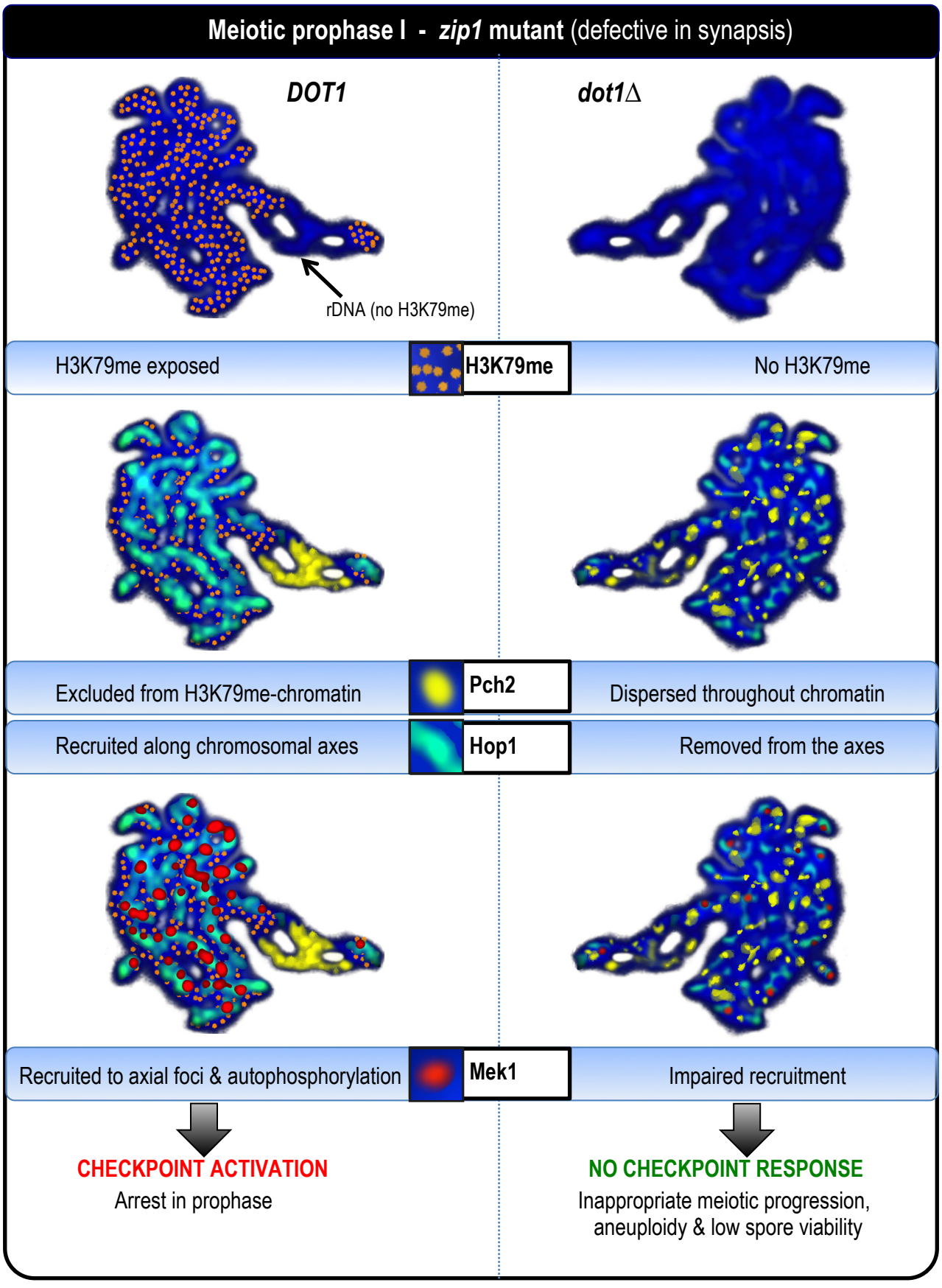

OPEN ACCESS Freely available online

PLOS | GENETICS

Dot1-Dependent Histone H3K79 Methylation Promotes Activation of the Mek1 Meiotic Checkpoint Effector Kinase by Regulating the Hop1 Adaptor

David Ontoso[1], Isabel Acosta[1], Fred van Leeuwen[2], Raimundo Freire[3], Pedro A. San-Segundo[1]*

1 Instituto de Biología Funcional y Genómica, Consejo Superior de Investigaciones Científicas and University of Salamanca, Salamanca, Spain, **2** Division of Gene Regulation, Netherlands Cancer Institute, Amsterdam, The Netherlands, **3** Unidad de Investigación, Hospital Universitario de Canarias, Tenerife, Spain

Abstract

During meiosis, accurate chromosome segregation relies on the proper interaction between homologous chromosomes, including synapsis and recombination. The meiotic recombination checkpoint is a quality control mechanism that monitors those crucial events. In response to defects in synapsis and/or recombination, this checkpoint blocks or delays progression of meiosis, preventing the formation of aberrant gametes. Meiotic recombination occurs in the context of chromatin and histone modifications, which play crucial roles in the maintenance of genomic integrity. Here, we unveil the role of Dot1-dependent histone H3 methylation at lysine 79 (H3K79me) in this meiotic surveillance mechanism. We demonstrate that the meiotic checkpoint function of Dot1 relies on H3K79me because, like the *dot1* deletion, *H3-K79A* or *H3-K79R* mutations suppress the checkpoint-imposed meiotic delay of a synapsis-defective *zip1* mutant. Moreover, by genetically manipulating Dot1 catalytic activity, we find that the status of H3K79me modulates the meiotic checkpoint response. We also define the phosphorylation events involving activation of the meiotic checkpoint effector Mek1 kinase. Dot1 is required for Mek1 autophosphorylation, but not for its Mec1/Tel1-dependent phosphorylation. Dot1-dependent H3K79me also promotes Hop1 activation and its proper distribution along *zip1* meiotic chromosomes, at least in part, by regulating Pch2 localization. Furthermore, *HOP1* overexpression bypasses the Dot1 requirement for checkpoint activation. We propose that chromatin remodeling resulting from unrepaired meiotic DSBs and/or faulty interhomolog interactions allows Dot1-mediated H3K79-me to exclude Pch2 from the chromosomes, thus driving localization of Hop1 along chromosome axes and enabling Mek1 full activation to trigger downstream responses, such as meiotic arrest.

Citation: Ontoso D, Acosta I, van Leeuwen F, Freire R, San-Segundo PA (2013) Dot1-Dependent Histone H3K79 Methylation Promotes Activation of the Mek1 Meiotic Checkpoint Effector Kinase by Regulating the Hop1 Adaptor. PLoS Genet 9(1): e1003262. doi:10.1371/journal.pgen.1003262

Editor: Michael Lichten, National Cancer Institute, United States of America

Received August 9, 2012; **Accepted** December 6, 2012; **Published** January 31, 2013

Funding: This work was supported by grants from MICINN (SAF2010-22357, CONSOLIDER-Ingenio 2010 CDS2007-0015) to RF; from the Dutch Cancer Society (KWF2009-4511) to FvL; and from the Ministry of Science and Innovation of Spain (BFU2009-07159), Junta de Castilla y León (CSI025A11-2), and Fundación Ramón Areces to PAS-S. DO was supported by a predoctoral fellowship (JAE-predoc) from the CSIC (Spain). The funders had no role in study design, data collection and analysis, decision to publish, or preparation of the manuscript.

Competing Interests: The authors have declared that no competing interests exist.

* E-mail: pedross@usal.es

Introduction

During the specialized meiotic cell cycle, two rounds of chromosome segregation follow a single phase of DNA replication dividing the number of chromosomes by half to generate haploid gametes. One of the hallmarks of meiosis is the complex interaction between homologous chromosomes (homologs) involving synapsis and recombination. During meiotic prophase I, homologs find each other, get aligned and finally closely associate along their entire length (synapsis) in the context of the synaptonemal complex (SC). The SC is a tripartite structure composed of two lateral elements (LEs), connected by transverse filaments, which constitute the central region. The chromatin of both sister chromatids of each homolog is organized in loops attached at their base to each of the LEs [1,2]. In budding yeast, the Red1 and Hop1 proteins localize to the LEs [3], whereas the Zip1 protein is a major component of the SC central region [4,5]. Concomitant with SC development, meiotic recombination takes place. Meiotic recombination initiates with programmed double-strand breaks (DSBs) introduced by Spo11 and accessory proteins [6]. Meiotic DSBs are preferentially repaired using an intact non-sister chromatid resulting in physical connections between homologs (chiasmata), which promote proper chromosome segregation.

Accurate distribution of chromosomes to the progeny is essential for generation of functional gametes; thus, meiotic cells are endowed with a meiosis-specific surveillance mechanism, the so-called pachytene checkpoint or meiotic recombination checkpoint, which contributes to faithful chromosome segregation. In response to defects in meiotic recombination and/or chromosome synapsis, the pachytene checkpoint is triggered and blocks or delays exit from prophase of meiosis I to prevent aberrant chromosome segregation and the formation of aneuploid meiotic products [7,8].

This evolutionary-conserved quality-control mechanism operates from yeast to mammals. In *S. cerevisiae*, the meiotic recombination checkpoint responding to unrepaired resected DSBs shares the same sensors with the DNA damage checkpoint operating in vegetative cells, including the Mec1/Ddc2 kinase, Rad24 and the 9-1-1 complex [9–11]. However, the Rad9 adaptor and the Rad53 checkpoint kinase are dispensable for this meiotic checkpoint. On the contrary, given the special chromosomal

Author Summary

In sexually reproducing organisms, meiosis divides the number of chromosomes by half to generate gametes. Meiosis involves a series of interactions between maternal and paternal chromosomes leading to the exchange of genetic material by recombination. Completion of these processes is required for accurate distribution of chromosomes to the gametes. Meiotic cells possess quality-control mechanisms (checkpoints) to monitor those critical events. When failures occur, the checkpoint blocks meiotic progression to prevent the formation of aneuploid gametes. Genetic information is packaged into chromatin; histone modifications regulate multiple aspects of DNA metabolism to maintain genomic integrity. Dot1 is a conserved methyltransferase, responsible for histone H3 methylation at lysine 79, that is required for the meiotic recombination checkpoint. Here we decipher the molecular mechanism underlying Dot1 meiotic checkpoint function. We show that Dot1 catalytic activity correlates with the strength of the checkpoint response. By regulating Pch2 chromatin distribution, Dot1 controls localization of the chromosome axial component Hop1, which, in turn, contributes to activation of Mek1, the major effector kinase of the checkpoint. Our findings suggest that, in response to meiotic defects, the chromatin environment created by a constitutive histone mark orchestrates distribution of structural components of the chromosomes supporting activation of the meiotic checkpoint.

context where meiotic recombination takes place, the meiosis-specific axial chromosomal components Red1 and Hop1 act as adaptors between the upstream sensors and the downstream Mek1 meiotic effector kinase, which, like Rad53, is hyperphosphorylated upon checkpoint activation [12,13]. In turn, the meiotic cell cycle delay is imposed by inhibition of crucial regulators of meiosis I progression, including the cyclin-dependent kinase Cdc28, the transcription factor Ndt80 and the polo-like kinase Cdc5 [14–19]. Budding yeast meiotic mutants, such as *zip1* (defective in SC and crossover formation) or *dmc1* (defective in the strand invasion step of interhomolog recombination), are invaluable genetic tools to activate the meiotic recombination checkpoint.

Meiotic recombination as well as detection and signaling of recombination intermediates by the checkpoint machinery occur in the context of chromatin; therefore, histone posttranslational modifications are expected to play important roles on these processes [20]. For example, Set1-dependent H3K4 methylation is linked to meiotic DSB formation [21,22]. On the other hand, the Dot1 histone methyltranferase, which targets H3K79 [23–25], is largely dispensable for unperturbed meiosis, but is essential for meiotic checkpoint function. Mutation of *DOT1* relieves the meiotic prophase arrest of *zip1* and *dmc1* mutants resulting in defective meiotic products [26]. Dot1 is also involved in several aspects of the DNA damage response in vegetative yeast cells and the DOT1L mammalian homolog also plays crucial cellular functions [27]. However, the molecular mechanisms underlying the meiotic checkpoint function of Dot1 are unknown.

Here, we investigated the role of Dot1-dependendent H3K79 methylation in *zip1*-induced checkpoint activation. By manipulation of Dot1 catalytic activity and levels, we found that the extent of H3K79 trimethylation correlates with the strength of checkpoint-imposed meiotic delay. We demonstrate that while the meiotic defects of a synapsis and recombination-deficient *zip1* mutant are correctly sensed by Mec1-Ddc2 in the absence of H3K79me, activation of the downstream effector kinase Mek1 is impaired. We dissected the Mek1 phosphorylation events and found that Dot1 promotes its Hop1-dependent dimerization and auto-phosphorylation. Finally, we show that the effect of Dot1-dependent H3K79me on Hop1 localization is exerted, at least in part, by excluding Pch2 from the chromosomes. Our results indicate that constitutive methylation of H3K79 by Dot1 is required for proper chromosomal recruitment of Hop1 to relay the checkpoint signal to Mek1 in response to meiotic defects.

Results

Histone H3K79 methylation regulates the meiotic recombination checkpoint

Dot1 catalyzes the mono-, di- and tri-methylation of histone H3K79 (Figure 1A) by a non-processive mechanism [27,28] and plays a crucial role in the meiotic recombination checkpoint [26]. Notably, we found that overall levels of H3K79me do not significantly change upon meiosis induction (Figure 1A, compare vegetative and meiotic cells; Figure S1A) or upon meiotic checkpoint activation (Figure 1A, compare wild type and *zip1* meiotic cells; Figure S1A). Moreover, H3K79me meiotic levels were not significantly altered in the *spo11* mutant, lacking meiotic recombination [6], or in other mutants defective in the meiotic recombination checkpoint, such as *rad24*, *pch2* and *ddc2* [10,11,29] (Figure S1B). Therefore, to determine whether regulation of the meiotic recombination checkpoint by Dot1 relies on H3K79me, we generated and analyzed *H3-K79R* and *H3-K79A* mutants, in which the lysine 79 targeted by Dot1 cannot be methylated (Figure 1A). Importantly, like *dot1*, both methylation-site mutants suppressed the pronounced checkpoint-imposed meiotic delay of the *zip1* mutant (Figure 1B). In an otherwise wild-type background, *DOT1* deletion has no or little meiotic effects and spore viability is high [26,30]; likewise, the *H3-K79R* and *H3-K79A* single mutants showed wild-type levels of spore viability (Figure 1C), suggesting that H3K79me is dispensable in unperturbed meiosis. However, similar to *zip1 dot1*, spore viability was strongly reduced in *zip1 H3-K79R* and *zip1 H3-K79A* (Figure 1C), indicating that the defects conferred by *zip1* persist in the double mutants despite their wild-type kinetics of meiotic progression. Thus, Dot1-dependent H3K79me is essential for meiotic recombination checkpoint function.

To further investigate the regulation of the meiotic checkpoint by H3K79me, we monitored checkpoint function in *zip1* diploid strains exhibiting gradually decreased Dot1 activity. In order to generate this set of strains, we used the combination of the *dot1-G401A* allele, which confers partial catalytic activity [28], with the expression of *DOT1* (or *dot1-G401A*) from a plasmid, which results in lower protein levels (Figure 1D; [31]). Analysis of H3K79-me1, -me2 and -me3 levels in meiotic cells confirmed a gradually reduced Dot1 activity following this order: *DOT1*>p[*DOT1*]> *dot1-G401A*>p[*dot1-G401A*]>*dot1Δ*, as manifested by progressively reduced H3K79-me3 and, conversely, progressively increased H3K79-me1 (Figure 1D). Interestingly, meiotic checkpoint activity, monitored as the ability to impose the *zip1* meiotic delay, also showed a gradual decrease mirroring the drop in Dot1 catalytic function (Figure 1E). Quantification of the relative levels of each H3K79 methylation state revealed a marked correlation between H3K79-me3 and checkpoint function (Figure 1F). Thus, the status of H3K79 methylation modulates the meiotic recombination checkpoint, with the H3K79-me3 form being the most relevant to sustain the checkpoint response.

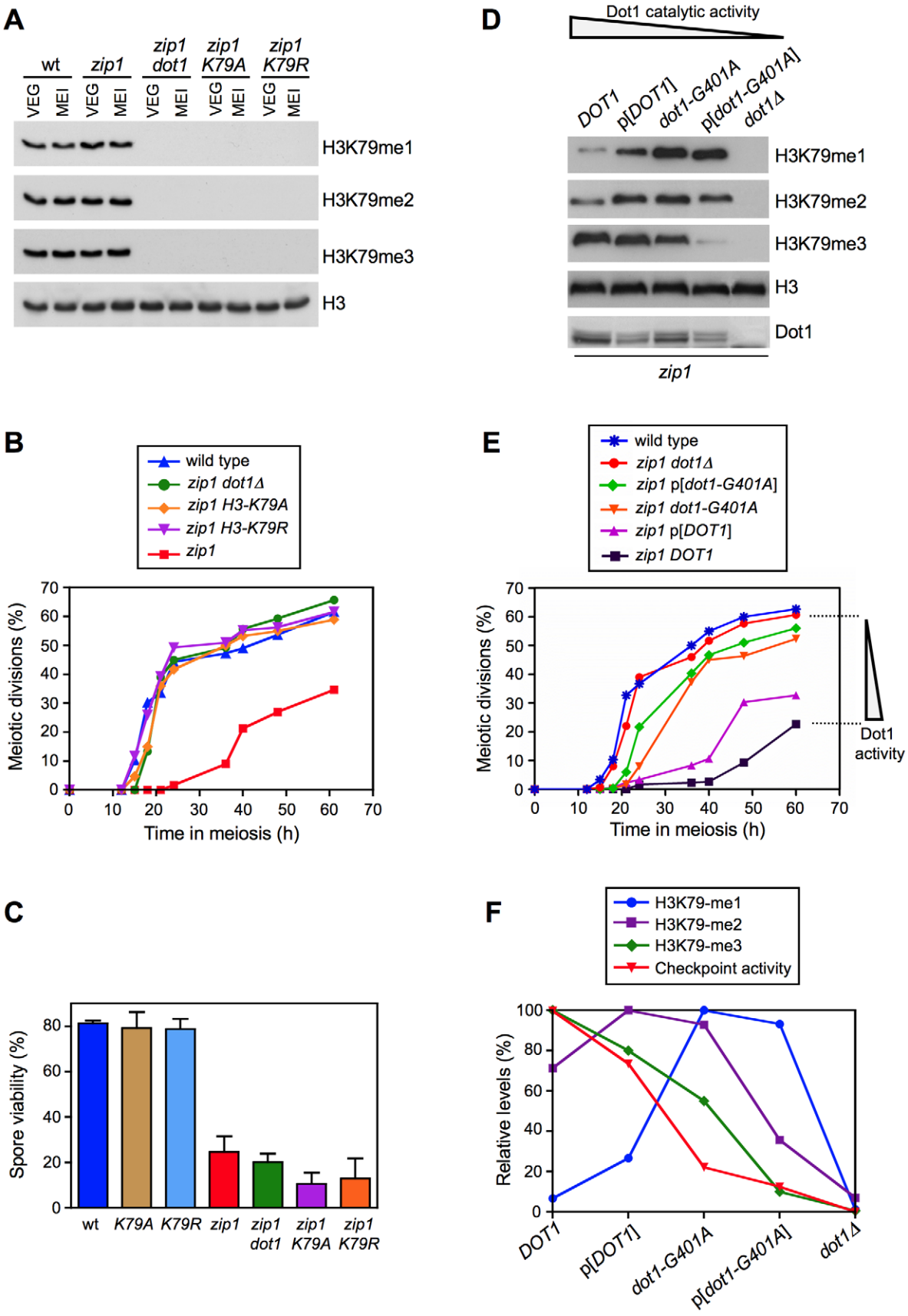

Figure 1. Methylation of H3K79 by Dot1 is essential for meiotic recombination checkpoint function. (A) Western blot analysis of H3K79 methylation in vegetative (VEG) and meiotic (MEI) cells to compare H3K79 methylation levels in different mutant backgrounds. Samples of meiotic

cells were taken 15 h after meiosis induction. Total histone H3 is shown as a loading control. (B) Suppression of *zip1* meiotic delay by *dot1* or by *H3-K79A* and *H3-K79R* mutations. Time course of meiotic nuclear divisions; the percentage of cells containing more than two nuclei is represented. (C) Spore viability determined by tetrad dissection. At least 240 spores were scored for each strain. Means and standard deviations are shown. Strains for (A), (B) and (C) are: DP806 (wild type), DP807 (*H3-K79A*), DP808 (*H3-K79R*), DP809 (*zip1*), DP812 (*zip1 dot1*), DP810 (*zip1 H3-K79A*) and DP811 (*zip1 H3-K79R*). (D) Western blot analysis of H3K79 methylation in *zip1* strains producing different versions of Dot1 either from the endogenous loci (*DOT1* and *dot1-G401A*) or from a centromeric plasmid (p[*DOT1*] and p[*dot1-G401A*]). Samples were taken 24 h after meiosis induction. Dot1 levels are also shown. Total histone H3 serves as a loading control. (E) Time course of meiotic nuclear divisions; the percentage of cells containing more than two nuclei is represented. (F) Quantification of the relative levels of H3K79 mono-, di-, and tri-methylation. The maximum value of each methylation state was considered 100%. Checkpoint activity represents the ability to impose the *zip1* meiotic delay according to data in (E). The meiotic nuclear division values for the latest time point (60 h) were considered in the calculations. Maximum checkpoint activity (100%) was assigned to the *zip1* strain expressing endogenous wild-type *DOT1*. Strains for (D), (E) and (F) are: DP421 + pRS315 (wild type), DP555 + pRS315 (*zip1 dot1Δ*), DP555 + pRS315-DOT1 (*zip1* p[*DOT1*]), DP555 + pFvL54 (*zip1* p[*dot1-G401A*]), DP556 + pRS315 (*zip1 DOT1*) and DP560 + pRS315 (*zip1 dot1-G401A*).
doi:10.1371/journal.pgen.1003262.g001

Dot1 is required for activation of the Mek1 effector kinase

Next, we sought to determine where in the meiotic recombination checkpoint pathway Dot1-dependent H3K79me is acting. We first analyzed checkpoint sensor function by monitoring the formation of *zip1*-induced Ddc2-GFP foci [11]. Formation of Ddc2 foci was not disrupted in the absence of Dot1 (Figure 2A), suggesting that H3K79me is not required for the ability of Mec1-Ddc2 to detect meiotic recombination intermediates. Upon checkpoint activation, the Mek1 effector kinase forms nuclear foci that can be detected both on chromosome spreads ([9]; see below) and in live meiotic cells (Figure 2A). Strikingly, we found that the *zip1* mutant accumulated multiple discrete Mek1-GFP foci during meiotic prophase, whereas most *zip1 dot1* cells displayed a diffuse Mek1 nuclear signal and only occasional foci were observed (Figure 2A) indicating that Dot1 promotes checkpoint-induced association of Mek1 to meiotic chromosomes (see below).

Mek1 is activated by phosphorylation in mutants that trigger the meiotic recombination checkpoint, including *zip1* [12,14,32,33]; therefore, we followed Mek1 phosphorylation throughout meiosis in wild-type, *zip1* and *zip1 dot1* cells using Phos-tag gels (Figure 2B). In the wild type, Mek1 was weakly and transiently activated during the peak of meiotic prophase in this strain background (around 12–15 h). In contrast, Mek1 was hyperactivated in *zip1* cells as evidenced by the presence of additional, more persistent, and stronger phosphorylated forms. However, Mek1 hyperactivation was not observed in the *zip1 dot1* double mutant; like in wild type, only a weak and transient phosphorylated form was detected. To rule out the possibility that the difference between *zip1* and *zip1 dot1* were due to their different kinetics of meiotic progression (*zip1* exhibits a marked delay that is bypassed in *zip1 dot1*; Figure 1B), we monitored Mek1 phosphorylation in *ndt80* pachytene-arrested cells. As presented in Figure 2C, *zip1*-induced hyperphosphorylation of Mek1 was severely impaired in the absence of Dot1.

In summary, these results place Dot1 function upstream of Mek1 in the meiotic recombination checkpoint pathway and indicate that, whereas Mec1/Ddc2 act independently of H3K79 methylation to sense meiotic defects, Dot1 is required for checkpoint-induced activation of Mek1.

Autophosphorylation of Mek1 depends on Dot1

In *ndt80*-arrested cells, using high-resolution Phos-tag gels, we were able to resolve several *zip1*-induced shifted forms of Mek1 above the basal band (Figure 3A–3D). Phosphatase treatment eliminated all band shifts indicating that they represent distinct phosphorylated forms (Figure 3A). We used different *mek1* versions carrying specific mutations, as well as mutants in upstream components of the checkpoint pathway, in order to determine the contribution of different phosphorylation events to the observed checkpoint-induced Mek1 forms in *zip1 ndt80* cells (Figure 3E). Mek1 phosphorylation was completely abolished in the *hop1* mutant, lacking a LE-component meiotic checkpoint adaptor [3,34,35] (Figure 3B) and in the *spo11* mutant, which does not initiate recombination [36] (Figure 3C). However, in the absence of Dot1, only the upper phosphorylated bands were eliminated (Figure 3B–3D, white arrowheads), but the form immediately above the basal Mek1 band remained intact (Figure 3B–3D, black arrowhead). Interestingly, this moderately-shifted form was reduced in *mec1* cells and virtually disappeared in *mec1 tel1* and *rad24 tel1* mutants (Figure 3C and 3D, black arrowhead), suggesting that it arises from Mec1/Tel1-dependent phosphorylation. On the other hand, the kinase-dead *mek1-K199R* allele, as well as the autophosphorylation-defective *mek1-T327A* and *mek1-T331A* mutants [33], specifically lacked the upper bands displaying the stronger mobility shift, suggesting that they result from Mek1 autophosphorylation (Figure 3D, white arrowheads). In contrast, the Mek1 form immediately above the basal band (i.e., resulting from Mec1/Tel1 action) remained invariable in those *mek1* mutants (Figure 3D, black arrowhead). Thus, interestingly, the *zip1 dot1* mutant showed a similar pattern to that of *zip1 mek1-K199R*, *zip1 mek1-T327A* or *zip1 mek1-T331A* (Figure 3D), strongly suggesting that Dot1 is mainly required for Mek1 autophosphorylation, but not for its Mec1/Tel1-dependent phosphorylation (Figure 3E).

It has been proposed that dimerization of Mek1 promotes its function, likely by facilitating *in trans* autophosphorylation [33,37]. Thus, we hypothesized that Dot1 could be required for Mek1 dimerization. Importantly, we found that GST-driven forced dimerization of Mek1 restored its full phosphorylation even in the absence of Dot1, although Mek1 activation was not maintained at late time points (Figure 2B). Consistently, expression of *GST-MEK1* in *zip1 dot1* strains conferred a brief, but significant, meiotic delay (Figure 2D). As previously reported, the *zip1 GST-MEK1* mutant was completely halted (Figure 2D) [37], and we found that this block was accompanied by the persistent hyperphosphorylation of GST-Mek1 (Figure 2B). The permanent or transient arrest conferred by GST-Mek1 in *zip1* or *zip1 dot1*, respectively, was completely relieved when inactive kinase (*GST-mek1-K199R*) or autophosphorylation-defective (*GST-mek1-T327A*) versions were introduced (Figure 2D), confirming that in *GST-MEK1* strains, meiotic progression was slowed down by forced Mek1 activation and not by another unrelated cause. To further support this conclusion, we monitored another downstream molecular marker of pachytene checkpoint activation, such as the inhibition of the production of the Cdc5 polo-like kinase [14,18]. As expected, whereas induction of Cdc5 was delayed in *zip1* cells, the *zip1 dot1* double mutant displayed wild-type kinetics of Cdc5 production (Figure 2B). Strikingly, consistent with the kinetics of meiotic progression (Figure 2D), expression of *GST-MEK1* in *zip1 dot1* cells restored a significant delay in Cdc5 induction. Furthermore, Cdc5 production was severely impaired in the arrested *zip1 GST-MEK1* strain (Figure 2B). In summary, these observations indicate that

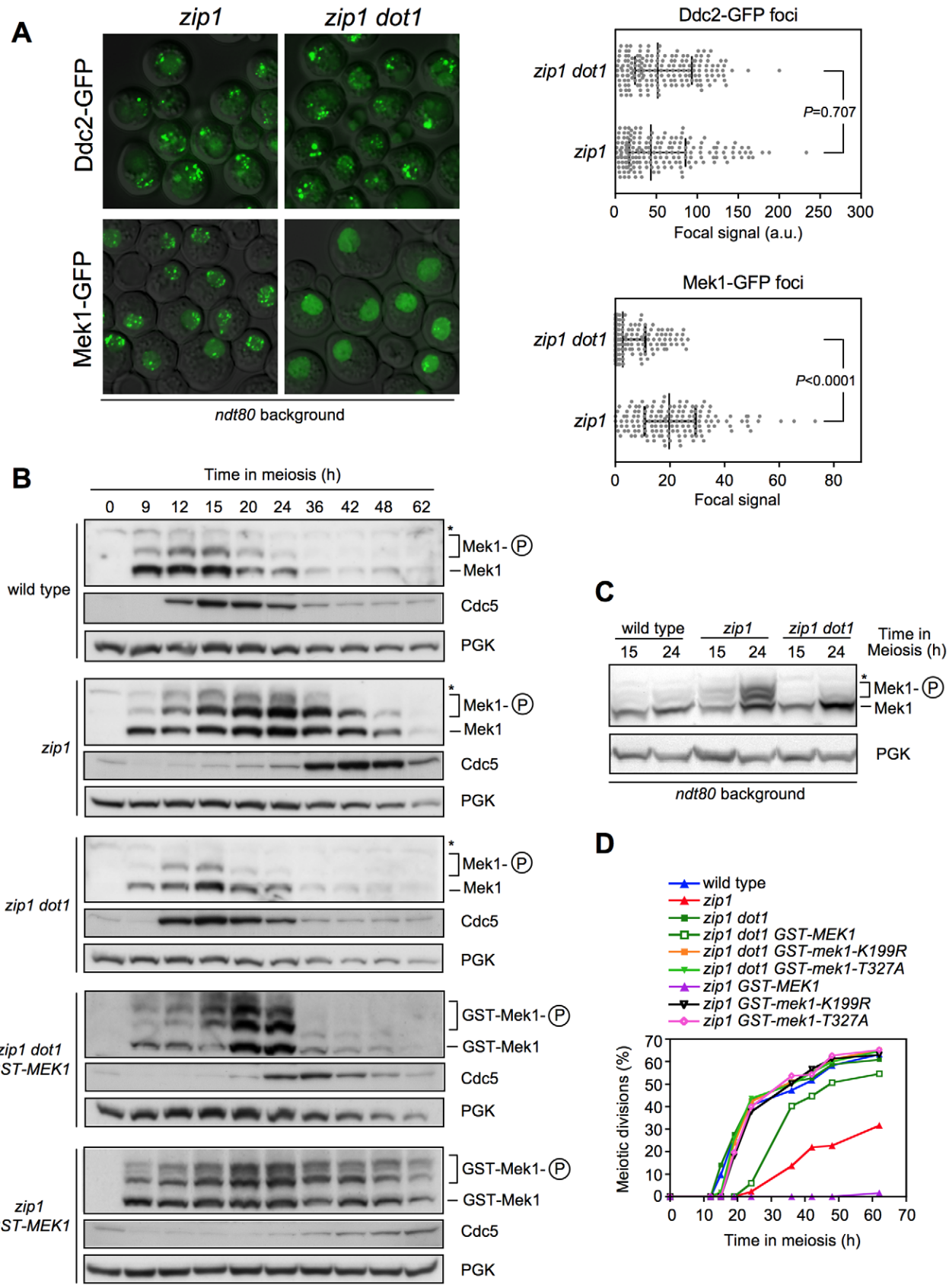

Figure 2. Dot1 is required for checkpoint-promoted localization and activation of Mek1. (A) Formation of *zip1*-induced Mek1 foci is defective in the absence of Dot1. Representative images of Ddc2-GFP and Mek1-GFP foci in *zip1* and *zip1 dot1* cells after 24 h in meiosis. Strains are DP460 (*zip1 DDC2-GFP*), DP579 (*zip1 dot1 DDC2-GFP*), DP582 (*zip1 MEK1-GFP*) and DP583 (*zip1 dot1 MEK1-GFP*). All strains are *ndt80*-arrested at

pachytene. The graphs show the quantification of Ddc2 and Mek1 foci formation from the same samples determined as the intensity of the total focal GFP signal relative to total nuclear signal (a.u., arbitrary units). Error bars represent the median with interquartile range. Each spot in the plot represents the foci intensity of every nucleus measured. 175 and 150 nuclei were analyzed for Ddc2-GFP and Mek1-GFP, respectively. (B) Western blot analysis of Mek1 activation by phosphorylation and Cdc5 production throughout meiosis in wild type (DP421), *zip1* (DP422), *zip1 dot1* (DP555), *zip1 dot1 GST-MEK1* (DP785) and *zip1 GST-MEK1* (DP792) using Phos-tag gels. PGK was used as a loading control. (C) Analysis of Mek1 activation in *ndt80*-arrested cells. Strains are DP424 (wild type), DP428 (*zip1*) and DP655 (*zip1 dot1*). (D) Time course of meiotic nuclear divisions; the percentage of cells containing more than two nuclei is represented. Strains are: DP421 (wild type), DP422 (*zip1*), DP555 (*zip1 dot1*), DP785 (*zip1 dot1 GST-MEK1*), DP783 (*zip1 dot1 GST-mek1-K199R*), DP784 (*zip1 dot1 GST-mek1-T327A*), DP792 (*zip1 GST-MEK1*), DP790 (*zip1 GST-mek1-K199R*) and DP791 (*zip1 GST-mek1-T327A*).
doi:10.1371/journal.pgen.1003262.g002

artificial dimerization of Mek1 partially overcomes Dot1 requirement for Mek1 activation and further supports the conclusion that Dot1 function promotes Mek1 autophosphorylation.

Dot1 is required for localization and activation of the Hop1 meiotic checkpoint adaptor

It has been reported that activated Hop1 promotes Mek1 dimerization via a C-terminal domain [33,38]; therefore, we investigated whether the effect of Dot1 on Mek1 phosphorylation was mediated by Hop1. First, we studied Hop1 localization on chromosome spreads of *ndt80*-arrested *zip1* and *zip1 dot1* strains. As previously described [3], Hop1 displayed a predominantly linear staining along the lateral elements of *zip1* chromosomes. In contrast, only short stretches of Hop1 could be detected in the *zip1 dot1* mutant, which showed a predominating Hop1 punctate pattern (Figure 4A and 4B, left panel). Consistent with our observations in live cells (Figure 2A), we also detected a marked reduction of Mek1 chromosomal foci in *zip1 dot1*, compared to the *zip1* single mutant (Figure 4A and 4B, right panel). In addition, we also analyzed Hop1 localization in *zip1* and *zip1 dot1* live meiotic cells expressing *HOP1-GFP*. In line with the aberrant distribution on spreads, we observed that Hop1-GFP signal was weaker and less continuous in *zip1 dot1* cells. (Figure 4C and 4D; Video S1). This discontinuous localization of Hop1 does not result from a pronounced alteration of overall chromosome structure, because the SC lateral component Red1 [3] displayed a linear distribution in both *zip1* and *zip1 dot1* strains (Figure S2). On the other hand, the *dot1* single mutant only showed a modest decrease of Hop1-GFP signal compared with the wild type (see Figure 7C and 7D below). Thus, upon *zip1*-induced checkpoint activation, Dot1 enables proper loading or maintenance of Hop1 onto chromosomes.

Since Mec1/Tel1-dependent phosphorylation of Hop1 at defined S/T-Q motifs is required for Mek1 activation and localization [34], we examined *zip1*-induced Hop1 phosphorylation in the absence of Dot1, by monitoring its gel mobility shift. As shown in Figure 4E, the *zip1 dot1* mutant displayed a severe defect in Hop1 phosphorylation, similar to the *zip1 mec1* and *zip1 spo11* mutants also analyzed as controls (Figure 4E and Figure S3). Even after long overexposure of the gels, only a barely visible phosphorylated form of Hop1 could be detected in the absence of Dot1 (Figure 4E).

These observations suggest that the defect in Mek1 autophosphorylation observed in the absence of Dot1 stems from impaired Hop1 function. To confirm this notion, we overexpressed *HOP1* from a high-copy plasmid in *zip1 dot1* cells. As shown in Figure 5, whereas the *zip1 dot1* mutant transformed with empty vector showed defective Mek1 localization and activation, *HOP1* overexpression in *zip1 dot1* restored Mek1 chromosomal foci (Figure 5A), Mek1 phosphorylation (Figure 5B), and reestablished a substantial meiotic delay (Figure 5C). We found that Hop1 overproduction also conferred a slight reduction in the efficiency of meiotic progression in the wild type (Figure 5C) and further enhanced the *zip1* meiotic delay, as expected from the strong hyperphosphorylation of Mek1 (Figure 5B and 5C). Notably, in all cases (wild type, *zip1* or *zip1 dot1*), the further delay in meiotic progression imposed by high levels of Hop1 was suppressed by the absence of Mek1 (Figure 5C), proving that it was caused from amplified pachytene checkpoint signaling and not from an unrelated cause.

H3K79me is required for Mek1 and Hop1 phosphorylation and localization

We have shown that, like *dot1*, mutation of H3K79 to non-methylatable residues completely bypasses the checkpoint-induced meiotic delay of *zip1* (Figure 1B). On the other hand, we have revealed that, in *zip1* cells, Dot1 orchestrates Hop1 and Mek1 activation and chromosomal distribution (Figure 2, Figure 3, Figure 4, and Figure 5). To confirm that Hop1 and Mek1 checkpoint functions are also directly regulated by H3K79me, and not by another possible methyltransferase-independent function of Dot1, we examined their phosphorylation and localization in the *zip1 H3-K79R* and *zip1 H3-K79A* mutants. We found that, indeed, these histone point mutants phenocopy the *dot1* defects in Mek1 foci formation (Figure 6A and 6B) and Mek1 autophosphorylation (Figure 6D; Figure S4). Likewise, the *zip1 H3-K79R* and *zip1 H3-K79A* mutants resemble *dot1* in the impaired Hop1 chromosomal distribution (Figure 6A and 6C; Figure S5) and checkpoint-induced phosphorylation (Figure 6E; Figure S4).

Thus, taken together, our results indicate that, upon meiotic recombination checkpoint triggering, Dot1-dependent H3K79 methylation promotes proper chromosomal localization and activation of Hop1, which in turn, is required to sustain Mek1 autophosphorylation and the ensuing checkpoint response.

H3K79me partially controls Hop1 chromosomal localization via Pch2

Previous studies have shown that whereas in the *zip1* mutant the Pch2 meiotic checkpoint protein is detected only in the nucleolar (rDNA) region, in the *zip1 dot1* double mutant Pch2 is distributed throughout all chromatin [26]. To confirm that the regulation of Pch2 localization by Dot1 depends on the histone H3 methyltransferase activity, we analyzed Pch2 distribution on spread meiotic chromosomes of the *zip1 H3-K79R* and *zip1 H3-K79A* mutants. Although global Pch2 protein levels remained fairly invariable in the different mutants (Figure S4), we found that, like in *zip1 dot1*, Pch2 mislocalized to chromatin outside the rDNA in *zip1 H3-K79R* and *zip1 H3-K79A* strains (Figure 7A), suggesting that H3K79me excludes Pch2 from chromosomes.

Several lines of evidence support a role for Pch2 in promoting the turnover of Hop1 from meiotic chromosomes, at least in unperturbed meiosis [29,39,40]; therefore, it was possible that the reduced localization of Hop1 in the absence of Dot1 could stem from the action of the Pch2 protein aberrantly present at chromosomal locations removing Hop1 from *zip1* chromosomes. To investigate this possibility, we monitored Hop1 localization in *zip1 dot1 pch2* strains. Interestingly, we found that deletion of *PCH2*

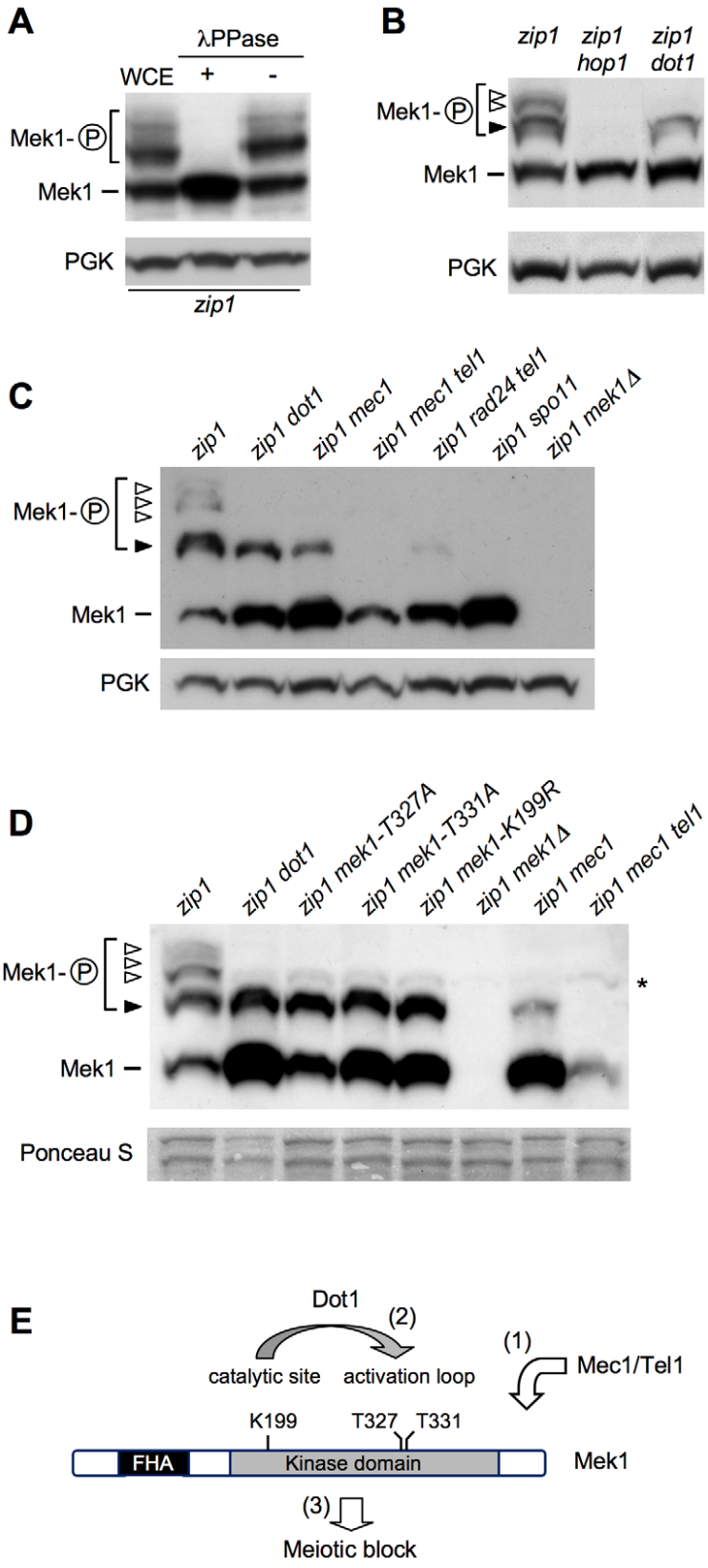

Figure 3. Dot1 contributes to Mek1 activation by autophosphorylation. (A) Whole cell extracts (WCE) from a *zip1 ndt80* culture at 24 h in meiosis were incubated in the presence (+) or absence (−) of lambda phosphatase (λPPase). (B), (C) and (D) Detection of different phosphorylated forms of Mek1 in *ndt80*-arrested cells after 24 h in meiosis using high-resolution Phos-tag gels. Basal Mek1 (line) and several phosphorylated forms (black and white arrowheads) are indicated; see text for explanation. PGK or Ponceau S staining were used as loading controls. Asterisk in (D) marks a weak non-specific band. (E) Schematic representation of a model for the sequential phosphorylation events leading to Mek1 activation and the relevant mutations analyzed above. (1) Priming phosphorylation by Mec1/Tel1 (black arrowhead in B, C, D) is followed by (2) autophosphorylation of

Mek1 (white arrowheads in B, C, D) leading to its full activation and (3) the checkpoint response. H3K79 methylation by Dot1 contributes to Mek1 autophosphorylation. Strains were: (A); DP428 (*zip1*). (B); DP428 (*zip1*), DP701 (*zip1 hop1*) and DP655 (*zip1 dot1*). (C); DP428 (*zip1*), DP655 (*zip1 dot1*), DP680 (*zip1 mec1*), DP861 (*zip1 mec1 tel1*), DP877 (*zip1 rad24 tel1*), DP728 (*zip1 spo11*) and DP674 (*zip1 mek1Δ*). (D); DP885 (*zip1*), DP890 (*zip1 dot1*), DP886 (*zip1 mek1-T327A*), DP887 (*zip1 mek1-T331A*), DP888 (*zip1 mek1-K199R*), DP674 (*zip1 mek1Δ*), DP680 (*zip1 mec1*) and DP861 (*zip1 mec1 tel1*).
doi:10.1371/journal.pgen.1003262.g003

alleviated to some extent the defective Hop1 localization pattern of *zip1 dot1*, although it did not fully restore the high and continuous Hop1 levels present in *zip1* (Figure 7B–7D). To determine whether the increased abundance of Hop1 along chromosomes in *zip1 dot1 pch2* restores the checkpoint-induced delay we analyzed meiotic divisions and Mek1 phosphorylation (Figure 7E–7F). We found that the checkpoint was still impaired in the *zip1 dot1 pch2* triple mutant because, like the *zip1 dot1* and the *zip1 pch2* double mutants, it displayed wild-type kinetics of meiotic progression (Figure 7E) and defective Mek1 activation (Figure 7F), implying a more complex contribution of Pch2's function to the pachytene checkpoint response (see Discussion).

In summary, these observations indicate that in the *zip1* mutant, methylation of H3K79 by Dot1 controls proper chromosomal distribution of Hop1 by maintaining Pch2 confined in the nucleolar region. The fact that Hop1 localization is still partially impaired in the *zip1 dot1 pch2* triple mutant suggests that Dot1 may also regulate Hop1 chromosomal recruitment by a Pch2-independent mechanism (Figure 8).

Discussion

Previous studies have shown that Dot1 is important for the pachytene checkpoint, but the molecular mechanism underlying such function remained unclear. Here, we provide evidence that methylation of H3K79 by Dot1 contributes to the meiotic recombination checkpoint response by enabling proper Hop1 chromosomal recruitment, which, in turn is a requisite for Mek1 activation by autophosphorylation.

We demonstrate that the function of Dot1 in the meiotic recombination checkpoint specifically relies on the methylation of H3K79, since the non-methylatable *H3-K79A* and *H3-K79R* mutations confer essentially the same meiotic phenotypes as the lack of Dot1. Moreover, by modulating Dot1 catalytic activity, we found that high levels of the H3K79-me3 are required for full checkpoint activation raising the possibility that this methylation state is particularly critical for promoting the proper localization of the Hop1 meiotic checkpoint adaptor (see below).

In mitotic cells, methylated histones are well-known chromatin marks for recognition of DSBs by checkpoint adaptors. In *S. cerevisiae*, the Rad9 adaptor is recruited to DSB sites by H3K79me [41,42], whereas in *S. pombe*, which lacks H3K79me, the recruitment of the Crb2 adaptor relies on H4K20me [43]. In mammalian cells, the Rad9 and Crb2 homolog 53BP1 appears to recognize both H3K79me and H4K20me [44–46]. All these DNA damage checkpoint adaptors (Rad9, Crb2 and 53BP1) contain tandem tudor domains that mediate the interaction with the methylated histones. Rad9, Crb2 and 53BP1 also possess BRCT motifs; in fact, the recognition of DSBs by Rad9 and Crb2 in *S. cerevisiae* and *S. pombe*, respectively, is also mediated by their binding to phosphorylated histone H2A (hereafter γH2AX) via the BRCT domains [47,48]. However, the Hop1 meiotic checkpoint adaptor lacks either tudor or BRCT motifs and contains a HORMA domain likely involved in protein-protein interactions [49], raising the possibility that its chromosomal recruitment can be mediated by different mechanisms.

As mentioned before, in DNA damaged vegetative cells, Rad9 function depends both on H3K79me and γH2AX [47,50–52]; however, the relevance of both histone modifications appears to be different in meiotic cells. Dot1-dependent H3K79me is crucial for checkpoint function, at least in Zip1-deficient cells, because deletion of *DOT1* (or mutation of H3K79) results in complete bypass of the *zip1* meiotic block. In contrast, an *H2A-S129** mutant, lacking the four C-terminal amino acids of histone H2A including the SQ phosphorylation site [53], has no defect in the *zip1*-induced checkpoint (Figure S6A). Moreover, like in both single mutants, meiotic progression and spore viability are essentially normal in the *dot1 H2A-S129** double mutant (Figure S6A, S6B).

We show here that Dot1 is required for Mek1 and Hop1 activation in meiotically-challenged cells, but in addition to the checkpoint function, Mek1 and Hop1 promote the repair of meiotic DSBs by Dmc1-dependent interhomolog recombination [34,37,38,54]. Consistent with this function, in the absence of Dmc1, Dot1 prevents the repair of DSBs by Rad54-dependent sister-chromatid recombination, which is controlled, at least in part, by inhibitory phosphorylation of Rad54 by Mek1 [26,54]. In principle, it could be possible that impaired Hop1/Mek1 function in the absence of Dot1 could induce an alternative intersister recombination pathway resulting in meiotic progression because of the disappearance of the meiotic defects initially triggering the checkpoint. However, deletion of *DOT1* alleviates the meiotic arrest of *zip1 rad54* and *dmc1 rad54* mutants, where intersister repair is impaired, strongly suggesting that Dot1 performs a bona-fide meiotic checkpoint function [26]. The fact that, unlike Mek1 and Hop1, the Dot1 protein is dispensable in otherwise unperturbed meiosis implies the H3K79me is mostly relevant to signal defects when meiotic chromosome metabolism is disturbed (i.e., *zip1* or *dmc1* mutants). Consistent with this notion, Hop1 localization on *zip1* chromosomes is dramatically altered in the absence of Dot1, but it is only slightly reduced in the *dot1* single mutant as compared with the wild type (Figure 7C and 7D).

In other studies, activation of the Mek1 effector meiotic kinase has been monitored either by a slight electrophoretic mobility shift [32,34] or by using an anti-phospho-Ser/Thr Akt substrate antibody, which specifically recognizes phosphorylation of Mek1 at T327 [33,37,55]. However, those assays do not permit one to delineate the different events contributing to Mek1 activation. Here, by using high-resolution Phos-tag gels, we identify several phosphorylated Mek1 forms and dissect the genetic requirements for sequential Mek1 activation. Our findings support a model (Figure 3E; Figure 8) in which the presence of unrepaired DSBs and/or unsynapsed chromosomes results in the initial phosphorylation of Mek1 by the redundant action of Mec1/Tel1. This priming phosphorylation is followed by autophosphorylation of Mek1 at T327 and T331 leading to full Mek1 activation supporting the checkpoint response. We found that Dot1 is chiefly required for this last step, which is mediated by Mek1 dimerization promoted by the Hop1 C-terminal domain [38]. Thus, the altered localization of Hop1 on *zip1 dot1* chromosomes likely explains the defect in Mek1 autophosphorylation. Interestingly, GST-mediated forced dimerization of Mek1 bypasses Dot1 requirement for its activation; however, this activation is only transient in the absence of Dot1, suggesting that proper chromosome axis architecture is required for maintenance of Mek1 activity.

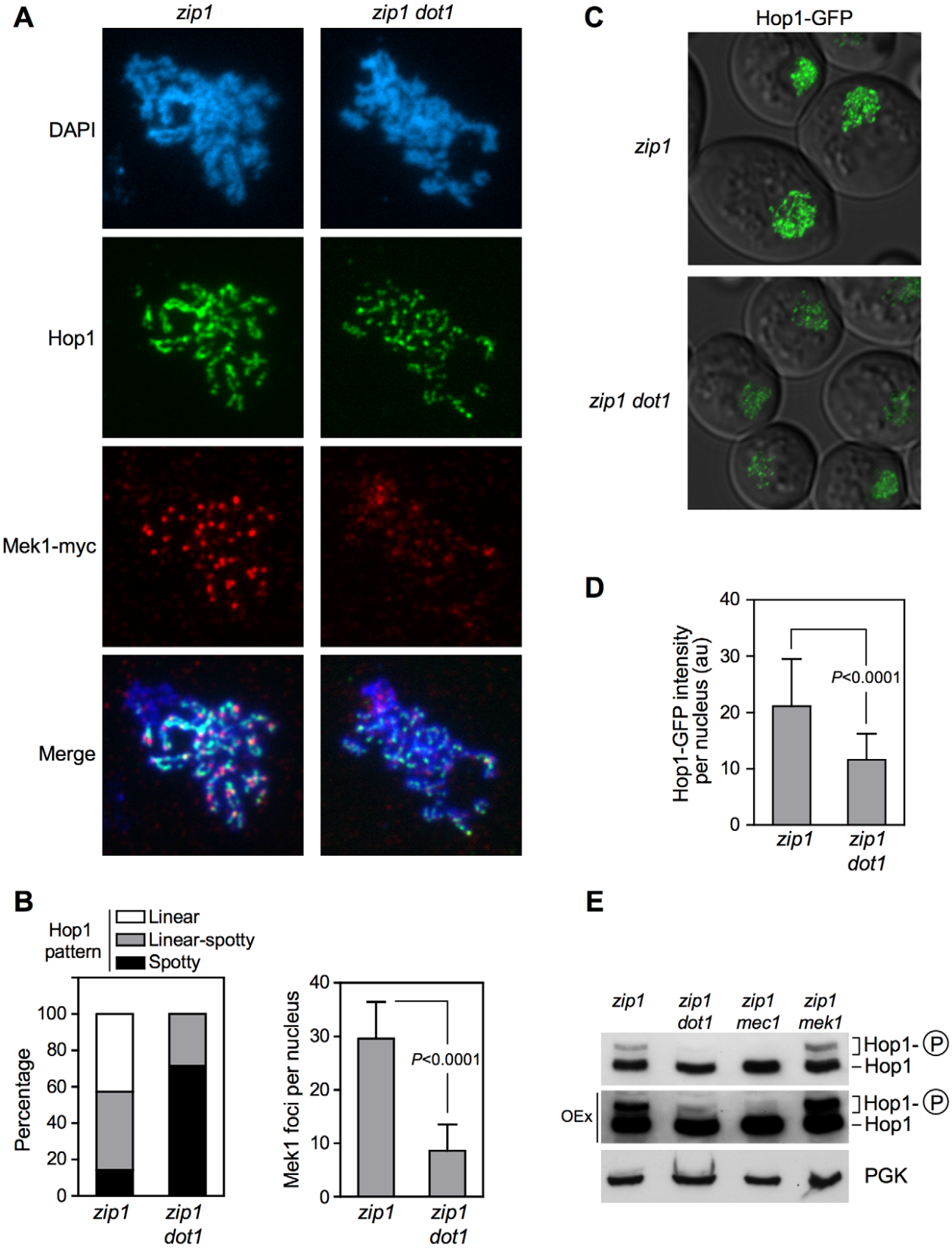

Figure 4. Dot1 is required for *zip1*-induced localization and activation of the Hop1 meiotic checkpoint adaptor. (A) Immunofluorescence of meiotic chromosome spreads stained with DAPI (blue), anti-Hop1 (green) and anti-myc (red) antibodies. Representative nuclei are shown. The same exposure time was used to capture the signal from the different strains. Spreads were prepared 24 h after meiotic induction of *ndt80* cells. Strains are: DP848 (*zip1*) and DP849 (*zip1 dot1*). (B) Quantification of the Hop1 staining pattern (left) and the number of Mek1 foci (right) on spread chromosomes analyzed as in (A). 14 and 21 nuclei were scored for *zip1* and *zip1 dot1*, respectively. (C) Representative images of

ndt80-arrested cells expressing *HOP1-GFP* in *zip1* (DP964) and *zip1 dot1* (DP965) captured after 24 h in meiosis. (D) Quantification of the Hop1-GFP signal intensity on fluorescence images (a.u., arbitrary units). 300 individual nuclei were analyzed for each strain. (E) Dot1 is required for Hop1 phosphorylation. Western blot analysis of Hop1 in cell extracts obtained 24 h after meiotic induction in *ndt80* cells. The middle panel corresponds to an overexposure (OEx) of the blot shown in the upper panel. PGK was used as a loading control. Strains are: DP428 (*zip1*), DP655 (*zip1 dot1*), DP680 (*zip1 mec1*) and DP674 (*zip1 mek1*). Means, standard deviations and *P*-values are shown in (B) and (D).
doi:10.1371/journal.pgen.1003262.g004

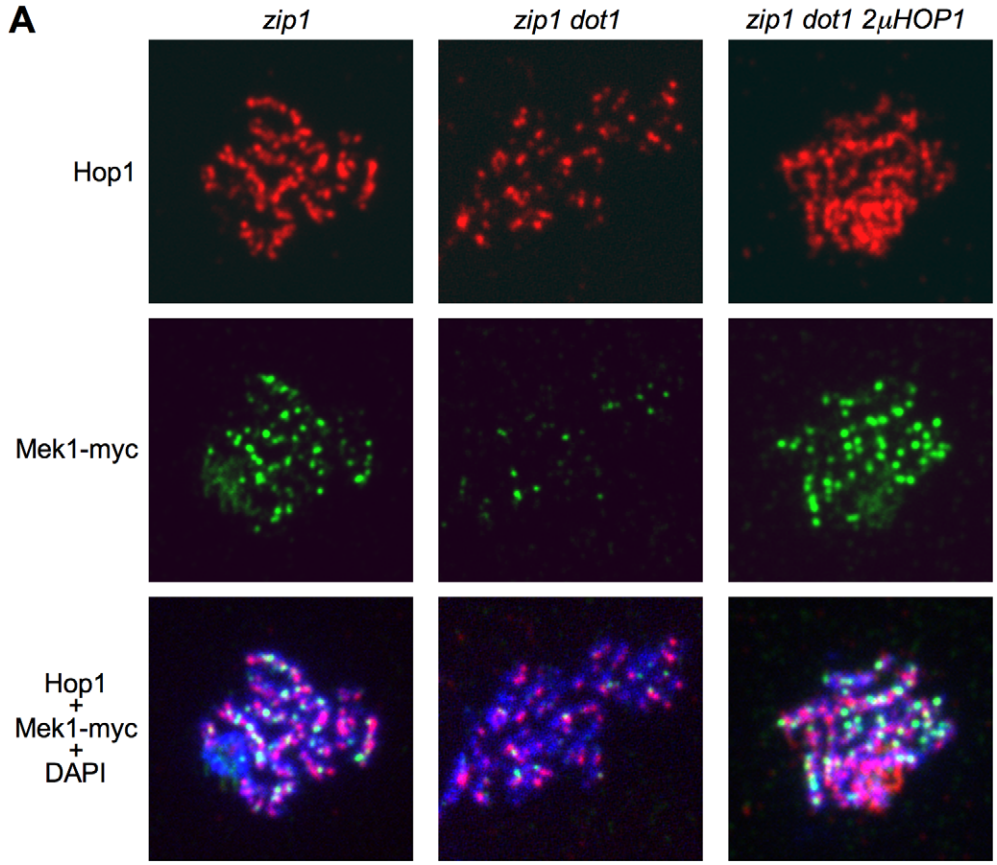

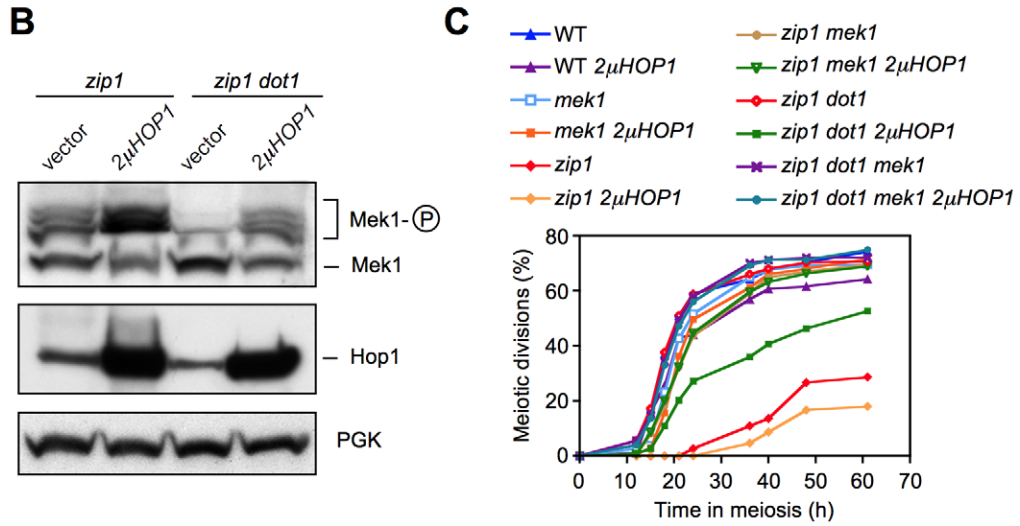

Figure 5. Hop1 overproduction restores Mek1 function in the absence of Dot1. (A) Immunofluorescence of meiotic chromosome spreads stained with DAPI (blue), anti-Hop1 (red) and anti-myc (green) antibodies. Spreads were prepared 24 h after meiotic induction of *ndt80* cells. Strains are: DP848 (*zip1*) and DP884 (*zip1 dot1*) transformed either with empty vector or with a *HOP1* high-copy plasmid (*2μHOP1*). (B) Western blot analysis of Mek1 phosphorylation and Hop1 production in *ndt80* cells after 24 h in meiosis. PGK was a loading control. Strains are DP428 (*zip1*) and DP655 (*zip1 dot1*) transformed either with empty vector or with *2μHOP1*. (C) Time course of meiotic nuclear divisions; the percentage of cells containing more than two nuclei is represented. Strains are DP421 (wild type), DP713 (*mek1*), DP422 (*zip1*), DP714 (*zip1 mek1*), DP555 (*zip1 dot1*) and DP716 (*zip1 dot1 mek1*), transformed either with empty vector or with *2μHOP1*.
doi:10.1371/journal.pgen.1003262.g005

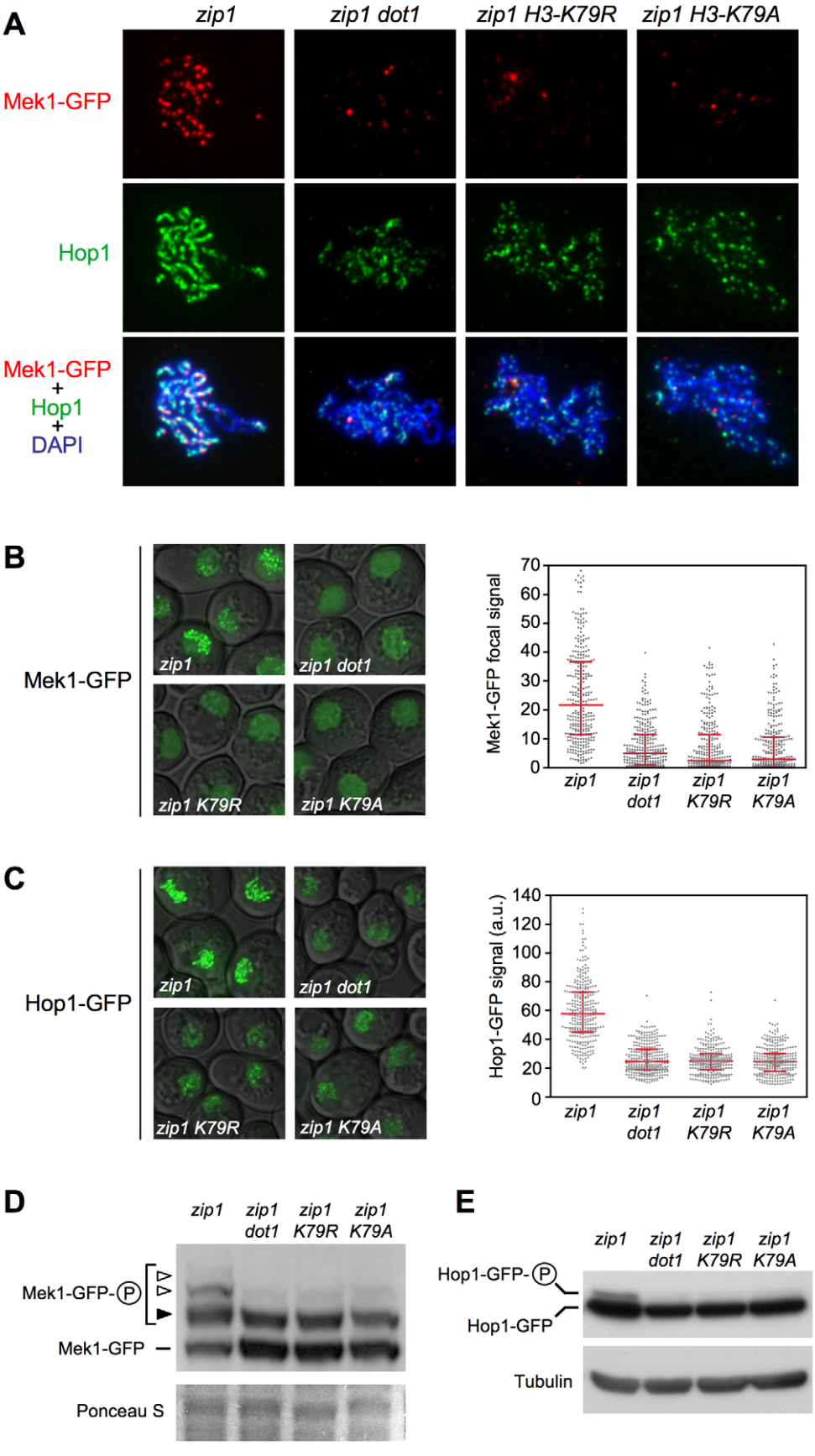
A
zip1
zip1 dot1
zip1 H3-K79R
zip1 H3-K79A
Mek1-GFP
Hop1
Mek1-GFP + Hop1 + DAPI
B
Mek1-GFP
zip1
zip1 dot1
zip1 K79R
zip1 K79A
Mek1-GFP focal signal
70
60
50
40
30
20
10
0
zip1
zip1 dot1
zip1 K79R
zip1 K79A
C
Hop1-GFP
zip1
zip1 dot1
zip1 K79R
zip1 K79A
Hop1-GFP signal (a.u.)
140
120
100
80
60
40
20
0
zip1
zip1 dot1
zip1 K79R
zip1 K79A
D
zip1
zip1 dot1
zip1 K79R
zip1 K79A
Mek1-GFP-P
Mek1-GFP
Ponceau S
E
zip1
zip1 dot1
zip1 K79R
zip1 K79A
Hop1-GFP-P
Hop1-GFP
Tubulin

Figure 6. The *H3-K79R* and *H3-K79A* mutations recapitulate *dot1* defects in checkpoint-induced Mek1 and Hop1 phosphorylation and localization. (A) Immunofluorescence of meiotic chromosome spreads stained with DAPI (blue), anti-Hop1 (green) and anti-GFP (red) antibodies. Representative nuclei are shown. The same exposure time was used to capture the signal from the different strains. (B) and (C) Representative images of meiotic cells expressing *MEK1-GFP* and *HOP1-GFP*, respectively. The scattered plots represent the quantification of the Mek1-GFP focal signal (B) and total Hop1-GFP signal intensity (C) on fluorescence images (a.u., arbitrary units). Error bars represent the median with interquartile range. 300 individual nuclei were analyzed for each strain. (D) Western blot analysis of *zip1*-induced Mek1-GFP phosphorylation in a Phos-tag gel using anti-Mek1 antibodies. The basal Mek1-GFP form (line), and the forms resulting from Mec1/Tel1-dependent phosphorylation (black arrowhead) and autophosphorylation (white arrowheads) are indicated. Ponceau S staining of the membrane is shown as a loading control. (E) Western blot analysis of *zip1*-induced Hop1-GFP phosphorylation using anti-GFP antibodies. Tubulin is shown as a loading control. Strains in (A), (B) and (D) are: DP1046 (*zip1*), DP1049 (*zip1 dot1*), DP1048 (*zip1 H3-K79R*) and DP1047 (*zip1 H3-K79A*). Strains in (C) and (E) are: DP1042 (*zip1*), DP1045 (*zip1 dot1*), DP1044 (*zip1 H3-K79R*) and DP1043 (*zip1 H3-K79A*). In all cases (A–E), spreads were made, GFP images were captured and cell extracts were prepared after 24 h of meiotic induction in *ndt80* strains.
doi:10.1371/journal.pgen.1003262.g006

We found that global levels of H3K79me do not significantly change in response to the meiotic defects of the *zip1* mutant, but this methylation is critical for the checkpoint response. The nature of the signal that triggers the meiotic checkpoint in *zip1* is still unclear. Like in mammals [56], the existence of a synapsis checkpoint in yeast has also been proposed [7,55,58]. Nevertheless, Dot1 is also required for the meiotic cell cycle arrest of the *dmc1* mutant that accumulates unrepaired DSBs [26], indicating that H3K79me is also involved in the response to meiotic DSBs. It has been reported that, under certain conditions, DSBs are efficiently repaired in *zip1* mutants [37] implying that the signal triggering the checkpoint could be different. However, Ddc2 foci marking the presence of recombination intermediates are detected in *zip1* [11] (Figure 2A), consistent with at least some DSBs remaining unrepaired in *zip1* mutants [57,59,60] sufficient to induce the checkpoint. Alternatively, or in addition, Mec1-Ddc2 may also sense defects in structural aspects of interhomolog interactions resulting from the lack of the central region of the SC [39]. In any case, independently of the nature of the signal triggering the meiotic checkpoint response(s), the question of how a constitutive histone mark, such as H3K79me, contributes to Hop1-mediated Mek1 activation specifically in challenged meiosis remains to be elucidated. In the DNA damage response in vegetative yeast cells or somatic mammalian cells it has been proposed, though never proven, that chromatin remodeling in the vicinity of DNA lesions may locally expose constitutive marks (i.e., H3K79me, H4K20me) supporting the recruitment of DNA damage checkpoint adaptors to activate the checkpoint [44,45]. In meiotic cells, the DSB metabolism is linked to the special architecture of the chromosome axis [61]. Therefore, we envision that unrepaired DSBs and/or defects in interhomolog connections may provoke chromatin conformational changes unmasking H3K79me capable to drive proper Hop1 distribution along the axes, enabling its activation by Mec1 to elicit the downstream checkpoint events including Mek1 full activation by autophosphorylation (Figure 8).

Although it is formally possible that H3K79me may directly facilitate Hop1 recruitment to some extent, we provide evidence indicating that the control of Hop1 chromosomal distribution by H3K79me is substantially driven by regulation of the Pch2 protein. Pch2 was initially discovered as a meiotic checkpoint protein required for the *zip1*-induced meiotic arrest [29], but more recent studies have shown that Pch2 impacts multiple aspects of meiotic chromosome dynamics [55,62–64]. In particular, Pch2 acts as a negative regulator of Hop1 chromosomal abundance [39,40]. In wild-type pachytene chromosomes, Pch2 localizes to the unsynapsed rDNA region (nucleolus) and also along synapsed chromosomes [29,40]. In contrast, Pch2 is solely detectable at the nucleolar region in the *zip1* mutant [29]; remarkably, in the absence of H3K79me, Pch2 is redistributed throughout all chromatin of *zip1* nuclei (Figure 7A). We hypothesize that, as a consequence of the synapsis defects of *zip1*, the H3K79me mark becomes exposed functioning as an anti-binding signal for Pch2, thus permitting the extensive Hop1 distribution found on *zip1* chromosomes (Figure 8). In the absence of Dot1 (or H3K79me), the presence of chromosomal Pch2 triggers the removal of Hop1 and the consequent defect in Mek1 activation. The reduced global levels of Hop1 detected in *zip1 dot1* (Figure S3 and Figure 6E) are also consistent with a higher protein turnover.

Interestingly, like in *zip1 dot1*, the synapsis checkpoint is still completely defective in the *zip1 dot1 pch2* triple mutant, despite the partial restoration of Hop1 localization. Since the excess of Hop1 induced by other means, such as *HOP1* overexpression, but in the presence of Pch2, does confer a meiotic delay in *zip1 dot1* and restores Mek1 phosphorylation (Figure 5), it is conceivable that nucleolar Pch2 performs an additional downstream function in Mek1 activation (Figure 8) and/or that the excess of Hop1 in the absence of Pch2 is not correctly assembled on chromosome axes to support checkpoint activation. In fact, the *zip1 pch2* mutant itself is also checkpoint deficient. Future studies will address these intriguing possibilities.

Dot1/DOT1L is structurally conserved throughout evolution from budding yeast to worms, flies, mice and humans; therefore, it is possible that members of the Dot1 family play similar roles in Metazoa. DOT1L is essential in mammals [65] functioning in embryogenesis, hematopoiesis and cardiac development [27]; however, much less is known about the impact of mammalian DOT1L in the DNA damage response. It would be interesting to determine whether, like the yeast counterpart, Dot1 orthologs are involved in meiotic checkpoint control in higher eukaryotes.

Materials and Methods

Yeast strains and plasmids

Yeast strains genotypes are listed in Table 1. All the strains are in the BR1919 background [66]. Gene deletions were made using a PCR-based approach [67,68] except for *dot1::URA3*, *zip1::LYS2* and *ndt80::LEU2*, which were previously described [19,26,29]. *MEK1-13myc*, *MEK1-GFP* and *HOP1-GFP* were made by a PCR approach [68]. The C-terminally tagged Mek1-13myc and Mek1-GFP proteins are functional because spore viability of homozygous tagged wild-type diploids was similar to that of untagged strains and, in addition, they supported the checkpoint-induced delay of a *hop2* mutant. In *zip1 HOP1-GFP* strains the meiotic block was less tight, but Hop1-GFP displayed a localization pattern indistinguishable from that of the untagged protein (Figure S5); therefore, we used the native GFP fluorescence for quantitation of Hop1 localization. N-terminal tagging of Pch2 with three copies of the HA epitope has been previously described [29]. Strains carrying *DOT1* or *dot1-G401A* at its genomic locus or in the pRS315 vector (plasmids pRS315-DOT1 and pFvL54, respectively) were described [28,31]. The *H3-K79A* and *H3-K79R* strains are deleted

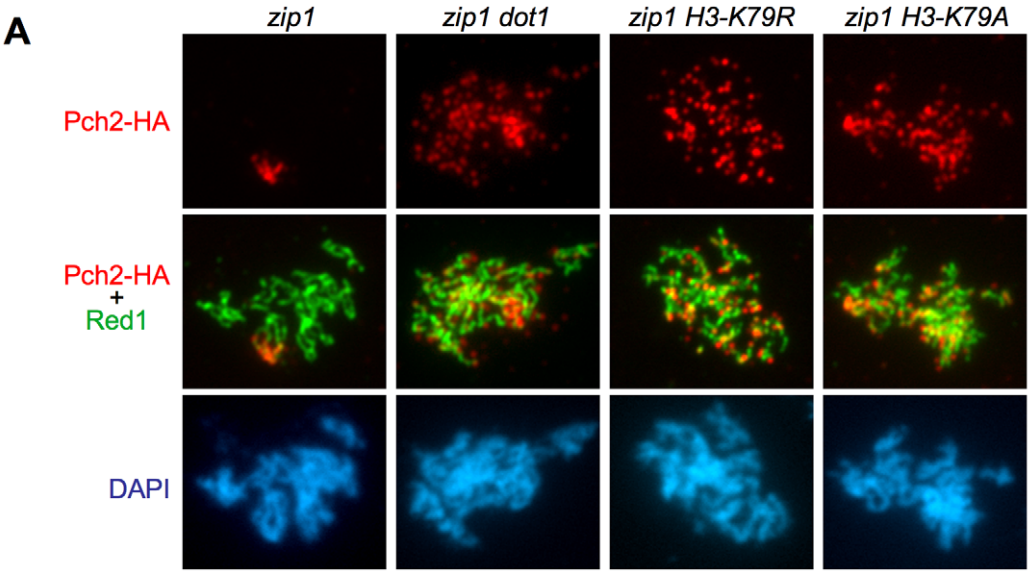
A
zip1
zip1 dot1
zip1 H3-K79R
zip1 H3-K79A
Pch2-HA
Pch2-HA + Red1
DAPI

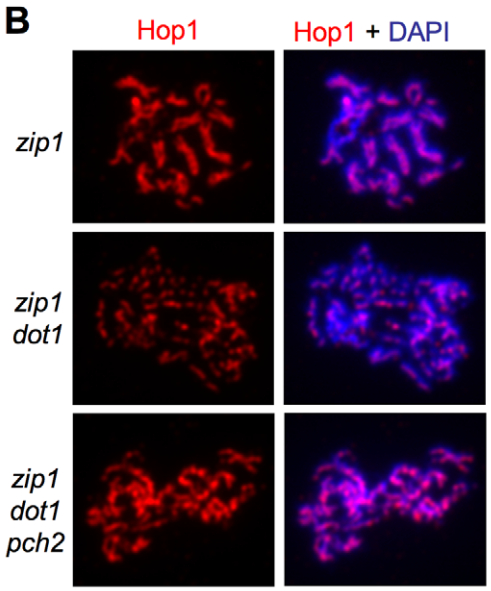
B
Hop1
Hop1 + DAPI
zip1
zip1 dot1
zip1 dot1 pch2

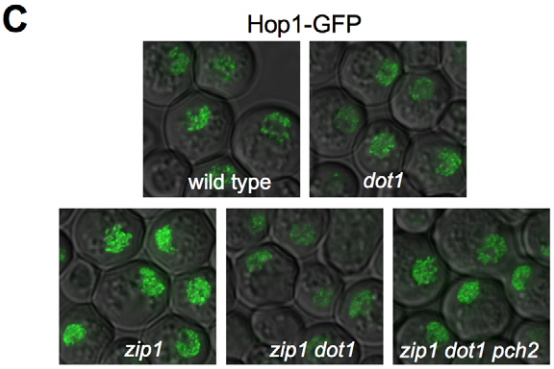
C
Hop1-GFP
wild type
dot1
zip1
zip1 dot1
zip1 dot1 pch2

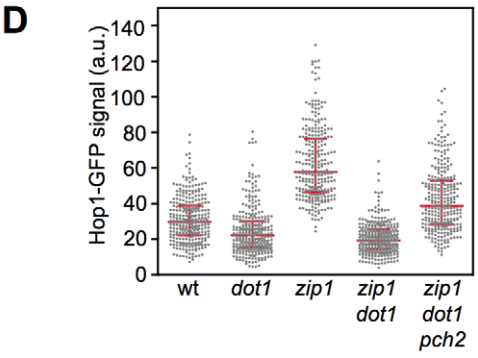
D
Hop1-GFP signal (a.u.)
0
20
40
60
80
100
120
140
wt
dot1
zip1
zip1 dot1
zip1 dot1 pch2

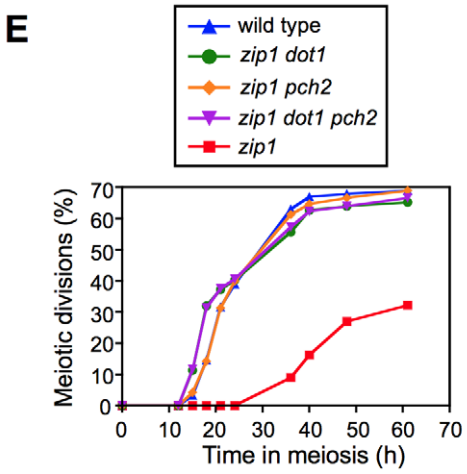
E
wild type
zip1 dot1
zip1 pch2
zip1 dot1 pch2
zip1
Meiotic divisions (%)
0
10
20
30
40
50
60
70
Time in meiosis (h)

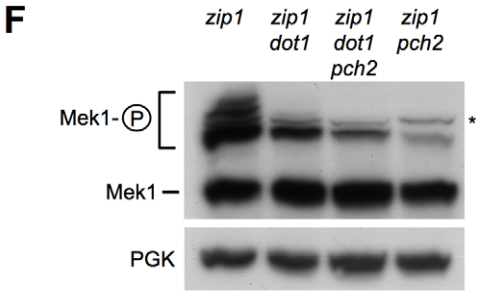
F
zip1
zip1 dot1
zip1 dot1 pch2
zip1 pch2
Mek1-P
Mek1
PGK
*

Figure 7. H3K79me controls Hop1 localization by excluding Pch2 from chromosomes. (A) H3K79me is required to prevent Pch2 localization outside of the rDNA. Immunofluorescence of meiotic chromosome spreads stained with DAPI (blue), anti-HA (red) and anti-Red1 (green) antibodies. Strains are: DP1050 (*zip1*), DP1053 (*zip1 dot1*), DP1052 (*zip1 H3-K79R*) and DP1051 (*zip1 H3-K79A*). (B–D) The absence of Pch2 partially restores Hop1 chromosomal abundance in *zip1 dot1*. (B) Immunofluorescence of meiotic chromosome spreads stained with DAPI (blue) and anti-Hop1 antibody (red). Strains are: DP428 (*zip1*), DP655 (*zip1 dot1*) and DP1054 (*zip1 dot1 pch2*). (C) Representative images of cells expressing *HOP1-GFP* in wild type (DP963), *dot1* (DP966), *zip1* (DP964), *zip1 dot1* (DP965) and *zip1 dot1 pch2* (DP1027). (D) Quantification of the Hop1-GFP signal intensity on fluorescence images (a.u., arbitrary units). 300 individual nuclei were analyzed for each strain. Each spot in the plot represents the fluorescence intensity of every nucleus measured. Error bars represent the median with interquartile range. $P<0.01$ in pairwise comparisons. In all cases (A–C), spreads were prepared and GFP images were taken 24 h after meiotic induction in *ndt80* strains. (E, F) The absence of Pch2 does not restore the pachytene checkpoint response in *zip1 dot1*. (E) Time course of meiotic nuclear divisions; the percentage of cells containing more than two nuclei is represented. Strains are: DP421 (wild type), DP422 (*zip1*), DP555 (*zip1 dot1*), DP1029 (*zip1 pch2*) and DP1041 (*zip1 dot1 pch2*). (F) Western blot analysis of *zip1*-induced Mek1 phosphorylation in *ndt80* strains. PGK was used as a loading control. The asterisk marks a presumed non-specific band (see Figure 3D). Strains are: DP428 (*zip1*), DP655 (*zip1 dot1*), DP881 (*zip1 pch2*) and DP1054 (*zip1 dot1 pch2*).
doi:10.1371/journal.pgen.1003262.g007

for all genomic copies of the histone H3-H4 encoding genes (*HHT1-HHF1 and HHT2-HHF2*) and express different versions of H3 from centromeric plasmids carrying either the *hht2(K79A)-HHF2* or *hht2(K79R)-HHF2* mutant genes (pFvL87 and pFvL88, respectively). The *mek1-T327A*, *mek1-T331A*, *mek1-K199R* mutations, as well as the *GST-MEK1* construct were introduced as described [33], using plasmids kindly provided by N. Hollingsworth (Stony Brook University, NY). The high-copy *HOP1* plasmid was also described [69]. Strains harboring the *hta1-S129** and *hta2-S129** mutations lacking the last four amino acids of the C-terminal tail of histone H2A including the serine 129 phosphorylated by Mec1/Tel1 [53] were made using plasmids pJHA16 and pJHA17 (provided by J. Downs, University of Sussex) following a pop-in/pop-out strategy. For meiotic time courses, strains were grown in 2×SC (3.5 ml) for 20–24 hours, then transferred to YPDA (2.5 ml) and incubated to saturation for additional 8 hours. Cells were harvested, washed with 2% potassium acetate (KAc), resuspended into 2% KAc (10 ml) and incubated at 30°C with vigorous shaking to induce meiosis and sporulation. Both YPDA and 2% KAc were supplemented with 20 mM adenine and 10 mM uracil. The culture volumes were scaled-up when needed.

Western blotting and analysis of Mek1 phosphorylation

TCA cell extracts from 5–10 ml of sporulating cultures were processed as described [14]. To resolve the phosphorylated forms of Mek1 or Mek1-GFP, 10% or 7% gels (acrylamide:bisacrylamide 29:1), respectively, containing 37.5 µM Phos-tag (Wako Chemicals) and 75 µM $MnCl_2$ were used. Gels were run on ice at 100 volts in a MiniProtean3 (Bio-Rad) for 3 h. After running, gels were washed with 1 mM EDTA before transfer to PVDF membranes.

For dephosphorylation assays, total TCA cell extracts solubilized in Laemmli buffer were diluted 10 times with phosphatase buffer supplemented with 1 mM $MnCl_2$. Diluted extracts were treated with 2000 units of lambda phosphatase (New England Biolabs) for 30 min at 30°C. As control, a similar aliquot of the diluted extract was incubated under the same conditions but without adding phosphatase. Samples were re-precipitated with 20% TCA, washed with acetone, boiled in Laemmli buffer and loaded in Phostag gels.

The following antibodies were used: rabbit polyclonal anti-Mek1 (1:1000 dilution) [11] and anti-Dot1 (1:2000 dilution) [31]. Rabbit polyclonal anti-H3K79-me1 (ab2886; 1:1000 dilution), anti-H3K79-me2 (ab3594; 1:2000 dilution), anti-H3K79-me3

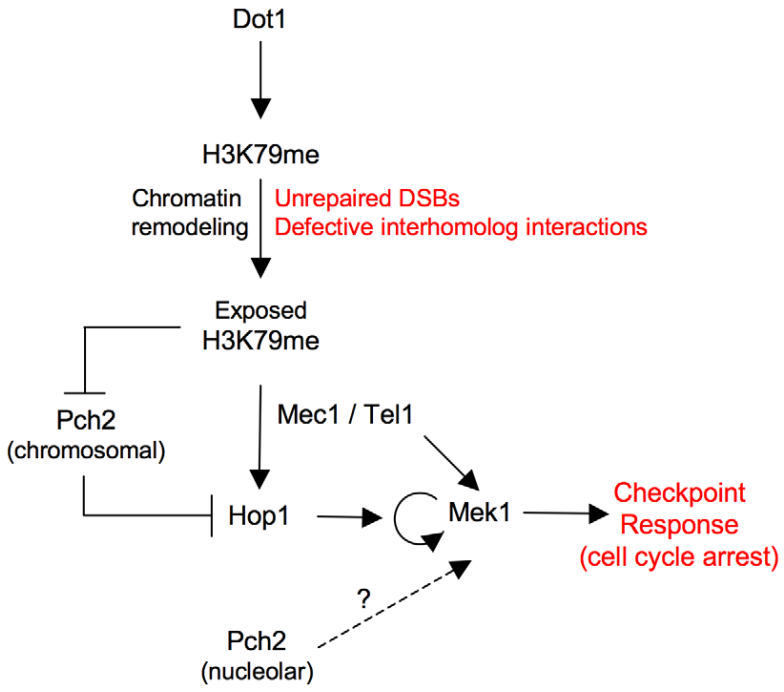

Figure 8. Model for Dot1 function in the meiotic recombination checkpoint. See text for details.
doi:10.1371/journal.pgen.1003262.g008

Table 1. *Saccharomyces cerevisiae* strains.

Strain	Genotype*
BR1919-2N	*MAT***a**/*MATα leu2-3,112 his4-260 ura3-1 ade2-1 thr1-4 trp1-289*
DP409	BR1919-2N *zip1::LEU2*
DP419	BR1919-2N *hta1-S129* hta2-S129**
DP420	BR1919-2N *hta1-S129* hta2-S129* zip1::LEU2*
DP421	BR1919-2N *lys2ΔNheI*
DP422	DP421 *zip1::LYS2*
DP424	DP421 *ndt80::LEU2*
DP428	DP421 *zip1::LYS2 ndt80::LEU2*
DP460	DP421 *zip1::LYS2 ndt80::LEU2 DDC2-GFP::TRP1*
DP555	DP421 *zip1::LYS2 dot1::kanMX6*
DP556	DP421 *zip1::LYS2 dot1::kanMX6::DOT1::URA3*
DP560	DP421 *zip1::LYS2 dot1::kanMX6::dot1-G401A::URA3*
DP579	DP421 *zip1::LYS2 ndt80::LEU2 dot1::URA3 DDC2-GFP::TRP1*
DP582	DP421 *zip1::LYS2 ndt80::LEU2 MEK1-GFP::kanMX6*
DP583	DP421 *zip1::LYS2 ndt80::LEU2 MEK1-GFP::kanMX6 dot1::URA3*
DP622	BR1919-2N *hta1-S129* hta2-S129* dot1::kanMX6*
DP623	BR1919-2N *hta1-S129* hta2-S129* dot1::kanMX6 zip1::LEU2*
DP624	DP421 *dot1::URA3*
DP625	DP421 *dot1::kanMX6*
DP655	DP421 *zip1::LYS2 ndt80::LEU2 dot1::kanMX6*
DP674	DP421 *zip1::LYS2 ndt80::LEU2 mek1::kanMX6*
DP680	DP421 *zip1::LYS2 ndt80::LEU2 sml1::kanMX6 mec1::KlURA3*
DP701	DP421 *zip1::LYS2 ndt80::LEU2 hop1::hphMX4*
DP713	DP421 *mek1::kanMX6*
DP714	DP421 *zip1::LYS2 mek1::kanMX6*
DP716	DP421 *zip1::LYS2 mek1::kanMX6 dot1::hphMX4*
DP728	BR1919-2N *zip1::kanMX6 ndt80::LEU2 spo11::hphMX4*
DP783	DP421 *zip1::LYS2 mek1::kanMX6 dot1::hphMX4 GST-mek1-K199R::URA3*
DP784	DP421 *zip1::LYS2 mek1::kanMX6 dot1::hphMX4 GST-mek1-T327A::URA3*
DP785	DP421 *zip1::LYS2 mek1::kanMX6 dot1::hphMX4 GST-MEK1::URA3*
DP790	DP421 *zip1::LYS2 mek1::kanMX6 GST-mek1-K199R::URA3*
DP791	DP421 *zip1::LYS2 mek1::kanMX6 GST-mek1-T327A::URA3*
DP792	DP421 *zip1::LYS2 mek1::kanMX6 GST-MEK1::URA3*
DP806	DP421 (*hht1-hhf1)::kanMX6 (hht2-hhf2)::natMX4 p[HHT2-HHF2]::TRP1*
DP807	DP421 (*hht1-hhf1)::kanMX6 (hht2-hhf2)::natMX4 p[hht2-K79A-HHF2]::TRP1*
DP808	DP421 (*hht1-hhf1)::kanMX6 (hht2-hhf2)::natMX4 p[hht2-K79R-HHF2]::TRP1*
DP809	DP421 (*hht1-hhf1)::kanMX6 (hht2-hhf2)::natMX4 p[HHT2-HHF2]::TRP1 zip1::LYS2*
DP810	DP421 (*hht1-hhf1)::kanMX6 (hht2-hhf2)::natMX4 p[hht2-K79A-HHF2]::TRP1 zip1::LYS2*
DP811	DP421 (*hht1-hhf1)::kanMX6 (hht2-hhf2)::natMX4 p[hht2-K79R-HHF2]::TRP1 zip1::LYS2*
DP812	DP421 (*hht1-hhf1)::kanMX6 (hht2-hhf2)::natMX4 p[HHT2-HHF2]::TRP1 zip1::LYS2 dot1:hphMX4*
DP848	DP421 *zip1::LYS2 ndt80::LEU2 MEK1-13myc::kanMX6*
DP849	DP421 *zip1::LYS2 ndt80::LEU2 MEK1-13myc::kanMX6 dot1::URA3*
DP861	DP421 *zip1::LYS2 ndt80::LEU2 sml1::kanMX6 mec1::KlURA3 tel1::hphMX4*
DP877	DP421 *zip1::LYS2 ndt80::LEU2 rad24::TRP1 tel1::hphMX4*
DP881	DP421 *zip1::LYS2 ndt80::LEU2 pch2::TRP1*
DP883	DP421 *zip1::LYS2 ndt80::LEU2 rad24::TRP1*
DP884	DP421 *zip1::LYS2 ndt80::LEU2 dot1::hphMX4 MEK1-13myc::kanMX6*
DP885	DP421 *zip1::LYS2 ndt80::LEU2 mek1::kanMX6 MEK1::URA3*
DP886	DP421 *zip1::LYS2 ndt80::LEU2 mek1::kanMX6 mek1-T327A::URA3*

Table 1. Cont.

Strain	Genotype*
DP887	DP421 *zip1::LYS2 ndt80::LEU2 mek1::kanMX6 mek1-T331A::URA3*
DP888	DP421 *zip1::LYS2 ndt80::LEU2 mek1::kanMX6 mek1-K199R::URA3*
DP890	DP421 *zip1::LYS2 ndt80::LEU2 mek1::kanMX6 MEK1::URA3 dot1::hphMX4*
DP963	DP421 *ndt80::LEU2 HOP1-GFP::kanMX6*
DP964	DP421 *zip1::LYS2 ndt80::LEU2 HOP1-GFP::kanMX6*
DP965	DP421 *zip1::LYS2 ndt80::LEU2 HOP1-GFP::kanMX6 dot1::URA3*
DP966	DP421 *ndt80::LEU2 HOP1-GFP::kanMX6 dot1::URA3*
DP1024	DP421 *zip1::LYS2 ndt80::LEU2 ddc2::TRP1 sml1::kanMX6*
DP1027	DP421 *zip1::LYS2 ndt80::LEU2 pch2::TRP1 dot1::URA3 HOP1-GFP::kanMX6*
DP1029	DP421 *zip1::LYS2 pch2::TRP1*
DP1041	DP421 *zip1::LYS2 pch2::TRP1 dot1::URA3*
DP1042	DP421 (*hht1-hhf1)::natMX4 (hht2-hhf2)::hphMX4 zip1::LYS2 ndt80::LEU2 HOP1-GFP::kanMX6 p[HHT2-HHF2]::TRP1*
DP1043	DP421 (*hht1-hhf1)::natMX4 (hht2-hhf2)::hphMX4 zip1::LYS2 ndt80::LEU2 HOP1-GFP::kanMX6 p[hht2-K79A-HHF2]::TRP1*
DP1044	DP421 (*hht1-hhf1)::natMX4 (hht2-hhf2)::hphMX4 zip1::LYS2 ndt80::LEU2 HOP1-GFP::kanMX6 p[hht2-K79R-HHF2]::TRP1*
DP1045	DP421 (*hht1-hhf1)::natMX4 (hht2-hhf2)::hphMX4 zip1::LYS2 ndt80::LEU2 dot1::URA3 HOP1-GFP::kanMX6 p[HHT2-HHF2]::TRP1*
DP1046	DP421 (*hht1-hhf1)::natMX4 (hht2-hhf2)::hphMX4 zip1::LYS2 ndt80::LEU2 MEK1-GFP::kanMX6 p[HHT2-HHF2]::TRP1*
DP1047	DP421 (*hht1-hhf1)::natMX4 (hht2-hhf2)::hphMX4 zip1::LYS2 ndt80::LEU2 MEK1-GFP::kanMX6 p[hht2-K79A-HHF2]::TRP1*
DP1048	DP421 (*hht1-hhf1)::natMX4 (hht2-hhf2)::hphMX4 zip1::LYS2 ndt80::LEU2 MEK1-GFP::kanMX6 p[hht2-K79R-HHF2]::TRP1*
DP1049	DP421 (*hht1-hhf1)::natMX4 (hht2-hhf2)::hphMX4 zip1::LYS2 ndt80::LEU2 dot1::URA3 MEK1-GFP::kanMX6 p[HHT2-HHF2]::TRP1*
DP1050	DP421 (*hht1-hhf1)::natMX4 (hht2-hhf2)::hphMX4 zip1::LEU2 PCH2-3HA p[HHT2-HHF2]::TRP1*
DP1051	DP421 (*hht1-hhf1)::natMX4 (hht2-hhf2)::hphMX4 zip1::LEU2 PCH2-3HA p[hht2-K79A-HHF2]::TRP1*
DP1052	DP421 (*hht1-hhf1)::natMX4 (hht2-hhf2)::hphMX4 zip1::LEU2 PCH2-3HA p[hht2-K79R-HHF2]::TRP1*
DP1053	DP421 (*hht1-hhf1)::natMX4 (hht2-hhf2)::hphMX4 zip1::LEU2 PCH2-3HA dot1::kanMX6 p[HHT2-HHF2]::TRP1*
DP1054	DP421 *zip1::LYS2 ndt80::LEU2 pch2::TRP1 dot1::URA3*

*All strains are isogenic diploids homozygous for the indicated markers.
doi:10.1371/journal.pgen.1003262.t001

(ab2621; 1:2000 dilution), and anti-histone H3 (ab1791: 1:5000) were from Abcam. Rabbit polyclonal anti-Hop1 (1:2000 dilution) [3], was from S. Roeder (Yale University). Anti-Cdc5 (sc-6733; 1:1000 dilution) was from Santa Cruz Biotechnology. Mouse monoclonal anti-HA (12CA5; 1:2000 dilution) was from Roche. Anti-phosphoglycerate kinase (PGK) (A-6457, 1:10000 dilution) was from Molecular Probes. The ECL or ECL+ reagents were used for detection. The signal was captured on film and/or with a ChemiDoc XRS (Bio-Rad) system and quantified with the Quantity One software (Bio-Rad).

Cytology

Immunofluorescence of chromosome spreads was performed essentially as described [29]. To detect Mek1-myc and Mek1-GFP, mouse monoclonal anti-myc (clone 4A6, Millipore) and mouse monoclonal anti-GFP (JL-8, Clontech) antibodies, respectively, were used at 1:200 dilution. Rabbit polyclonal anti-Red1 and anti-Hop1 antibodies (gifts from S. Roeder) have been previously described [3,5]. Anti-mouse and/or anti-rabbit AF-488 and AF-594 conjugated secondary antibodies (Molecular Probes) were used at 1:200 dilution. Images were captured with a Nikon Eclipse 90i fluorescence microscope controlled with the MetaMorph software and equipped with an Orca-AG (Hammamatsu) CCD camera and a PlanApo VC 100×1.4 NA objective.

Whole cell images were captured with an Olympus IX71 fluorescence microscope equipped with a personal DeltaVision system (Applied Precision), a CoolSnap HQ2 (Photometrics) camera and a 100× UPLSAPO 1.4 NA objective. Exposure times were 800 ms, 400 ms and 300 ms for Ddc2-GFP, Mek1-GFP, and Hop1-GFP, respectively. Stacks of 20 planes at 0.2 μm intervals were captured. Maximum intensity projections of deconvolved images were generated with the SoftWoRx 5.0 software (Applied Precision). Quantification of GFP signals in the projections of individual nuclei was performed with the Image J software (http://rsb.info.nih.gov/ij/). Background signal was subtracted using the Otsu's or the Renyi's entropy threshold methods in Image J. To outline the contour of the cells in the representative whole-cell images presented, an overlay of the DIC image with 15–20% transparency over the GFP signal is shown.

Other techniques

To analyze meiotic nuclear divisions, cells were fixed in 70% ethanol, washed in PBS and stained with 1 μg/μl DAPI for 15 minutes at room temperature. At least 300 cells of every strain were scored at each time point. Analyses of meiotic kinetics were repeated several times; representative time courses are shown. Spore viability was determined by tetrad dissection. To calculate the statistical significance of differences a two-tailed Student *t*-test was used. *P*-values were calculated using the GraphPad Prism 4.0 software. $P<0.01$ was considered significant.

Supporting Information

Figure S1 H3K79 is constitutively methylated during meiosis. (A) Western blot analysis of H3K79 methylation dynamics

throughout meiosis. Total histone H3 is shown as a loading control. Strains are: DP421 (wild type), DP625 (*dot1*), DP422 (*zip1*) and DP555 (*zip1 dot1*). (B) H3K79 methylation does not change in other mutants defective in the meiotic recombination checkpoint. Western blot analysis of H3K79me in *ndt80*-arrested cells at 24 h after meiosis induction. Total histone H3 is shown as a loading control. Strains are: DP428 (*zip1*), DP728 (*zip1 spo11*), DP881 (*zip1 pch2*), DP883 (*zip1 rad24*) and DP1024 (*zip1 ddc2*).
(TIF)

Figure S2 Red1 linear localization in *zip1* chromosomes is not significantly altered in the absence of Dot1. Immunofluorescence of meiotic chromosome spreads stained with DAPI (blue) and anti-Red1 (green) antibody. Representative nuclei are shown. Spreads were prepared 24 h after meiotic induction of *ndt80* cells. Strains are: DP848 (*zip1*) and DP849 (*zip1 dot1*).
(TIF)

Figure S3 Dot1 is required for *zip1*-induced Hop1 phosphorylation. Western blot analysis of Hop1 in cell extracts obtained 24 h after meiotic induction in *ndt80* cells. Ponceau S staining of the membrane was used a loading control. Strains are: DP428 (*zip1*), DP674 (*zip1 mek1*), DP655 (*zip1 dot1*), DP728 (*zip1 spo11*) and DP680 (*zip1 mec1*).
(TIF)

Figure S4 Pch2 protein levels do not change in the absence of H3K79me. Western blot analysis of Pch2-HA in cell extracts obtained 15 h after meiotic induction. PGK is shown as a loading control. Hop1 and Mek1 phosphorylation were also analyzed in the same samples to demonstrate their defective activation in the *H3-K79R* and *H3-K79A* mutants. See Figure 3 for explanation of the black and white arrowheads pointing to phosphorylated Mek1 forms. Strains are: DP1050 (*zip1*), DP1053 (*zip1 dot1*), DP1052 (*zip1 H3-K79R*) and DP1051 (*zip1 H3-K79A*).
(TIF)

Figure S5 Hop1-GFP localization is impaired in the absence of H3K79me. Immunofluorescence of meiotic chromosome spreads stained with DAPI (blue), anti-Red1 (green) and anti-GFP (red) antibodies. Representative nuclei are shown. Spreads were prepared 24 h after meiotic induction of *ndt80* cells. Strains are: DP1042 (*zip1*), DP1045 (*zip1 dot1*), DP1044 (*zip1 H3-K79R*) and DP1043 (*zip1 H3-K79A*).
(TIF)

Figure S6 Analysis of γH2AX meiotic function. (A) Unlike H3K79me, γH2AX is not required for the checkpoint-induced by *zip1* because the *H2A-S129** mutation does not suppress *zip1* meiotic block. Time course of meiotic nuclear divisions; the percentage of cells containing more than two nuclei is represented. Strains are: BR1919-2N (wild type), DP409 (*zip1*), DP419 (*H2A-S129**), DP420 (*zip1 H2A-S129**), DP622 (*dot1 H2A-S129**) and DP623 (*zip1 dot1 H2A-S129**). (B) Spore viability is high in the absence of γH2AX and H3K79me, suggesting that both histone modifications are not required in unperturbed meiosis. At least 288 spores were scored for each strain. Means and standard deviations are shown. Strains are: BR1919-2N (wild type), DP419 (*H2A-S129**), DP622 (*dot1 H2A-S129**) and DP624 (*dot1*).
(TIF)

Video S1 Hop1 chromosomal distribution is impaired in the absence of Dot1. 3D reconstruction of deconvolved Z-stack images showing Hop1-GFP signal in *zip1* and *zip1 dot1* cells. Two different nuclei of each strain are shown during the movie.
(MOV)

Acknowledgments

We are indebted to J. Downs, N. Hollingsworth, and S. Roeder for invaluable reagents. We thank J. Pérez-Martín for useful comments and discussion and Simone Meidhof for help in strains construction.

Author Contributions

Conceived and designed the experiments: DO PAS-S. Performed the experiments: DO IA. Analyzed the data: DO IA PAS-S. Contributed reagents/materials/analysis tools: DO IA FvL RF PAS-S. Wrote the paper: PAS-S.

References

1. Roeder GS (1997) Meiotic chromosomes: it takes two to tango. Genes Dev 11: 2600–2621.
2. Zickler D, Kleckner N (1999) Meiotic chromosomes: integrating structure and function. Annu Rev Genet 33: 603–754.
3. Smith AV, Roeder GS (1997) The yeast Red1 protein localizes to the cores of meiotic chromosomes. J Cell Biol 136: 957–967.
4. Dong H, Roeder GS (2000) Organization of the yeast Zip1 protein within the central region of the synaptonemal complex. J Cell Biol 148: 417–426.
5. Sym M, Engebrecht JA, Roeder GS (1993) ZIP1 is a synaptonemal complex protein required for meiotic chromosome synapsis. Cell 72: 365–378.
6. Keeney S (2001) Mechanism and control of meiotic recombination initiation. Curr Top Dev Biol 52: 1–53.
7. MacQueen AJ, Hochwagen A (2011) Checkpoint mechanisms: the puppet masters of meiotic prophase. Trends Cell Biol 21: 393–400.
8. Roeder GS, Bailis JM (2000) The pachytene checkpoint. Trends Genet 16: 395–403.
9. Hong EJ, Roeder GS (2002) A role for Ddc1 in signaling meiotic double-strand breaks at the pachytene checkpoint. Genes Dev 16: 363–376.
10. Lydall D, Nikolsky Y, Bishop DK, Weinert T (1996) A meiotic recombination checkpoint controlled by mitotic checkpoint genes. Nature 383: 840–843.
11. Refolio E, Cavero S, Marcon E, Freire R, San-Segundo PA (2011) The Ddc2/ATRIP checkpoint protein monitors meiotic recombination intermediates J Cell Sci 124: 2488–2500.
12. Bailis JM, Roeder GS (2000) Pachytene exit controlled by reversal of Mek1-dependent phosphorylation. Cell 101: 211–221.
13. Wan L, de los Santos T, Zhang C, Shokat K, Hollingsworth NM (2004) Mek1 kinase activity functions downstream of *RED1* in the regulation of meiotic double strand break repair in budding yeast. Mol Biol Cell 15: 11–23.
14. Acosta I, Ontoso D, San-Segundo PA (2011) The budding yeast polo-like kinase Cdc5 regulates the Ndt80 branch of the meiotic recombination checkpoint pathway. Mol Biol Cell 22: 3478–3490.
15. Chu S, Herskowitz I (1998) Gametogenesis in yeast is regulated by a transcriptional cascade dependent on Ndt80. Mol Cell 1: 685–696.
16. Leu JY, Roeder GS (1999) The pachytene checkpoint in *S. cerevisiae* depends on Swe1-mediated phosphorylation of the cyclin-dependent kinase Cdc28. Mol Cell 4: 805–814.
17. Pak J, Segall J (2002) Role of Ndt80, Sum1, and Swe1 as targets of the meiotic recombination checkpoint that control exit from pachytene and spore formation in *Saccharomyces cerevisiae*. Mol Cell Biol 22: 6430–6440.
18. Sourirajan A, Lichten M (2008) Polo-like kinase Cdc5 drives exit from pachytene during budding yeast meiosis. Genes Dev 22: 2627–2632.
19. Tung KS, Hong EJ, Roeder GS (2000) The pachytene checkpoint prevents accumulation and phosphorylation of the meiosis-specific transcription factor Ndt80. Proc Natl Acad Sci U S A 97: 12187–12192.
20. Brachet E, Sommermeyer V, Borde V (2011) Interplay between modifications of chromatin and meiotic recombination hotspots. Biol Cell 104: 51–69.
21. Borde V, Robine N, Lin W, Bonfils S, Geli V, et al. (2009) Histone H3 lysine 4 trimethylation marks meiotic recombination initiation sites. EMBO J 28: 99–111.
22. Sollier J, Lin W, Soustelle C, Suhre K, Nicolas A, et al. (2004) Set1 is required for meiotic S-phase onset, double-strand break formation and middle gene expression. EMBO J 23: 1957–1967.
23. Feng Q, Wang H, Ng HH, Erdjument-Bromage H, Tempst P, et al. (2002) Methylation of H3-lysine 79 is mediated by a new family of HMTases without a SET domain. Curr Biol 12: 1052–1058.
24. Ng HH, Feng Q, Wang H, Erdjument-Bromage H, Tempst P, et al. (2002) Lysine methylation within the globular domain of histone H3 by Dot1 is important for telomeric silencing and Sir protein association. Genes Dev 16: 1518–1527.
25. van Leeuwen F, Gafken PR, Gottschling DE (2002) Dot1p modulates silencing in yeast by methylation of the nucleosome core. Cell 109: 745–756.
26. San-Segundo PA, Roeder GS (2000) Role for the silencing protein Dot1 in meiotic checkpoint control. Mol Biol Cell 11: 3601–3615.
27. Nguyen AT, Zhang Y (2011) The diverse functions of Dot1 and H3K79 methylation. Genes Dev 25: 1345–1358.

28. Frederiks F, Tzouros M, Oudgenoeg G, van Welsem T, Fornerod M, et al. (2008) Nonprocessive methylation by Dot1 leads to functional redundancy of histone H3K79 methylation states. Nat Struct Mol Biol 15: 550–557.
29. San-Segundo PA, Roeder GS (1999) Pch2 links chromatin silencing to meiotic checkpoint control. Cell 97: 313–324.
30. Lui DY, Peoples-Holst TL, Mell JC, Wu HY, Dean EW, et al. (2006) Analysis of close stable homolog juxtaposition during meiosis in mutants of *Saccharomyces cerevisiae*. Genetics 173: 1207–1222.
31. Conde F, Ontoso D, Acosta I, Gallego-Sanchez A, Bueno A, et al. (2010) Regulation of tolerance to DNA alkylating damage by Dot1 and Rad53 in Saccharomyces cerevisiae. DNA Repair 9: 1038–1049.
32. Cartagena-Lirola H, Guerini I, Viscardi V, Lucchini G, Longhese MP (2006) Budding Yeast Sae2 is an In Vivo Target of the Mec1 and Tel1 Checkpoint Kinases During Meiosis. Cell Cycle 5: 1549–1559.
33. Niu H, Li X, Job E, Park C, Moazed D, et al. (2007) Mek1 kinase is regulated to suppress double-strand break repair between sister chromatids during budding yeast meiosis. Mol Cell Biol 27: 5456–5467.
34. Carballo JA, Johnson AL, Sedgwick SG, Cha RS (2008) Phosphorylation of the axial element protein Hop1 by Mec1/Tel1 ensures meiotic interhomolog recombination. Cell 132: 758–770.
35. Woltering D, Baumgartner B, Bagchi S, Larkin B, Loidl J, et al. (2000) Meiotic segregation, synapsis, and recombination checkpoint functions require physical interaction between the chromosomal proteins Red1p and Hop1p. Mol Cell Biol 20: 6646–6658.
36. Keeney S, Giroux CN, Kleckner N (1997) Meiosis-specific DNA double-strand breaks are catalyzed by Spo11, a member of a widely conserved protein family. Cell 88: 375–384.
37. Wu HY, Ho HC, Burgess SM (2010) Mek1 kinase governs outcomes of meiotic recombination and the checkpoint response. Curr Biol 20: 1707–1716.
38. Niu H, Wan L, Baumgartner B, Schaefer D, Loidl J, et al. (2005) Partner choice during meiosis is regulated by Hop1-promoted dimerization of Mek1. Mol Biol Cell 16: 5804–5818.
39. Borner GV, Barot A, Kleckner N (2008) Yeast Pch2 promotes domainal axis organization, timely recombination progression, and arrest of defective recombinosomes during meiosis. Proc Natl Acad Sci U S A 105: 3327–3332.
40. Joshi N, Barot A, Jamison C, Borner GV (2009) Pch2 links chromosome axis remodeling at future crossover sites and crossover distribution during yeast meiosis. PLoS Genet 5: e1000557. doi:10.1371/journal.pgen.1000557.
41. Grenon M, Costelloe T, Jimeno S, O'Shaughnessy A, Fitzgerald J, et al. (2007) Docking onto chromatin via the *Saccharomyces cerevisiae* Rad9 Tudor domain. Yeast 24: 105–119.
42. Wysocki R, Javaheri A, Allard S, Sha F, Cote J, et al. (2005) Role of Dot1-dependent histone H3 methylation in G1 and S phase DNA damage checkpoint functions of Rad9. Mol Cell Biol 25: 8430–8443.
43. Sanders SL, Portoso M, Mata J, Bahler J, Allshire RC, et al. (2004) Methylation of histone H4 lysine 20 controls recruitment of Crb2 to sites of DNA damage. Cell 119: 603–614.
44. Botuyan MV, Lee J, Ward IM, Kim JE, Thompson JR, et al. (2006) Structural basis for the methylation state-specific recognition of histone H4-K20 by 53BP1 and Crb2 in DNA repair. Cell 127: 1361–1373.
45. Huyen Y, Zgheib O, Ditullio RA, Jr., Gorgoulis VG, Zacharatos P, et al. (2004) Methylated lysine 79 of histone H3 targets 53BP1 to DNA double-strand breaks. Nature 432: 406–411.
46. Wakeman TP, Wang Q, Feng J, Wang XF (2012) Bat3 facilitates H3K79 dimethylation by DOT1L and promotes DNA damage-induced 53BP1 foci at G1/G2 cell-cycle phases. EMBO J 31: 2169–2181.
47. Hammet A, Magill C, Heierhorst J, Jackson SP (2007) Rad9 BRCT domain interaction with phosphorylated H2AX regulates the G1 checkpoint in budding yeast. EMBO Rep 8: 851–857.
48. Sanders SL, Arida AR, Phan FP (2010) Requirement for the phospho-H2AX binding module of Crb2 in double-strand break targeting and checkpoint activation. Mol Cell Biol 30: 4722–4731.
49. Hunter N (2008) Hop1 and the meiotic DNA-damage response. Cell 132: 731–732.
50. Conde F, Refolio E, Cordon-Preciado V, Cortes-Ledesma F, Aragon L, et al. (2009) The Dot1 histone methyltransferase and the Rad9 checkpoint adaptor contribute to cohesin-dependent double-strand break repair by sister chromatid recombination in *Saccharomyces cerevisiae*. Genetics 182: 437–446.
51. Javaheri A, Wysocki R, Jobin-Robitaille O, Altaf M, Cote J, et al. (2006) Yeast G1 DNA damage checkpoint regulation by H2A phosphorylation is independent of chromatin remodeling. Proc Natl Acad Sci U S A 103: 13771–13776.
52. Toh GW, O'Shaughnessy AM, Jimeno S, Dobbie IM, Grenon M, et al. (2006) Histone H2A phosphorylation and H3 methylation are required for a novel Rad9 DSB repair function following checkpoint activation. DNA Repair 5: 693–703.
53. Downs JA, Lowndes NF, Jackson SP (2000) A role for *Saccharomyces cerevisiae* histone H2A in DNA repair. Nature 408: 1001–1004.
54. Niu H, Wan L, Busygina V, Kwon Y, Allen JA, et al. (2009) Regulation of meiotic recombination via Mek1-mediated Rad54 phosphorylation. Mol Cell 36: 393–404.
55. Ho HC, Burgess SM (2011) Pch2 acts through Xrs2 and Tel1/ATM to modulate interhomolog bias and checkpoint function during meiosis. PLoS Genet 7: e1002351. doi:10.1371/journal.pgen.1002351.
56. Wojtasz L, Cloutier JM, Baumann M, Daniel K, Varga J, et al. (2012) Meiotic DNA double-strand breaks and chromosome asynapsis in mice are monitored by distinct HORMAD2-independent and -dependent mechanisms. Genes Dev 26: 958–973.
57. Bishop DK (1994) RecA homologs Dmc1 and Rad51 interact to form multiple nuclear complexes prior to meiotic chromosome synapsis. Cell 79: 1081–1092.
58. Hochwagen A, Amon A (2006) Checking your breaks: surveillance mechanisms of meiotic recombination. Curr Biol 16: R217–228.
59. Borner GV, Kleckner N, Hunter N (2004) Crossover/noncrossover differentiation, synaptonemal complex formation, and regulatory surveillance at the leptotene/zygotene transition of meiosis. Cell 117: 29–45.
60. Storlazzi A, Xu L, Schwacha A, Kleckner N (1996) Synaptonemal complex (SC) component Zip1 plays a role in meiotic recombination independent of SC polymerization along the chromosomes. Proc Natl Acad Sci U S A 93: 9043–9048.
61. Panizza S, Mendoza MA, Berlinger M, Huang L, Nicolas A, et al. (2011) Spo11-accessory proteins link double-strand break sites to the chromosome axis in early meiotic recombination. Cell 146: 372–383.
62. Farmer S, Hong EJ, Leung WK, Argunhan B, Terentyev Y, et al. (2012) Budding yeast Pch2, a widely conserved meiotic protein, is involved in the initiation of meiotic recombination. PLoS ONE 7: e39724. doi:10.1371/journal.pone.0039724.
63. Vader G, Blitzblau HG, Tame MA, Falk JE, Curtin L, et al. (2011) Protection of repetitive DNA borders from self-induced meiotic instability. Nature 477: 115–119.
64. Zanders S, Alani E (2009) The *pch2Δ* mutation in baker's yeast alters meiotic crossover levels and confers a defect in crossover interference. PLoS Genet 5: e1000571. doi:10.1371/journal.pgen.1000571.
65. Jones B, Su H, Bhat A, Lei H, Bajko J, et al. (2008) The histone H3K79 methyltransferase Dot1L is essential for mammalian development and heterochromatin structure. PLoS Genet 4: e1000190. doi:10.1371/journal.pgen.1000190.
66. Rockmill B, Roeder GS (1990) Meiosis in asynaptic yeast. Genetics 126: 563–574.
67. Goldstein AL, McCusker JH (1999) Three new dominant drug resistance cassettes for gene disruption in *Saccharomyces cerevisiae*. Yeast 15: 1541–1553.
68. Longtine MS, McKenzie A, 3rd, Demarini DJ, Shah NG, Wach A, et al. (1998) Additional modules for versatile and economical PCR-based gene deletion and modification in *Saccharomyces cerevisiae*. Yeast 14: 953–961.
69. Hollingsworth NM, Ponte L (1997) Genetic interactions between *HOP1*, *RED1* and *MEK1* suggest that *MEK1* regulates assembly of axial element components during meiosis in the yeast *Saccharomyces cerevisiae*. Genetics 147: 33–42.

Figure S1

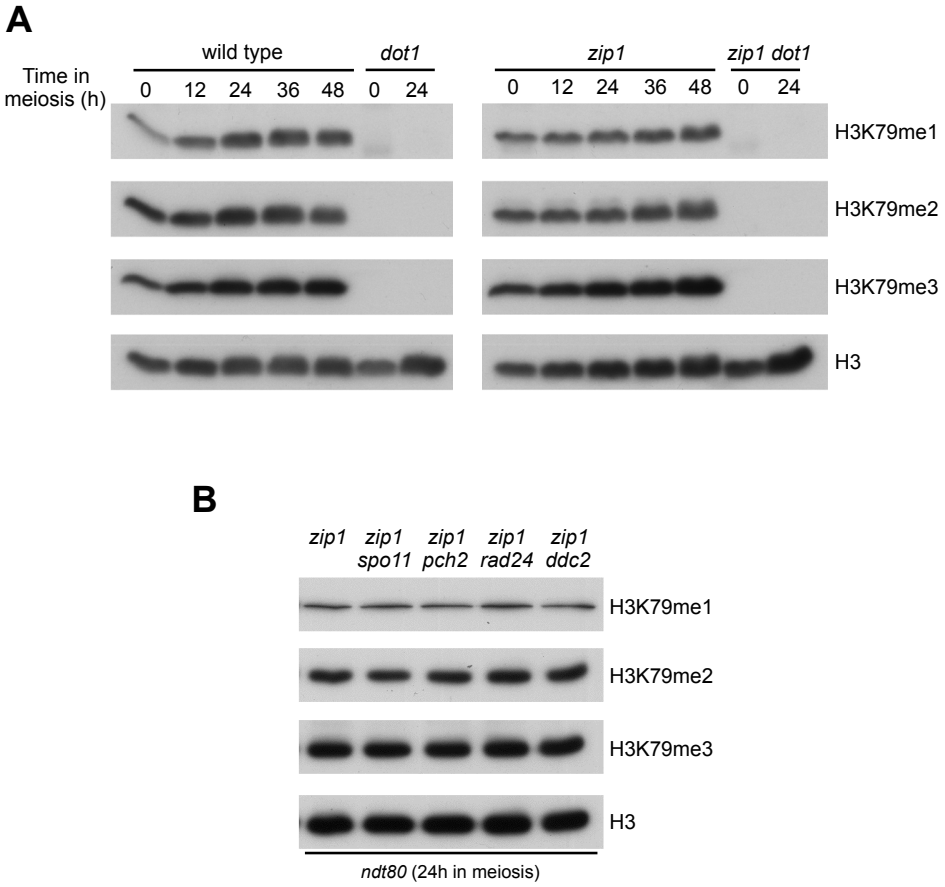

Figure S1 H3K79 is constitutively methylated during meiosis. (A) Western blot analysis of H3K79 methylation dynamics throughout meiosis. Total histone H3 is shown as a loading control. Strains are: DP421 (wild type), DP625 (*dot1*), DP422 (*zip1*) and DP555 (*zip1 dot1*). (B) H3K79 methylation does not change in other mutants defective in the meiotic recombination checkpoint. Western blot analysis of H3K79me in *ndt80*-arrested cells at 24 h after meiosis induction. Total histone H3 is shown as a loading control. Strains are: DP428 (*zip1*), DP728 (*zip1 spo11*), DP881 (*zip1 pch2*), DP883 (*zip1 rad24*) and DP1024 (*zip1 ddc2*).

Figure S2

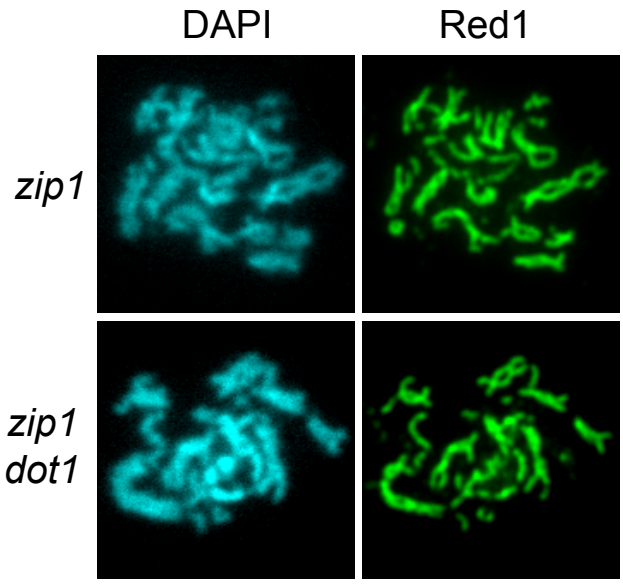

Figure S2 Red1 linear localization in *zip1* chromosomes is not significantly altered in the absence of Dot1. Immunofluorescence of meiotic chromosome spreads stained with DAPI (blue) and anti-Red1 (green) antibody. Representative nuclei are shown. Spreads were prepared 24 h after meiotic induction of *ndt80* cells. Strains are: DP848 (*zip1*) and DP849 (*zip1 dot1*).

Figure S3

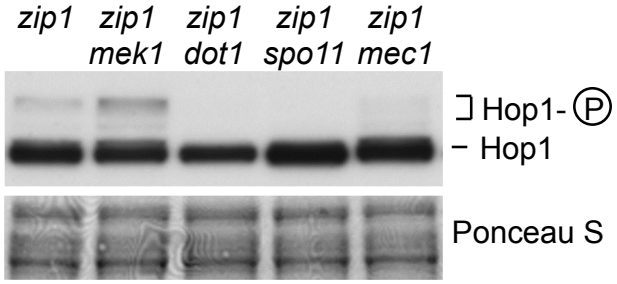

Figure S3 Dot1 is required for *zip1*-induced Hop1 phosphorylation. Western blot analysis of Hop1 in cell extracts obtained 24 h after meiotic induction in *ndt80* cells. Ponceau S staining of the membrane was used a loading control. Strains are: DP428 (*zip1*), DP674 (*zip1 mek1*), DP655 (*zip1 dot1*), DP728 (*zip1 spo11*) and DP680 (*zip1 mec1*).

Figure S4

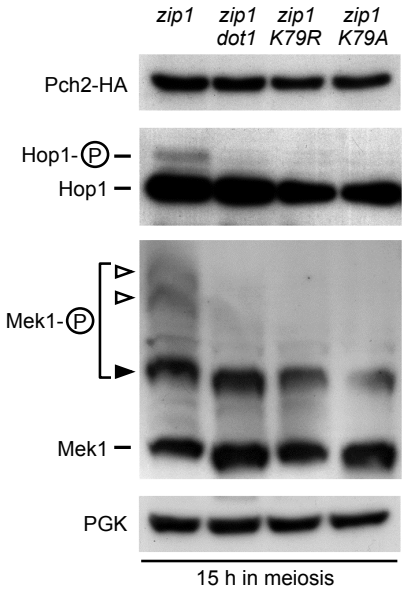

Figure S4 Pch2 protein levels do not change in the absence of H3K79me. Western blot analysis of Pch2-HA in cell extracts obtained 15 h after meiotic induction. PGK is shown as a loading control. Hop1 and Mek1 phosphorylation were also analyzed in the same samples to demonstrate their defective activation in the *H3-K79R* and *H3-K79A* mutants. See Figure 3 for explanation of the black and white arrowheads pointing to phosphorylated Mek1 forms. Strains are: DP1050 (*zip1*), DP1053 (*zip1 dot1*), DP1052 (*zip1 H3-K79R*) and DP1051 (*zip1 H3-K79A*).

Figure S5

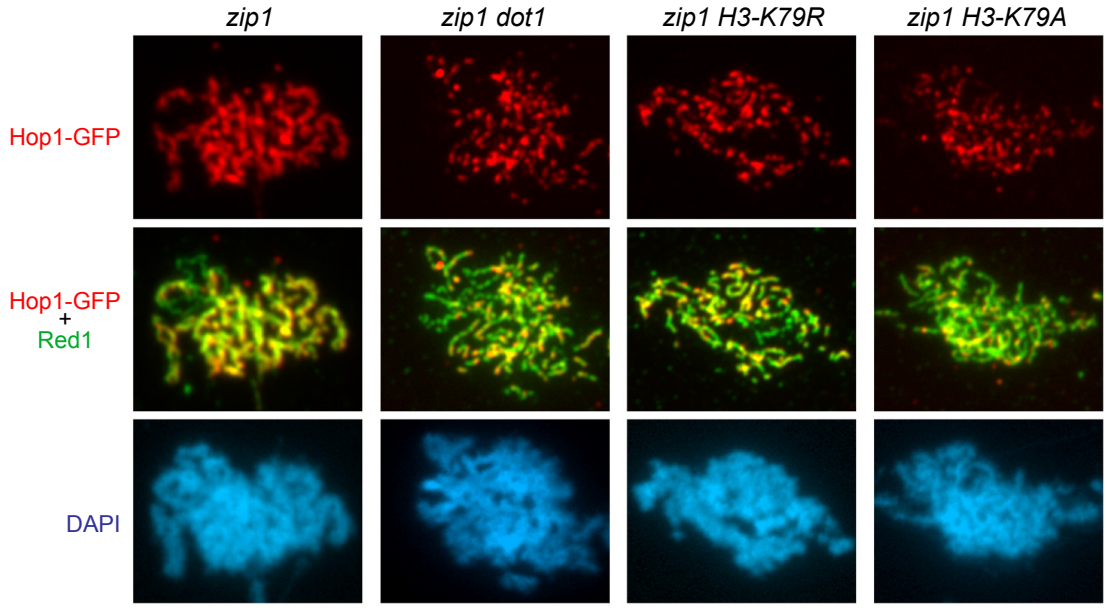

Figure S5 Hop1-GFP localization is impaired in the absence of H3K79me. Immunofluorescence of meiotic chromosome spreads stained with DAPI (blue), anti-Red1 (green) and anti-GFP (red) antibodies. Representative nuclei are shown. Spreads were prepared 24 h after meiotic induction of *ndt80* cells. Strains are: DP1042 (*zip1*), DP1045 (*zip1 dot1*), DP1044 (*zip1 H3-K79R*) and DP1043 (*zip1 H3-K79A*).

Figure S6

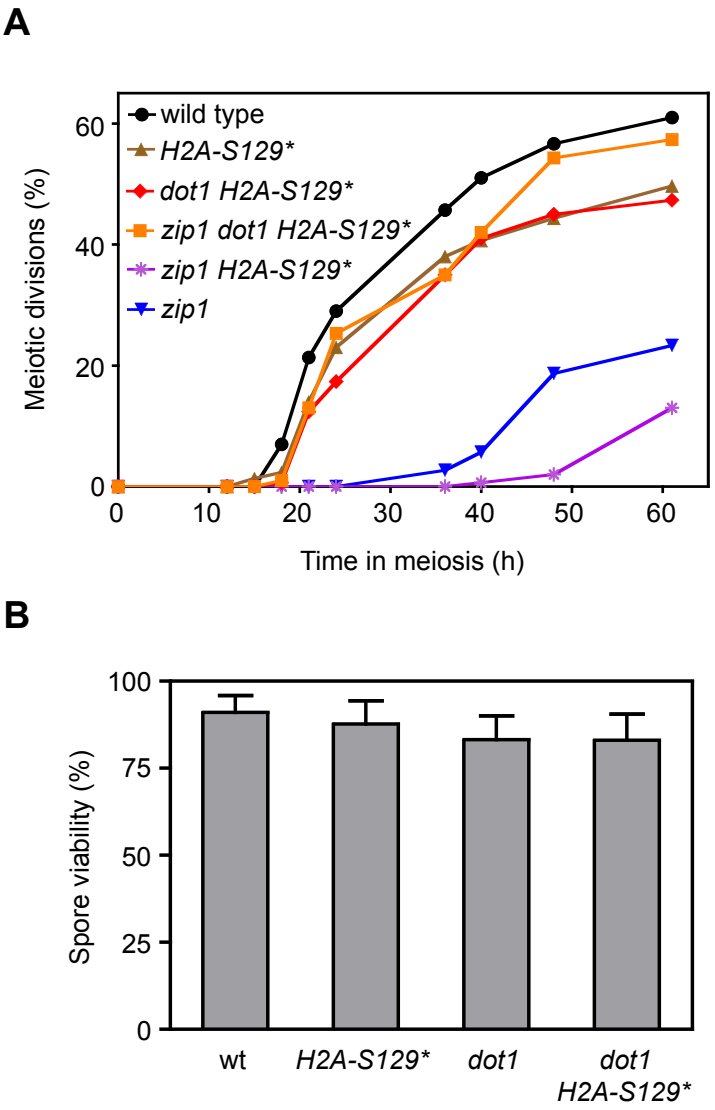

Figure S6 Analysis of γH2AX meiotic function. (A) Unlike H3K79me, γH2AX is not required for the checkpoint-induced by *zip1* because the *H2A-S129** mutation does not suppress *zip1* meiotic block. Time course of meiotic nuclear divisions; the percentage of cells containing more than two nuclei is represented. Strains are: BR1919-2N (wild type), DP409 (*zip1*), DP419 (*H2A-S129**), DP420 (*zip1 H2A-S129**), DP622 (*dot1 H2A-S129**) and DP623 (*zip1 dot1 H2A-S129**). (B) Spore viability is high in the absence of γH2AX and H3K79me, suggesting that both histone modifications are not required in unperturbed meiosis. At least 288 spores were scored for each strain. Means and standard deviations are shown. Strains are: BR1919-2N (wild type), DP419 (*H2A-S129**), DP622 (*dot1 H2A-S129**) and DP624 (*dot1*).

Video S1

Available at:
www.plosgenetics.org/article/fetchSingleRepresentation.action?uri=info:doi/10.1371/journal.pgen.1003262.s007

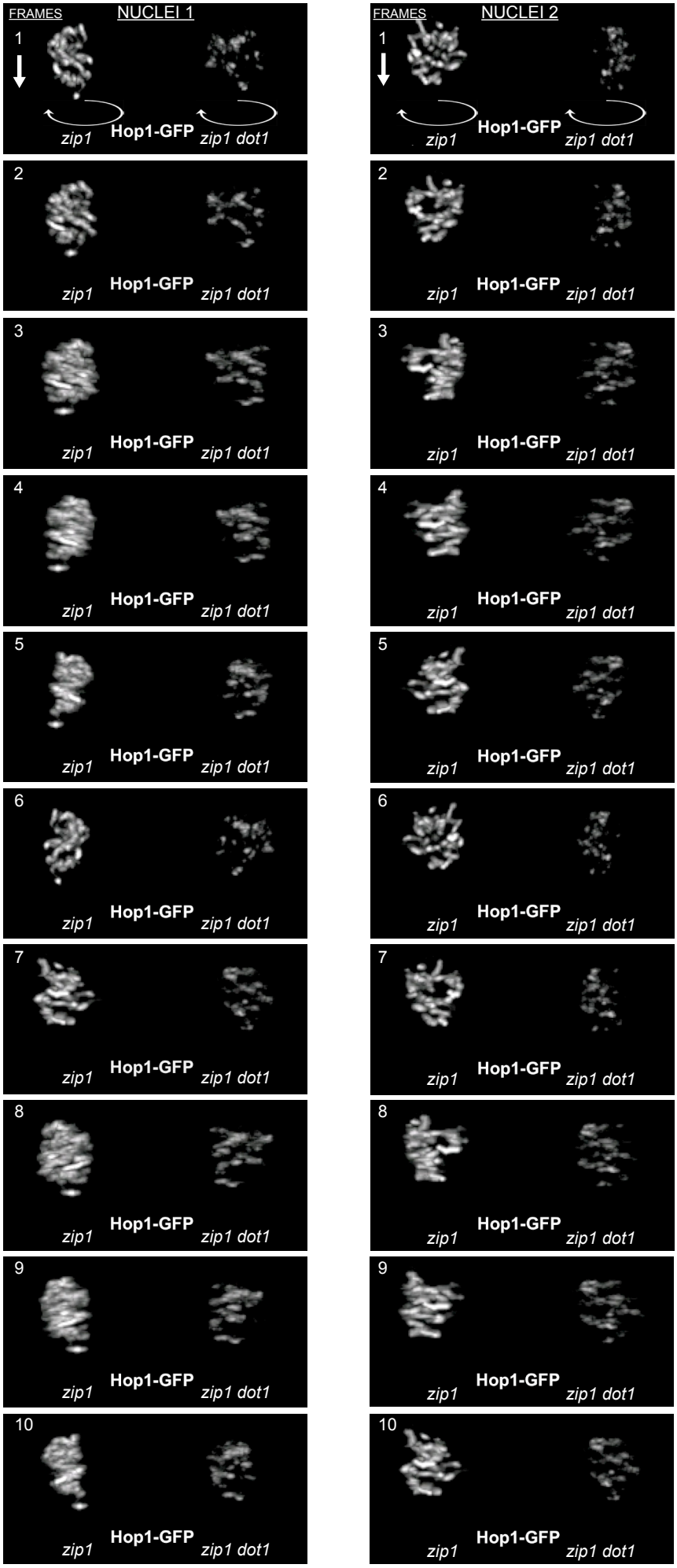

Video S1 Hop1 chromosomal distribution is impaired in the absence of Dot1. 3D reconstruction of deconvolved Z-stack images showing Hop1-GFP signal in *zip1* and *zip1 dot1* cells. Two different nuclei of each strain are shown during the movie.

Available at:
www.plosgenetics.org/article/fetchSingleRepresentation.action?uri=info:doi/10.1371/journal.pgen.1003262.s007

CONCLUSIONES

1. Los niveles globales de H3K79me, catalizados en exclusiva por Dot1, no cambian ni por la inducción de la meiosis, ni ante defectos meióticos. Sin embargo, esta modificación epigenética es esencial para permitir la respuesta del *checkpoint* de recombinación meiótica en *Saccharomyces cerevisiae*.

2. La función de Dot1 en este *checkpoint* meiótico se debe exclusivamente a su actividad catalítica metilando H3K79, siendo la forma H3K79me3 la más relevante.

3. La activación completa de la quinasa efectora del *checkpoint* de recombinación meiótica, Mek1, se produce por eventos secuenciales de fosforilación por las quinasas sensoras Mec1/Tel1 y de autofosforilación en *trans* por la propia Mek1.

4. La metilación de H3K79 es necesaria para el reclutamiento de Mek1 a los cromosomas meióticos y su autofosforilación, promoviendo así su plena activación y el establecimiento de la respuesta del *checkpoint*.

5. La metilación de H3K79 catalizada por Dot1 controla la fosforilación del adaptador Hop1 y su localización en los ejes de los cromosomas del mutante *zip1*, lo que permite la activación de Mek1.

6. La regulación de la localización de Hop1 por H3K79me se ejerce, al menos en parte, mediante la exclusión de la proteína Pch2 de la cromatina y su confinamiento en la región del DNA ribosómico (nucléolo).

CONCLUSIONS

1. Global levels of H3K79me, exclusively catalyzed by Dot1, do not change in response to either meiosis induction or meiotic defects. However, this epigenetic modification is essential for proper meiotic recombination checkpoint response in *Saccharomyces cerevisiae*.

2. Dot1 function in this meiotic checkpoint relies solely on the methylation of H3K79, with H3K79me3 being the most relevant form to sustain this function.

3. Full activation of the meiotic recombination checkpoint effector kinase, Mek1, is achieved in two sequential phosphorylation events: initial phosphorylation of Mek1 mediated by the sensor kinases Mec1/Tel1 is followed by *in trans* autophosphorylation of Mek1 itself.

4. Dot1-dependent H3K79me is required for both Mek1 recruitment to meiotic chromosomes and Mek1 autophosphorylation, thereby promoting its full activation and the ensuing checkpoint response.

5. Dot1-dependent H3K79me controls phosphorylation of the Hop1 adaptor and its localization along the chromosome axes of the *zip1* mutant, thus enabling Mek1 activation.

6. Regulation of H3K79me-mediated Hop1 localization is exerted, at least in part, by excluding the Pch2 meiotic checkpoint protein from the chromatin and its confinement in the ribosomal DNA region (nucleolus).

ARTÍCULO 2

Dynamics of DOT1L localization and H3K79 methylation during meiotic prophase I in mouse spermatocytes

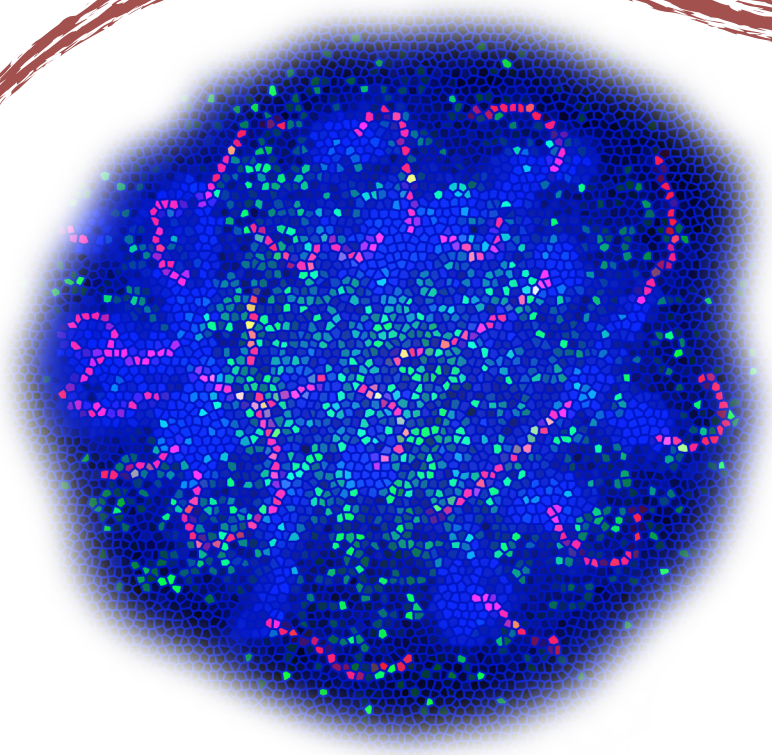

Dinámica de la localización de DOT1L y de la metilación de H3K79 durante la profase meiótica I en espermatocitos de ratón

RESUMEN

Durante la profase meiótica I tienen lugar numerosas interacciones entre los cromosomas homólogos, dando lugar a conexiones entre los mismos que promueven su correcta distribución a la progenie meiótica. Estos procesos se encuentran bajo la supervisión de mecanismos de *checkpoint* meióticos. En los seres humanos, las aneuploidías resultantes de defectos meióticos causan abortos espontáneos y síndromes genéticos. Los eventos de la profase meiótica ocurren en el contexto de la cromatina, por lo que las modificaciones post-traduccionales de las histonas deben desempeñar funciones importantes en estos procesos. En este artículo, describimos la localización de la metil-transferasa conservada evolutivamente, DOT1L, y de los diferentes estados de metilación de su diana, la lisina 79 de la histona H3 (mono–, di– y tri-metilación: H3K79me1, –me2 o –me3, respectivamente), durante la profase meiótica I en espermatocitos de ratón. Para ello, hemos empleado inmunofluorescencia de extensiones de núcleos. Así, encontramos que, en la estirpe silvestre, los niveles de H3K79me1 permanecen bajos y uniformes a lo largo de toda la profase I, mientras que los niveles de DOT1L, H3K79me2 y H3K79me3 muestran un notable aumento a partir de paquitene, pero con patrones de distribución subnuclear diferenciales. Las regiones de heterocromatina centromérica y el cuerpo sexual están enriquecidos en H3K79me3, mientras que H3K79me2 está presente por toda la cromatina excepto en el cuerpo sexual, a pesar de la acumulación de DOT1L que se observa en esta región. En ratones mutantes con meiosis defectuosas, la acumulación de DOT1L y H3K79me progresa hasta alcanzar los niveles característicos del último estadio de la profase en el que está bloqueado cada mutante. Los patrones de H3K79me combinados con el análisis citológico de las variantes de histonas H3.3, macroH2A, H2A.Z y γH2AX apuntan a una función diferencial para estas marcas epigenéticas durante la espermatogénesis en ratón. Así, proponemos que H3K79me2 está relacionada con la reactivación transcripcional de los autosomas durante paquitene, mientras que H3K79me3 puede contribuir al mantenimiento de la cromatina silenciada en las regiones centroméricas y en el cuerpo sexual.

GRAPHICAL ABSTRACT

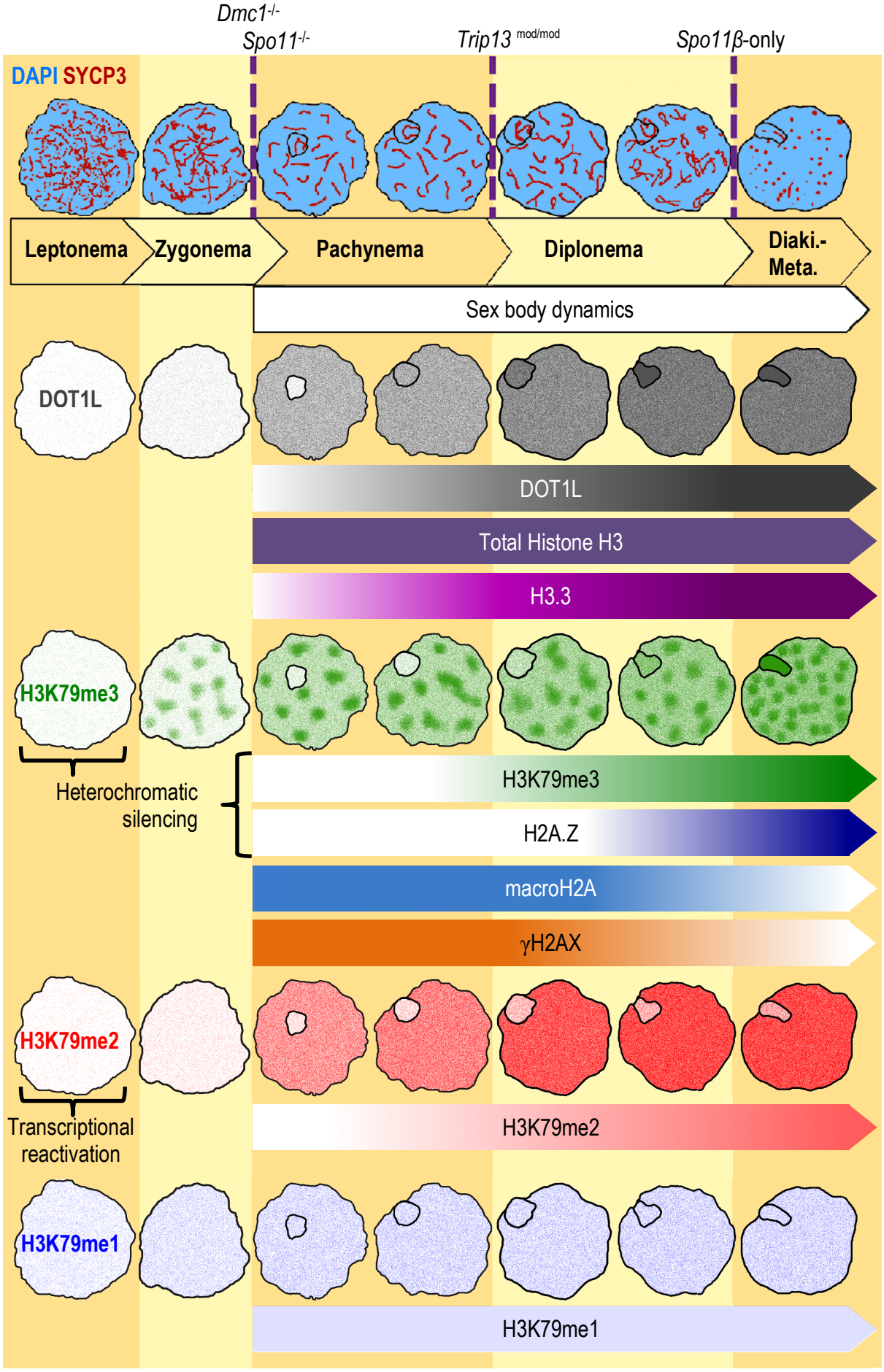

Chromosoma
DOI 10.1007/s00412-013-0438-5

RESEARCH ARTICLE

Dynamics of DOT1L localization and H3K79 methylation during meiotic prophase I in mouse spermatocytes

David Ontoso · Liisa Kauppi · Scott Keeney · Pedro A. San-Segundo

Received: 2 July 2013 / Revised: 6 September 2013 / Accepted: 24 September 2013

Abstract During meiotic prophase I, interactions between maternal and paternal chromosomes, under checkpoint surveillance, establish connections between homologs that promote their accurate distribution to meiotic progeny. In human, faulty meiosis causes aneuploidy resulting in miscarriages and genetic diseases. Meiotic processes occur in the context of chromatin; therefore, histone post-translational modifications are expected to play important roles. Here, we report the cytological distribution of the evolutionarily conserved DOT1L methyltransferase and the different H3K79 methylation states resulting from its activity (mono-, di- and tri-methylation; H3K79me1, me2 and me3, respectively) during meiotic prophase I in mouse spermatocytes. In the wild type, whereas low amounts of H3K79me1 are rather uniformly present throughout prophase I, levels of DOT1L, H3K79me2 and H3K79me3 exhibit a notable increase from pachynema onwards, but with differential subnuclear distribution patterns. The heterochromatic centromeric regions and the sex body are enriched for H3K79me3. In contrast, H3K79me2 is present all over the chromatin, but is largely excluded from the sex body despite the accumulation of DOT1L. In meiosis-defective mouse mutants, the increase of DOT1L and H3K79me is blocked at the same stage where meiosis is arrested. H3K79me patterns, combined with the cytological analysis of the H3.3, γH2AX, macroH2A and H2A.Z histone variants, are consistent with a differential role for these epigenetic marks in male mouse meiotic prophase I. We propose that H3K79me2 is related to transcriptional reactivation on autosomes during pachynema, whereas H3K79me3 may contribute to the maintenance of repressive chromatin at centromeric regions and the sex body.

Electronic supplementary material The online version of this article (doi:10.1007/s00412-013-0438-5) contains supplementary material, which is available to authorized users.

D. Ontoso · P. A. San-Segundo (✉)
Instituto de Biología Funcional y Genómica, Consejo Superior de Investigaciones Científicas and University of Salamanca, 37007 Salamanca, Spain
e-mail: pedross@usal.es

L. Kauppi · S. Keeney
Molecular Biology Program, Memorial Sloan-Kettering Cancer Center, 1275 York Avenue, New York, NY 10065, USA

Present Address:
L. Kauppi
Research Programs Unit (Genome-Scale Biology) and Institute of Biomedicine (Biochemistry and Developmental Biology), University of Helsinki, Haartmaninkatu 8, Helsinki, Finland

Introduction

Meiosis is a specialized cell division that generates haploid gametes required for sexual reproduction because two rounds of chromosome segregation are preceded by a single phase of DNA replication. In order to accomplish this reduction in the number of chromosomes, a sequence of finely regulated, coordinated and monitored events takes place. Thus, the unique meiotic prophase I is the most prolonged and elaborate stage of meiosis, during which pairing, synapsis and recombination between homologous chromosomes occur (Cohen et al. 2006). Meiotic recombination begins with programmed DNA double-strand breaks (DSBs), introduced by Spo11 and accessory proteins (Keeney 2008). In many organisms, including budding yeast and mouse, meiotic DSBs trigger a complex program in which their repair is coupled to homologous chromosome pairing and synapsis. Interactions between homologs are stabilized by a proteinaceous structure, the synaptonemal complex (SC), which keeps homologs tightly associated during pachynema and facilitates completion of crossover recombination to generate physical linkages required for the subsequent accurate segregation (Pawlowski and Cande 2005). Progression and completion of meiotic events are monitored by checkpoints, specific surveillance mechanisms that block meiotic

Published online: 09 October 2013

progression in response to defects and, in the case of Metazoa, lead to apoptosis of aberrant meiocytes avoiding generation of aneuploid gametes (Hochwagen and Amon 2006; Macqueen and Hochwagen 2011).

Meiotic recombination takes place in the context of chromatin; accordingly, several histone post-translational modifications (PTMs) have been found to influence various aspects of meiosis (Bolcun-Filas and Schimenti 2012; Brachet et al. 2012). For example, there is an association between trimethylation of histone H3 at Lysine 4 (H3K4me3) and the determination of meiotic DSB sites, mediated by the Set1 complex and its subunit Spp1 in yeast (Borde et al. 2009; Acquaviva et al. 2013; Sommermeyer et al. 2013) and the meiosis-specific histone H3 methyltransferase PRDM9 in mouse (Baudat et al. 2000; Grey et al. 2011; Smagulova et al. 2011).

Another histone PTM with a known meiotic function is the methylation of H3K79 mediated by Dot1 in *Saccharomyces cerevisiae*. In yeast, H3K79me is largely dispensable for unperturbed meiosis, but it is essential for meiotic recombination checkpoint function (San-Segundo and Roeder 2000; Ontoso et al. 2013). Dot1 is the only methyltransferase responsible for catalyzing mono-, di- and trimethylation at H3K79 in a non-processive manner (Lacoste et al. 2002; van Leeuwen et al. 2002; Ng et al. 2002; Frederiks et al. 2008). To date, there is no demethylase known capable of reverting H3K79me. With a few exceptions — such as *Schizosaccharomyces pombe*, which lacks Dot1 and H3K79me — this histone methyltransferase has been conserved through evolution; the mammalian homolog is called DOT1L (for Dot1-like) (Feng et al. 2002; Jones et al. 2008). In human cells and *Drosophila*, DOT1L/dDot1 has been isolated forming part of a large macromolecular complex, DotCom, which modulates its activity (Mohan et al. 2010). DOT1L-mediated H3K79me performs important roles in transcriptional regulation (Steger et al. 2008; Kim et al. 2012a) and affects multiple biological processes (Nguyen and Zhang 2011). In particular, DOT1L activity is involved in embryonic development and differentiation (Jones et al. 2008; Barry et al. 2009), cardiac function (Nguyen et al. 2011), hematopoiesis (Feng et al. 2010; Jo et al. 2011), cell proliferation and aging (Kim et al. 2012b) and chondrogenesis (Castaño Betancourt et al. 2012). Alteration of DOT1L function is related with some types of mixed lineage leukemia (Okada et al. 2005; Krivtsov et al. 2008; Bernt et al. 2011), neural tube defects (Zhang et al. 2013) and osteoarthritis (Castaño Betancourt et al. 2012). The discovery of an increasing number of pathologies related with altered DOT1L-mediated H3K79me patterns points to DOT1L as a promising therapeutic target (Daigle et al. 2011; Yao et al. 2011; Anglin et al. 2012). However, little is known about DOT1L activity in mammalian meiosis; only a study on H3K79me2/3 in mouse oocytes and preimplantation embryos has been reported (Ooga et al. 2008).

Here, we report the characterization of DOT1L localization and the chromatin distribution of the distinct H3K79 methylation states (me1, me2 and me3) during meiotic prophase I in spermatocytes of wild-type mice and various meiotic mutants. Our results reveal a progressive increment of DOT1L activity as prophase I advances, and the existence of differential spatio-temporal patterns for H3K79me2 and H3K79me3. Furthermore, the comparison of the distribution of these epigenetic marks with that of the H3.3, γH2AX, macroH2A and H2A.Z histone variants hints at a functional contribution of H3K79me2 and H3K79me3 to the characteristic transcriptional states of the different subnuclear territories in spermatocyte nuclei.

Materials and methods

Mice

Animals in this study were of C57BL/6 background or C57BL/6 X 129/Sv mixed background. The *Spo11* β-only transgenic mice, the hypomorphic *Trip13*$^{mod/mod}$, and the *Spo11*$^{-/-}$ and *Dmc1*$^{-/-}$ null mice were previously described (Pittman et al. 1998; Baudat et al. 2000; Roig et al. 2010; Kauppi et al. 2011). To minimize variability due to strain background in the studies involving mutant mice, experimental animals were compared to control animals from the same litter. Experiments conformed to relevant regulatory standards and were approved by the MSKCC Institutional Animal Care and Use Committee.

Immunofluorescence

Mouse testicular cells were prepared for surface spreading and subsequent immunofluorescence as previously described (Barchi et al. 2005), with slight modifications. Testis cell preparations were resuspended in 0.1 M sucrose were added onto glass slides previously coated with a 1% paraformaldehyde, 0.1% Triton X-100 solution, incubated for 3 h in a humidified chamber at room temperature, rinsed in 0.4% Kodak Photo-Flo 200 and dried briefly. Slides were treated with blocking/antibody dilution buffer (B/ADB: 2 mg/ml BSA, 0.05% Tween-20, 0.2% gelatin in PBS) for 30 min at room temperature, and incubated overnight at 4°C with the primary antibody diluted in B/ADB. After four washes of 5 min with B/ADB, slides were incubated with the secondary antibody diluted in B/ADB for 1 h at 37°C in the dark. After four washing steps again, slides were mounted in Vectashield mounting medium (Vector) with 5 μg/ml DAPI. Images were captured using an Axio2 microscope (Zeiss) connected to a CCD camera and processed using the SlideBook software package (Intelligent Imaging Innovations).

The following primary antibodies and dilutions were used. Rabbit polyclonal anti-DOT1L (ab64077; 1:200 dilution), anti-H3K79-me1 (ab2886; 1:1,000 dilution), anti-H3K79-me2 (ab3594; 1:2,000), anti-H3K79-me3 (ab2621; 1:2,000

dilution), anti-histone H3 (ab1791; 1:100), and anti-histone H3.3 (ab62642; 1:400) were from Abcam. Mouse monoclonal anti-γH2AX (05-636; 1:800), rabbit polyclonal anti-H2A.Z (07-594; 1:400) and rabbit polyclonal anti-macroH2A (07-219; 1:400) were from Millipore. Mouse monoclonal anti-SYCP3 (sc-74569; 1:500) was from Santa Cruz and goat polyclonal anti-SYCP3 (1:400) was from Terry Ashley.

The following secondary antibodies conjugated with Alexa Fluor were from Molecular Probes and used at 1:200 dilution. Anti-rabbit-AF488 (A-21206), anti-mouse-AF594 (A-21203), anti-mouse-AF647 (A-31571), and anti-goat-AF594 (A-11058).

Quantification of fluorescence intensities of individual nuclei was performed with the ImageJ 1.47f software (National Institutes of Health, USA; http://imagej.nih.gov/ij/). The contours of the nuclei, the centromeric areas and the sex bodies were identified based on DAPI and SYCP3 staining. The intensity values within these regions of interest were quantified. Background signal was subtracted using the Otsu's entropy threshold methods in ImageJ. This threshold tool was also used to reproducibly outline without bias the more intense DAPI-stained centromeric regions and the sex body, as shown in Fig. 2. The parameters used for quantification purposes were the integrated density (the result of multiplying the area by the mean of the fluorescence intensity values) and the percentage of area with signal from the total area of interest.

For graphs showing centromeric regions/uncondensed chromatin ratios (Fig. 2e and Fig. S4 b, d), a threshold was fixed in every image; then, the percentage of area with DOT1L or H3K79me signal was obtained for all the centromeric regions and a mean value was calculated (numerator). The signal was also measured for the uncondensed chromatin (the whole nucleus except the centromeric regions and the sex body) (denominator). Finally, a ratio between these two values was calculated for each nucleus. The graphs show the mean of these ratios.

For graphs showing XY body/whole nucleus ratios (Fig. 2f and Fig. S4 a, c) a threshold was fixed in every image. The percentage of area with DOT1L or H3K79me signal was obtained for the XY body (numerator), and for the remaining of nucleus (denominator). A ratio between these two values was calculated for each nucleus. The graphs show the mean of these ratios.

For pairwise comparisons of mutants versus controls, two-tailed Mann–Whitney tests were applied and *P* values were calculated using the GraphPad Prism 5.0 software (http://www.graphpad.com/).

Bioinformatics

The protein sequence alignment was performed with CLUSTALW (http://www.ebi.ac.uk/Tools/msa/clustalw2/). The PDB ID references for human nucleosomes containing histone variant H3.1, H3.2 and H3.3 are 3AFA, 3av1 and 3av2, respectively (Tachiwana et al. 2010, 2011), available at the Research Collaboratory for Structural Bioinformatics (RCSB) Protein Data Bank (http://www.rcsb.org/pdb/). Molecular graphics and H3K79 highlighting were performed with the UCSF Chimera package (http://www.cgl.ucsf.edu/chimera)

Results

Spatial and temporal patterns of DOT1L and H3K79me distribution during meiotic prophase I

To investigate the localization of mammalian DOT1L and the associated mono-, di- and tri-methylation of histone H3 at lysine 79 (H3K79me1, me2, and me3, respectively), we performed immunofluorescence of surface-spread meiotic chromosomes from wild-type mouse spermatocytes. We tracked SYCP3, a component of the axial/lateral elements of the SC (Lammers et al. 1994), to define the stage of prophase I of each spermatocyte nucleus based on the degree of synapsis exhibited by the chromosomes (Fig. 1 and Fig. S1). At the beginning of prophase I, short stretches of SYCP3 start to develop during leptonema. At zygonema, synapsis of homologs begins and thickened SYCP3 areas along the already synapsed regions are detected. At pachynema, synapsis between the autosomes is completed, resulting in a thick and uniform SYCP3 signal. A subnuclear domain formed by the sex chromosomes, the so-called "XY body" or "sex body", begins to emerge around the end of zygonema, and is fully formed in pachynema. This chromosome pair displays a short synapsed area on a limited distal region of homology, the pseudoautosomal region (PAR). The PAR exhibits thickened SYCP3 staining, whereas a thinner signal is visible along the unsynapsed non-homologous regions (e.g., see yellow arrows in Fig. 1a and Fig. S1, where the sex body is pointed). At diplonema, homologs progressively desynapse revealing spaces between the SYCP3 axes, but they still remain joined at chiasmata sites where crossovers have occurred. In addition, from late pachynema, but more evident during diplonema, the chromosomes show thickenings at the ends, which correspond with their attachment to the inner nuclear membrane (Liebe et al. 2004). Meanwhile, in the sex body desynapsis also occurs, the X and Y chromosomes are joined end-to-end, and the X chromosome shows thickenings along its length (Fig. S1, diplotene panels). At diakinesis-metaphase I, SC disassembly is general, SYCP3 staining is mainly concentrated at the centromeric areas, and only remnants persist on chromosome arms. The X chromosome remnants are the last ones to disappear (Fig. S1, diaki.-meta. panels) (Parra et al. 2004; Barchi et al. 2008).

First, we monitored DOT1L localization throughout meiotic prophase I (Fig. 1a). Interestingly, we found a progressive increment of the association of this histone methyltransferase with meiotic chromatin correlating with the progression through prophase I stages. DOT1L nuclear staining started at very low levels at leptonema, increased slightly in zygonema, followed by a dramatic increment in DOT1L levels at pachynema and, especially, during the diplonema and diakinesis stages (Fig. 1a). The sex body exhibited particularly dynamic patterns, detailed below.

Next, we analyzed the distribution of the three possible methylated states of H3K79 resulting from DOT1L action: H3K79me1, -me2 and -me3 (Fig. 1b, c and d, respectively). Overall levels of H3K79me1 were uniformly weak at all stages (Fig. 1b). In contrast, H3K79me2 exhibited a progressive enrichment concurrent with prophase I progression, achieving relatively strong staining during pachynema, diplonema and diakinesis/metaphase I (Fig. 1c). H3K79me3 staining also intensified during meiotic prophase I, reaching the highest levels in diakinesis/metaphase I (Fig. 1d).

These observations indicate that overall levels of chromatin-associated DOT1L and H3K79 methylation undergo significant change during male mouse meiotic prophase I. The enrichment of DOT1L is accompanied by higher amounts of two particular methylation states, H3K79me2 and H3K79me3; however, their dynamics and subnuclear distribution were different.

We examined DOT1L and H3K79me in more detail starting from the stage when they became more abundant, pachynema, and focused on the distinctive chromatin regions that can be distinguished according with their intensity of DAPI staining and chromosome positioning, marked by SYCP3. In this way, we discriminated areas with weaker DAPI fluorescence signal, corresponding to euchromatin and encompassing most of the autosome domains. On the other hand, subnuclear territories with more intense DAPI staining were classified into two groups: the constitutive heterochromatin located at the centromeric regions surrounding one end of each mouse autosome (which are telocentric; Kalitsis et al. 2006), and the facultative heterochromatin of the sex body (differentially outlined in Fig. 2a–d). We quantified the signal intensity of DOT1L and the different H3K79me states in the DAPI-bright regions relative to the remaining chromatin (Fig. 2e). Strikingly, we found that, as soon as the large centromeric regions became apparent after mid-zygonema, they exhibited strong accumulation (about 7-fold) of H3K79me3 (Fig. 2d, e). These areas continued to be highly trimethylated at H3K79 through metaphase I, enclosing the centromere-proximal SYCP3 remnants (Parra et al. 2004). Furthermore, strong H3K79me3 staining could be still detected at the chromocenter in round spermatids (Fig. 3). In contrast, neither DOT1L, H3K79me1, nor H3K79me2 showed this centromeric accumulation (Fig. 2a–c), with ratios relative to euchromatin regions close to 1 (Fig. 2e), denoting a more uniform distribution between both types of subnuclear territories.

Fig. 1 DOT1L and H3K79me localization patterns throughout male mouse meiotic prophase I. Immunofluorescence of surface-spread wild-type spermatocytes stained with antibodies to SYCP3 (*red*) and to either DOT1L (**a**), H3K79me1 (**b**), H3K79me2 (**c**) or H3K79me3 (**d**), shown in *white* or *green*, as indicated on the panels. DAPI staining of chromatin is shown in *blue*. Representative nuclei for each prophase I stage are presented, determined by the SYCP3 localization pattern (see also Fig. S1). In **a**, the sex body is indicated by a *yellow arrow*. Quantification of the signal intensity for DOT1L and the different H3K79me states is shown in arbitrary units (a.u.) on the *right graphs*. Each dot in the scatter plot indicates the value for an individual nucleus. The *central horizontal line* is the median. Scale bar: 10 μm

Sex body development involves massive chromatin remodeling events to establish a heterochromatin configuration that leads to a transcriptional inactivation program, the so-called "meiotic sex chromosome inactivation" (MSCI) (Handel 2004; Turner 2007). Little is known about the contribution of DOT1L and H3K79me to MSCI, so we analyzed their distribution in the sex body from pachynema to metaphase I (Fig. 2a–d, f). At pachynema, the amount of DOT1L in the sex body was roughly at the average level of the rest of the nucleus, but during diplonema and at diakinesis-metaphase I it significantly increased (2- and 4-fold, respectively) (Fig. 2a, f). H3K79me1 maintained a stable, relatively uniform pattern over the entire nucleus at all stages (Fig. 2b, f), while H3K79me2 was underrepresented in the sex body from pachynema up to diakinesis/metaphase I (Fig. 2c, f). Finally, XY-associated H3K79me3 started at low amounts during pachynema, matched autosome levels at diplonema and reached a 2-fold higher level at diakinesis-metaphase (Fig. 2d, f). In more advanced stages of spermatogenesis, such as in round spermatids, the more intense DAPI-stained territory adjacent to the chromocenter contains the sex chromosome X or Y (Greaves et al. 2006). We found that H3K79me3 was also detected in this region, although at lower levels than in the chromocenter (Fig. 3).

Thus, DOT1L and the ensuing H3K79me states exhibit characteristic spatio-temporal dynamics suggestive of possible differential roles during male mouse meiotic prophase I.

Impaired DOT1L localization and H3K79 methylation patterns in meiotic mutants

To determine whether DOT1L and H3K79 methylation patterns are functionally tied to meiotic progression and/or recombination, we examined mutants affected at different stages during meiosis: *Spo11* β-only, *Trip13*$^{mod/mod}$, *Spo11*$^{-/-}$ and *Dmc1*$^{-/-}$ (Fig. 4, Fig. S2, S3 and Fig. 5, respectively; ordered from the one that reaches the furthest stage to the mutant with the least progression). These mutants exhibit defects in synapsis and/or recombination, with different degrees of severity that are incompatible with a successful meiosis program and lead to widespread checkpoint-induced arrest and apoptosis before the first meiotic division. The arrest point varies in the different

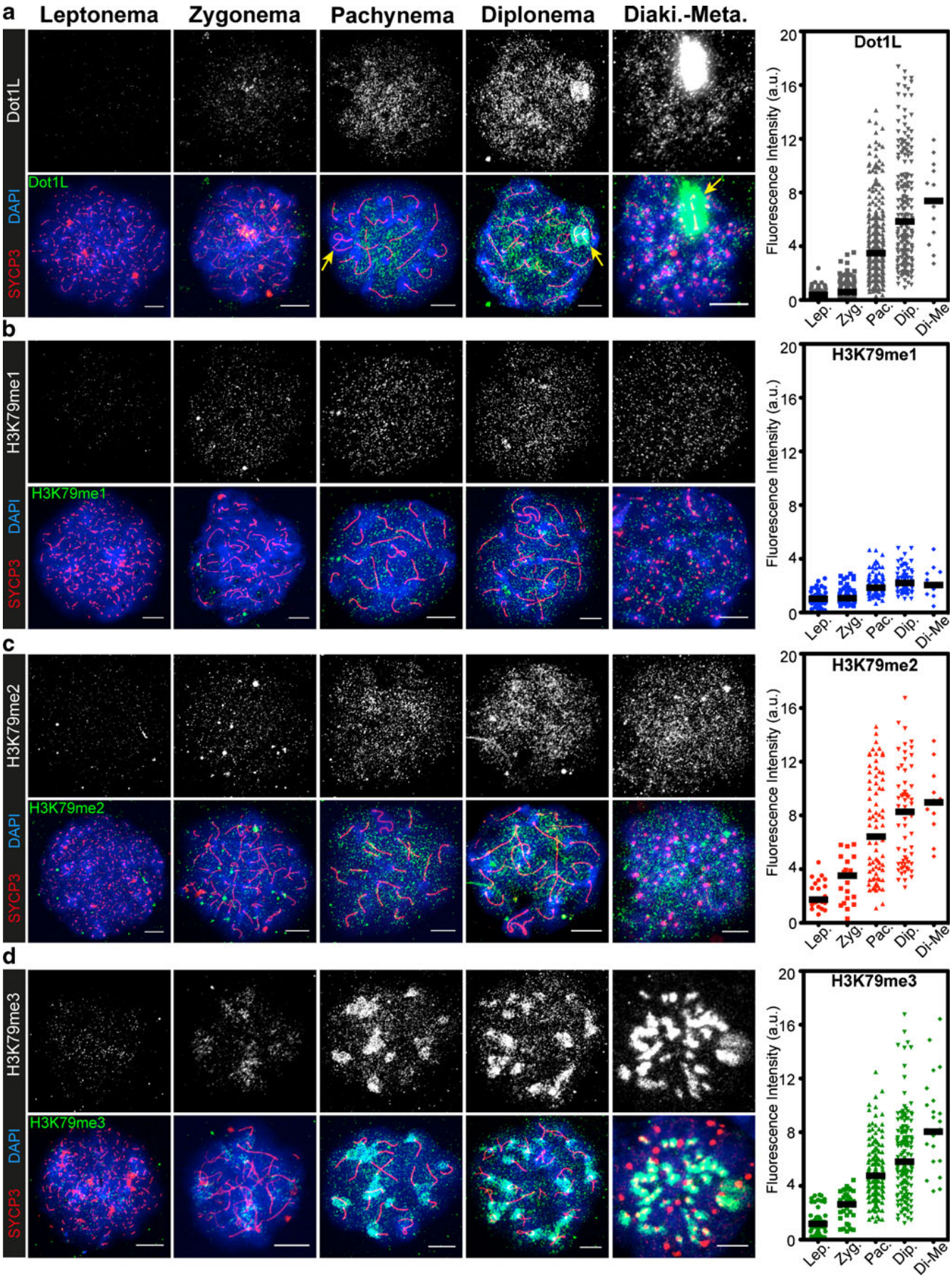
a
Leptonema
Zygonema
Pachynema
Diplonema
Diaki.-Meta.
Dot1L
Dot1L
DAPI
SYCP3
Fluorescence Intensity (a.u.)
Lep.
Zyg.
Pac.
Dip.
Di-Me
b
H3K79me1
H3K79me1
c
H3K79me2
H3K79me2
d
H3K79me3
H3K79me3

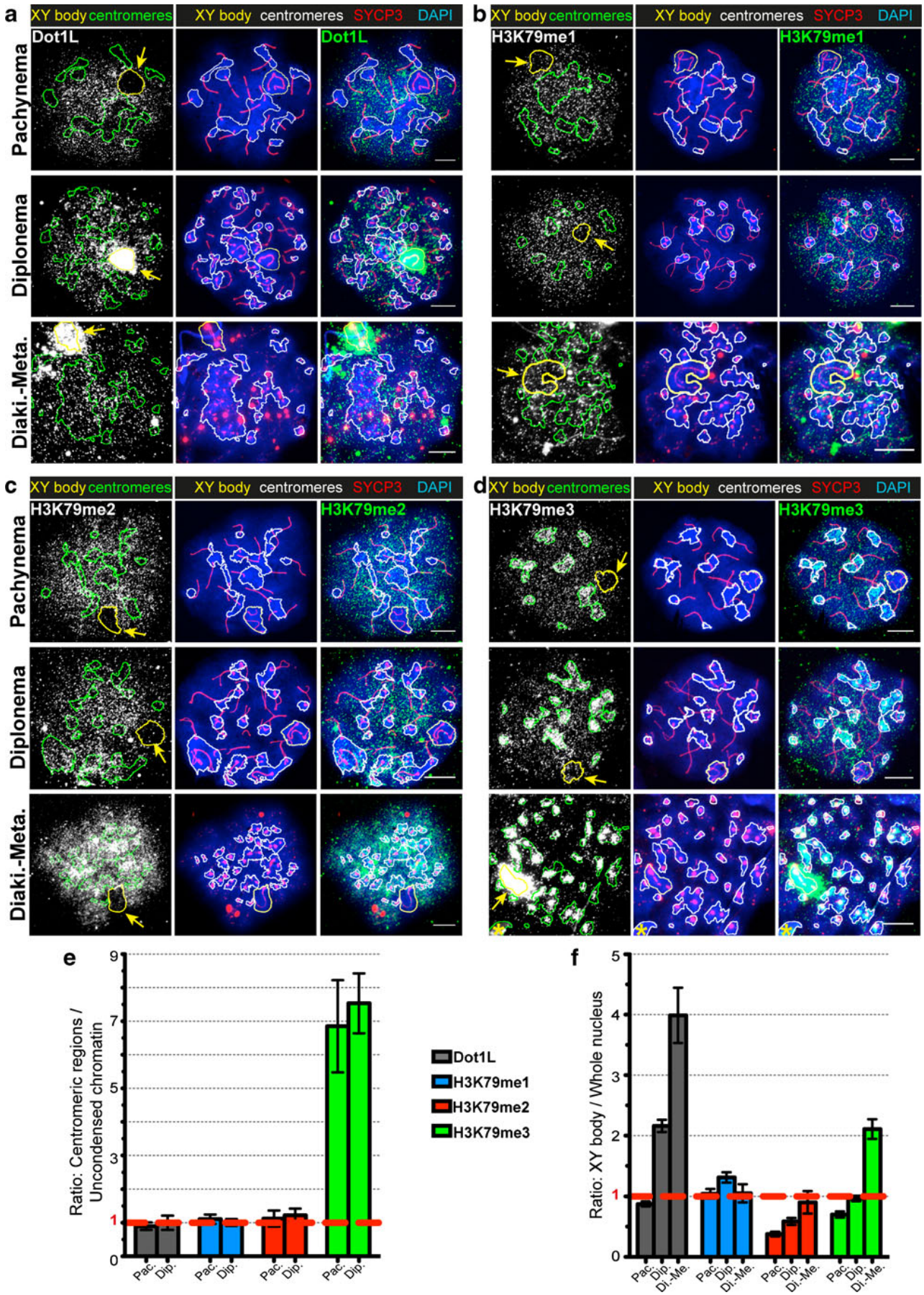
a
XY body centromeres
XY body centromeres SYCP3 DAPI
Dot1L
Dot1L
Pachynema
Diplonema
Diaki.-Meta.
b
XY body centromeres
XY body centromeres SYCP3 DAPI
H3K79me1
H3K79me1
c
XY body centromeres
XY body centromeres SYCP3 DAPI
H3K79me2
H3K79me2
d
XY body centromeres
XY body centromeres SYCP3 DAPI
H3K79me3
H3K79me3
e
Ratio: Centromeric regions / Uncondensed chromatin
0
1
3
5
7
9
Pac.
Dip.
Dot1L
H3K79me1
H3K79me2
H3K79me3
f
Ratio: XY body / Whole nucleus
0
1
2
3
4
5
Pac.
Dip.
Di.-Me.

◀ **Fig. 2** Subnuclear distribution of DOT1L and H3K79me. Localization of DOT1L (**a**), H3K79me1 (**b**), H3K79me2 (**c**) and H3K79me3 (**d**) in representative pachytene, diplotene and diakinesis-metaphase nuclei. In every group of panels, the *left column* is for either DOT1L or each particular H3K79me state (*white*), with the centromeric areas (centromeres) outlined in *green*, and the sex body outlined in *yellow* and marked with an *arrow*. The central column is the merging of SYCP3 (*red*) and DAPI (*blue*), with the centromeric areas (centromeres) outlined in *white* and the sex body in *yellow*. The right column additionally displays DOT1L or the corresponding H3K79me state in *green*. *Yellow asterisks* mark an adjacent cell. Scale bar: 10 μm. **e** Ratio of the area of centromeric regions containing DOT1L or H3K79me signal, relative to the area of the remaining uncondensed autosomal chromatin domains with the corresponding signal. **f** Ratio of the area of the sex body with DOT1L or H3K79me signal, relative to the area of the whole nucleus with signal (excluding the sex body). A more detailed explanation of quantification could be found in the Materials and methods section. *Pac* pachynema, *Dip* diplonema, *Di.-Me.* diakinesis-metaphase I. Error bars are the standard error of mean (*SEM*)

male mouse mutants, but all are infertile (Barchi et al. 2005; Burgoyne et al. 2009; Handel and Schimenti 2010; Kauppi et al. 2011).

Spo11 β-only

The *Spo11*$^{-/-}$ *Tg(Xmr-Spo11* β_B*)*$^{+/+}$ transgenic mouse (hereafter, *Spo11* β-only) exclusively expresses the *Spo11* β splice

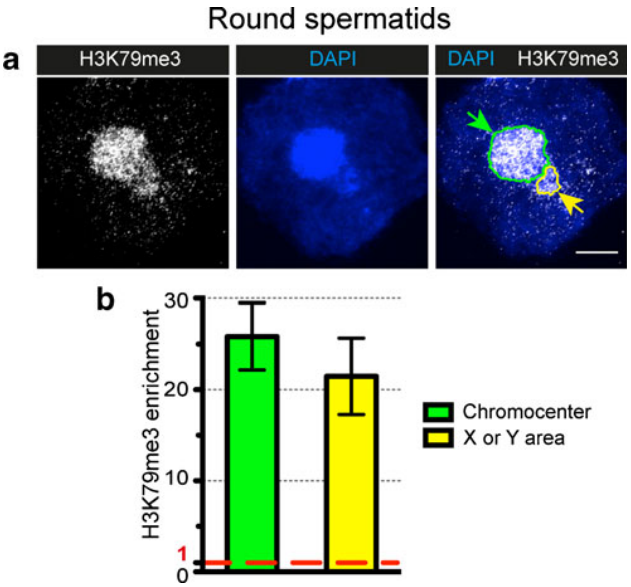

Fig. 3 H3K79me3 accumulates in the chromocenter and the sex chromosome domain at post-meiotic stages. **a** A representative round spermatid stained with DAPI (*blue*) and antibodies to H3K79me3 (*white*) is shown. The chromocenter (*green arrow*) and the sex chromosome, X or Y, domain (*yellow arrow*), displaying differential DAPI intensities, are outlined on the merged panel. **b** Quantification of the H3K79me3 signal present in the chromocenter (*green bar*) and the sex chromosome (*yellow bar*) relative to the signal in the remaining uncondensed chromatin. A total of 15 spermatids were quantified. Scale bar: 10 μm.

variant, which is capable of supporting crossing-over, pairing, and synapsis normally in autosomes, but is defective in promoting late, efficient DSB formation specifically at the PAR (Kauppi et al. 2011). *Spo11* β-only spermatocytes frequently display X-Y association defects that trigger the spindle checkpoint causing apoptosis at metaphase I, so few spermatocytes reach later stages (Kauppi et al. 2011). We analyzed DOT1L localization and the H3K79me state in *Spo11* β-only from leptonema to diplonema (Fig. 4 and Fig. S4a, b). Consistent with prior results, although some sperm were seen (note the sperm head in the lower left corner of the zygotene panel in Fig. 4a, asterisk), few spermatocytes at diakinesis or more advanced stages were found. Also as described previously, the X-Y chromosomes were unsynapsed in most sex bodies (surrounded in yellow in Fig. 4). *Spo11* β-only spermatocytes showed DOT1L staining similar to wild type: little or no signal at leptonema and zygonema, but significant signal during the pachytene and diplotene stages with accumulation at the sex body especially in diplotene nuclei (Fig. 4a and Fig. S4a). H3K79me1 also showed no significant differences from control spermatocytes (Fig. 4b). In contrast, overall H3K79me2 levels were reduced in *Spo11* β-only diplotene nuclei relative to the wild type, although close to the control values for the remaining stages (Fig. 4c). As in the control, the H3K79me2 signal in the *Spo11* β-only sex body was lower than the average for the rest of the nucleus (Fig. S4a). Finally, although H3K79me3 staining in *Spo11* β-only displayed the characteristic increasing trend throughout prophase I progression, the levels were significantly reduced during pachynema and diplonema (Fig. 4d). Nevertheless, H3K79me3 was enriched at centromeric regions in the mutant (Fig. 4d and Fig. S4b).

Trip13$^{mod/mod}$

We analyzed mice carrying a hypomorphic mutation of the yeast *PCH2* ortholog, *Trip13*, referred to as *Trip13*$^{mod/mod}$ for "moderate" defect (Li et al. 2007; Roig et al. 2010). *Trip13*$^{mod/mod}$ males show apparently fully synapsed chromosomes, but there is inefficient repair of meiotic DSBs, aberrant SC development and abnormal sex body formation, triggering a checkpoint response that leads to meiotic arrest and apoptosis at pachynema (Li et al. 2007; Wojtasz et al. 2009; Roig et al. 2010). We found no significant differences between wild type and *Trip13*$^{mod/mod}$ spermatocytes with respect to either distribution or amount of DOT1L, H3K79me1, H3K79me2 or H3K79me3 in leptotene through pachytene spermatocytes (Fig. S2a, b, c, and d, respectively; too few spermatocytes at diplonema or further are found in this mutant, precluding analysis of later stages). H3K79me3 localization in the sex body and centromeric regions was also unaltered (Figs. S2d and S4c, d).

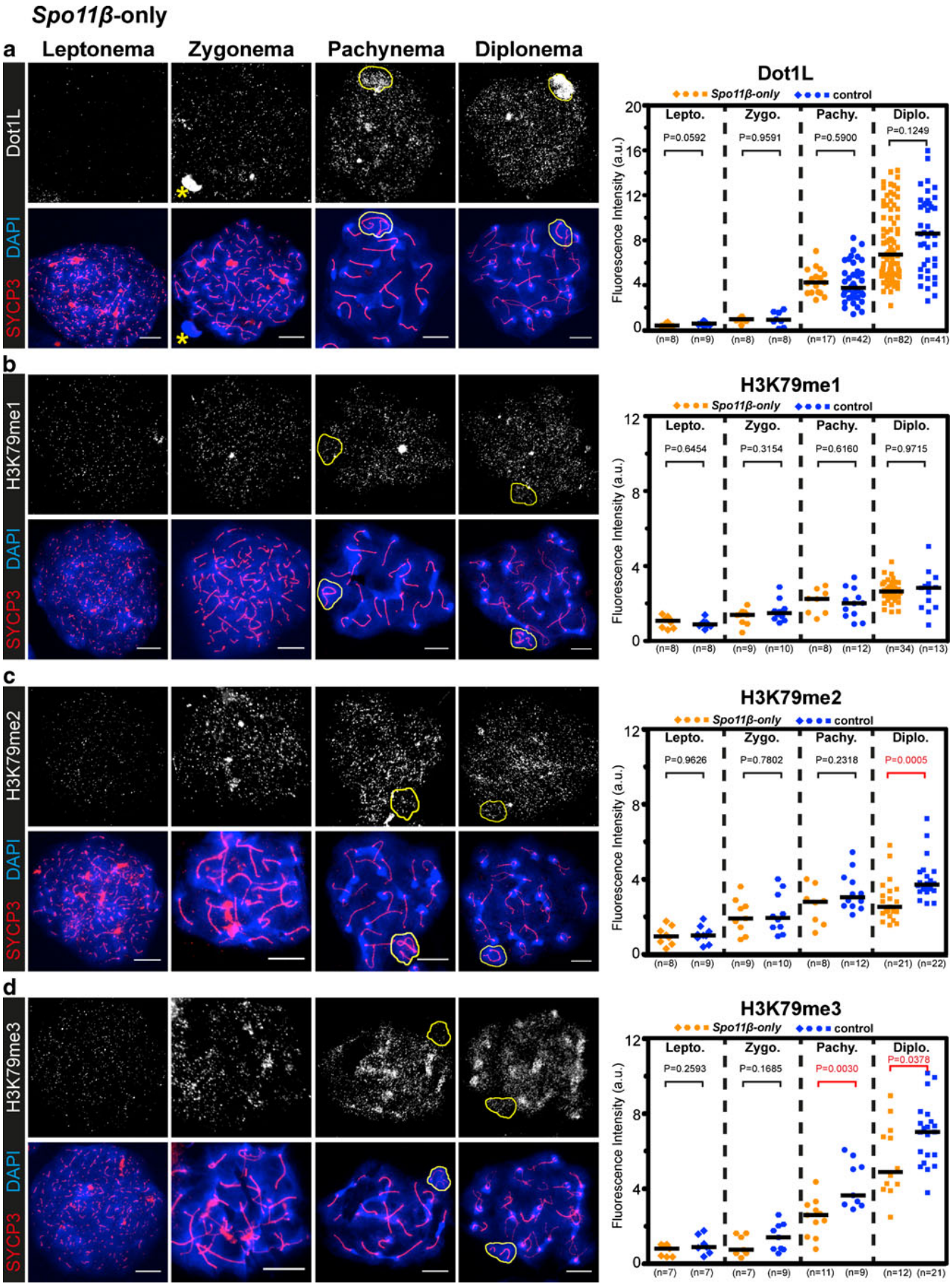
Spo11β-only
a
Leptonema
Zygonema
Pachynema
Diplonema
Dot1L
DAPI
SYCP3
Dot1L
Spo11β-only
control
Lepto.
Zygo.
Pachy.
Diplo.
P=0.0592
P=0.9591
P=0.5900
P=0.1249
Fluorescence Intensity (a.u.)
(n=8) (n=9) (n=8) (n=8) (n=17) (n=42) (n=82) (n=41)
b
H3K79me1
H3K79me1
P=0.6454
P=0.3154
P=0.6160
P=0.9715
(n=8) (n=8) (n=9) (n=10) (n=8) (n=12) (n=34) (n=13)
c
H3K79me2
H3K79me2
P=0.9626
P=0.7802
P=0.2318
P=0.0005
(n=8) (n=9) (n=9) (n=10) (n=8) (n=12) (n=21) (n=22)
d
H3K79me3
H3K79me3
P=0.2593
P=0.1685
P=0.0030
P=0.0378
(n=7) (n=7) (n=7) (n=9) (n=11) (n=9) (n=12) (n=21)

◀ **Fig. 4** DOT1L and H3K79 methylation patterns in the *Spo11* β-only mutant. Immunofluorescence of surface-spread spermatocytes from the *Spo11* β-only mutant stained with antibodies to SYCP3 (*red*) and either DOT1L (**a**), H3K79me1 (**b**), H3K79me2 (**c**) or H3K79me3 (**d**) shown in *white*. DAPI staining of chromatin is shown in *blue*. Representative nuclei for the indicated prophase I stages are presented. The sex body is outlined in *yellow*. Scale bar, 10 μm. The scatter plots show the quantification of the indicated immunofluorescence signal (*a.u.*, arbitrary units) in spermatocytes from the *Spo11* β-only mutant and a littermate heterozygous control [$Spo11^{+/-}$ $Tg(Xmr\text{-}Spo11\ \beta_B)^{+/+}$]. Each *dot* in the graph indicates the value for an individual nucleus. The *central horizontal line* is the median and *n* is the number of nuclei evaluated at each stage. *P* values were calculated by two-tailed Mann–Whitney tests of the indicated pairwise comparisons. $P<0.05$ was considered statistically significant (marked in *red*)

$Spo11^{-/-}$

This mutant lacks the evolutionary-conserved Spo11 transesterase that catalyzes meiotic DSBs, so it exhibits no meiotic recombination and fails in homolog pairing and synapsis. These defects trigger a DNA damage-independent checkpoint that leads to apoptosis at the zygotene–pachytene transition, a so-called zygotene-like stage (Baudat et al. 2000; Romanienko and Camerini-Otero 2000). We examined $Spo11^{-/-}$ spermatocytes from leptotene to the zygotene-like stage, dividing the latter into two classes: early, with shorter SYCP3 stretches and low levels of axial association; and late, with full-length SYCP3 and extensive aberrant non-homologous synapsis (Fig. S3). We found only very low levels of DOT1L and H3K79me1 staining throughout these stages in the $Spo11^{-/-}$ mutant (Fig. S3a, b). H3K79me2 and H3K79me3 increased slightly at the zygotene-like stage (Fig. S3a, b), but in all cases, the signal intensity of DOT1L and all H3K79 methylation states was significantly reduced in the $Spo11^{-/-}$ mutant (Fig. S3).

$Dmc1^{-/-}$

The $Dmc1^{-/-}$ mutant fails to repair meiotic DSBs and exhibits impaired synapsis, leading to arrest and apoptosis in a zygotene-like stage similar to that of $Spo11^{-/-}$ (Pittman et al. 1998; Yoshida et al. 1998). However, molecular markers have revealed differences between the arrests in these two mutants. Specifically, unlike $Spo11^{-/-}$, $Dmc1^{-/-}$ spermatocytes maintain the TopBP1 and γH2AX DNA damage checkpoint factors associated with chromatin, lack the H1t histone variant, and do not establish pseudo-sex bodies (Barchi et al. 2005). Therefore, although both mutants undergo apoptosis at a cytologically similar zygotene-like stage, molecular events indicate that $Dmc1^{-/-}$ spermatocytes are arrested earlier. We monitored DOT1L and H3K79me in $Dmc1^{-/-}$ from leptotene to zygotene-like stages (Fig. 5), divided into early and late categories, as above. Similar to $Spo11^{-/-}$, we found that the levels of DOT1L and all the H3K79 methylation states were significantly lower than in the wild-type control, especially in late zygotene-like spermatocytes (Fig. 5).

Sex body-specific dynamics of H3K79me3 and particular histone variants

To achieve MSCI, chromatin remodeling takes place in the sex body during pachynema. Histone H3 plays an important role in this process, via eviction of the canonical H3.1 and H3.2 forms and replacement by the H3.3 histone variant. As a consequence of this replacement, the PTMs carried by the H3.1/H3.2–H4 tetramers are removed; thus, the chance to establish new marks and/or the need to recover some of the lost ones emerges (van der Heijden et al. 2007). Other histone variants, such as H2A.Z, macroH2A and γH2AX, also exhibit remarkable changes during sex body development (Hoyer-Fender et al. 2000; Fernandez-Capetillo et al. 2003; Greaves et al. 2006). Therefore, we compared the spatio-temporal pattern of DOT1L-dependent H3K79me3 at the sex body with that of those specific histone variants.

In agreement with previous observations (van der Heijden et al. 2007), we found an approximately 4-fold enrichment for the H3.3 variant in the sex body during pachynema and diplonema (Fig. 6a, c). The incorporation of H3.3 appeared to be exclusive for the sex body, since the centromeric regions did not show any particular accumulation of this histone variant (Fig. 6a). Total histone H3 distribution at these stages remained more uniform (Fig. 6b, c).

We found that the progressive enrichment of DOT1L in the sex body from early diplonema correlated with a decrease in γH2AX (Fig. 7a). In addition, the strong accumulation of H3K79me3 in the sex body during diakinesis-metaphase coincided with the complete disappearance of detectable γH2AX signal (Fig. 7b). Therefore, these two histone PTMs (H3K79me3 and γH2AX) are largely mutually exclusive, at least in the sex body. During these stages, H3K79me2 remained low and the H3K79me1 was uniformly weak (see above; Fig. 2b, c).

Finally, we analyzed the dynamics of the histone H2A variants macroH2A and H2A.Z in the sex body. The macroH2A variant defines heterochromatin areas, is enriched in the sex body from pachynema onward, participates in MSCI and disappears at later stages during diakinesis-metaphase I (Hoyer-Fender et al. 2000) (Fig. S5a). In turn, it has been reported that the expression of H2A.Z begins in pachynema and peaks in round spermatids, supporting a role for H2A.Z in maintaining MSCI after disappearance of macroH2A and γH2AX (Greaves et al. 2006). We found H2A.Z all over the nucleus, except for strong exclusion from the sex body during pachynema and early-mid diplonema (Fig. S5b, c). Then, H2A.Z became progressively more abundant in the sex body starting in late diplonema, reaching the same overall levels as the rest of the chromatin during diakinesis-metaphase I (Fig. S5b, c). Therefore, whereas H3K79me3 exhibits limited coexistence with macroH2A at the sex body, its

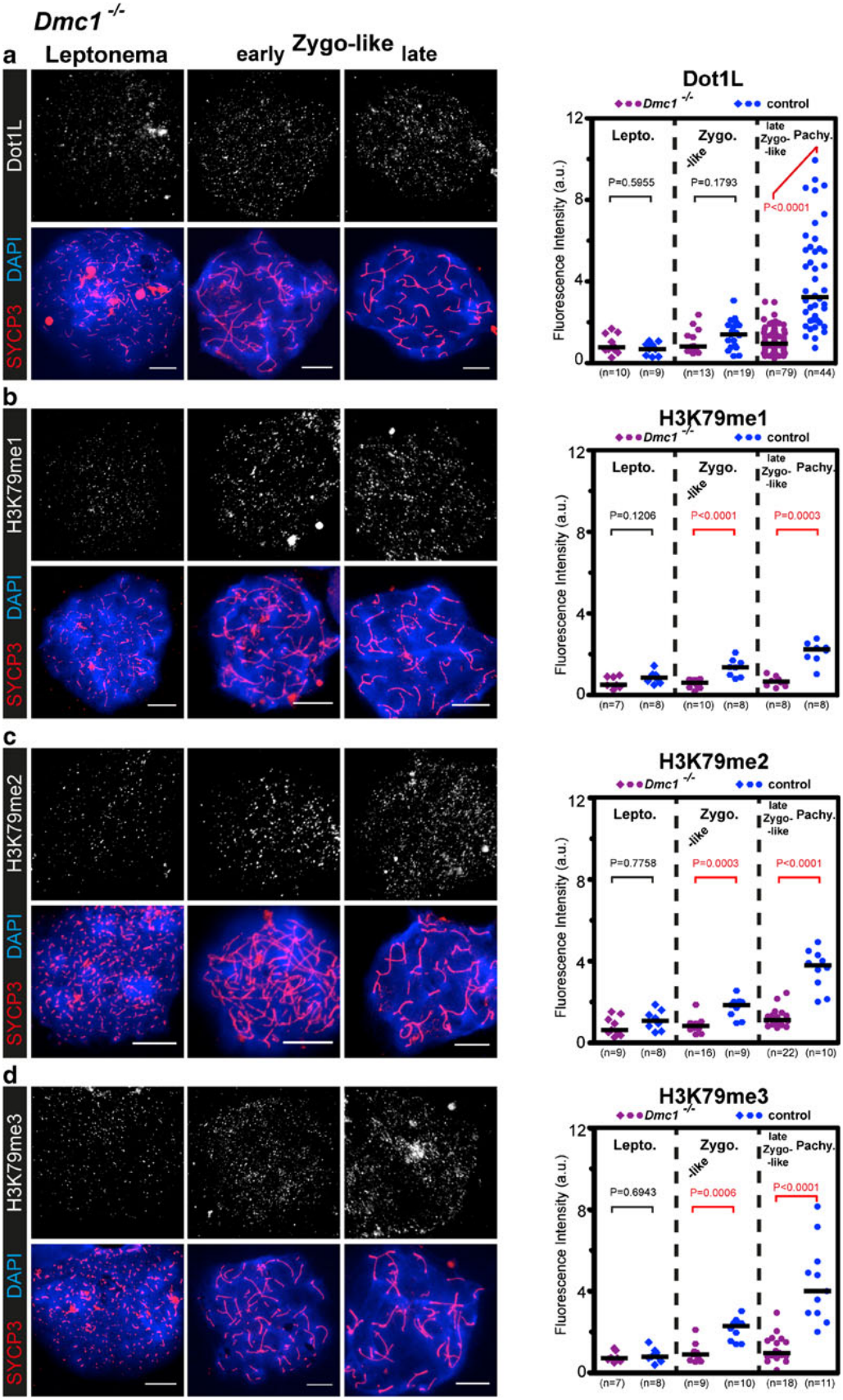

Fig. 5 DOT1L and H3K79 methylation patterns in the *Dmc1*$^{-/-}$ mutant. **a**–**d** Spermatocytes from the *Dmc1*$^{-/-}$ mutant and a littermate *Dmc1*$^{+/-}$ control were analyzed as indicated in Fig. 4

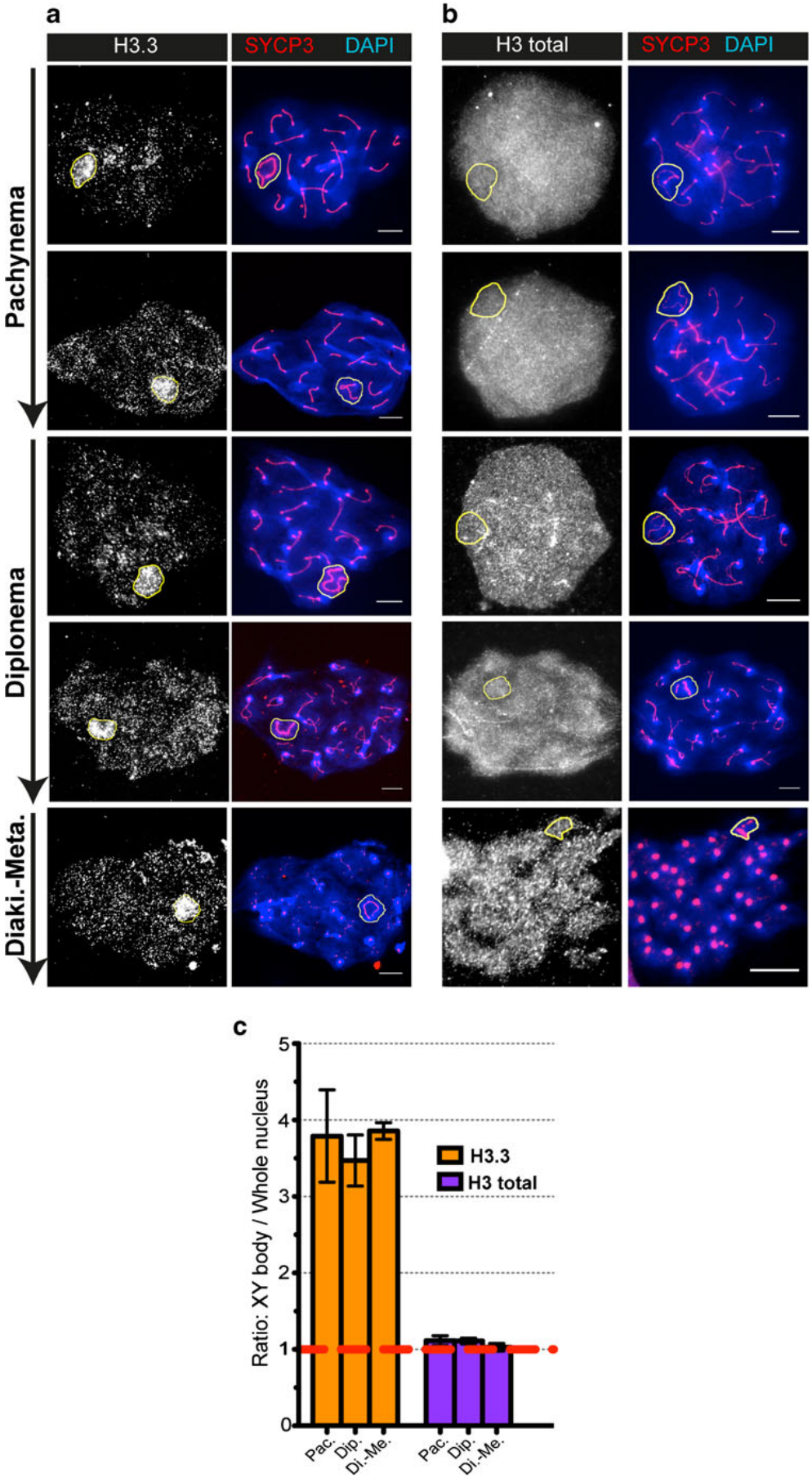

Fig. 6 Enrichment of the H3.3 histone variant in the sex body. **a**, **b** Immunofluorescence of surface-spread wild-type spermatocytes stained with antibodies specific to the H3.3 histone variant (**a**; *white color*) and total histone H3 (**b**; *white color*). The merged images of SYCP3 (*red*) and DAPI (*blue*) are also shown. Representative nuclei for the indicated prophase I stages, determined by the SYCP3 localization pattern, are presented. The sex body is outlined in *yellow*. Scale bars: 10 μm. **c** Ratio of the area of the sex body with H3.3 (*orange bars*) or total H3 (*purple bars*) signal, relative to the area of the whole nucleus with signal (excluding the sex body). *Pac* pachynema, *Dip* diplonema, *Di.-Me.* diakinesis-metaphase. Error bars are the standard error of mean (SEM)

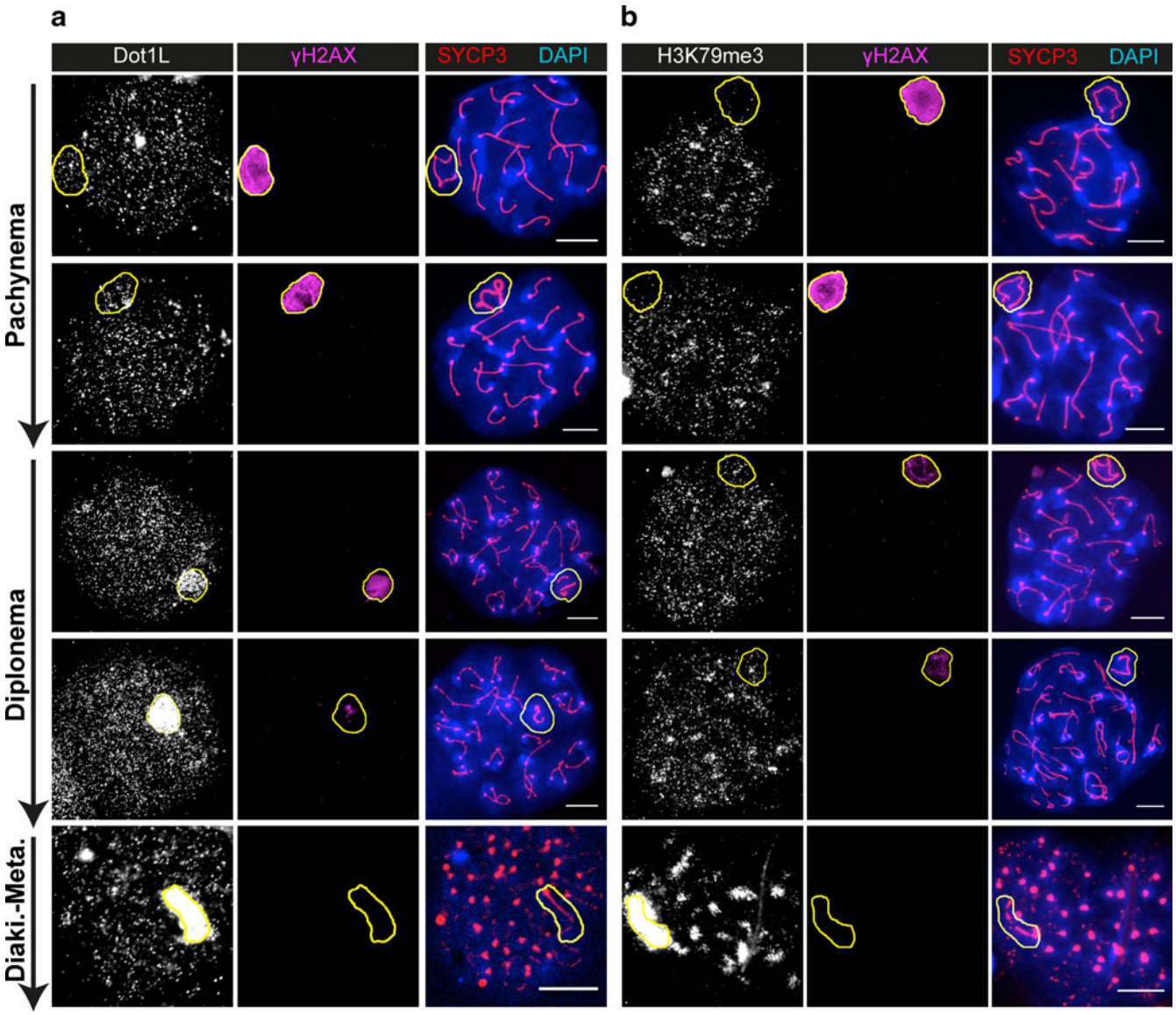

Fig. 7 Accumulation of γH2AX and DOT1L/H3K79me3 at the sex body display largely opposite dynamics. Representative nuclei for pachytene, diplotene and diakinesis-metaphase I stages stained with antibodies to DOT1L (*white*) and γH2AX (*purple*) in **a**, or antibodies to H3K79me3 (*white*) and γH2AX (*purple*) in **b**. The merged images of SYCP3 (*red*) and DAPI (*blue*) are also shown. The XY body is outlined in *yellow*. Scale bars: 10 μm.

accumulation at this region correlates with the deposition of H2A.Z during late prophase I.

Discussion

In this report, we describe the localization of the histone methyltransferase DOT1L during male mouse meiotic prophase I. Since Dot1/DOT1L can mono-, di-, or tri-methylate H3K79, we also followed the dynamics of each individual methylation state resulting from DOT1L activity. Our cytological analyses show that the association of DOT1L with meiotic chromatin increases as prophase I progresses. Interestingly, although the H3K79me2 and H3K79me3 states, but not H3K79me1, also display a progressive increment, they show remarkable differences with respect to the subnuclear distribution, particularly in autosomal chromatin domains, centromeric chromatin, and the sex body. A summary of DOT1L localization and H3K79me patterns throughout prophase I is depicted in Fig. 8. The findings suggest that each H3K79 methylation state may have a specific role during mammalian spermatogenesis. This highly dynamic scenario contrasts with the situation in yeast, where global levels of H3K79me do not significantly change during meiosis (Ontoso et al. 2013). Although the precise chromosomal distribution of the different methylation states remains to be tested in yeast, it

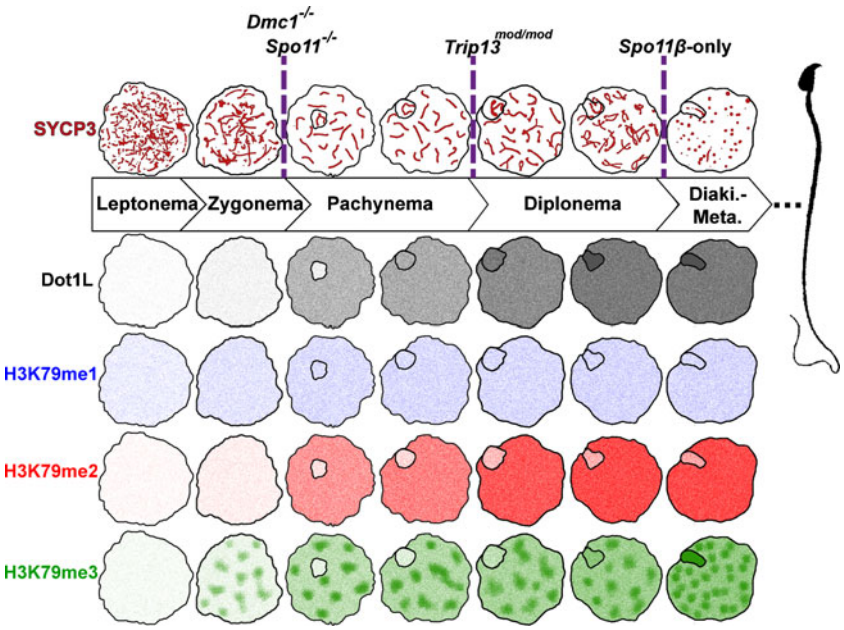

Fig. 8 Summary of DOT1L and H3K79me localization patterns throughout prophase I in mouse spermatocytes. Schematic representation of spermatocytes at different stages of prophase I displaying the characteristic arrangement of SYCP3 (*dark red lines*) and the corresponding pattern for DOT1L (*grey*), H3K79me1 (*blue*), H3K79me2 (*red*) and H3K79me3 (*green*). The color gradation reflects the signal intensity for each marker. The sex body is outlined. The *dashed purple lines* mark the last developmental stage reached by each mutant analyzed (see text for details)

is likely that DOT1L activity during male mouse meiosis is subjected to a more complex regulation.

H3K79me3 in the sex body

Of the extensive chromatin remodeling that accompanies MSCI during early pachynema (Handel 2004; Turner 2007), one of the most dramatic changes is the replacement of histone H3.1/2 by the H3.3 variant, which implies the loss of most of the PTMs already established in the XY chromatin and the opportunity to introduce novel or additional marks (van der Heijden et al. 2007). Tri-methylation of histone H3 at other sites, such as H3K27, is among the repressive PTMs lost from the XY body during pachynema (van der Heijden et al. 2007). We find that the gradual increase of DOT1L all over the nucleus is especially evident in the sex body from diplonema onwards, coincident with the pronounced accumulation of H3.3. The H3.3 histone variant differs from H3.1 or H3.2 only in five or four amino acids, respectively (Fig. S6a), and the H3K79 position, as well as the structure of nucleosomes containing either one of these three H3 variants, is conserved (Fig. S6b–d) (Tachiwana et al. 2011). Moreover, in somatic mammalian cells, the presence of K79me1 and K79me2 in H3.3 has been reported (Hake et al. 2006; Sweet et al. 2010; Zee et al. 2010). Therefore, since DOT1L is the only methyltransferase known for H3K79, it is conceivable that DOT1L is responsible for the extensive tri-methylation of the H3.3 variant at K79 in the sex body during the late stages of meiotic prophase I (Figs. 1 and 2). We note that there is a temporal shift between the prominent localization of DOT1L in the sex body (at diplonema) and the strong accumulation of H3K79me3 (at diakinesis). The additional regulation of DOT1L activity and/or substrate accessibility by other histone PTMs (i.e., H2BK120 ubiquitylation; McGinty et al. 2008) may account for this displacement.

H3K79me3 has been related with transcriptional repression in mammalian somatic cells (Barski et al. 2007). The H3K79me3 enrichment at the XY pair takes place during the diplotene/diakinesis transition when the staining for γH2AX and the repressive macroH2A variant becomes weaker. Nevertheless, it is possible that, although undetectable with our spreading technique, at least a fraction of these histone variants remains associated with the sex chromosomes until later meiotic stages, as occurs in other mammalian species (de la Fuente et al. 2007, 2012; Namekawa et al. 2007). Conversely, H2A.Z, which is initially excluded from the sex body, arrives at this location at the same time as H3K79me3 accumulates. Most of the gene repression started with MSCI remains at postmeiotic stages, and may be linked with imprinted X-inactivation, although a subset of sex chromosome genes is upregulated postmeiotically (Namekawa et al. 2006; Mueller et al. 2008). As has been proposed for H2A.Z (Greaves et al. 2006) and other chromatin modifications, such as H3K9me2 and the recruitment of the heterochromatin proteins HP1β and HP1γ (Namekawa et al. 2006), our results are consistent with a role for DOT1L-mediated H3K79me3 in maintaining silencing of sex chromosomes from diplonema onwards. Curiously, in yeast, H2A.Z and H3K79 methylation also collaborate in the maintenance of differentiated chromatin domains contributing to the establishment of boundaries between the subtelomeric silenced chromatin and the active euchromatin (van Leeuwen et al. 2002; Ng et al. 2003; Meneghini et al. 2003). On the other hand, we demonstrate that the H3K79me2 mark, which is related with active

transcription in somatic cells (Kouskouti and Talianidis 2005; Miao and Natarajan 2005; Zhou et al. 2011), remains largely excluded from the sex body with a faint signal only during late prophase I and metaphase I stages, presumably corresponding to the small fraction of X-linked genes expressed after MSCI (Mueller et al. 2008).

H3K79me3 at the centromeric heterochromatin

H3K79me3 also exhibits strong enrichment in the constitutive heterochromatin at centromeric regions during meiotic prophase I. This tendency was also reported in mouse somatic cells and oocytes, where H3K79me3 colocalizes with the heterochromatin protein HP1β (Ooga et al. 2008). Another histone PTM associated with transcriptional silencing, such as H3K9me3 (Cowell et al. 2002; Wu et al. 2005), similarly accumulates at centromeric regions during mid-prophase I (Page et al. 2012). However, this mark has a wider localization all over the nucleus until mid-pachynema and, unlike H3K79me3, displays a reduced signal in the sex chromosomes from mid-pachynema onwards (Page et al. 2012), coincident with the replacement of H3.1/2 by H3.3. These observations are consistent with a specific role for H3K9me3 in transcriptional repression of the autosomes during early prophase I, and together with H3K79me3 in the establishment of centromeric heterochromatin. However, whereas the H3.3 newly incorporated at the sex body appears to be a favorable substrate for DOT1L and becomes highly tri-methylated at K79 during diplonema/diakinesis, it does not seem to be a target for the Suv39h methyltransferases responsible for H3K9me. Additional histone PTMs at centromeric regions, such as H3K9me2, H4K5ac and H4K16ac (ac, acetylation) also undergo particular dynamics during meiotic prophase I (Khalil and Driscoll 2010). Therefore, distinctive PTM combinations could set up spatial and temporal control of transcriptional repression or (re)activation during particular stages (Greaves et al. 2006; Namekawa et al. 2006; van der Heijden et al. 2007; Mueller et al. 2008; Khalil and Driscoll 2010; Page et al. 2012). Our results suggest that DOT1L-dependent H3K79me3 also impinges on this exquisite control. Consistent with a role for H3K79 methylation in heterochromatin formation it has been shown that DOT1L-deficient mouse embryonic stem cells possess reduced levels of constitutive heterochromatin marks, such as H4K20me3, at subtelomeric regions (Jones et al. 2008). Since DOT1L appears to be the only methyltransferase responsible for H3K79me in mouse (Jones et al. 2008), it is somehow surprising that the accumulation of H3K79me3 at centromeric domains does not correlate with stronger DOT1L staining in these regions. It is possible that the crosstalk with other(s) centromeric-specific histone PTMs may stimulate DOT1L activity specifically at these locations to reach higher levels of the maximum methylation state (i.e., H3K79me3). Alternatively, slower dynamics of histone H3 replacement at centromeres could also explain the accumulation of H3K79me3 (De Vos et al. 2011).

A potential role for H3K79me2 in autosomal transcriptional reactivation

In contrast to H3K79me3, we found a rather homogeneous distribution of H3K79me2 all over the nucleus, except for the exclusion from the sex body. Similar widespread localization has been described in mouse oocytes (Ooga et al. 2008). H3K79me2, like H3K4me3 and various H3 acetylation events, are characteristic marks of active genes in mammalian somatic cells (Kouskouti and Talianidis 2005; Miao and Natarajan 2005; Zhou et al. 2011). The H3K79me2 increase that we detect starting at pachynema and following DOT1L accumulation coincides temporally with the general transcriptional reactivation occurring on autosomes during the transition from mid to late pachynema and continuing in diplonema (Page et al. 2012). In addition, H3K79me2 distribution during prophase I exhibits a similar spatio-temporal pattern to that of H3K9ac and the active form of RNA polymerase II (RNAPII), both strongly associated with active transcription (Page et al. 2012). Furthermore, human DOT1L functionally interacts with actively transcribing RNAPII, which targets the methyltransferase to active genes (Kim et al. 2012a). Therefore, widespread DOT1L-dependent H3K79me2 from pachynema onwards could be an additional element contributing to the resumption of transcription in autosomes when recombination intermediates are resolved and characteristic marks, like γH2AX, and Dmc1/Rad51 foci, disappear. Alternatively, it could be also possible that accumulation of H3K79me2 is a consequence of transcriptional reactivation.

H3K79 methylation in challenged meiosis

Dot1/DOT1L-mediated H3K79me has multiple functions in a variety of biological processes from yeast to mammals (see Introduction; Nguyen and Zhang 2011); but the functional contribution of Dot1 to meiosis has been investigated mostly in budding yeast. Dot1 is not required in unperturbed meiosis, but is essential for the checkpoint responses to the accumulation of unrepaired meiotic DSBs and synapsis defects that occur in yeast *dmc1* and *zip1* mutants, respectively (San-Segundo and Roeder 2000; Ontoso et al. 2013). Unlike other chromatin marks, e.g., γH2AX, neither DOT1L nor H3K79me showed evidence for relocalization or redistribution in various mouse mutants defective at different steps in prophase I. The reduced levels of DOT1L, H3K79me2 and H3K79me3 at the latest stage of development reached in *Spo11*$^{-/-}$ and *Dmc1*$^{-/-}$ mutants are likely the consequence of the arrested meiosis that hampers the progressive accumulation of DOT1L observed in the wild type (Fig. 8). Higher levels of H3K79me2/3 are present in the *Spo11* β-only mouse,

which shows milder meiotic defects, compared to the severely affected and prematurely arrested *Spo11*$^{-/-}$ and *Dmc1*$^{-/-}$ mutants, which barely accumulate those marks. The fact that DOT1L-dependent H3K79 modifications do not relocalize to sites of unrepaired DSBs or unsynapsed chromosomes in these mutants does not preclude a role for DOT1L in the mammalian checkpoints responding to meiotic defects. Actually, in the synapsis-defective *zip1* mutant of budding yeast, global H3K79me levels do not change compared with the wild type, despite the essential role of Dot1-dependent H3K79me in the checkpoint response promoting the *zip1* meiotic delay (Ontoso et al. 2013). Furthermore, in the DNA damage checkpoint triggered by unrepaired DSBs in somatic cells, a similar situation exists, because neither global nor local changes in H3K79 methylation occur, despite its role in the recruitment of mammalian 53BP1 or yeast Rad9 checkpoint adaptors (Huyen et al. 2004; Wysocki et al. 2005). Models involving chromatin remodeling events that locally expose methylated H3K79 residues under certain faulty circumstances have been invoked to explain these findings (Huyen et al. 2004; Wysocki et al. 2005; Ontoso et al. 2013). In the yeast *zip1* mutant, Dot1 promotes the accumulation of the HORMAD1/2 homolog Hop1 on unsynapsed axes to enable activation of the Mek1 checkpoint effector kinase. H3K79me-dependent chromosonal exclusion of the Trip13-homolog Pch2 contributes in part to the regulation of Hop1 localization (Ontoso et al. 2013). Although Pch2's checkpoint role is not restricted to yeast and it also exists in worms and flies (San-Segundo and Roeder 1999; Bhalla and Dernburg 2005; Joyce and McKim 2009), no evidence of the participation of Trip13 in mouse meiotic checkpoints has been found so far (Li et al. 2007; Roig et al. 2010). Therefore, if DOT1L also performs a meiotic checkpoint function in mouse it is unlikely to be exerted via Trip13 regulation.

Concluding remarks

Although functional interpretations from cytological analysis must be taken with caution, our results are consistent with a role for DOT1L and H3K79me at least in the special dynamics of chromatin repression/(re)activation that takes place during male mouse meiotic prophase I. Our observations open several intriguing questions, and more work needs to be done to expand our knowledge about DOT1L and H3K79me meiotic function(s) and regulation. For example, how is the same methyltransferase responsible for two methylated stages at the same target with such different roles? Undoubtedly, a fine regulation must be involved, perhaps mediated through the crosstalk with neighboring PTMs and/or histone variants in each moment and location. Alternatively, or in addition, the several DOT1L splicing isoforms in mice (Zhang et al. 2004) may have different affinities and/or requirements for catalytic activity, or the regulation could be imposed by other components of the DotCom complex (Mohan et al. 2010). Since DOT1L-knockout mice are not viable and die by embryonic day 10.5 (Jones et al. 2008), the development of conditional testis-specific DOT1L-deficient mice would be an invaluable tool to address the functional contribution of H3K79me to various meiotic events.

Acknowledgments We thank the members of the SK and PSS laboratories for useful comments and discussion. We also thank the reviewers for their constructive comments and suggestions improving the manuscript. DO was supported by a predoctoral fellowship (JAE-Predoc) from the CSIC (Spain) and an EMBO short-term fellowship. Research was supported by NIH grant R01 GM105421 (to Maria Jasin and SK) and grants from MINECO (BFU2012-35748), Junta de Castilla y León (CSI025A11-2), and Fundación Ramón Areces to PSS.

References

Acquaviva L, Székvölgyi L, Dichtl B, Dichtl BS, de La Roche Saint André C, Nicolas A, Géli V (2013) The COMPASS subunit Spp1 links histone methylation to initiation of meiotic recombination. Science 339:215–218. doi:10.1126/science.1225739

Anglin JL, Deng L, Yao Y, Cai G, Liu Z, Jiang H, Cheng G, Chen P et al (2012) Synthesis and structure–activity relationship investigation of adenosine-containing inhibitors of histone methyltransferase DOT1L. J Med Chem 55:8066–8074. doi:10.1021/jm300917h

Barchi M, Mahadevaiah S, Di Giacomo M, Baudat F, de Rooij DG, Burgoyne PS, Jasin M, Keeney S (2005) Surveillance of different recombination defects in mouse spermatocytes yields distinct responses despite elimination at an identical developmental stage. Mol Cell Biol 25:7203–7215. doi:10.1128/MCB.25.16.7203-7215.2005

Barchi M, Roig I, Di Giacomo M, de Rooij DG, Keeney S, Jasin M (2008) ATM promotes the obligate XY crossover and both crossover control and chromosome axis integrity on autosomes. PLoS Genet 4:e1000076. doi:10.1371/journal.pgen.1000076

Barry ER, Krueger W, Jakuba CM, Veilleux E, Ambrosi DJ, Nelson CE, Rasmussen TP (2009) ES cell cycle progression and differentiation require the action of the histone methyltransferase Dot1L. Stem Cells 27:1538–1547. doi:10.1002/stem.86

Barski A, Cuddapah S, Cui K, Roh T-Y, Schones DE, Wang Z, Wei G, Chepelev I et al (2007) High-resolution profiling of histone methylations in the human genome. Cell 129:823–837. doi:10.1016/j.cell.2007.05.009

Baudat F, Manova K, Yuen JP, Jasin M, Keeney S (2000) Chromosome synapsis defects and sexually dimorphic meiotic progression in mice lacking Spo11. Mol Cell 6:989–998

Bernt KM, Zhu N, Sinha AU, Vempati S, Faber J, Krivtsov AV, Feng Z, Punt N et al (2011) MLL-rearranged leukemia is dependent on aberrant H3K79 methylation by DOT1L. Cancer Cell 20:66–78. doi:10.1016/j.ccr.2011.06.010

Bhalla N, Dernburg AF (2005) A conserved checkpoint monitors meiotic chromosome synapsis in *Caenorhabditis elegans*. Science 310:1683–1686. doi:10.1126/science.1117468

Bolcun-Filas E, Schimenti JC (2012) Genetics of meiosis and recombination in mice. Int Rev Cell Mol Biol 298:179–227. doi:10.1016/B978-0-12-394309-5.00005-5

Borde V, Robine N, Lin W, Bonfils S, Géli V, Nicolas A (2009) Histone H3 lysine 4 trimethylation marks meiotic recombination initiation sites. EMBO J 28:99–111. doi:10.1038/emboj.2008.257

Brachet E, Sommermeyer V, Borde V (2012) Interplay between modifications of chromatin and meiotic recombination hotspots. Biol Cell 104:51–69. doi:10.1111/boc.201100113

Burgoyne PS, Mahadevaiah SK, Turner JMA (2009) The consequences of asynapsis for mammalian meiosis. Nat Rev Genet 10:207–216. doi:10.1038/nrg2505

Castaño Betancourt MC, Cailotto F, Kerkhof HJ, Cornelis FMF, Doherty SA, Hart DJ, Hofman A, Luyten FP et al (2012) Genome-wide association and functional studies identify the DOT1L gene to be involved in cartilage thickness and hip osteoarthritis. Proc Natl Acad Sci U S A 109:8218–8223. doi:10.1073/pnas.1119899109

Cohen PE, Pollack SE, Pollard JW (2006) Genetic analysis of chromosome pairing, recombination, and cell cycle control during first meiotic prophase in mammals. Endocr Rev 27:398–426. doi:10.1210/er.2005-0017

Cowell I, Aucott R, Mahadevaiah S, Huskisson N, Bongiorni S, Prantera G, Fanti L, Pimpinelli S et al (2002) Heterochromatin, HP1 and methylation at lysine 9 of histone H3 in animals. Chromosoma 111: 22–36. doi:10.1007/s00412-002-0182-8

Daigle SR, Olhava EJ, Therkelsen CA, Majer CR, Sneeringer CJ, Song J, Johnston LD, Scott MP et al (2011) Selective killing of mixed lineage leukemia cells by a potent small-molecule DOT1L inhibitor. Cancer Cell 20:53–65. doi:10.1016/j.ccr.2011.06.009

de la Fuente R, Parra MT, Viera A, Calvente A, Gómez R, Suja JA, Rufas JS, Page J (2007) Meiotic pairing and segregation of achiasmate sex chromosomes in eutherian mammals: the role of SYCP3 protein. PLoS Genet 3:e198. doi:10.1371/journal.pgen.0030198

de la Fuente R, Sánchez A, Marchal JA, Viera A, Parra MT, Rufas JS, Page J (2012) A synaptonemal complex-derived mechanism for meiotic segregation precedes the evolutionary loss of homology between sex chromosomes in arvicolid mammals. Chromosoma 121:433–446. doi:10.1007/s00412-012-0374-9

De Vos D, Frederiks F, Terweij M, van Welsem T, Verzijlbergen KF, Iachina E, de Graaf EL, Maarten Altelaar AF et al (2011) Progressive methylation of ageing histones by Dot1 functions as a timer. EMBO Rep 12:956–962. doi:10.1038/embor.2011.131

Feng Q, Wang H, Ng HH, Erdjument-Bromage H, Tempst P, Struhl K, Zhang Y (2002) Methylation of H3-lysine 79 is mediated by a new family of HMTases without a SET domain. Curr Biol 12:1052–1058

Feng Y, Yang Y, Ortega MM, Copeland JN, Zhang M, Jacob JB, Fields TA, Vivian JL et al (2010) Early mammalian erythropoiesis requires the Dot1L methyltransferase. Blood 116:4483–4491. doi:10.1182/blood-2010-03-276501

Fernandez-Capetillo O, Mahadevaiah SK, Celeste A, Romanienko PJ, Camerini-Otero RD, Bonner WM, Manova K, Burgoyne P et al (2003) H2AX is required for chromatin remodeling and inactivation of sex chromosomes in male mouse meiosis. Dev Cell 4:497–508

Frederiks F, Tzouros M, Oudgenoeg G, van Welsem T, Fornerod M, Krijgsveld J, van Leeuwen F (2008) Nonprocessive methylation by Dot1 leads to functional redundancy of histone H3K79 methylation states. Nat Struct Mol Biol 15:550–557. doi:10.1038/nsmb.1432

Greaves IK, Rangasamy D, Devoy M, Marshall Graves JA, Tremethick DJ (2006) The X and Y chromosomes assemble into H2A.Z, containing facultative heterochromatin, following meiosis. Mol Cell Biol 26:5394–5405. doi:10.1128/MCB.00519-06

Grey C, Barthès P, Chauveau-Le Friec G, Langa F, Baudat F, de Massy B (2011) Mouse PRDM9 DNA-binding specificity determines sites of histone H3 lysine 4 trimethylation for initiation of meiotic recombination. PLoS Biol 9:e1001176. doi:10.1371/journal.pbio.1001176

Hake SB, Garcia BA, Duncan EM, Kauer M, Dellaire G, Shabanowitz J, Bazett-Jones DP, Allis CD et al (2006) Expression patterns and post-translational modifications associated with mammalian histone H3 variants. J Biol Chem 281:559–568. doi:10.1074/jbc.M509266200

Handel MA (2004) The XY body: a specialized meiotic chromatin domain. Exp Cell Res 296:57–63. doi:10.1016/j.yexcr.2004.03.008

Handel MA, Schimenti JC (2010) Genetics of mammalian meiosis: regulation, dynamics and impact on fertility. Nat Rev Genet 11: 124–136. doi:10.1038/nrg2723

Hochwagen A, Amon A (2006) Checking your breaks: surveillance mechanisms of meiotic recombination. Curr Biol 16:R217–228. doi:10.1016/j.cub.2006.03.009

Hoyer-Fender S, Costanzi C, Pehrson JR (2000) Histone macroH2A1.2 is concentrated in the XY-body by the early pachytene stage of spermatogenesis. Exp Cell Res 258:254–260. doi:10.1006/excr.2000.4951

Huyen Y, Zgheib O, Ditullio RA, Gorgoulis VG, Zacharatos P, Petty TJ, Sheston EA, Mellert HS et al (2004) Methylated lysine 79 of histone H3 targets 53BP1 to DNA double-strand breaks. Nature 432:406–411. doi:10.1038/nature03114

Jo SY, Granowicz EM, Maillard I, Thomas D, Hess JL (2011) Requirement for Dot1l in murine postnatal hematopoiesis and leukemogenesis by MLL translocation. Blood 117:4759–4768. doi:10.1182/blood-2010-12-327668

Jones B, Su H, Bhat A, Lei H, Bajko J, Hevi S, Baltus GA, Kadam S et al (2008) The histone H3K79 methyltransferase Dot1L is essential for mammalian development and heterochromatin structure. PLoS Genet 4:e1000190. doi:10.1371/journal.pgen.1000190

Joyce EF, McKim KS (2009) Drosophila PCH2 is required for a pachytene checkpoint that monitors double-strand-break-independent events leading to meiotic crossover formation. Genetics 181:39–51. doi:10.1534/genetics.108.093112

Kalitsis P, Griffiths B, Choo KHA (2006) Mouse telocentric sequences reveal a high rate of homogenization and possible role in Robertsonian translocation. Proc Natl Acad Sci U S A 103:8786–8791. doi:10.1073/pnas.0600250103

Kauppi L, Barchi M, Baudat F, Romanienko PJ, Keeney S, Jasin M (2011) Distinct properties of the XY pseudoautosomal region crucial for male meiosis. Science 331:916–920. doi:10.1126/science.1195774

Keeney S (2008) Spo11 and the formation of DNA double-strand breaks in meiosis. Genome Dyn Stab 2:81–123. doi:10.1007/7050_2007_026

Khalil AM, Driscoll DJ (2010) Epigenetic regulation of pericentromeric heterochromatin during mammalian meiosis. Cytogenet Genome Res 129:280–289. doi:10.1159/000315903

Kim S-K, Jung I, Lee H, Kang K, Kim M, Jeong K, Kwon CS, Han Y-M et al (2012a) Human histone H3K79 methyltransferase DOT1L binds actively transcribing RNA polymerase II to regulate gene expression. J Biol Chem 287:39698–39709. doi:10.1074/jbc.M112.384057

Kim W, Kim R, Park G, Park J-W, Kim J-E (2012b) Deficiency of H3K79 histone methyltransferase Dot1-like protein (DOT1L) inhibits cell proliferation. J Biol Chem 287:5588–5599. doi:10.1074/jbc.M111.328138

Kouskouti A, Talianidis I (2005) Histone modifications defining active genes persist after transcriptional and mitotic inactivation. EMBO J 24:347–357. doi:10.1038/sj.emboj.7600516

Krivtsov AV, Feng Z, Lemieux ME, Faber J, Vempati S, Sinha AU, Xia X, Jesneck J et al (2008) H3K79 methylation profiles define murine and human MLL-AF4 leukemias. Cancer Cell 14:355–368. doi:10.1016/j.ccr.2008.10.001

Lacoste N, Utley RT, Hunter JM, Poirier GG, Côte J (2002) Disruptor of telomeric silencing-1 is a chromatin-specific histone H3 methyltransferase. J Biol Chem 277:30421–30424. doi:10.1074/jbc.C200366200

Lammers JH, Offenberg HH, van Aalderen M, Vink AC, Dietrich AJ, Heyting C (1994) The gene encoding a major component of the lateral elements of synaptonemal complexes of the rat is related to X-linked lymphocyte-regulated genes. Mol Cell Biol 14:1137–1146. doi:10.1128/MCB.14.2.1137.Updated

Li XC, Li X, Schimenti JC (2007) Mouse Pachytene Checkpoint 2 (Trip13) is required for completing meiotic recombination but not synapsis. PLoS Genet 3:e130. doi:10.1371/journal.pgen.0030130

Liebe B, Alsheimer M, Höög C, Benavente R, Scherthan H (2004) Telomere attachment, meiotic chromosome condensation, pairing, and bouquet stage duration are modified in spermatocytes lacking axial elements. Mol Biol Cell 15:827–837. doi:10.1091/mbc.E03-07-0524

Macqueen AJ, Hochwagen A (2011) Checkpoint mechanisms: the puppet masters of meiotic prophase. Trends Cell Biol 21:393–400. doi:10.1016/j.tcb.2011.03.004

McGinty RK, Kim J, Chatterjee C, Roeder RG, Muir TW (2008) Chemically ubiquitylated histone H2B stimulates hDot1L-mediated intranucleosomal methylation. Nature 453:812–816. doi:10.1038/nature06906

Meneghini MD, Wu M, Madhani HD (2003) Conserved histone variant H2A.Z protects euchromatin from the ectopic spread of silent heterochromatin. Cell 112:725–736

Miao F, Natarajan R (2005) Mapping global histone methylation patterns in the coding regions of human genes. Mol Cell Biol 25:4650–4661. doi:10.1128/MCB.25.11.4650-4661.2005

Mohan M, Herz H, Takahashi Y, Lin C, Lai KC, Zhang Y, Washburn MP, Florens L et al (2010) Linking H3K79 trimethylation to Wnt signaling through a novel Dot1-containing complex (DotCom). Genes Dev 24:574–589. doi:10.1101/gad.1898410

Mueller JL, Mahadevaiah SK, Park PJ, Warburton PE, Page DC, Turner JMA (2008) The mouse X chromosome is enriched for multicopy testis genes showing postmeiotic expression. Nat Genet 40:794–799. doi:10.1038/ng.126

Namekawa SH, Park PJ, Zhang L-F, Shima JE, McCarrey JR, Griswold MD, Lee JT (2006) Postmeiotic sex chromatin in the male germline of mice. Curr Biol 16:660–667. doi:10.1016/j.cub.2006.01.066

Namekawa SH, VandeBerg JL, McCarrey JR, Lee JT (2007) Sex chromosome silencing in the marsupial male germ line. Proc Natl Acad Sci U S A 104:9730–9735. doi:10.1073/pnas.0700323104

Ng HH, Feng Q, Wang H, Erdjument-Bromage H, Tempst P, Zhang Y, Struhl K (2002) Lysine methylation within the globular domain of histone H3 by Dot1 is important for telomeric silencing and Sir protein association. Genes Dev 16:1518–1527. doi:10.1101/gad.1001502

Ng HH, Ciccone DN, Morshead KB, Oettinger MA, Struhl K (2003) Lysine-79 of histone H3 is hypomethylated at silenced loci in yeast and mammalian cells: a potential mechanism for position-effect variegation. Proc Natl Acad Sci U S A 100:1820–1825. doi:10.1073/pnas.0437846100

Nguyen AT, Zhang Y (2011) The diverse functions of Dot1 and H3K79 methylation. Genes Dev 25:1345–1358. doi:10.1101/gad.2057811

Nguyen AT, Xiao B, Neppl RL, Kallin EM, Li J, Chen T, Wang D-Z, Xiao X et al (2011) DOT1L regulates dystrophin expression and is critical for cardiac function. Genes Dev 25:263–274. doi:10.1101/gad.2018511

Okada Y, Feng Q, Lin Y, Jiang Q, Li Y, Coffield VM, Su L, Xu G et al (2005) hDOT1L links histone methylation to leukemogenesis. Cell 121:167–178. doi:10.1016/j.cell.2005.02.020

Ontoso D, Acosta I, van Leeuwen F, Freire R, San-Segundo PA (2013) Dot1-dependent histone H3K79 methylation promotes activation of the Mek1 meiotic checkpoint effector kinase by regulating the Hop1 adaptor. PLoS Genet 9:e1003262. doi:10.1371/journal.pgen.1003262

Ooga M, Inoue A, Kageyama S, Akiyama T, Nagata M, Aoki F (2008) Changes in H3K79 methylation during preimplantation development in mice. Biol Reprod 78:413–424. doi:10.1095/biolreprod.107.063453

Page J, de la Fuente R, Manterola M, Parra MT, Viera A, Berríos S, Fernández-Donoso R, Rufas JS (2012) Inactivation or non-reactivation: what accounts better for the silence of sex chromosomes during mammalian male meiosis? Chromosoma 121:307–326. doi:10.1007/s00412-012-0364-y

Parra MT, Viera A, Gómez R, Page J, Benavente R, Santos JL, Rufas JS, Suja JA (2004) Involvement of the cohesin Rad21 and SCP3 in monopolar attachment of sister kinetochores during mouse meiosis I. J Cell Sci 117:1221–1234. doi:10.1242/jcs.00947

Pawlowski WP, Cande WZ (2005) Coordinating the events of the meiotic prophase. Trends Cell Biol 15:674–681. doi:10.1016/j.tcb.2005.10.005

Pittman DL, Cobb J, Schimenti KJ, Wilson LA, Cooper DM, Brignull E, Handel MA, Schimenti JC (1998) Meiotic prophase arrest with failure of chromosome synapsis in mice deficient for Dmc1, a germline-specific RecA homolog. Mol Cell 1:697–705

Roig I, Dowdle JA, Toth A, de Rooij DG, Jasin M, Keeney S (2010) Mouse TRIP13/PCH2 is required for recombination and normal higher-order chromosome structure during meiosis. PLoS Genet 6:e1001062. doi:10.1371/journal.pgen.1001062

Romanienko PJ, Camerini-Otero RD (2000) The mouse Spo11 gene is required for meiotic chromosome synapsis. Mol Cell 6:975–987

San-Segundo PA, Roeder GS (1999) Pch2 links chromatin silencing to meiotic checkpoint control. Cell 97:313–324

San-Segundo PA, Roeder GS (2000) Role for the silencing protein Dot1 in meiotic checkpoint control. Mol Biol Cell 11:3601–3615

Smagulova F, Gregoretti IV, Brick K, Khil P, Camerini-Otero RD, Petukhova G V (2011) Genome-wide analysis reveals novel molecular features of mouse recombination hotspots. Nature 472:375–378. doi:10.1038/nature09869

Sommermeyer V, Béneut C, Chaplais E, Serrentino ME, Borde V (2013) Spp1, a member of the Set1 Complex, promotes meiotic DSB formation in promoters by tethering histone H3K4 methylation sites to chromosome axes. Mol Cell 49:43–54. doi:10.1016/j.molcel.2012.11.008

Steger DJ, Lefterova MI, Ying L, Stonestrom AJ, Schupp M, Zhuo D, Vakoc AL, Kim J-E et al (2008) DOT1L/KMT4 recruitment and H3K79 methylation are ubiquitously coupled with gene transcription in mammalian cells. Mol Cell Biol 28:2825–2839. doi:10.1128/MCB.02076-07

Sweet SMM, Li M, Thomas PM, Durbin KR, Kelleher NL (2010) Kinetics of re-establishing H3K79 methylation marks in global human chromatin. J Biol Chem 285:32778–32786. doi:10.1074/jbc.M110.145094

Tachiwana H, Kagawa W, Osakabe A, Kawaguchi K, Shiga T, Hayashi-Takanaka Y, Kimura H, Kurumizaka H (2010) Structural basis of instability of the nucleosome containing a testis-specific histone variant, human H3T. Proc Natl Acad Sci U S A 107:10454–10459. doi:10.1073/pnas.1003064107

Tachiwana H, Osakabe A, Shiga T, Miya Y, Kimura H, Kagawa W, Kurumizaka H (2011) Structures of human nucleosomes containing major histone H3 variants. Acta Crystallogr D Biol Crystallogr 67:578–583. doi:10.1107/S0907444911014818

Turner JMA (2007) Meiotic sex chromosome inactivation. Development 134:1823–1831. doi:10.1242/dev.000018

van der Heijden GW, Derijck AAHA, Pósfai E, Giele M, Pelczar P, Ramos L, Wansink DG, van der Vlag J et al (2007) Chromosome-wide nucleosome replacement and H3.3 incorporation during mammalian meiotic sex chromosome inactivation. Nat Genet 39:251–258. doi:10.1038/ng1949

van Leeuwen F, Gafken PR, Gottschling DE (2002) Dot1p modulates silencing in yeast by methylation of the nucleosome core. Cell 109:745–756

Wojtasz L, Daniel K, Roig I, Bolcun-Filas E, Xu H, Boonsanay V, Eckmann CR, Cooke HJ et al (2009) Mouse HORMAD1 and HORMAD2, two conserved meiotic chromosomal proteins, are depleted from synapsed chromosome axes with the help of TRIP13 AAA-ATPase. PLoS Genet 5:e1000702. doi:10.1371/journal.pgen.1000702

Wu R, Terry AV, Singh PB, Gilbert DM (2005) Differential subnuclear localization and replication timing of histone H3 lysine 9 methylation states. Mol Biol Cell 16:2872–2881. doi:10.1091/mbc.E04

Wysocki R, Javaheri A, Allard S, Sha F, Côté J, Kron SJ (2005) Role of Dot1-dependent histone H3 methylation in G1 and S phase DNA damage checkpoint functions of Rad9. Mol Cell Biol 25:8430–8443. doi:10.1128/MCB.25.19.8430-8443.2005

Yao Y, Chen P, Diao J, Cheng G, Deng L, Anglin JL, Prasad BVV, Song Y (2011) Selective inhibitors of histone methyltransferase DOT1L: design, synthesis, and crystallographic studies. J Am Chem Soc 133: 16746–16749. doi:10.1021/ja206312b

Yoshida K, Kondoh G, Matsuda Y, Habu T, Nishimune Y, Morita T (1998) The mouse RecA-like gene Dmc1 is required for homologous chromosome synapsis during meiosis. Mol Cell 1:707–718

Zee BM, Levin RS, Dimaggio PA, Garcia BA (2010) Global turnover of histone post-translational modifications and variants in human cells. Epigenetics & Chromatin 3:22. doi:10.1186/1756-8935-3-22

Zhang W, Hayashizaki Y, Kone BC (2004) Structure and regulation of the mDot1 gene, a mouse histone H3 methyltransferase. Biochem J 377: 641–651. doi:10.1042/BJ20030839

Zhang Q, Xue P, Li H, Bao Y, Wu L, Chang S, Niu B, Yang F et al (2013) Histone modification mapping in human brain reveals aberrant expression of histone H3 lysine 79 dimethylation in neural tube defects. Neurobiol Dis 54:404–413. doi:10.1016/j.nbd.2013.01.014

Zhou VW, Goren A, Bernstein BE (2011) Charting histone modifications and the functional organization of mammalian genomes. Nat Rev Genet 12:7–18. doi:10.1038/nrg2905

Electronic Supplementary Materials

Dynamics of DOT1L localization and H3K79 methylation during meiotic prophase I in mouse spermatocytes

Ontoso D, Kauppi L, Keeney S and San-Segundo PA

Supplementary Fig. 1

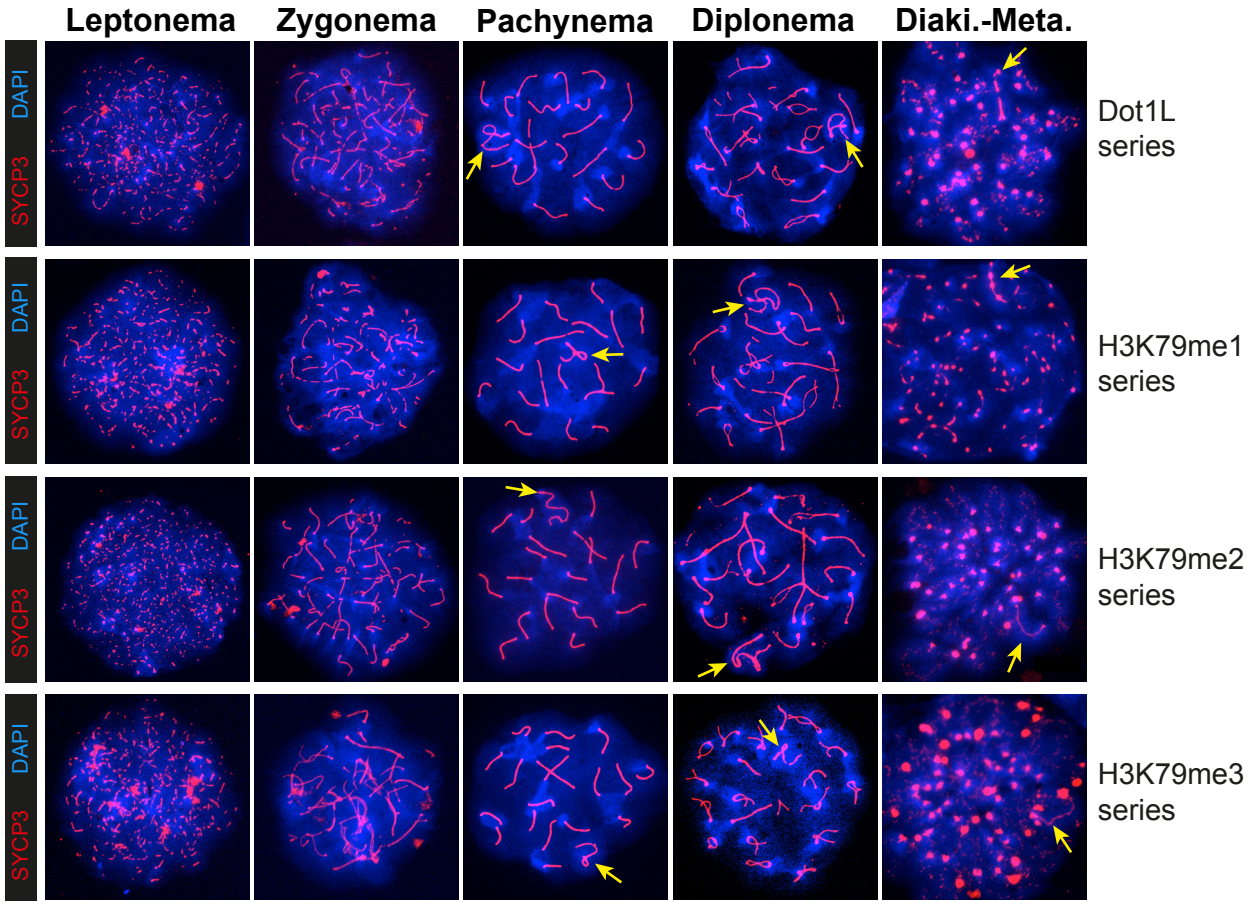

Supplementary Fig. 1 SC morphology in the spermatocytes displayed on Fig. 1. The DAPI and SYCP3 staining corresponding exactly to the same panels presented in the main Fig. 1 are shown alone to facilitate the clear discrimination of SCYP3 morphology in the different prophase I stages. DOT1L, H3K79me1, H3K79me2 and H3K79me3 series refer to the panels shown in the main Fig. 1 displaying those signals, respectively. The sex body is pointed by a yellow arrow.

Supplementary Fig. 2

Trip13 $^{mod/mod}$

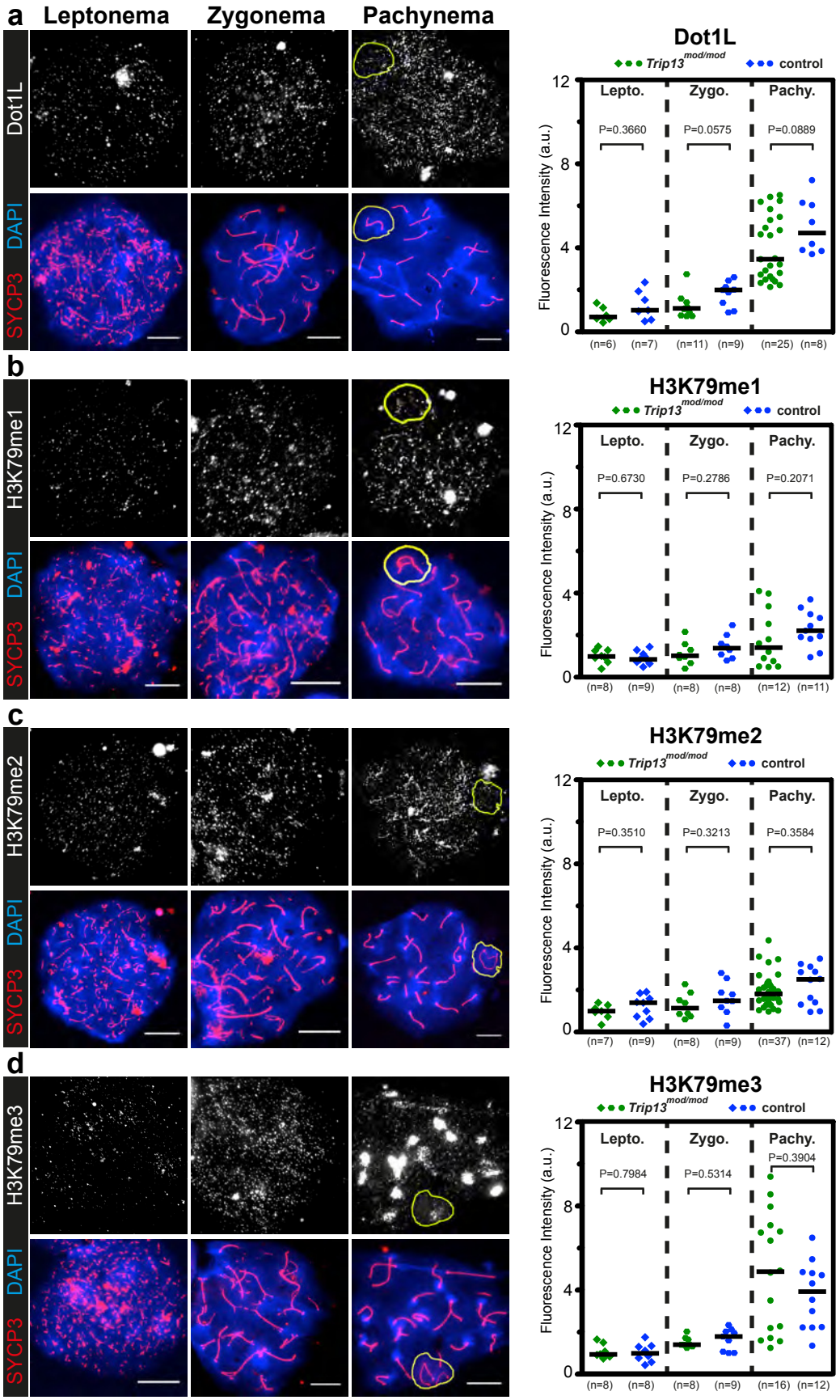

Supplementary Fig. 2 DOT1L and H3K79 methylation patterns in the *Trip13* $^{mod/mod}$ mutant. **a-d** Spermatocytes from the *Trip13*$^{mod/mod}$ mutant and a littermate *Trip13* $^{+/mod}$ control were analyzed as indicated in Fig. 4.

Supplementary Fig. 3

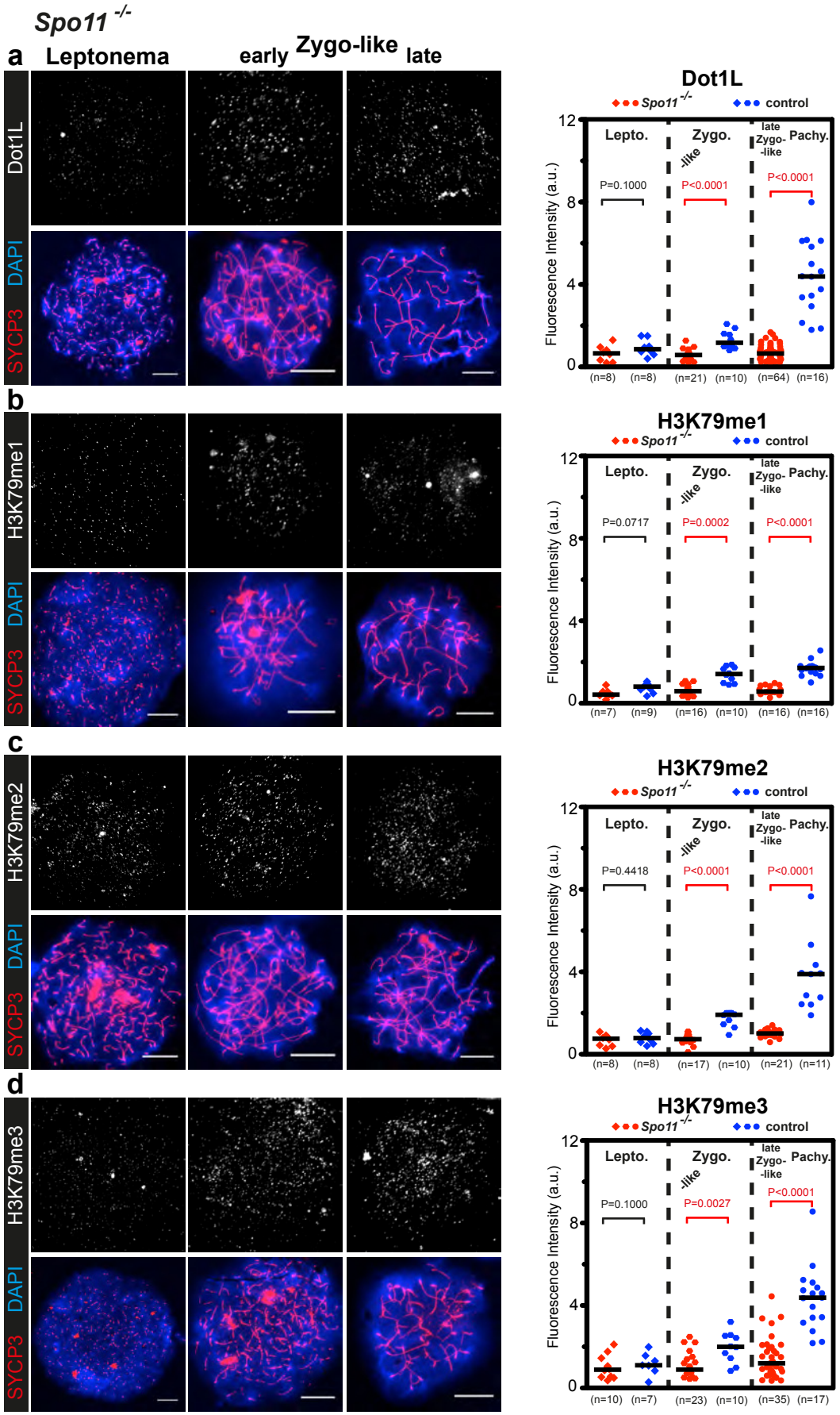

Supplementary Fig. 3 DOT1L and H3K79 methylation patterns in the *Spo11* $^{-/-}$ mutant. **a-d** Spermatocytes from the *Spo11* $^{-/-}$ mutant and a littermate *Spo11* $^{+/-}$ control were analyzed as indicated in Fig. 4.

Supplementary Fig. 4

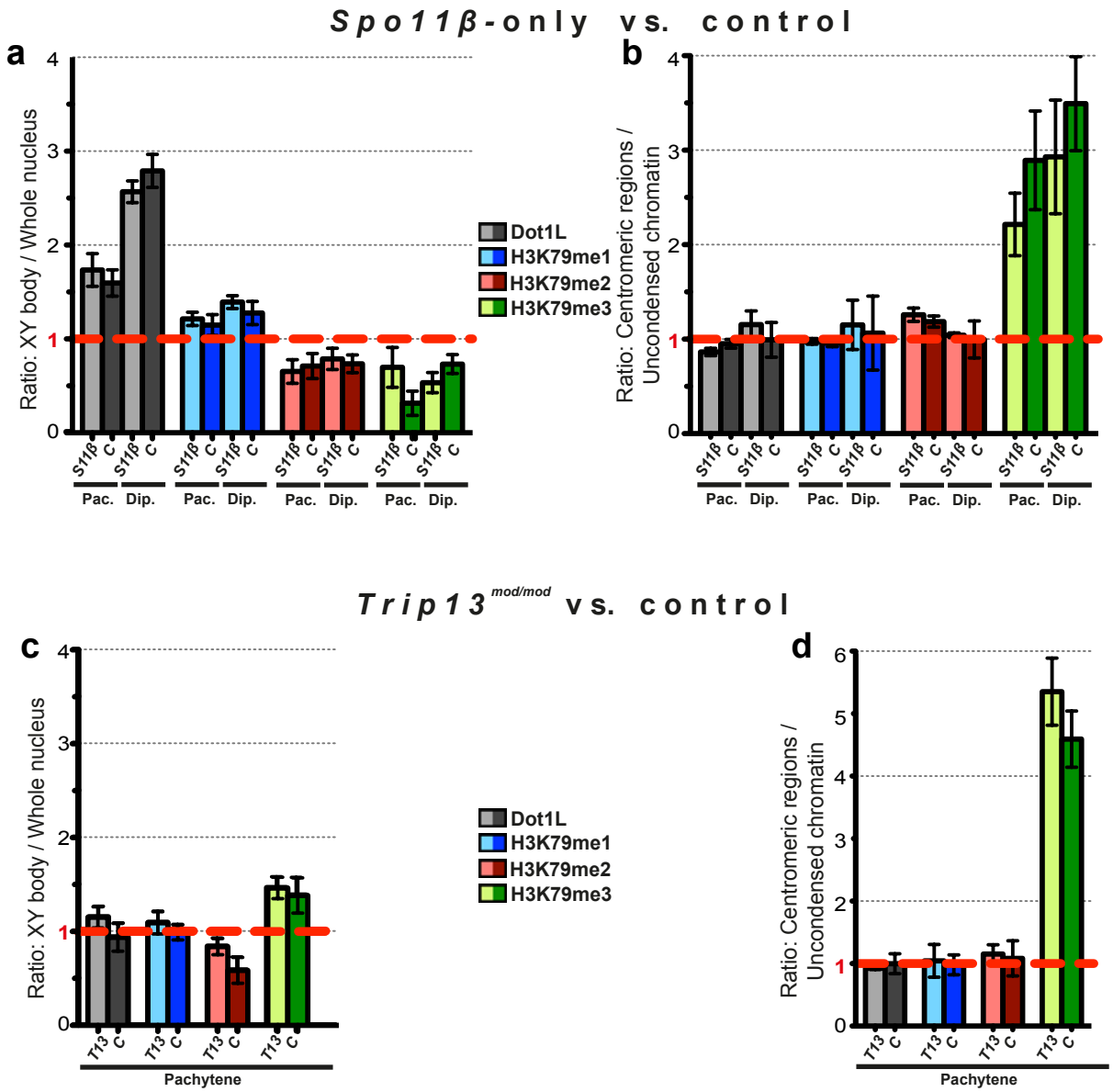

Supplementary Fig. 4 Quantification of DOT1L and H3K79me staining at the sex body and pericentromeric areas in *Spo11β*-only and *Trip13*$^{mod/mod}$ mutants. **a-d** The graphs represent the ratio of the area of the sex body (**a, c**) or the pericentromeric regions (**b, d**) with DOT1L, H3K79me1, H3K79me2 or H3K79me3 signal, relative to the area of the rest of the nucleus with the corresponding signal in the *Spo11β*-only (**a, b**) or the *Trip13*$^{mod/mod}$ (**c, d**) mutants. The indicated prophase stages were analyzed. S11β, *Spo11β*-only; T13, *Trip13*$^{mod/mod}$; C, control; Pac, pachynema; Dip, diplonema. Error bars are the standard error of mean (SEM).

Supplementary Fig. 5

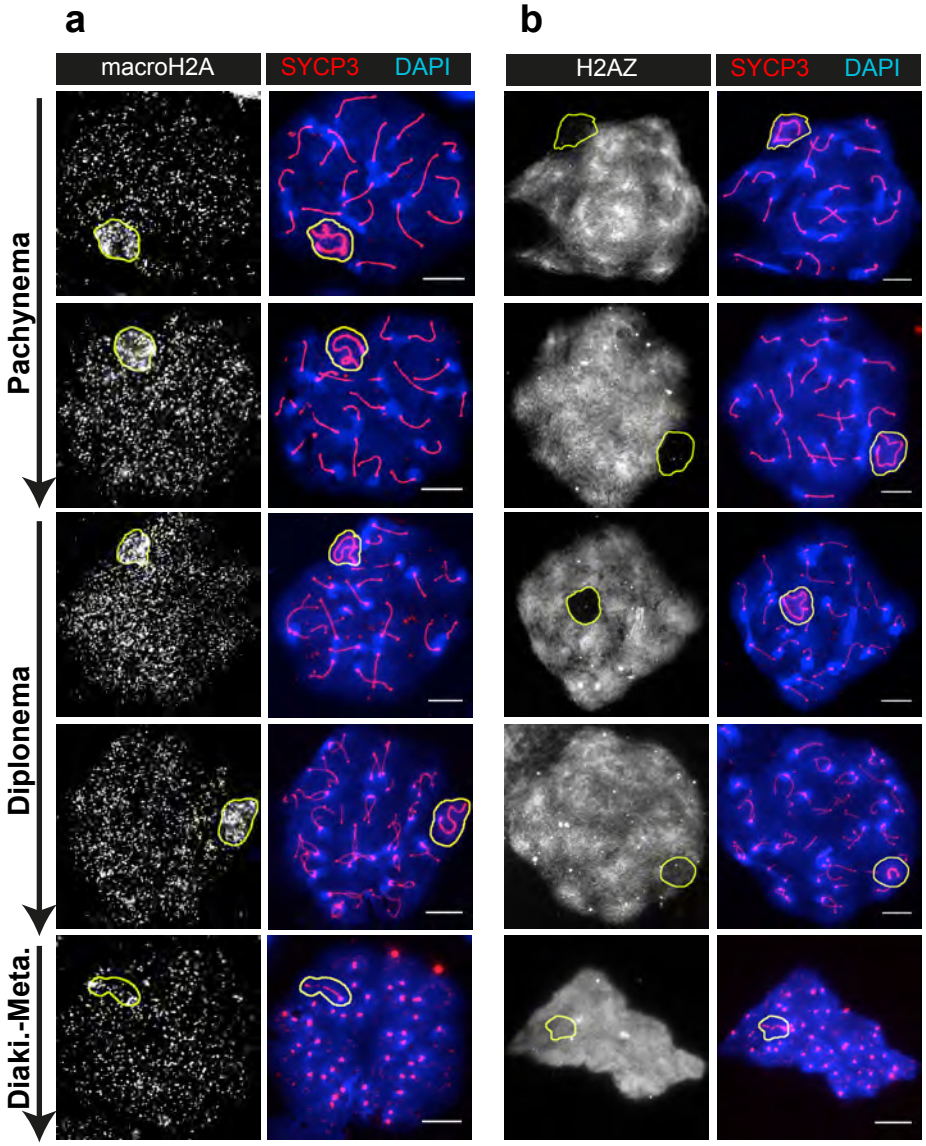

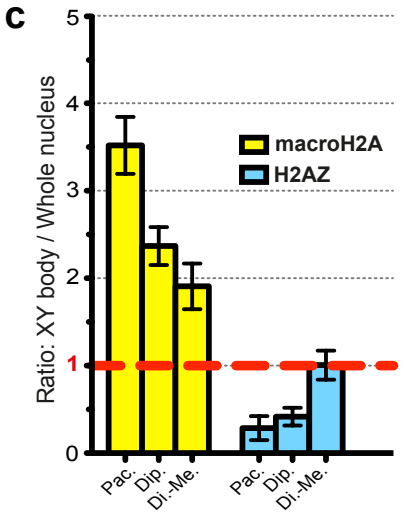

Supplementary Fig. 5 Differential subnuclear distribution of the macroH2A and H2A.Z histone variants. **a, b** Representative nuclei for pachytene, diplotene and diakinesis-metaphase I stages stained with antibodies to macroH2A (**a**; white), or to H2A.Z (**b**; white). The merged images of SYCP3 (red) and DAPI (blue) are also shown. The XY body is outlined in yellow. Scale bars: 10 μm.

c Ratio of the area of the sex body with macroH2A (yellow bars) or H2A.Z (blue bars) signal, relative to the area of the whole nucleus with signal (excluding the sex body). Pac, pachynema; Dip, diplonema and Di.-Me., diakinesis-metaphase. Error bars are the standard error of mean (SEM).

Supplementary Fig. 6

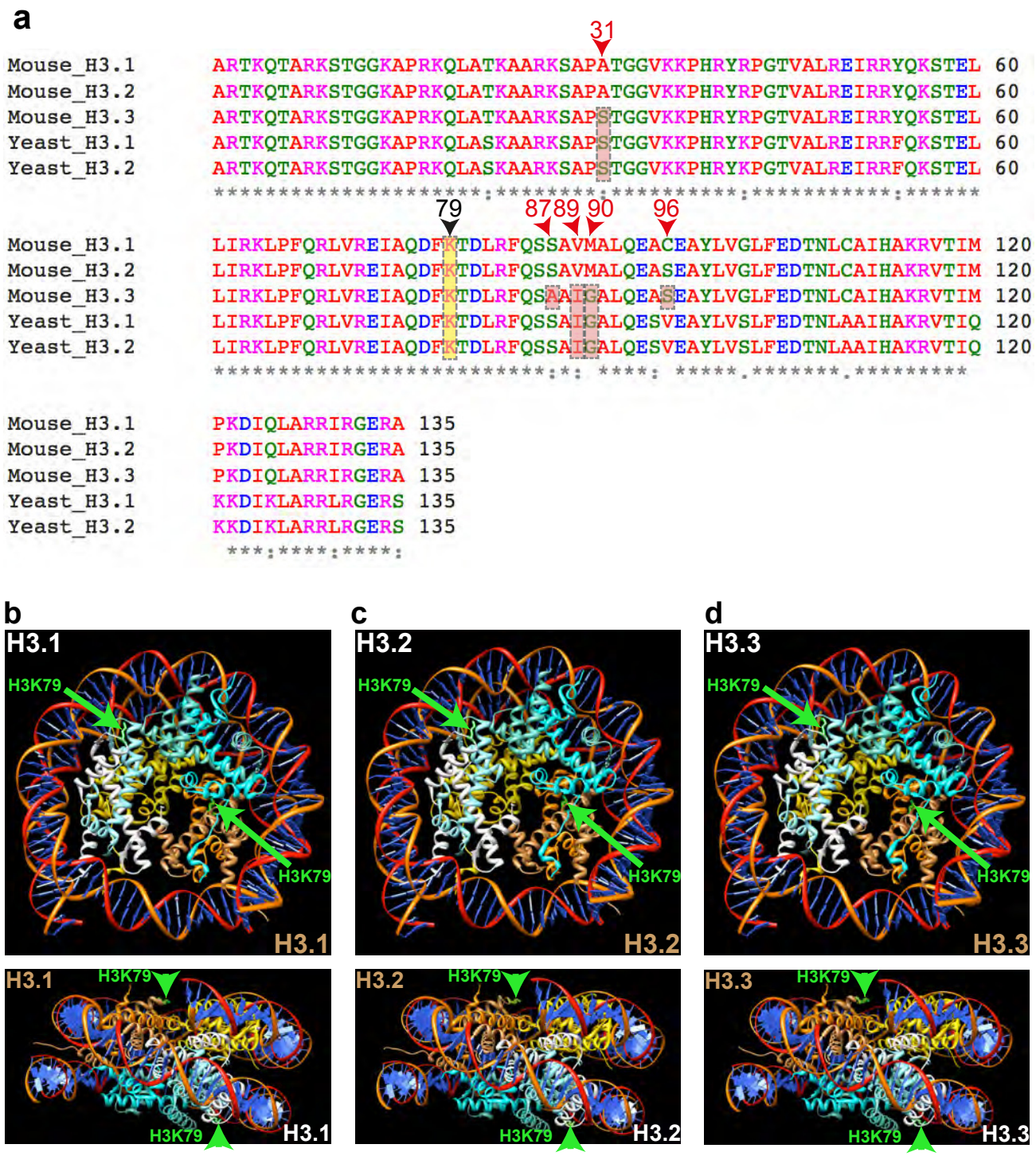

Supplementary Fig. 6 Structural analysis of the K79 position in various histone H3 forms. **a** Sequence alignment of the mouse H3.1, H3.2 and H3.3, and the *Saccharomyces cerevisiae* H3.1 and H3.2 histones. The K79 position (shaded in yellow) is among the majority of evolutionarily conserved residues present in the five sequences. The variant residues are shaded in red. Note that H3.3 only differs in four residues with H3.2 (positions 31, 87, 89 and 90), and in five residues with H3.1 (the previous ones plus the position 96). Curiously, three of the mouse H3.3 specific positions (S31, I89 and G90) are conserved in the yeast H3.1 and H3.2. The A87 is the only exclusive residue of H3.3 compared with all the other H3 histones. **b-d** Crystal structure of human nucleosomes containing H3.1 (**b**), H3.2 (**c**) and H3.3 (**d**) (Tachiwana et al. 2010; Tachiwana et al. 2011). The PDB IDs are 3AFA, 3av1 and 3av2, respectively. The structure of the nucleosomes carrying either H3.1, H3.2, or H3.3 is almost identical. The surface-exposed H3K79 position (green arrow) is not affected by the variant residues in H3.3, even though most of them are in its neighborhood.

CONCLUSIONES

1. La metil-transferasa DOT1L y los distintos estados de metilación de H3K79 presentan dinámicas de localización espacio-temporal específicas a lo largo de la profase meiótica I en espermatocitos de ratón, lo que sugiere funciones diferenciales para cada una de ellas.

2. Aunque H3K79me2 se excluye significativamente del cuerpo sexual, los niveles de H3K79me2 aumentan en las regiones autosómicas a partir de paquitene, de acuerdo con una función relacionada con la reactivación transcripcional autosómica en los estadios tardíos de la profase.

3. La forma H3K79me3 muestra un enriquecimiento progresivo en el cuerpo sexual que correlaciona con el de H2A.Z, con la sustitución de H3.1/H3.2 por la variante H3.3, y con la pérdida de γH2AX y macroH2A, por lo que su incorporación en H3.3 podría contribuir, junto con H2A.Z, al mantenimiento del silenciamiento en determinadas regiones de los cromosomas sexuales a partir de diplotene.

4. La forma H3K79me3 también se concentra en las regiones de heterocromatina centromérica, por lo que podría tener un papel en el silenciamiento estas zonas.

5. La localización de DOT1L y la distribución los distintos estados de metilación de H3K79 no se altera en mutantes de ratón con defectos en sinapsis y/o recombinación, aunque la acumulación de las formas metiladas se interrumpe en el estadio de la profase correspondiente al bloqueo meiótico de cada mutante analizado.

CONCLUSIONS

1. The DOT1L methyltransferase and the different H3K79me states exhibit characteristic spatio-temporal dynamics during meiotic prophase I in mouse spermatocytes, suggesting differential roles for each methylation state.

2. H3K79me2 is largely excluded from the sex body, but H3K79me2 levels increase in autosomal regions from pachynema onwards, consistent with a role in the resumption of transcription in autosomes during late prophase I stages.

3. H3K79me3 shows a progressive enrichment at the sex body, which correlates with that of H2A.Z, with the replacement of H3.1/H3.2 by H3.3 and with the loss of γH2AX and macroH2A. Therefore, trimethylation of K79 in the H3.3 variant at the sex body, together with H2A.Z incorporation, supports a contribution in maintaining silencing of sex chromosomes from diplonema onward.

4. H3K79me3 is also enriched at pericentromeric heterochromatin areas, consistent with a role in silencing these regions.

5. The chromosomal distribution of DOT1L and the different H3K79me states is not altered in mutant mice with defects in synapsis and/or recombination, although the accumulation of H3K79me is blocked at the corresponding prophase I stage where each mutant analyzed undergoes meiotic arrest.

ARTÍCULO 3

Regulation of tolerance to DNA alkylating damage by Dot1 and Rad53 in *Saccharomyces cerevisiae*

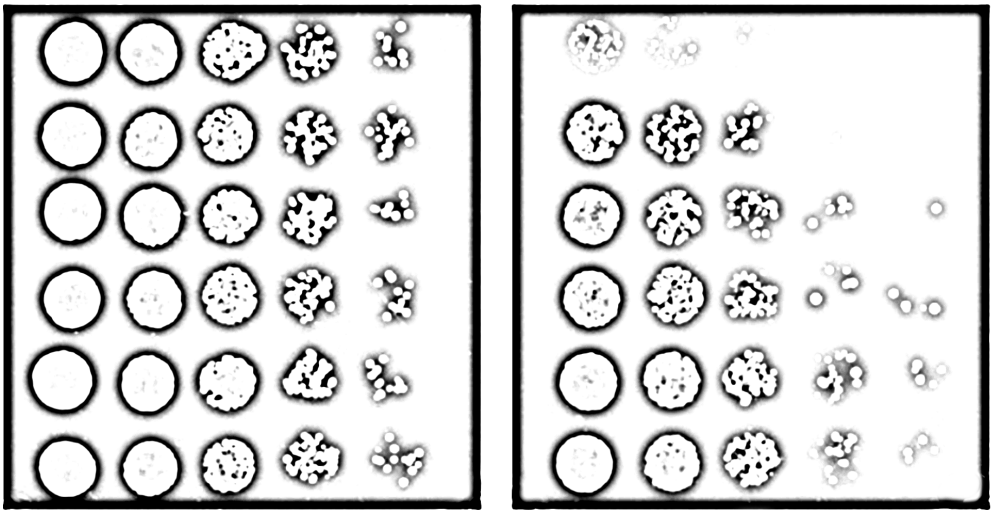

Regulación de la tolerancia al daño alquilante en el DNA por Dot1 y Rad53 en *Saccharomyces cerevisiae*

RESUMEN

Para mantener la integridad genómica, las células tienen que responder correctamente a una variedad de factores tanto exógenos, como endógenos, que provocan lesiones en el genoma e interfieren con la replicación del DNA. Los *checkpoints* de integridad del DNA coordinan esta respuesta ralentizando la progresión del ciclo celular para conceder tiempo a la célula para reparar el daño, estabilizar las horquillas de replicación y estimular la reparación del DNA para recuperar la secuencia y estructura original del DNA. Además, también existen mecanismos de tolerancia al daño, como la síntesis a través de lesión (TLS, del inglés *translesion synthesis*), que es importante para la supervivencia después del daño en el DNA. TLS permite que la replicación continúe sin eliminar la lesión, pero da lugar a una mayor frecuencia de mutagénesis. En este trabajo, hemos investigado la contribución funcional de la metiltransferasa de histona Dot1 y de la quinasa del *checkpoint* Rad53 a la regulación de TLS en *Saccharomyces cerevisiae*. Demostramos que los niveles de metilación de H3K79 mediados por Dot1 modulan la resistencia ante el agente alquilante metil-metano-sulfonato (MMS), que depende de la ubiquitinación de PCNA en la lisina 164. Curiosamente, tanto la ausencia de *DOT1*, que impide la plena activación de Rad53, como la expresión de una versión de *RAD53* etiquetada con *HA*, que produce menos cantidad de la quinasa, confieren un aumento en la resistencia a MMS. Sin embargo, el doble mutante *dot1Δ rad53-HA* es hipersensible al MMS y los niveles de quinasa activada son prácticamente indetectables. Además la sobre-expresión moderada de *RAD53* suprime parcialmente la resistencia a MMS de *dot1Δ*. También encontramos que las células *dot1Δ* y *rad53-HA* tratadas con MMS muestran un aumento en el número de focos de Rev1 asociados a los cromosomas. Proponemos que el umbral de actividad de Rad53 modula de forma precisa la tolerancia al daño por alquilación, al menos en parte, mediante el control de la abundancia del factor clave para la TLS Rev1 unido a la cromatina.

GRAPHICAL ABSTRACT

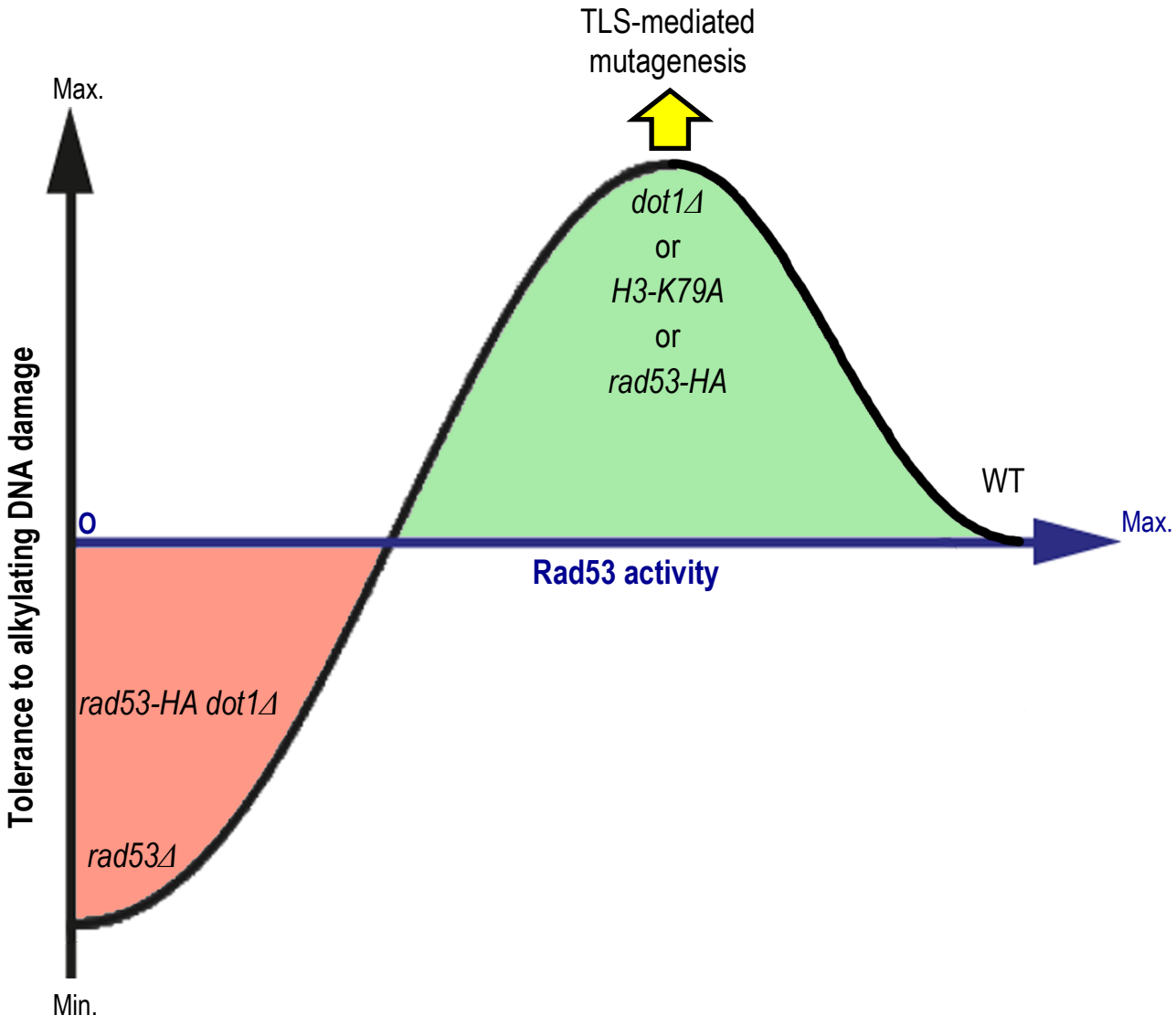

DNA Repair 9 (2010) 1038–1049

Contents lists available at ScienceDirect

DNA Repair

journal homepage: www.elsevier.com/locate/dnarepair

Regulation of tolerance to DNA alkylating damage by Dot1 and Rad53 in *Saccharomyces cerevisiae*

Francisco Conde[a], David Ontoso[a], Isabel Acosta[a], Alfonso Gallego-Sánchez[b], Avelino Bueno[b], Pedro A. San-Segundo[a,*]

[a] Instituto de Microbiología Bioquímica, Consejo Superior de Investigaciones Científicas and University of Salamanca, 37007 Salamanca, Spain
[b] Instituto de Biología Celular y Molecular del Cáncer, Consejo Superior de Investigaciones Científicas and University of Salamanca, 37007 Salamanca, Spain

ARTICLE INFO

Article history:
Received 23 April 2010
Received in revised form 24 June 2010
Accepted 5 July 2010
Available online 31 July 2010

Keywords:
Dot1
Histone modification
Rad53
TLS
DNA damage tolerance

ABSTRACT

To maintain genomic integrity cells have to respond properly to a variety of exogenous and endogenous factors that produce genome injuries and interfere with DNA replication. DNA integrity checkpoints coordinate this response by slowing cell cycle progression to provide time for the cell to repair the damage, stabilizing replication forks and stimulating DNA repair to restore the original DNA sequence and structure. In addition, there are also mechanisms of damage tolerance, such as translesion synthesis (TLS), which are important for survival after DNA damage. TLS allows replication to continue without removing the damage, but results in a higher frequency of mutagenesis. Here, we investigate the functional contribution of the Dot1 histone methyltransferase and the Rad53 checkpoint kinase to TLS regulation in *Saccharomyces cerevisiae*. We demonstrate that the Dot1-dependent status of H3K79 methylation modulates the resistance to the alkylating agent MMS, which depends on PCNA ubiquitylation at lysine 164. Strikingkly, either the absence of *DOT1*, which prevents full activation of Rad53, or the expression of an HA-tagged version of *RAD53*, which produces low amounts of the kinase, confer increased MMS resistance. However, the *dot1Δ rad53-HA* double mutant is hypersensitive to MMS and shows barely detectable amounts of activated kinase. Furthermore, moderate overexpression of *RAD53* partially suppresses the MMS resistance of *dot1Δ*. In addition, we show that MMS-treated *dot1Δ* and *rad53-HA* cells display increased number of chromosome-associated Rev1 foci. We propose that threshold levels of Rad53 activity exquisitely modulate the tolerance to alkylating damage at least by controlling the abundance of the key TLS factor Rev1 bound to chromatin.

1. Introduction

The genome is constantly hit by multiple sources of exogenous and endogenous damage that compromise its integrity. Eukaryotic cells respond to the presence of genome injuries by activating surveillance mechanisms referred to as DNA damage or DNA integrity checkpoints. The inability to properly react to DNA damage results in genome instability, which in mammalian systems is linked to tumor development [1–3].

In *Saccharomyces cerevisiae*, DNA damage is initially detected by the Mec1/Ddc2 (ATR/ATRIP) and the clamp-like Ddc1-Rad17-Mec3 ('9-1-1') complexes. These checkpoint sensors are independently recruited to the sites of damage and trigger the activation of the Rad53 and Chk1 effector kinases in a process mediated by the Rad9 and Mrc1 adaptors. In turn, the effector kinases act on the corresponding targets to promote the different cellular responses to cope with the DNA damage, including cell cycle arrest, stabilization of replication forks and activation of DNA repair [4].

Eukaryotic cells are equipped with a broad range of specialized DNA repair pathways to confront and eliminate the great variety of genomic insults of different nature that can arise during different cell cycle stages, but lesions occurring during S phase that can stall replication forks are particularly threatening [5,6]. Thus, in addition to the repair pathways to remove the lesions, cells possess tolerance mechanisms, such as translesion synthesis (TLS) and template switching, that allow replication to continue despite the presence of DNA damage [7]. These tolerance pathways are critical for survival in the face of DNA damage. TLS is mediated by specialized polymerases that, in contrast to replicative polymerases, are able to insert nucleotides opposite damaged templates, although at the cost of increasing the mutagenesis rate. Therefore, this tolerance pathway must be tightly controlled. In yeast, TLS is performed

Abbreviations: IR, ionizing radiation; MMS, methylmethane sulfonate; PCNA, proliferating cell nuclear antigen; TLS, translesion synthesis; UV, ultraviolet.

* Corresponding author at: Instituto de Microbiología Bioquímica, CSIC-USAL, Edificio Departamental, Lab 313-316, Campus Unamuno, 37007-Salamanca, Spain. Tel.: +34 923124517; fax: +34 923 224876.
E-mail address: pedross@usal.es (P.A. San-Segundo).

1568-7864/$ – see front matter © 2010 Elsevier B.V. All rights reserved.
doi:10.1016/j.dnarep.2010.07.003

Table 1
Saccharomyces cerevisiae strains.

Strain	Genotype	Source/reference
BR1919a	*MATa leu2-3,112 his4-260 ura3-1 ade2-1 thr1-4 trp1-289*	[75]
YP712	BR1919a *lys2ΔNheI zip1::LYS2*	This study
YP1175	BR1919a *lys2ΔNheI zip1::LYS2 dot1::kanMX6*	This study
YP1181	BR1919a *lys2ΔNheI zip1::LYS2 dot1::kanMX6::dot1-G401V::URA3*	This study
YP1185	BR1919a *lys2ΔNheI zip1::LYS2 dot1::kanMX6::dot1-G401A::URA3*	This study
W303-1A	*MATa leu2-3,112 trp1-1 ura3-1 ade2-1 his3-11,15 can1-100 rad5-G535R*	R. Rothstein
W303-1B	*MATα leu2-3,112 trp1-1 ura3-1 ade2-1 his3-11,15 can1-100 rad5-G535R*	R. Rothstein
YAF120	W303-1A *hhf2-hht2::natMX hta1-htb1::hphMX4 hht1-hhf1::kanMX hta2-htb2::natMX GAL1::YLR454w::TRP1* ⟨pRS315-*HTA1-Flag-HTB1*, *HHT1-HHF1*⟩	[46]
YAF124	W303-1A *hhf2-hht2::natMX hta1-htb1::hphMX4 hht1-hhf1::kanMX hta2-htb2::natMX GAL1::YLR454w::TRP1* ⟨pRS315-*HTA1-Flag-HTB1*, *hht1-K79A-HHF1*⟩	[46]
YP1332	YAF120 *dot1::URA3*	This study
YP813[a]	W303-1A *RAD5 bar1::LEU2*	[51]
YP814	W303-1A *RAD5 bar1::LEU2 rad53-3HA::TRP1*	This study
YP1215	W303-1A *RAD5 bar1::LEU2 dot1:kanMX6*	This study
YP1216	W303-1A *RAD5 bar1::LEU2 dot1:kanMX6 rad53-3HA::TRP1*	This study
TH291	W303-1A *RAD5 pol30-K164R*	[48]
YP1553	W303-1B *RAD5 bar1::URA3 pol30-K164R*	This study
YP1554	W303-1A *RAD5 bar1::URA3 pol30-K164R rad53-3HA::TRP1*	This study
YP1217	W303-1B *RAD5 bar1::URA3 pol30-K164R dot1::kanMX6*	This study
U952-3B	W303-1A *RAD5 sml1::HIS3*	[76]
YP558	W303-1A *RAD5 sml1::HIS3 dot1::URA3*	This study
U960-5C	W303-1A *RAD5 sml1-1 rad53::HIS3*	[76]
YP755	W303-1A *RAD5 rad53::HIS3 sml1-1 dot1::kanMX6*	This study
YP1471	W303-1A *RAD5 bar1::LEU2 REV1::13myc::HISMX6*	This study
YP1458	W303-1A *RAD5 bar1::LEU2 REV1::13myc::HISMX6 dot1::kanMX6*	This study
YP1460	W303-1A *RAD5 bar1::LEU2 REV1::13myc::HISMX6 rad53-3HA::TRP1*	This study
YP1531	W303-1A *RAD5 bar1::LEU2 REV1::13myc::HISMX6 pol30-K164R*	This study
BY4742	*MATα his3Δ1 leu2Δ0 ura3Δ0 lys2Δ0*	[77]
NKI3002	BY4742 *dot1::natMX4*	[42]
NKI3018	BY4742 *dot1Δ::dot1-G401V*	F. van Leeuwen

[a] Corresponds to strain YLW70 [51].

by the Polη polymerase (encoded by the *RAD30* gene), and by the Polζ polymerase composed by the Rev3 (catalytic) and Rev7 (regulatory) subunits [8]. In addition, the Rev1 protein also plays a critical role in TLS. Although Rev1 possesses deoxycytidyl transferase activity, its main TLS function is structural and does not rely on the catalytic activity [9,10]. In eukaryotes, DNA damage tolerance is exquisitely controlled by ubiquitylation of the DNA sliding clamp PCNA at the lysine 164 [11]. Thus, Rad6/Rad18-dependent monoubiquitylation of PCNA-K164 triggers TLS, whereas polyubiquitylation of PCNA-K164 through Ubc13/Mms2/Rad5 induces the template-switch error-free mode of damage bypass by sister-strand recombination [7,12–14].

Genome injuries do not occur on the naked DNA, but rather in the context of the highly organized chromatin. Indeed, during the recent years significant advances have been made in understanding the contribution of chromatin modifications to several aspects of the DNA damage response, such as detection, signaling and repair of the damage [15–20]. However, little is known about how chromatin structure may impinge on DNA damage tolerance, although a recent report has described a role for the INO80 remodeling complex in DNA damage tolerance through modulation of PCNA ubiquitylation [21]. Methylation of lysine 79 in histone H3 (hereafter H3K79-me) by the Dot1 methyltransferase is one of the various histone modifications involved in the cellular responses to DNA damage. Dot1 orchestrates several aspects of chromosome metabolism both in mitotic and meiotic cells, including transcriptional silencing [22–25], activation of the meiotic recombination checkpoint and regulation of recombination partner choice in meiosis [26], repair of double-strand breaks by sister-chromatid recombination in mitotic cells [27], and repair of IR- and UV-induced lesions [28–31]. In addition, Dot1 participates in the DNA damage checkpoint in vegetative yeast cells being required for Rad9-mediated activation of the Rad53 effector kinase, at least during the G1-S cell cycle transitions [32,33]. Moreover, we have recently reported that Dot1 negatively regulates the Polζ/Rev1-dependent pathway of tolerance to alkylating DNA damage. Indeed, deletion of *DOT1* results in increased Rev3-dependent mutagenesis [34]. Dot1 is conserved form yeast to human; importantly, altered function of human DOT1L is linked to leukemia development [35–39].

Here we investigate in more detail how Dot1 function contributes to the regulation of DNA damage tolerance. We find that Dot1 modulates the response to the alkylating agent MMS through its catalytic activity on H3K79. In fact, progressively reduced levels of H3K79 tri-methylation result in gradually increased resistance to MMS. In addition, we examine the functional interaction between Dot1 and an HA-tagged version of the Rad53 checkpoint kinase that also promotes increased MMS resistance and mutagenesis [40]. Our results indicate that there is a window of opportunity for TLS to act in the face of MMS lesions that is delineated by threshold levels of Rad53 activity. Moreover, we present evidence indicating that the contribution of Dot1 to DNA damage tolerance is exerted via Rad53 and controls the levels of Rev1 protein associated with chromosomes.

2. Materials and methods

2.1. Strains and plasmids

Yeast strains and plasmids used in this work are listed in Tables 1 and 2, respectively. *REV1-13myc::HISMX6* and *rad53-3HA::TRP1* tagging, as well as *dot1::kanMX6* gene deletion, were performed using standard PCR-based approaches [41]. Plasmid pSS30 was used to generate *dot1::URA3* [26]. Gene modifications were introduced either by direct transformation or by genetic crosses always in an isogenic background. To generate the strains carrying the *dot1-G401A* and *dot1-G401V* alleles at the genomic

Table 2
Plasmids.

Plasmid	Description	Source/reference
pRS315	*CEN LEU2*	[78]
pRS315-DOT1	*CEN LEU2 DOT1*	[42]
pFvL54	*CEN LEU2 dot1-G401A*	[42]
pRS306	*URA3*	[78]
pFF003	*URA3 dot1-G401A*	F. van Leeuwen
pTW043	*URA3 dot1-G401V*	F. van Leeuwen
pRS426	*2μ URA3*	[79]
pSS145	*2μ URA3 RAD53*	This study

locus, the pRS306-based plasmids pFF003 and pTW043, kindly provided by Fred van Leeuwen (NKI, Netherlands) were cut with *Mlu*I and targeted to the *DOT1* promoter in *dot1::kanMX6* strains lacking the whole *DOT1* coding region. Plasmids pRS315-DOT1 and pFvL54, which contain *DOT1* and *dot1-G401V* respectively, in the pRS315 low-copy vector were also provided by F. van Leeuwen [42]. Strains YP712, YP1175, YP1181 and YP1185 carry the *zip1::LYS2* deletion. Zip1 is a meiosis-specific structural component of the yeast synaptonemal complex [43]; therefore, the presence or absence of the *ZIP1* gene does not have any effect in vegetative haploid yeast. Strains harboring the *hht1-K79A* and *pol30-K164R* alleles were kindly provided by Mary Ann Osley (University of New Mexico) and Takashi Hishida (Osaka University), respectively. Functionality of the *REV1-myc* tagged gene was confirmed by the lack of MMS sensitivity. The high-copy plasmid pSS145 containing *RAD53* was constructed by cloning the 3.6-kb *Eco*RI fragment from pCB583 (provided by the lab of M. Foiani, IFOM, Italy) into the 2μ vector pRS426.

2.2. MMS sensitivity assays

Exponentially growing cells were serially diluted in water and 5 μl were spotted onto YPDA plates (YPD supplemented with 50 μg/ml adenine) or YPDA plates containing MMS (Sigma) at various concentrations and incubated at 30 °C. MMS plates were always freshly made. When the strains to be analyzed contained plasmids, cells were grown on selective medium (SC) lacking the corresponding nutrient. Quantification of the MMS resistance was carried out by plating the same number of exponentially growing cells onto YPDA and MMS-containing plates. The MMS resistance was determined by counting the colonies growing on MMS plates relative to the YPDA. Colonies were counted using the colony counting tool of the Quantity One software (Bio-Rad). The quantification was always done at least in triplicate. To calculate the statistical significance of differences in MMS resistance in Fig. 6C, a two-tailed unpaired Student *t*-test was performed using the GraphPad Prism version 4.0 software.

2.3. Western blot analysis

TCA cell extracts were prepared and analyzed essentially as described [34]. SDS-PAGE gels at 15%, 10% and 7.5% were used for detection of histone H3, Dot1 and Rad53, respectively. Antibodies that specifically recognize H3K79-me1 (ab2886), H3K79-me2 (ab3594), H3K79-me3 (ab2621) and total histone H3 (ab1791) were from Abcam and were used at 1:1000 dilution for H3K79-me1 and 1:4000 dilution for the rest. The anti-Rad53 (sc-6749; Santa Cruz Biotechnology) and anti-HA (12CA5; Roche) antibodies were used at 1:2000 dilution. The rabbit polyclonal anti-Dot1 antibody was a kind gift from R. Freire (HUC, Tenerife, Spain) and was used at 1:1000 dilution. HRP-conjugated secondary antibodies were from Santa Cruz or GE Healthcare. The ECL or ECL-Plus reagents (GE Healthcare) were used for detection. For quantification of H3K79 methylation levels, the chemiluminescence signal was captured with a ChemiDoc XRS (Bio-Rad) apparatus and analyzed with the Quantity One software. Only non-saturated bands in the linear range of detection were considered for quantification.

2.4. Citology

Immunofluorescence of nuclear spreads was performed essentially as described [44]. The anti-myc tag antibody (clone 4A6, 05-724; Millipore) was used at 1:500 dilution and the Alexa Fluor 594-conjugated anti-mouse secondary antibody (A11032; Molecular Probes) was used at 1:200 dilution. Images were captured using a Nikon Eclipse 90i fluorescence microscope equipped with an Orca-AG (Hamamatsu) CCD camera and a PlanApo VC 100X/1.4 objective. Images were processed and analyzed with the MetaMorph software (Molecular Devices). Quantification of chromosome-associated Rev1 was performed by counting the number of Rev1 foci in the DAPI-stained area delimited using the MetaMorph tools.

3. Results

3.1. Dot1-dependent histone H3K79 methylation regulates tolerance to alkylating DNA damage

We have previously reported that the absence of Dot1 results in increased resistance to chronic MMS exposure as a consequence of enhanced TLS-mediated tolerance [34]. The only known biochemical function of Dot1 is the mono-, di-, and tri-methylation of lysine 79 in histone H3 [25]. To determine whether regulation of MMS resistance by Dot1 relies on its methyltransferase activity, we analyzed a catalytically inactive *dot1-G401V* mutant, in which the glycine at position 401 in the Dot1 active site has been substituted by a valine (Fig. 1A; [45]). Like *dot1Δ*, the *dot1-G401V* mutant completely lacked detectable H3K79 methyltransferase activity (Fig. 1B) and also displayed enhanced MMS resistance relative to the isogenic wild-type strain (Figs. 1C and 2B), indicating that the catalytic activity of Dot1 is required for its function in MMS tolerance. The only known substrate of Dot1 is H3K79; therefore, to confirm that the MMS resistance of *dot1Δ* is due to the lack of H3K79 methylation, we analyzed an *H3-K79A* mutant, in which the lysine 79 targeted by Dot1 has been replaced by an alanine and cannot be methylated [46]. Like *dot1Δ*, the *H3-K79A* allele conferred increased MMS resistance (Fig. 1D).

To investigate in more detail the regulation of DNA damage tolerance by H3K79 methylation, we examined MMS resistance in strains exhibiting gradually diminished Dot1 catalytic activity. We utilized the combination of two genetic tools to alter the levels of Dot1 activity: (a) use of a *dot1-G401A* mutant (Fig. 1A), which produces a partially active protein [42], and (b) expression of the gene under its own promoter, but from a single-copy plasmid (p[*DOT1*] or p[*dot1-G401A*]), which results in reduced amount of protein (Fig. 2A). Given the distributive mode of action of Dot1 [42], the wild-type strain expressing *DOT1* from its endogenous locus displayed the maximal activity with the highest levels of H3K79-me3 and the lowest levels of H3K79-me1 (Fig. 2A). The catalytic activity was then gradually reduced, as manifested by decreasing levels of H3K79-me3 and increasing levels of H3K79-me1, following this sequence: *DOT1* > p[*DOT1*] > *dot1-G401A* > p[*dot1-G401A*] > *dot1-G401V* ≈ *dot1Δ* (Fig. 2A). Interestingly, we found that the progressive reduction of Dot1 activity led to a gradually elevated MMS resistance (Fig. 2B and D). In particular, quantification of the relative levels of each methylation state revealed a clear correlation between the drop of H3K79-me3 and the enhanced resistance to MMS (Fig. 2C and D). Thus, tolerance to alkylating damage is finely modulated by H3K79 methylation levels.

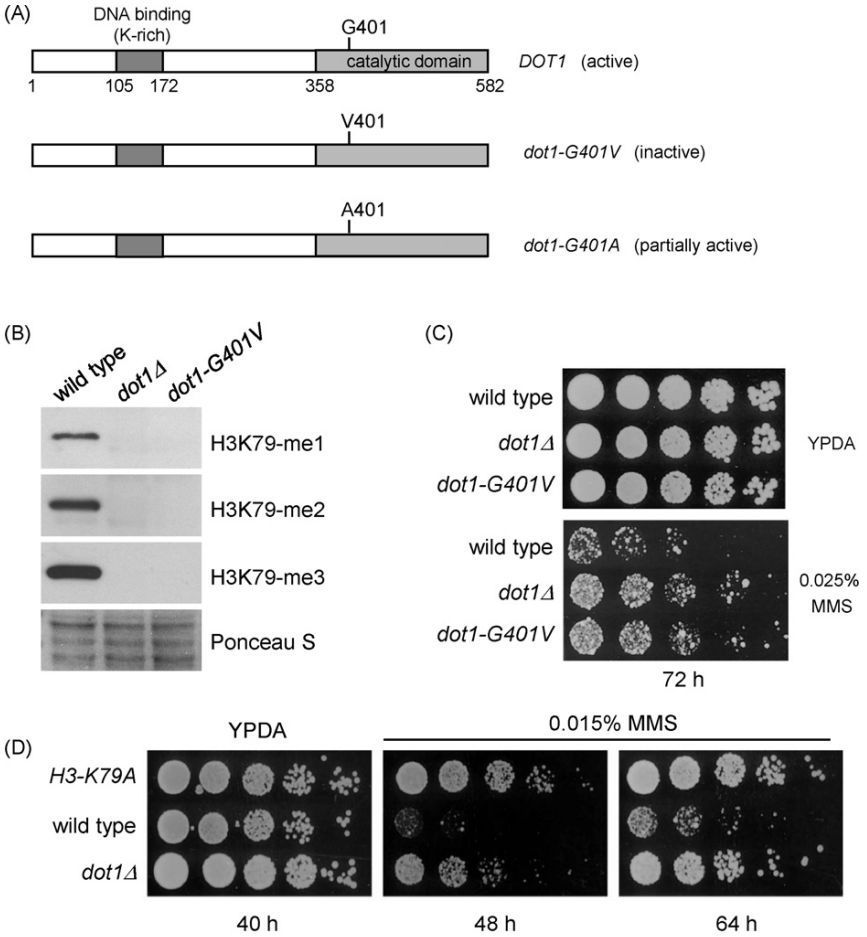

Fig. 1. The regulation of MMS resistance by Dot1 relies on its H3K79 methyltransferase activity. (A) Schematic representation of the Dot1 protein with the glycine at position 401 in the catalytic domain that has been mutated to valine or alanine in the *dot1* alleles generated, as indicated. (B) Western blot analysis of H3K79 mono-, di- and tri-methylation in wild type (BY4742), *dot1Δ* (NKI3002) and *dot1-G401V* (NKI3018) strains. Ponceau S staining is shown as a loading control. (C) Five-fold serial dilutions of exponentially growing cells from the strains used in (B) were spotted onto YPDA and 0.025% MMS plates and incubated for 72 h. (D) Five-fold serial dilutions of exponentially growing wild-type (YAF120), *H3-K79A* (YAF124) and *dot1Δ* (YP1332) cells were spotted onto YPDA and 0.015% MMS plates and incubated for the indicated time.

3.2. The MMS resistance of dot1Δ depends on PCNA ubiquitylation at lysine 164

Our previous observations indicated that the increased MMS resistance and mutagenesis frequency of *dot1Δ* is as a consequence of enhanced tolerance mediated by the TLS pathway of DNA damage bypass, because it is abolished in the absence of Polζ/Rev1 [34]. DNA damage-induced PCNA ubiquitylation at lysine 164 is carried out by the Rad6/Rad18 (E2–E3) complex [7,11,47] and it is a key regulator of the tolerance to genotoxic insults (Fig. 3A; [12]). Therefore, to determine whether the MMS resistance conferred by the absence of Dot1-promoted H3K79 methylation relies on this PCNA modification, we deleted *DOT1* in a PCNA ubiquitylation-deficient *pol30-K164R* mutant [48]. As expected, the *pol30-K164R* mutant was extremely sensitive even to low MMS concentrations (Fig. 3B), underscoring the importance of DNA damage tolerance pathways in promoting viability after alkylating damage [11]. However, although the absence of Dot1 suppresses the sensitivity of an ample range of mutants impaired in coping with MMS-induced lesions [34], deletion of *DOT1* failed to suppress the MMS sensitivity of *pol30-K164R* (Fig. 3B). Moreover, the *dot1Δ pol30-K164R* double mutant was more sensitive to MMS than *pol30-K164R* (Fig. 3B). Likewise, the *rev3Δ dot1Δ* or *rev1Δ dot1Δ* double mutants are also more sensitive to MMS than *rev3Δ* or *rev1Δ* [34]. These observations unveil the additional role of Dot1 in another process, such as homologous recombination [27], which becomes more relevant to deal with MMS damage in the absence of TLS.

3.3. Threshold levels of Rad53 activity modulate DNA damage tolerance

Previous studies have shown that, like *dot1Δ*, cells expressing an HA-tagged version of the Rad53 checkpoint kinase display increased MMS resistance and increased MMS-induced mutagenesis frequency ([40]; see also Fig. 5C). Moreover, recent observations indicate that the enhanced MMS resistance of *rad53-HA* also requires PCNA-K164 ubiquitylation (Fig. 3B) and TLS activity (AGS and AB, unpublished results).

Thus, the similar phenotypes of *dot1Δ* and *rad53-HA* prompted us to further explore the possible relationship between Dot1 and Rad53 in the regulation of MMS resistance, as we have previously proposed [34]. Indeed, we found that the enhanced MMS resistance of *dot1Δ* was abolished in the absence of Rad53 because a *rad53Δ dot1Δ* double mutant showed similar MMS sensitivity than *rad53Δ* (Fig. 4); therefore, MMS resistance conferred by *dot1Δ* requires Rad53 function.

Activation of Rad53 can be monitored by a well-characterized phosphorylation-dependent electrophoretic mobility shift [49]. In the *dot1Δ* mutant, Rad53 is not fully activated in response to MMS

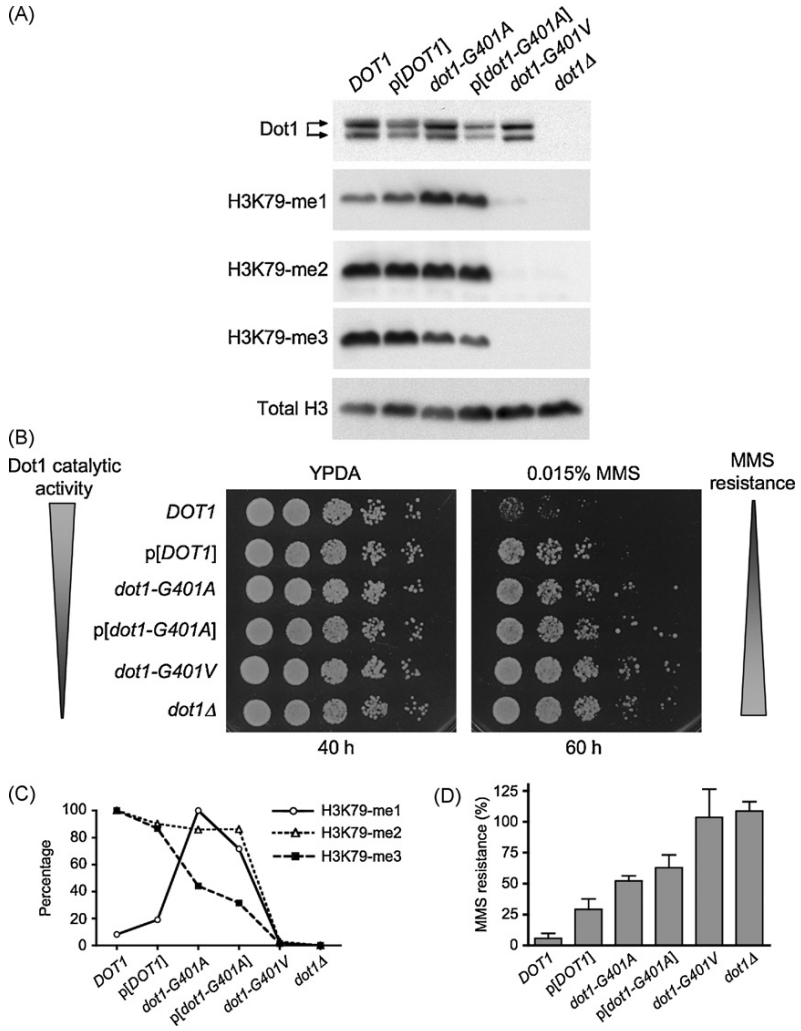

Fig. 2. The status of H3K79 methylation modulates tolerance to MMS. (A) Western blot analysis of strains producing the different versions of Dot1 either from the endogenous loci (*DOT1*, *dot1-G401A* and *dot1-G401V*) or from a single-copy plasmid (p[*DOT1*] and p[*dot1-G401A*]), as indicated. The *dot1Δ* mutant was also included. Note that the two isoforms of Dot1 detected correspond to two alternative translational start sites [74]. Exponentially growing cells on SC-Leu were treated with 0.02% MMS for 2 h. Cell extracts were analyzed with anti-Dot1 antibodies and with antibodies that specifically recognize the mono-, di- and tri-methylated forms of H3K79 or the total histone H3, as indicated. Strains are: YP712 + pRS315 (*DOT1*), YP1175 + pRS315-DOT1 (p[*DOT1*]), YP1185 + pRS315 (*dot1-G401A*), YP1175 + pFvL54 (p[*dot1-G401A*]), YP1181 + pRS315 (*dot1-G401V*) and YP1175 + pRS315 (*dot1Δ*). (B) Five-fold serial dilutions of cultures from the same strains analyzed in (A) were spotted onto YPDA and 0.015% MMS plates incubated for the indicated time. (C) Quantification of the relative levels of H3K79 mono-, di- and tri-methylation from the same strains used in (A). The maximum value of each methylation state resulting from the average of three experiments was considered 100%. (D) Quantification of the MMS resistance. Colonies were counted after 40 h of incubation on YPDA and 0.015% MMS plates. Average and standard deviation from three independent counts are presented.

([32]; Fig. 5A, lanes 3 and 4). In contrast, in the *rad53-HA* mutant, although the Rad53-HA protein can be activated to the same extent as the wild-type protein, it is produced in much lower amounts and, consequently, also renders reduced levels of Rad53 activity ([40]; Fig. 5A and B). These observations suggest that the sub-optimal levels of Rad53 activity present in *dot1Δ* or *rad53-HA* cells lead to increased MMS resistance. Therefore, we generated a *dot1Δ rad53-HA* double mutant to analyze the extent of Rad53-HA phosphorylation (activation) and MMS resistance. Using anti-Rad53 antibodies, the Rad53-HA protein was not detectable in *rad53-HA* and *dot1Δ rad53-HA* cells in the absence of DNA damage (Fig. 5A, lanes 5 and 6). Interestingly, in the *dot1Δ rad53-HA* double mutant, in addition to the low amount of Rad53-HA protein characteristic of this tagged version, the levels of MMS-induced phosphorylated (and therefore active) Rad53-HA were further reduced compared with the *rad53-HA* single mutant (Fig. 5A, lanes 7 and 8). Indeed, the phosphorylated species of Rad53-HA induced by MMS were only barely detectable after long exposure of the membranes (Fig. 5A, middle panels). Using anti-HA antibodies, it was possible to detect a faint band corresponding to the basal form of Rad53-HA (Fig. 5B, lanes 1 and 2), which was not detectable with anti-Rad53. In addition, upon MMS treatment, only the phosphorylated species of Rad53-HA were detected, and the reduced levels of activated Rad53-HA in the *dot1Δ rad53-HA* double mutant compared with the *rad53-HA* single mutant were also manifested (Fig. 5B, lanes 3–6). Strinkingly, whereas both *dot1Δ* and *rad53-HA* single mutants display increased MMS resistance (Fig. 5C; see also Figs. 1, 2, 3 and 6; [34,40]), the *dot1Δ rad53-HA* double mutant was extremely sensitive to MMS (Fig. 5C), resembling a *rad53Δ* mutant (Fig. 4).

Moreover, if the increase in MMS resistance observed in *dot1Δ* results from the inability to fully activate Rad53, we reasoned that raising the levels of active Rad53 kinase in the *dot1Δ* mutant by overproducing the protein should bring the MMS resistance closer to wild-type levels. Indeed, we found that moderate overexpression of *RAD53* from a high-copy plasmid significantly restored the levels of MMS-activated Rad53 in a *dot1Δ* mutant (Fig. 6A) and partially

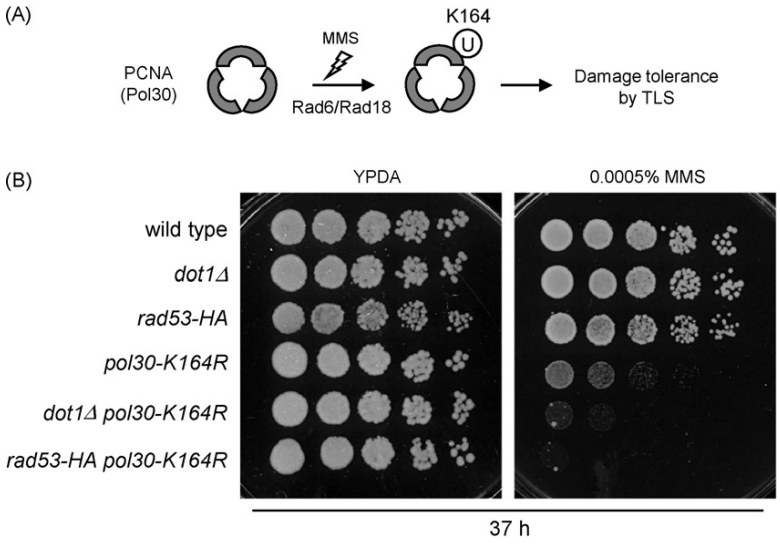

Fig. 3. The MMS resistance of *dot1Δ* and *rad53-HA* depends on PCNA-K164 ubiquitylation (A) Schematic diagram of the PCNA sliding clamp with the relevant MMS-induced ubiquitylation event. (B) Five-fold serial dilutions of exponentially growing cells were spotted onto YPDA and 0.0005% MMS plates. Note that the strong MMS sensitivity of the *pol30-K164R* mutant requires the use of a very low MMS concentration, at which *dot1Δ* and *rad53-HA* single mutants do not show increased resistance. Strains are YP813 (wild type), YP1215 (*dot1Δ*), YP814 (*rad53-HA*), YP1553 (*pol30-K164R*), YP1217 (*dot1Δ pol30-K164R*) and YP1554 (*rad53-HA pol30-K164R*).

suppressed the increased MMS resistance of *dot1Δ* (Fig. 6B and C). Collectively, these results suggest that intermediate Rad53 activity (below wild-type levels) supports enhanced resistance to MMS, as occurs in *dot1Δ* or *rad53-HA* mutants. However, when Rad53 function drops below certain threshold level the cells become very sensitive to this genotoxic agent, which is the situation present in the *dot1Δ rad53-HA* double mutant and in *rad53Δ* (see Section 4).

3.4. Dot1 and Rad53 modulate binding of Rev1 to chromatin

Current models for TLS propose that when the replication machinery stalls at a lesion, binding of the Rev1 protein to monoubiquitylated PCNA serves as scaffold for recruiting the Polζ polymerase to the stalled fork by virtue of the interaction between Rev1 and the Rev7 accessory subunit of Polζ [50–52]. This would promote the switch of the replicative polymerase by the TLS polymerase to continue replication past the lesion [53–55]. However, compelling evidence supports that DNA damage tolerance mechanisms function during the G2/M phase acting on gaps behind replication forks [56–59]. In any case, Rev1 is a key regulator of Polζ activity [10], and it has been shown that forms chromosomal foci [60,61]; therefore, we examined MMS-induced Rev1 localization in nuclear spreads of wild-type, *dot1Δ* and *rad53-HA* strains.

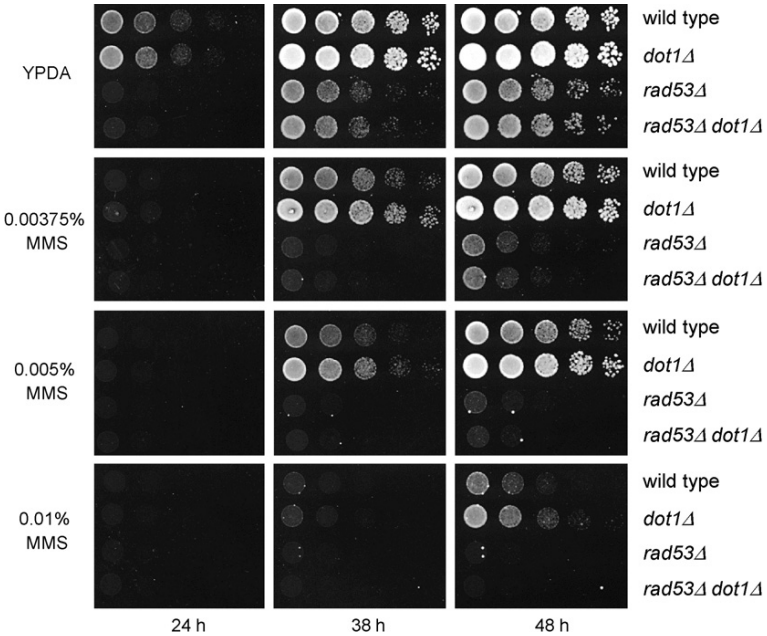

Fig. 4. The MMS resistance conferred by *dot1Δ* requires Rad53. Five-fold serial dilutions of exponentially growing cells were spotted onto YPDA, 0.00375% MMS, 0.005% MMS and 0.01% MMS plates incubated for the indicated time. Strains are U952-3B (wild type), YP558 (*dot1Δ*), U960-5C (*rad53Δ*) and YP755 (*dot1Δ rad53Δ*). Note that all strains are in an *sml1* background to maintain *rad53Δ* viability.

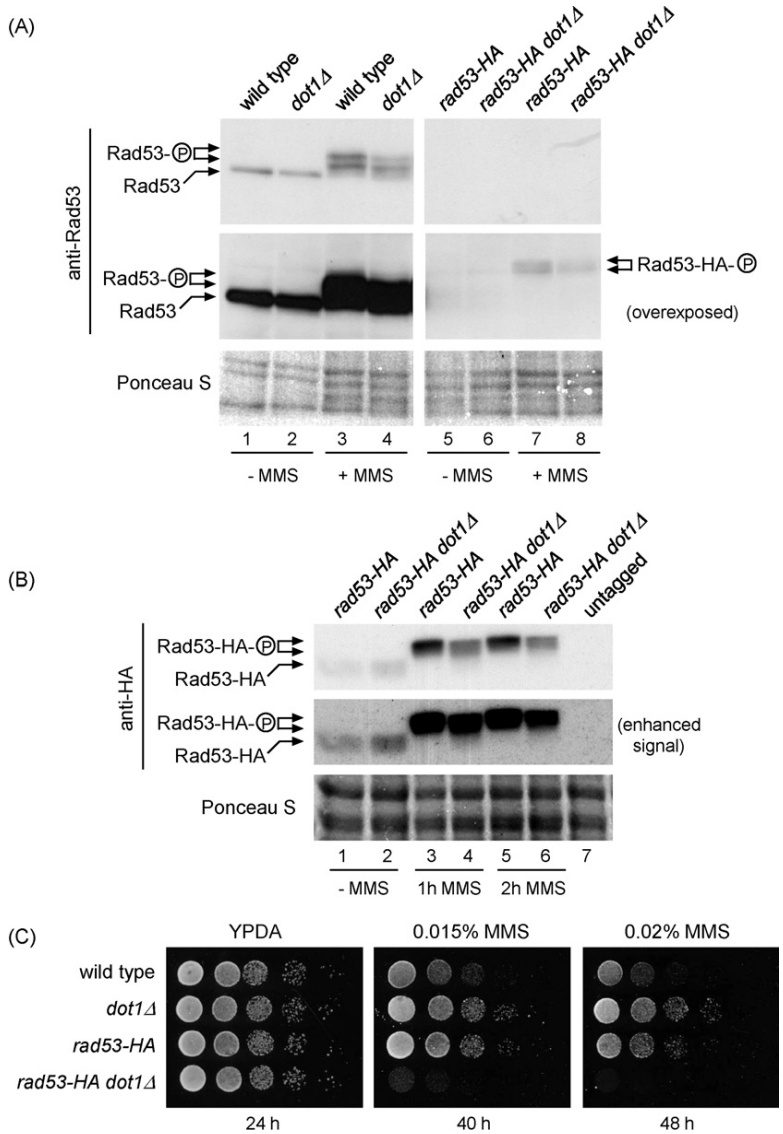

Fig. 5. Analysis of Rad53 activation and MMS resistance in *dot1Δ rad53-HA*. (A) Western blot analysis with anti-Rad53 antibodies of wild-type, *dot1Δ*, *rad53-HA* and *rad53-HA dot1Δ* exponentially growing cells either untreated or treated with 0.03% MMS for 1 h, as indicated. Double arrows mark the phosphorylated (activated) species of Rad53 (or Rad53-HA). The middle panels show an overexposure of the film to visualize the low levels of phosphorylated Rad53-HA in the absence of Dot1. Ponceau S staining was used as a loading control. (B) Western blot analysis with anti-HA antibodies of *rad53-HA* and *rad53-HA dot1Δ* exponentially growing cells either untreated or treated with 0.03% MMS for 1 h or 2 h, as indicated. The wild-type strain was included as an untagged control. Double arrows mark the phosphorylated (activated) species of Rad53-HA. The middle panel represents a computer-enhanced display of the upper blot to make more perceptible the basal form of Rad53-HA detected only in untreated cells (single arrow). Ponceau S staining was used as a loading control. (C) Five-fold serial dilutions of exponentially growing cells were spotted onto YPDA, 0.015% MMS and 0.02% MMS plates incubated for the indicated time. Strains are YP813 (wild type), YP1215 (*dot1Δ*), YP814 (*rad53-HA*) and YP1216 (*rad53-HA dot1Δ*).

Chromatin-associated Rev1 signal was observed both in untreated and MMS-treated cells (Fig. 7A). To analyze in more detail the binding of Rev1 to chromosomes, we quantified the number of Rev1 foci detected in the nuclear spreads and established three categories (Fig. 7B). In the absence of damage, all strains analyzed contained a high number of Rev1 foci on chromosomes; most nuclei corresponded to class III (i.e., more than 30 foci per nucleus). However, after MMS treatment, the number of Rev1 foci remarkably diminished in chromosome spreads from the wild-type strain, but remained high in the *dot1Δ* and *rad53-HA* mutants (Fig. 7). Indeed, whereas most nuclei from the MMS-treated *dot1Δ* and *rad53-HA* mutants contained more than 30 Rev1 foci (79% and 61% of nuclei belonged to class III, respectively), only 34% of wild-type nuclei fell into this category (Fig. 7B). Representative images of the most abundant class of nuclei for each condition are shown in Fig. 7A.

In summary, these results suggest that full activation of Rad53 promotes Rev1 disassembly from chromosomes upon MMS treatment, but the reduced Rad53 activity present in *dot1Δ* and *rad53-HA* allows extended Rev1 binding to chromatin accounting for the increased MMS resistance of these mutants.

4. Discussion

We have previously described a role for the histone H3K79 methyltransferase Dot1 in the tolerance to alkylating DNA damage [34]. Here, we have further characterized this function of Dot1 by first analyzing the impact of different methylation states of H3K79 in the response to continuous MMS exposure. We provide evidence indicating that the regulation of DNA damage tolerance by Dot1 depends on its catalytic activity on H3K79 and not on other possi-

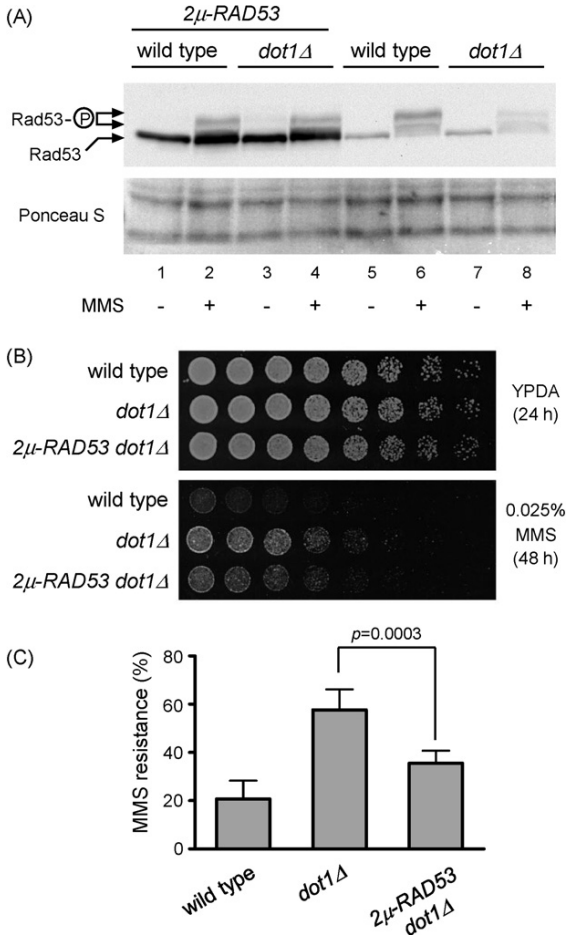

Fig. 6. Overexpression of *RAD53* partially suppresses the increased MMS resistance of *dot1Δ*. (A) Western blot analysis of Rad53 in wild-type (YP813) and *dot1Δ* strains (YP1215) transformed with vector alone (pRS426; lanes 5–8) or with a high-copy plasmid expressing *RAD53* (pSS145; lanes 1–4) either untreated or treated with 0.03% MMS for 1.5 h, as indicated. Double arrows mark the phosphorylated species of Rad53. Ponceau S was used as a loading control. (B) 2.5-fold serial dilutions of cells grown on SC-Ura to log phase were spotted onto YPDA and 0.025% MMS plates incubated for the indicated time. Strains are YP813 + pRS426 (wild type), YP1215 + pRS426 (*dot1Δ*) and YP1215 + pSS145 (*2μ-RAD53 dot1Δ*). (D) Quantification of the MMS resistance. Colonies were counted after 48 h of incubation on YPDA and 0.025% MMS plates. Average and standard deviation from six independent counts are presented. The *p* value of the statistical comparison is also shown.

ble unknown substrate(s) because, like *dot1Δ*, both a catalytically defective *dot1-G401V* allele, and a non-methylatable *H3-K79A* version of histone H3 confer MMS hyper-resistance. To investigate how different degrees of H3K79 methylation affect MMS resistance, we have engineered and analyzed a set of strains with progressively crippled Dot1 activity, ranging between wild-type *DOT1* and *dot1Δ* as the maximal and minimal Dot1 catalytic activity, respectively. We find a striking correlation between the decline of Dot1 activity and the increase in MMS resistance. This correlation was particularly evident for the loss of H3K79-me3, suggesting that this methylation state is the most relevant for the MMS response. Similarly, different functional relevance for the different methylation states of H3K79 in the coordination of DNA repair and checkpoint activation in response to UV has been proposed [62]. In contrast, it has been clearly demonstrated that chromatin silencing relies on global levels of H3K79 methylation, and not on specific methylation states [42]. Importantly, the MMS resistance conferred by the absence of Dot1 is independent of the silencing SIR complex [34].

The role of Dot1 in multiple nuclear processes, such as transcriptional silencing, meiotic checkpoint, DNA damage checkpoint or DSB repair, relies on the regulated binding of various key factors to specific chromosomal regions [25–27,33]. In principle, the impact of Dot1 (i.e. H3K79 methylation) in MMS resistance and the higher number of MMS-induced chromosome-associated Rev1 foci in the *dot1Δ* mutant could emanate from a direct effect of a peculiar chromatin structure dictated by the H3K79 methylation status modulating the recruitment of the TLS machinery. However, our results support an alternative possibility implying that the effect of Dot1 in DNA damage tolerance is exerted indirectly through the regulation of the Rad53 checkpoint kinase. The fact that a *rad53-HA* mutant, characterized by reduced levels of the kinase, substantially phenocopies *dot1Δ* in the response to chronic MMS exposure ([34,40]; this work) suggested a possible relationship between Dot1 and Rad53 in the regulation of tolerance to alkylating damage. Supporting this possibility, we find that the MMS resistance of both *dot1Δ* and *rad53-HA* depends on ubiquitylation of PCNA at K164, which is a crucial regulator of the TLS mechanism of DNA damage tolerance. Moreover, we show here that the increased MMS resistance of the *dot1Δ* mutant depends on Rad53.

Both *dot1Δ* and *rad53-HA* mutants display enhanced resistance to alkylating damage and increased TLS-dependent MMS-induced mutagenesis. Strinkingly, in both mutants, the levels of Rad53 activated by MMS treatment are reduced compared to the wild type, but for different reasons. In the case of *dot1Δ*, Rad53 is produced at normal levels (see Figs. 5A, lanes 1 and 2 and 6A, lanes 5 and 7), but the inability to properly recruit the Rad9 adaptor to DNA damage sites results in defective activation of Rad53 ([27,32,33]; Fig. 5). On the other hand, the *rad53-HA* allele gives rise to a functional protein, which can be fully activated; however, it is highly unstable, resulting in the production of low levels of MMS-induced active kinase ([40]; see also Fig. 5A, lane 7). In the *dot1Δ rad53-HA* double mutant, the activation of the low amounts of kinase produced by the HA-tagged allele is further hampered by the absence of *DOT1* resulting in barely detectable levels of phosphorylated kinase. Remarkably, whereas the *dot1Δ* and *rad53-HA* single mutants show increased MMS resistance, the *dot1Δ rad53-HA* double mutant shows strong MMS sensitivity implying that threshold levels of Rad53 activity determine the outcome of the cellular response to alkylating damage. We favor the scenario presented in Fig. 8 to explain our findings. In the face of MMS challenge that prevents the advance of replication forks, the wild-type strain fully activates Rad53 and the subsequent checkpoint responses controlled by this effector kinase, including cell cycle arrest, stabilization of replication forks and induction of DNA repair mechanisms [5]. In addition, high levels of Rad53 activity would negatively regulate the TLS mechanism of damage tolerance to prevent excessive mutagenesis. We propose that the sub-optimal levels of activated Rad53 present in *rad53-HA* mutants or in mutants that cripple H3K79 methylation (*dot1-G401A*, *dot1-G401V*, *dot1Δ*), while still preventing replication fork collapse, allow cell cycle progression and TLS-dependent replication across damage. Consistent with this idea, analysis of MMS-treated cells lacking the Rad53 phosphatases Pph3 an Ptc2 suggested that a graded response to the level of Rad53 phosphorylation occurs controlling replication fork restart [63,64]. These authors propose that a cycle of Rad53 activation and deactivation coordinates DNA repair with TLS-dependent replication fork progression through damaged DNA by a mechanism involving the Cdc7-Dbf4 kinase activity [64]. Indeed, the cooperation of a functional Rad53-dependent checkpoint response with multiple pathways involving base excision repair, recombination and DNA damage tolerance has been shown to be crucial for a proper cellular response to alkylated DNA [65,66]. Our analysis of the *dot1Δ rad53-HA* double mutant suggests that when Rad53 activity drops below a critical threshold level, damaged replication forks would

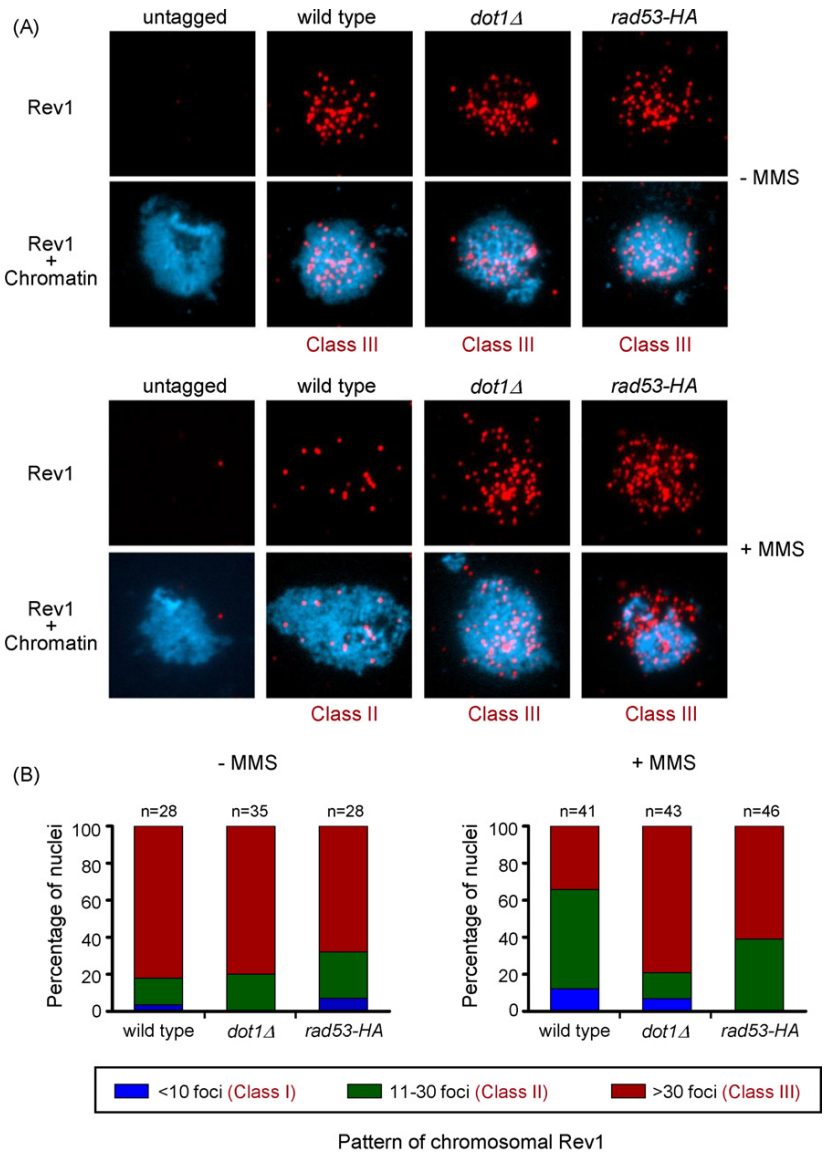

Fig. 7. The *dot1Δ* and *rad53-HA* mutants display increased number of chromosome-associated Rev1 foci upon MMS treatment. (A) Spread nuclei of wild-type (YP1471), *dot1Δ* (YP1458) and *rad53-HA* (YP1460) strains carrying *REV1* tagged with the *myc* epitope, as well as the untagged control strain (YP813), were stained with DAPI (blue) and anti-myc antibodies (red). Cells were untreated (upper panels) or treated with 0.03% MMS for 1 h (lower panels). Representative nuclei of the indicated categories (see below) are presented. (B) Quantification of the number of Rev1 foci in spread nuclei of the strains analyzed in (A) either untreated (left graph) or treated with MMS (right graph). The nuclei were classified in three categories according to the number of chromatin-bound Rev1 foci, as indicated. The percentage of nuclei belonging to each category is represented. The number of nuclei analyzed for each strain is indicated (*n*).

irreversibly collapse, like in *rad53Δ* [67,68], resulting in cell death and pronounced MMS sensitivity (Fig. 8). We note, however, that in contrast with *rad53Δ*, the low amounts of the Rad53-HA protein in the *dot1Δ rad53-HA* mutant must be sufficient to support viability in undamaged cells.

The Rev1 protein is a crucial regulator of TLS activity because of its structural function [10]; therefore, we focused on Rev1 to investigate how Dot1/Rad53 function impinges on TLS-dependent mutagenic bypass of MMS-induced lesions. In particular, we examined Rev1 localization to chromatin by immunofluorescence of nuclear spreads. We found that Rev1 foci are present in most nuclei even in the absence of MMS damage, suggesting that there is a constitutive localization of Rev1 to chromosomes. Similar results have been reported for 4NQO-treated cells [61]. Since PCNA ubiquitylation is triggered by DNA damage [11], these observations imply that the basal formation of Rev1 foci does not depend on the interaction with ubiquitylated PCNA. Consistent with this possibility, we detect Rev1 foci in the ubiquitylation-deficient *pol30-K164R* mutant (Supplementary Fig. 1). In fact, studies of mouse and yeast Rev1 suggest that the BRCT domain of Rev1 is required for its constitutive recruitment to foci, whereas the ubiquitin-binding motifs specifically drive Rev1 to damaged replication forks [60,69,70]. Moreover, in DT40 chicken cells, Rev1 maintains progression of replication forks upon DNA damage independently of PCNA ubiquitylation [71].

Strikingly, although most nuclei maintain Rev1 signal, we observe a decrease in the number of Rev1 foci per nucleus in MMS-treated wild-type cells. Since mutagenic TLS is induced by

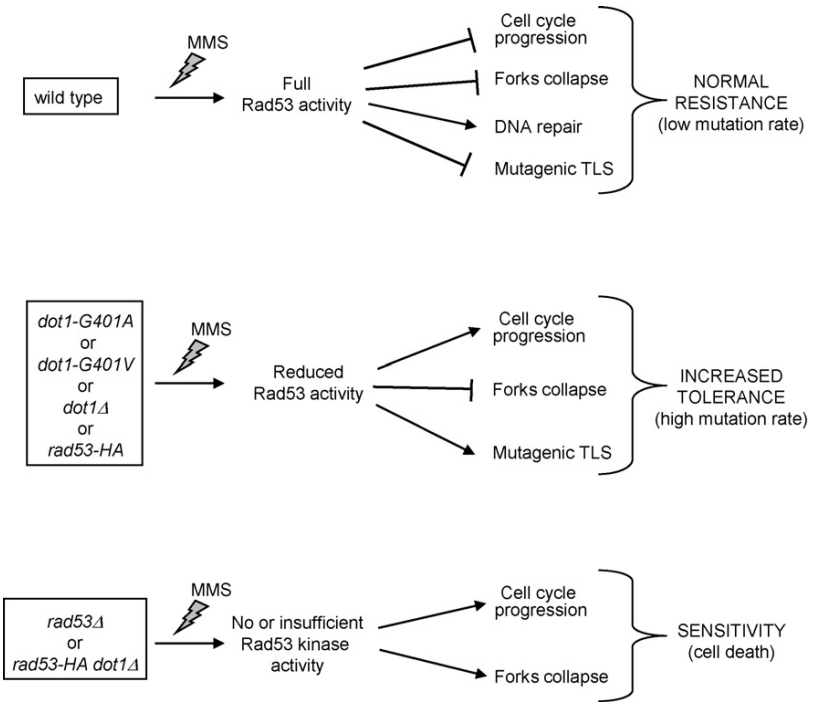

Fig. 8. Threshold levels of Rad53 activity modulate the tolerance to alkylating DNA damage. See discussion for details.

alkylating damage [34], this reduced number of Rev1 foci (or a significant fraction of them) must by actively engaged in TLS. In contrast, the number of chromatin-bound Rev1 foci remains elevated in the *dot1Δ* or *rad53-HA* mutants, providing the opportunity for more TLS-dependent mutagenic events once DNA damage-induced ubiquitylation of PCNA occurs. We propose that full activation of the Rad53 checkpoint kinase, which depends on Dot1, somehow restrains TLS activity by preventing promiscuous formation of Rev1 foci associated with chromosomes. Rev1 undergoes Mec1-dependent phosphorylation, which promotes Polζ activity only in NER-deficient cells [61,72]. Phosphorylation of Rev1 also requires the checkpoint clamp '9-1-1′ and the clamp loader Rad24; however, it is independent of Rad53 [72]. Therefore, it is unlikely that this posttranslational modification of Rev1 controls the formation of TLS-active Rev1 foci. Perhaps, Rad53 acts on other regulators of TLS that mediate Rev1 chromosomal binding or stability. Future studies will be aimed to unveil these mechanisms.

In summary, our studies provide insight into how a chromatin modification, namely Dot1-dependent H3K79 methylation, regulates the tolerance to alkylating damage by TLS through modulation of Rad53 activity. TLS constitutes one important aspect of the coordinated global cellular response to DNA damage because of the ability to bypass lesions that impede replication progression, thus preventing fork collapse and eventual formation of DNA breaks potentially leading to chromosomal rearrangements. However, given the error-prone nature of TLS, this process must be kept under strict control to avoid excessive mutagenesis, which can also have deleterious consequences. Therefore, an appropriate balance between error-prone and error-free processes to face DNA damage is essential to avoid genomic instability, which is directly linked to cancer development. Our studies in yeast reveal that the conserved Rad53 checkpoint kinase contributes to finely tune this balance at least by regulating the levels of chromatin-bound Rev1. Recent studies using a mouse model point to the influence of correct Rev1 levels in reducing the incidence of carcinogen-induced lung cancer [73], highlighting the importance of these mechanisms for the maintenance of genomic stability.

Conflict of interest

None

Acknowledgements

We thank M. Foiani, T. Hishida, R. Rothstein, M.A. Osley and G.C. Walker for providing plasmids and/or strains. We are indebted to F. van Leeuwen for sharing reagents and results prior to publication. We are especially grateful to R. Freire for raising the anti-Dot1 antibody and to F. Prado and J.A. Tercero for comments on the manuscript. DO and AGS were supported by predoctoral fellowships from CSIC and MEC (Spain), respectively. Research in our labs is supported by grants from Ministry of Science and Innovation of Spain (BFU2009-06938 to AB and BFU2009-07159 to PSS) and a grant from Fundación Ramón Areces to PSS.

Appendix A. Supplementary data

Supplementary data associated with this article can be found, in the online version, at doi:10.1016/j.dnarep.2010.07.003.

References

[1] A. Aguilera, B. Gomez-Gonzalez, Genome instability: a mechanistic view of its causes and consequences, Nat. Rev. Genet. 9 (2008) 204–217.
[2] M.B. Kastan, J. Bartek, Cell-cycle checkpoints and cancer, Nature 432 (2004) 316–323.
[3] C. Kerzendorfer, M. O'Driscoll, Human DNA damage response and repair deficiency syndromes: linking genomic instability and cell cycle checkpoint proficiency, DNA Repair 8 (2009) 1139–1152.
[4] J.C. Harrison, J.E. Haber, Surviving the breakup: the DNA damage checkpoint, Annu. Rev. Genet. 40 (2006) 209–235.

[5] D. Branzei, M. Foiani, Maintaining genome stability at the replication fork, Nat. Rev. Mol. Cell. Biol. 11 (2010) 208–219.
[6] A.M. Friedel, B.L. Pike, S.M. Gasser, ATR/Mec1: coordinating fork stability and repair, Curr. Opin. Cell Biol. 21 (2009) 237–244.
[7] H.D. Ulrich, The RAD6 pathway: control of DNA damage bypass and mutagenesis by ubiquitin and SUMO, Chembiochem 6 (2005) 1735–1743.
[8] B.A. Kunz, A.F. Straffon, E.J. Vonarx, DNA damage-induced mutation: tolerance via translesion synthesis, Mutat. Res. 451 (2000) 169–185.
[9] P.L. Andersen, F. Xu, W. Xiao, Eukaryotic DNA damage tolerance and translesion synthesis through covalent modifications of PCNA, Cell. Res. 18 (2008) 162–173.
[10] L.S. Waters, B.K. Minesinger, M.E. Wiltrout, S. D'Souza, R.V. Woodruff, G.C. Walker, Eukaryotic translesion polymerases and their roles and regulation in DNA damage tolerance, Microbiol. Mol. Biol. Rev. 73 (2009) 134–154.
[11] C. Hoege, B. Pfander, G.L. Moldovan, G. Pyrowolakis, S. Jentsch, RAD6-dependent DNA repair is linked to modification of PCNA by ubiquitin and SUMO, Nature 419 (2002) 135–141.
[12] A. Gallego-Sanchez, F. Conde, P. San Segundo, A. Bueno, Control of PCNA deubiquitylation in yeast, Biochem. Soc. Trans. 38 (2010) 104–109.
[13] H.L. Klein, Reversal of fortune: Rad5 to the rescue, Mol. Cell 28 (2007) 181–183.
[14] S. Prakash, R.E. Johnson, L. Prakash, Eukaryotic translesion synthesis DNA polymerases: specificity of structure and function, Annu. Rev. Biochem. 74 (2005) 317–353.
[15] Y. Bao, X. Shen, Chromatin remodeling in DNA double-strand break repair, Curr. Opin. Genet. Dev. 17 (2007) 126–131.
[16] M. Downey, D. Durocher, γH2AX as a checkpoint maintenance signal, Cell Cycle 5 (2006) 1376–1381.
[17] J.A. Downs, M.C. Nussenzweig, A. Nussenzweig, Chromatin dynamics and the preservation of genetic information, Nature 447 (2007) 951–958.
[18] C.L. Peterson, J. Cote, Cellular machineries for chromosomal DNA repair, Genes Dev. 18 (2004) 602–616.
[19] T. Schleker, S. Nagai, S.M. Gasser, Posttranslational modifications of repair factors and histones in the cellular response to stalled replication forks, DNA Repair 8 (2009) 1089–1100.
[20] H. van Attikum, S.M. Gasser, The histone code at DNA breaks: a guide to repair? Nat. Rev. Mol. Cell. Biol. 6 (2005) 757–765.
[21] K.B. Falbo, C. Alabert, Y. Katou, S. Wu, J. Han, T. Wehr, J. Xiao, X. He, Z. Zhang, Y. Shi, K. Shirahige, P. Pasero, X. Shen, Involvement of a chromatin remodeling complex in damage tolerance during DNA replication, Nat. Struct. Mol. Biol. 16 (2009) 1167–1172.
[22] Q. Feng, H. Wang, H.H. Ng, H. Erdjument-Bromage, P. Tempst, K. Struhl, Y. Zhang, Methylation of H3-lysine 79 is mediated by a new family of HMTases without a SET domain, Curr. Biol. 12 (2002) 1052–1058.
[23] N. Lacoste, R.T. Utley, J.M. Hunter, G.G. Poirier, J. Cote, Disruptor of telomeric silencing-1 is a chromatin-specific histone H3 methyltransferase, J. Biol. Chem. 277 (2002) 30421–30424.
[24] H.H. Ng, Q. Feng, H. Wang, H. Erdjument-Bromage, P. Tempst, Y. Zhang, K. Struhl, Lysine methylation within the globular domain of histone H3 by Dot1 is important for telomeric silencing and Sir protein association, Genes Dev. 16 (2002) 1518–1527.
[25] F. van Leeuwen, P.R. Gafken, D.E. Gottschling, Dot1p modulates silencing in yeast by methylation of the nucleosome core, Cell 109 (2002) 745–756.
[26] P.A. San-Segundo, G.S. Roeder, Role for the silencing protein Dot1 in meiotic checkpoint control, Mol. Biol. Cell 11 (2000) 3601–3615.
[27] F. Conde, E. Refolio, V. Cordon-Preciado, F. Cortes-Ledesma, L. Aragon, A. Aguilera, P.A. San-Segundo, The Dot1 histone methyltransferase and the Rad9 checkpoint adaptor contribute to cohesin-dependent double-strand break repair by sister chromatid recombination in *Saccharomyces cerevisiae*, Genetics 182 (2009) 437–446.
[28] L.J. Bostelman, A.M. Keller, A.M. Albrecht, A. Arat, J.S. Thompson, Methylation of histone H3 lysine-79 by Dot1p plays multiple roles in the response to UV damage in *Saccharomyces cerevisiae*, DNA Repair 6 (2007) 383–395.
[29] J.C. Game, M.S. Williamson, C. Baccari, X-ray survival characteristics and genetic analysis for nine *Saccharomyces* deletion mutants that show altered radiation sensitivity, Genetics 169 (2005) 51–63.
[30] J.C. Game, M.S. Williamson, T. Spicakova, J.M. Brown, The *RAD6/BRE1* histone modification pathway in *Saccharomyces* confers radiation resistance through a *RAD51*-dependent process that is independent of *RAD18*, Genetics 173 (2006) 1951–1968.
[31] G.W. Toh, A.M. O'Shaughnessy, S. Jimeno, I.M. Dobbie, M. Grenon, S. Maffini, A. O'Rorke, N.F. Lowndes, Histone H2A phosphorylation and H3 methylation are required for a novel Rad9 DSB repair function following checkpoint activation, DNA Repair 5 (2006) 693–703.
[32] M. Giannattasio, F. Lazzaro, P. Plevani, M. Muzi-Falconi, The DNA damage checkpoint response requires histone H2B ubiquitination by Rad6-Bre1 and H3 methylation by Dot1, J. Biol. Chem. 280 (2005) 9879–9886.
[33] R. Wysocki, A. Javaheri, S. Allard, F. Sha, J. Cote, S.J. Kron, Role of Dot1-dependent histone H3 methylation in G1 and S phase DNA damage checkpoint functions of Rad9, Mol. Cell. Biol. 25 (2005) 8430–8443.
[34] F. Conde, P.A. San-Segundo, Role of Dot1 in the response to alkylating DNA damage in *Saccharomyces cerevisiae*: regulation of DNA damage tolerance by the error-prone polymerases Polζ/Rev1, Genetics 179 (2008) 1197–1210.
[35] M.G. Guenther, L.N. Lawton, T. Rozovskaia, G.M. Frampton, S.S. Levine, T.L. Volkert, C.M. Croce, T. Nakamura, E. Canaani, R.A. Young, Aberrant chromatin at genes encoding stem cell regulators in human mixed-lineage leukemia, Genes Dev. 22 (2008) 3403–3408.
[36] A.V. Krivtsov, Z. Feng, M.E. Lemieux, J. Faber, S. Vempati, A.U. Sinha, X. Xia, J. Jesneck, A.P. Bracken, L.B. Silverman, J.L. Kutok, A.L. Kung, S.A. Armstrong, H3K79 methylation profiles define murine and human MLL-AF4 leukemias, Cancer Cell 14 (2008) 355–368.
[37] Y.H. Lin, P.M. Kakadia, Y. Chen, Y.Q. Li, A.J. Deshpande, C. Buske, K.L. Zhang, Y. Zhang, G.L. Xu, S.K. Bohlander, Global reduction of the epigenetic H3K79 methylation mark and increased chromosomal instability in CALM-AF10-positive leukemias, Blood 114 (2009) 651–658.
[38] Y. Okada, Q. Feng, Y. Lin, Q. Jiang, Y. Li, V.M. Coffield, L. Su, G. Xu, Y. Zhang, hDOT1L links histone methylation to leukemogenesis, Cell 121 (2005) 167–178.
[39] Y. Okada, Q. Jiang, M. Lemieux, L. Jeannotte, L. Su, Y. Zhang, Leukaemic transformation by CALM-AF10 involves upregulation of Hoxa5 by hDOT1L, Nat. Cell. Biol. 8 (2006) 1017–1024.
[40] V. Cordon-Preciado, S. Ufano, A. Bueno, Limiting amounts of budding yeast Rad53 S-phase checkpoint activity results in increased resistance to DNA alkylation damage, Nucleic Acids Res. 34 (2006) 5852–5862.
[41] M.S. Longtine, A. McKenzie, D.J. 3rd, N.G. Demarini, A. Shah, A. Wach, P. Brachat, J.R. Philippsen, Pringle, Additional modules for versatile and economical PCR-based gene deletion and modification in *Saccharomyces cerevisiae*, Yeast 14 (1998) 953–961.
[42] F. Frederiks, M. Tzouros, G. Oudgenoeg, T. van Welsem, M. Fornerod, J. Krijgsveld, F. van Leeuwen, Nonprocessive methylation by Dot1 leads to functional redundancy of histone H3K79 methylation states, Nat. Struct. Mol. Biol. 15 (2008) 550–557.
[43] M. Sym, J.A. Engebrecht, G.S. Roeder, ZIP1 is a synaptonemal complex protein required for meiotic chromosome synapsis, Cell 72 (1993) 365–378.
[44] P.A. San-Segundo, G.S. Roeder, Pch2 links chromatin silencing to meiotic checkpoint control, Cell 97 (1999) 313–324.
[45] K. Sawada, Z. Yang, J.R. Horton, R.E. Collins, X. Zhang, X. Cheng, Structure of the conserved core of the yeast Dot1p, a nucleosomal histone H3 lysine 79 methyltransferase, J. Biol. Chem. 279 (2004) 43296–43306.
[46] A.B. Fleming, C.F. Kao, C. Hillyer, M. Pikaart, M.A. Osley, H2B ubiquitylation plays a role in nucleosome dynamics during transcription elongation, Mol. Cell 31 (2008) 57–66.
[47] S. Bergink, S. Jentsch, Principles of ubiquitin and SUMO modifications in DNA repair, Nature 458 (2009) 461–467.
[48] T. Hishida, T. Ohya, Y. Kubota, Y. Kamada, H. Shinagawa, Functional and physical interaction of yeast Mgs1 with PCNA: impact on *RAD6*-dependent DNA damage tolerance, Mol. Cell. Biol. 26 (2006) 5509–5517.
[49] A. Pellicioli, C. Lucca, G. Liberi, F. Marini, M. Lopes, P. Plevani, A. Romano, P.P. Di Fiore, M. Foiani, Activation of Rad53 kinase in response to DNA damage and its effect in modulating phosphorylation of the lagging strand DNA polymerase, EMBO J. 18 (1999) 6561–6572.
[50] M. Bienko, C.M. Green, N. Crosetto, F. Rudolf, G. Zapart, B. Coull, P. Kannouche, G. Wider, M. Peter, A.R. Lehmann, K. Hofmann, I. Dikic, Ubiquitin-binding domains in Y-family polymerases regulate translesion synthesis, Science 310 (2005) 1821–1824.
[51] S. D'Souza, L.S. Waters, G.C. Walker, Novel conserved motifs in Rev1 C-terminus are required for mutagenic DNA damage tolerance, DNA Repair 7 (2008) 1455–1470.
[52] C. Guo, P.L. Fischhaber, M.J. Luk-Paszyc, Y. Masuda, J. Zhou, K. Kamiya, C. Kisker, E.C. Friedberg, Mouse Rev1 protein interacts with multiple DNA polymerases involved in translesion DNA synthesis, EMBO J. 22 (2003) 6621–6630.
[53] N. Acharya, R.E. Johnson, S. Prakash, L. Prakash, Complex formation with Rev1 enhances the proficiency of *Saccharomyces cerevisiae* DNA polymerase ζ for mismatch extension and for extension opposite from DNA lesions, Mol. Cell. Biol. 26 (2006) 9555–9563.
[54] A.R. Lehmann, A. Niimi, T. Ogi, S. Brown, S. Sabbioneda, J.F. Wing, P.L. Kannouche, C.M. Green, Translesion synthesis: Y-family polymerases and the polymerase switch, DNA Repair 6 (2007) 891–899.
[55] Z. Zhuang, R.E. Johnson, L. Haracska, L. Prakash, S. Prakash, S.J. Benkovic, Regulation of polymerase exchange between Polη and Polδ by monoubiquitination of PCNA and the movement of DNA polymerase holoenzyme, Proc. Natl. Acad. Sci. U.S.A. 105 (2008) 5361–5366.
[56] Y. Daigaku, A.A. Davies, H.D. Ulrich, Ubiquitin-dependent DNA damage bypass is separable from genome replication, Nature 465 (2010) 951–955.
[57] G.I. Karras, S. Jentsch, The *RAD6* DNA damage tolerance pathway operates uncoupled from the replication fork and is functional beyond S phase, Cell 141 (2010) 255–267.
[58] M. Lopes, M. Foiani, J.M. Sogo, Multiple mechanisms control chromosome integrity after replication fork uncoupling and restart at irreparable UV lesions, Mol. Cell 21 (2006) 15–27.
[59] L.S. Waters, G.C. Walker, The critical mutagenic translesion DNA polymerase Rev1 is highly expressed during G(2)/M phase rather than S phase, Proc. Natl. Acad. Sci. U.S.A. 103 (2006) 8971–8976.
[60] C. Guo, T.S. Tang, M. Bienko, J.L. Parker, A.B. Bielen, E. Sonoda, S. Takeda, H.D. Ulrich, I. Dikic, E.C. Friedberg, Ubiquitin-binding motifs in REV1 protein are required for its role in the tolerance of DNA damage, Mol. Cell. Biol. 26 (2006) 8892–8900.
[61] S. Sabbioneda, I. Bortolomai, M. Giannattasio, P. Plevani, M. Muzi-Falconi, Yeast Rev1 is cell cycle regulated, phosphorylated in response to DNA damage and its binding to chromosomes is dependent upon *MEC1*, DNA Repair 6 (2007) 121–127.
[62] M.L. Evans, L.J. Bostelman, A.M. Albrecht, A.M. Keller, N.T. Strande, J.S. Thompson, UV sensitive mutations in histone H3 in *Saccharomyces cerevisiae* that alter

specific K79 methylation states genetically act through distinct DNA repair pathways, Curr. Genet. 53 (2008) 259–274.
[63] B.M. O'Neill, S.J. Szyjka, E.T. Lis, A.O. Bailey, J.R. Yates, O.M. 3rd, F.E. Aparicio, Romesberg, Pph3-Psy2 is a phosphatase complex required for Rad53 dephosphorylation and replication fork restart during recovery from DNA damage, Proc. Natl. Acad. Sci. U.S.A. 104 (2007) 9290–9295.
[64] S.J. Szyjka, J.G. Aparicio, C.J. Viggiani, S. Knott, W. Xu, S. Tavare, O.M. Aparicio, Rad53 regulates replication fork restart after DNA damage in *Saccharomyces cerevisiae*, Genes Dev. 22 (2008) 1906–1920.
[65] M. Segurado, J.A. Tercero, The S-phase checkpoint: targeting the replication fork, Biol. Cell 101 (2009) 617–627.
[66] M.V. Vazquez, V. Rojas, J.A. Tercero, Multiple pathways cooperate to facilitate DNA replication fork progression through alkylated DNA, DNA Repair 7 (2008) 1693–1704.
[67] J.A. Tercero, J.F. Diffley, Regulation of DNA replication fork progression through damaged DNA by the Mec1/Rad53 checkpoint, Nature 412 (2001) 553–557.
[68] J.A. Tercero, M.P. Longhese, J.F. Diffley, A central role for DNA replication forks in checkpoint activation and response, Mol. Cell 11 (2003) 1323–1336.
[69] M.G. Bomar, S. D'Souza, M. Bienko, I. Dikic, G.C. Walker, P. Zhou, Unconventional ubiquitin recognition by the ubiquitin-binding motif within the Y family DNA polymerases ι and Rev1, Mol. Cell 37 (2010) 408–417.
[70] C. Guo, E. Sonoda, T.S. Tang, J.L. Parker, A.B. Bielen, S. Takeda, H.D. Ulrich, E.C. Friedberg, REV1 protein interacts with PCNA: significance of the REV1 BRCT domain in vitro and in vivo, Mol. Cell 23 (2006) 265–271.
[71] C.E. Edmunds, L.J. Simpson, J.E. Sale, PCNA ubiquitination and REV1 define temporally distinct mechanisms for controlling translesion synthesis in the avian cell line DT40, Mol. Cell 30 (2008) 519–529.
[72] V. Pages, S.R. Santa Maria, L. Prakash, S. Prakash, Role of DNA damage-induced replication checkpoint in promoting lesion bypass by translesion synthesis in yeast, Genes Dev. 23 (2009) 1438–1449.
[73] C.A. Dumstorf, S. Mukhopadhyay, E. Krishnan, B. Haribabu, W.G. McGregor, REV1 is implicated in the development of carcinogen-induced lung cancer, Mol. Cancer Res. 7 (2009) 247–254.
[74] F. Frederiks, G.J. Heynen, S.J. van Deventer, H. Janssen, F. van Leeuwen, Two Dot1 isoforms in *Saccharomyces cerevisiae* as a result of leaky scanning by the ribosome, Nucleic Acids Res. 37 (2009) 7047–7058.
[75] B. Rockmill, G.S. Roeder, Meiosis in asynaptic yeast, Genetics 126 (1990) 563–574.
[76] X. Zhao, E.G. Muller, R. Rothstein, A suppressor of two essential checkpoint genes identifies a novel protein that negatively affects dNTP pools, Mol. Cell 2 (1998) 329–340.
[77] C.B. Brachmann, A. Davies, G.J. Cost, E. Caputo, J. Li, P. Hieter, J.D. Boeke, Designer deletion strains derived from *Saccharomyces cerevisiae* S288C: a useful set of strains and plasmids for PCR-mediated gene disruption and other applications, Yeast 14 (1998) 115–132.
[78] R.S. Sikorski, P. Hieter, A system of shuttle vectors and yeast host strains designed for efficient manipulation of DNA in *Saccharomyces cerevisiae*, Genetics 122 (1989) 19–27.
[79] T.W. Christianson, R.S. Sikorski, M. Dante, J.H. Shero, P. Hieter, Multifunctional yeast high-copy-number shuttle vectors, Gene 110 (1992) 119–122.

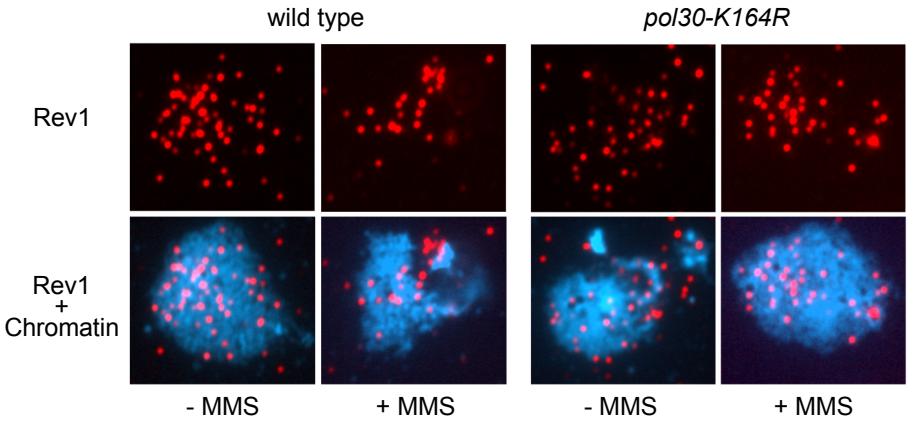

Supplementary Figure 1. Spread nuclei of wild-type (YP1471) or *pol30-K164R* (YP1561) strains carrying *REV1* tagged with the *myc* epitope, stained with DAPI (blue) and anti-myc antibodies (red). Cells were either untreated or treated with 0.03% MMS, as indicated.

CONCLUSIONES

1. La regulación de la resistencia a MMS mediada por Dot1 se debe a su actividad metiltransferasa sobre H3K79.

2. Los niveles de metilación de H3K79me modulan finamente la tolerancia al daño por alquilación en el DNA.

3. La resistencia a MMS en los mutantes depende de la ubiquitilación de PCNA-K164.

4. El umbral de actividad de Rad53 determina la tolerancia al daño en el DNA, de forma que los niveles intermedios presentes en los mutantes *dot1Δ* y *rad53-HA* confieren una mayor resistencia a MMS, mientras que la baja actividad del doble mutante *dot1Δ rad53-HA* o la carencia completa del mutante *rad53Δ* confieren sensibilidad a MMS.

5. La regulación de TLS por Dot1 y Rad53 se ejerce, al menos en parte, mediante el control de la unión de Rev1 a la cromatina.

CONCLUSIONS

1. The regulation of MMS resistance by Dot1 relies on its H3K79 methyltransferase activity.

2. H3K79me levels finely modulate the degree of tolerance to alkylating DNA damage.

3. The MMS resistance of *dot1Δ* and *rad53-HA* depends on PCNA-K164 ubiquitylation

4. Threshold levels of Rad53 activity modulate DNA damage tolerance: whereas the sub-optimal levels of Rad53 activity present in *dot1Δ* or *rad53-HA* cells lead to increased MMS resistance, the low levels in the *dot1Δ rad53-HA* double mutant or the complete lack of activity in *rad53Δ* confer MMS sensitivity.

5. Dot1 and Rad53 regulate TLS, at least partially, by controlling Rev1 chromatin binding.

Role of Dot1

in the meiotic recombination checkpoint

and in DNA damage tolerance

Role of Dot1 in the meiotic recombination checkpoint and in DNA damage tolerance

SUMMARY

Eukaryotic DNA is condensed in the cell nucleus through the interaction of roughly 147 base pairs wrapped around each histone octamer (an H3/H4 heterotetramer and two H2A/H2B dimers) to form the nucleosome, the basic repeating unit of chromatin (Kornberg and Lorch 1999). Histones are composed of a globular domain, which form the nucleosome core, and unstructured tails that protrude from the core. Histone proteins are subjected to multiple posttranslational modifications (PTMs) especially at the tails. Well-known PTMs include acetylation, methylation, phosphorylation, ubiquitylation and sumoylation, being always residue specific and with different degree of reversibility. PTMs modify chromatin condensation, thus controlling the accessibility of other DNA-binding proteins. Moreover, there are histone chaperones, histone variants, architectural chromatin proteins and chromatin remodelers that also transform chromatin structure. Many biological processes are regulated in this way; for example, transcription, heterochromatin formation, replication and DNA repair (Kouzarides 2007; Luger et al. 2012; Becker and Workman 2013).

An essential process in all sexually reproducing organisms, influenced by chromatin modifications, is the meiotic cell division. This specialized reductional division generates haploid products (spores in yeast or gametes in Metazoa) from a single diploid cell, because two rounds of chromosome segregation are preceded by a single phase of DNA replication. During meiosis, the unique meiotic prophase I is the most prolonged and elaborate stage, during which pairing, synapsis and recombination between homologous chromosomes occur (Cohen et al. 2006). Progression and completion of meiotic events are specifically monitored by a surveillance mechanism, the meiotic recombination checkpoint or pachytene checkpoint. Thus, in response to meiotic defects this checkpoint is triggered and blocks or delays meiotic progression in order to prevent aberrant chromosome segregation and the ensuing formation of aneuploid meiotic products (Roeder and Bailis 2000; Macqueen and Hochwagen 2011).

Precisely, the *dot1* mutant was isolated in a genetic screen for pachytene-checkpoint defective mutants in *Saccharomyces cerevisiae*. In the absence of *DOT1*, whose enzymatic activity was unknown at that time, the checkpoint-induced meiotic arrest of a synapsis-defective mutant (i.e., *zip1*) or recombination-defective mutant (i.e., *dmc1*) is abolished (San-Segundo and Roeder 2000). *DOT1* had already been independently isolated in a genetic screen for high-copy disruptors of telomeric silencing, hence its name "*Disruptor Of Telomeric silencing 1*" (Singer et al. 1998). A few years later, several groups, independently and using different approaches, discovered that Dot1 in budding yeast, and its human homolog DOT1L (for Dot1-like), were the methyltransferase of lysine 79 on histone H3 (H3K79). This methylation reaction occurs in the context of

nucleosomes and H3K79 is the only known methylated residue that lies within a histone globular domain (Feng et al. 2002; Lacoste et al. 2002; van Leeuwen et al. 2002; Ng et al. 2002).

Since the discovery of Dot1 activity as histone-lysine N-methyltransferase (EC 2.1.1.43), more and more work has been done to improve its characterization. Dot1 is the only methyltransferase that targets H3K79, because deletion mutants in yeast, flies or mice do not exhibit any methylation level at this lysine (van Leeuwen et al. 2002; Shanower et al. 2005; Jones et al. 2008). Dot1 is responsible for catalyzing mono-, di- and trimethylation of H3K79 (H3K79me1, -me2 y –me3, respectively) in a non-processive (or distributive) manner, which differs from the rest of histone methyltransferases, which possess a SET-domain and a processive mechanism of action (Frederiks et al. 2008). To date, there is no demethylase known capable of reverting H3K79me.

Major advances have been made in uncovering the multiple Dot1/DOT1L biological functions (Nguyen and Zhang 2011). Starting with the roles of Dot1 in *Saccharomyces cerevisiae* and regarding its first described function in telomeric silencing, it is now known that is mediated by Dot1 competing with the silencing protein Sir3 for same binding site on the nucleosomes and the inability of Sir3 for binding to methylated H3K79 nucleosomes (van Welsem et al. 2008). Furthermore, Dot1 plays numerous roles in the DNA damage response during the vegetative cycle. Thus, Dot1 is needed for Rad9-mediated activation of Rad53 in the G_1/S and intra-S DNA damage checkpoints (Giannattasio et al. 2005; Wysocki et al. 2005). In addition, Dot1 modulates DNA damage repair pathways in response to ionizing or ultraviolet radiation (Game et al. 2006; Toh et al. 2006; Bostelman et al. 2007).

Our laboratory has been interested in studying the role of Dot1 in the response to alkylating DNA damage caused by methyl methanesulfonate (MMS) and in double-strand break (DSB) repair by sister chromatid recombination (Conde and San-Segundo 2008; Conde et al. 2009). Unexpectedly, deletion of *DOT1* results in increased resistance to chronic MMS exposure. Our results indicate that Dot1 negatively regulates the tolerance to DNA alkylating damage response mediated by translesion synthesis (TLS). The MMS resistance observed in *dot1* results from the enhanced TLS activity, but at the expense of elevated mutagenesis frequency (Conde and San-Segundo 2008). We further focused on characterizing in more detail how Dot1 regulates DNA damage tolerance. The results are presented in the third research article that composes this doctoral thesis, entitled “Regulation of tolerance to DNA alkylating damage by Dot1 and Rad53 in *Saccharomyces cerevisiae*” (Conde et al. 2010). My contribution to this work consisted in demonstrating that the role of Dot1 in the TLS pathway is due to its methyltransferase activity on H3K79.

Regarding the research on the meiotic roles of Dot1, it was previously shown to be essential for meiotic recombination checkpoint function in *S. cerevisiae* (San-Segundo and Roeder 2000). However, the molecular mechanisms involved remained largely unknown. Therefore, the main goal of my thesis was to uncover the

role of Dot1-dependendent H3K79 methylation in meiotic checkpoint activation. The results obtained were published in the first article shown in this thesis report, entitled "Dot1-dependent histone H3K79 methylation promotes activation of the Mek1 meiotic checkpoint effector kinase by regulating the Hop1 adaptor" (Ontoso et al. 2013a).

Dot1 is conserved through evolution and the biological functions of Dot1 homologues in a wide range of organisms, such as *Dictyostelium*, *Trypanosoma*, *Caenorhabditis*, *Drosophila*, mice and humans have been progressively discovered (Feng et al. 2002; Shanower et al. 2005; Jones et al. 2008; Müller-Taubenberger et al. 2011; Cecere et al. 2013). Of note, *Schizosaccharomyces pombe* lacks Dot1 and H3K79me. In mammals, DOT1L-mediated H3K79me participates in multiple biological processes (Nguyen and Zhang 2011). Thus, DOT1L performs important roles in transcriptional regulation (Steger et al. 2008; Kim et al. 2012a), is involved in embryonic development and differentiation (Jones et al. 2008; Barry et al. 2009), cardiac function (Nguyen et al. 2011), hematopoiesis (Feng et al. 2010; Jo et al. 2011), cell proliferation and aging (Kim et al. 2012b) and chondrogenesis (Castaño Betancourt et al. 2012). Alteration of DOT1L function is related with some types of mixed lineage leukemia (Okada et al. 2005; Krivtsov et al. 2008; Bernt et al. 2011), neural tube defects (Zhang et al. 2013) and osteoarthritis (Castaño Betancourt et al. 2012). The discovery of an increasing number of pathologies related with altered DOT1L-mediated H3K79me patterns points to DOT1L as a promising therapeutic target (Daigle et al. 2011; Yao et al. 2011; Anglin et al. 2012; Helin and Dhanak 2013). However, little was known about DOT1L activity in mammalian meiosis; only a study in mouse oocytes has been reported (Ooga et al. 2008). Therefore, another aim of my thesis was the initial cytological characterization of DOT1L and H3K79me during meiotic prophase I in mouse spermatocytes. The findings were published in the second article presented in this report, entitled "Dynamics of DOT1L localization and H3K79 methylation during meiotic prophase I in mouse spermatocytes" (Ontoso et al. 2013b).

Thus, three sections compose the present thesis report entitled "Function of Dot1 in the meiotic recombination checkpoint and in the tolerance to DNA damage"; each of one is based on a published research article:

ARTICLE 1: "Dot1-dependent histone H3K79 methylation promotes activation of the Mek1 meiotic checkpoint effector kinase by regulating the Hop1 adaptor"

ARTICLE 2: "Dynamics of DOT1L localization and H3K79 methylation during meiotic prophase I in mouse spermatocytes"

ARTICLE 3: "Regulation of tolerance to DNA alkylating damage by Dot1 and Rad53 in *Saccharomyces cerevisiae*"

ARTICLE 1:

Dot1-dependent histone H3K79 methylation promotes activation of the Mek1 meiotic checkpoint effector kinase by regulating the Hop1 adaptor

Here, we investigated the role of Dot1-dependendent H3K79 methylation in *zip1*-induced checkpoint activation. By manipulation of Dot1 catalytic activity and levels, we found that the extent of H3K79 trimethylation correlates with the strength of checkpoint-imposed meiotic delay. We demonstrate that while the meiotic defects of a synapsis and recombination-deficient *zip1* mutant are correctly sensed by Mec1-Ddc2 in the absence of H3K79me, activation of the downstream effector kinase Mek1 is impaired. We dissected the Mek1 phosphorylation events and found that Dot1 promotes its Hop1-dependent dimerization and auto-phosphorylation. Finally, we show that the effect of Dot1-dependent H3K79me on Hop1 localization is exerted, at least in part, by excluding Pch2 from the chromosomes. Our results indicate that constitutive methylation of H3K79 by Dot1 is required for proper chromosomal recruitment of Hop1 to relay the checkpoint signal to Mek1 in response to meiotic defects.

Histone H3K79 methylation regulates the meiotic recombination checkpoint

Dot1 catalyzes the mono-, di- and tri-methylation of histone H3K79 by a non-processive mechanism (Frederiks et al. 2008; Nguyen and Zhang 2011) and plays a crucial role in the meiotic recombination checkpoint (San-Segundo and Roeder 2000). Notably, we found that overall levels of H3K79me do not significantly change upon meiosis induction or upon meiotic checkpoint activation. Moreover, H3K79me meiotic levels were not significantly altered in the *spo11* mutant, lacking meiotic recombination (Keeney 2001), or in other mutants defective in the meiotic recombination checkpoint, such as *rad24*, *pch2* and *ddc2* (Lydall et al. 1996; Refolio et al. 2011; San-Segundo and Roeder 1999). Therefore, to determine whether regulation of the meiotic recombination checkpoint by Dot1 relies on H3K79me, we generated and analyzed *H3-K79R* and *H3-K79A* mutants, in which the lysine 79 targeted by Dot1 cannot be methylated. Importantly, like *dot1*, both methylation-site mutants suppressed the pronounced checkpoint-imposed meiotic delay of the *zip1* mutant. In an otherwise wild-type background, *DOT1* deletion has no or little meiotic effects and spore viability is high (Lui et al. 2006; San-Segundo and Roeder 2000); likewise, the *H3-K79R* and *H3-K79A* single mutants showed wild-type levels of spore viability, suggesting that H3K79me is dispensable in unperturbed meiosis. However, similar to *zip1 dot1*, spore viability was strongly reduced in *zip1 H3-K79R* and *zip1 H3-K79A*, indicating that the defects conferred by *zip1* persist in the double mutants despite their wild-type kinetics of meiotic progression. Thus, Dot1-dependent H3K79me is essential for meiotic recombination checkpoint function.

To further investigate the regulation of the meiotic checkpoint by H3K79me, we monitored checkpoint function in *zip1* diploid strains exhibiting gradually decreased Dot1 activity. In order to generate this set of

strains, we used the combination of the *dot1-G401A* allele, which confers partial catalytic activity (Frederiks et al. 2008), with the expression of *DOT1* (or *dot1-G401A)* from a plasmid, which results in lower protein levels (Conde et al., 2010). Analysis of H3K79-me1, -me2 and -me3 levels in meiotic cells confirmed a gradually reduced Dot1 activity following this order: *DOT1*>p[*DOT1*]>*dot1-G401A*>p[*dot1-G401A*]>*dot1D*, as manifested by progressively reduced H3K79-me3 and, conversely, progressively increased H3K79-me1. Interestingly, meiotic checkpoint activity, monitored as the ability to impose the *zip1* meiotic delay, also showed a gradual decrease mirroring the drop in Dot1 catalytic function. Quantification of the relative levels of each H3K79 methylation state revealed a marked correlation between H3K79-me3 and checkpoint function. Thus, the status of H3K79 methylation modulates the meiotic recombination checkpoint, with the H3K79-me3 form being the most relevant to sustain the checkpoint response.

Dot1 is required for activation of the Mek1 effector kinase

Next, we sought to determine where in the meiotic recombination checkpoint pathway Dot1-dependent H3K79me is acting. We first analyzed checkpoint sensor function by monitoring the formation of *zip1*-induced Ddc2-GFP foci (Refolio et al. 2011). Formation of Ddc2 foci was not disrupted in the absence of Dot1, suggesting that H3K79me is not required for the ability of Mec1-Ddc2 to detect meiotic recombination intermediates. Upon checkpoint activation, the Mek1 effector kinase forms nuclear foci that can be detected both on chromosome spreads (Hong and Roeder 2002) and in live meiotic cells. Strikingly, we found that the *zip1* mutant accumulated multiple discrete Mek1-GFP foci during meiotic prophase, whereas most *zip1 dot1* cells displayed a diffuse Mek1 nuclear signal and only occasional foci were observed indicating that Dot1 promotes checkpoint-induced association of Mek1 to meiotic chromosomes.

Mek1 is activated by phosphorylation in mutants that trigger the meiotic recombination checkpoint, including *zip1* (Acosta et al. 2011; Bailis and Roeder 2000; Cartagena-Lirola et al. 2006; Niu et al. 2007); therefore, we followed Mek1 phosphorylation throughout meiosis in wild-type, *zip1* and *zip1 dot1* cells using Phos-tag gels. In the wild type, Mek1 was weakly and transiently activated during the peak of meiotic prophase in this strain background (around 12-15 h). In contrast, Mek1 was hyperactivated in *zip1* cells as evidenced by the presence of additional, more persistent, and stronger phosphorylated forms. However, Mek1 hyperactivation was not observed in the *zip1 dot1* double mutant; like in wild type, only a weak and transient phosphorylated form was detected. To rule out the possibility that the difference between *zip1* and *zip1 dot1* were due to their different kinetics of meiotic progression (*zip1* exhibits a marked delay that is bypassed in *zip1 dot1*), we monitored Mek1 phosphorylation in *ndt80* pachytene-arrested cells. Meanwhile, *zip1*-induced hyperphosphorylation of Mek1 was severely impaired in the absence of Dot1.

In summary, these results place Dot1 function upstream of Mek1 in the meiotic recombination checkpoint pathway and indicate that, whereas Mec1/Ddc2 act independently of H3K79 methylation to sense meiotic defects, Dot1 is required for checkpoint-induced activation of Mek1.

Autophosphorylation of Mek1 depends on Dot1

In *ndt80*-arrested cells, using high-resolution Phos-tag gels, we were able to resolve several *zip1*-induced shifted forms of Mek1 above the basal band. Phosphatase treatment eliminated all band shifts indicating that they represent distinct phosphorylated forms. We used different *mek1* versions carrying specific mutations, as well as mutants in upstream components of the checkpoint pathway, in order to determine the contribution of different phosphorylation events to the observed checkpoint-induced Mek1 forms in *zip1 ndt80* cells. Mek1 phosphorylation was completely abolished in the *hop1* mutant, lacking a LE-component meiotic checkpoint adaptor (Carballo et al. 2008; Smith and Roeder 1997; Woltering et al. 2000) and in the *spo11* mutant, which does not initiate recombination (Keeney et al. 1997). However, in the absence of Dot1, only the upper phosphorylated bands were eliminated, but the form immediately above the basal Mek1 band remained intact. Interestingly, this moderately-shifted form was reduced in *mec1* cells and virtually disappeared in *mec1 tel1* and *rad24 tel1* mutants, suggesting that it arises from Mec1/Tel1-dependent phosphorylation. On the other hand, the kinase-dead *mek1-K199R* allele, as well as the autophosphorylation-defective *mek1-T327A* and *mek1-T331A* mutants (Niu et al. 2007), specifically lacked the upper bands displaying the stronger mobility shift, suggesting that they result from Mek1 autophosphorylation. In contrast, the Mek1 form immediately above the basal band (i.e., resulting from Mec1/Tel1 action) remained invariable in those *mek1* mutants. Thus, interestingly, the *zip1 dot1* mutant showed a similar pattern to that of *zip1 mek1-K199R*, *zip1 mek1-T327A* or *zip1 mek1-T331A*, strongly suggesting that Dot1 is mainly required for Mek1 autophosphorylation, but not for its Mec1/Tel1-dependent phosphorylation.

It has been proposed that dimerization of Mek1 promotes its function, likely by facilitating *in trans* autophosphorylation (Niu et al. 2007; Wu et al. 2010). Thus, we hypothesized that Dot1 could be required for Mek1 dimerization. Importantly, we found that GST-driven forced dimerization of Mek1 restored its full phosphorylation even in the absence of Dot1, although Mek1 activation was not maintained at late time points. Consistently, expression of *GST-MEK1* in *zip1 dot1* strains conferred a brief, but significant, meiotic delay. As previously reported, the *zip1 GST-MEK1* mutant was completely halted (Wu et al. 2010), and we found that this block was accompanied by the persistent hyperphosphorylation of GST-Mek1. The permanent or transient arrest conferred by GST-Mek1 in *zip1* or *zip1 dot1*, respectively, was completely relieved when inactive kinase (*GST-mek1-K199R*) or autophosphorylation-defective (*GST-mek1-T327A*) versions were introduced, confirming that in *GST-MEK1* strains, meiotic progression was slowed down by forced Mek1 activation and not by another unrelated cause. To further support this conclusion, we monitored another downstream molecular

marker of pachytene checkpoint activation, such as the inhibition of the production of the Cdc5 polo-like kinase (Acosta et al. 2011; Sourirajan and Lichten 2008). As expected, whereas induction of Cdc5 was delayed in *zip1* cells, the *zip1 dot1* double mutant displayed wild-type kinetics of Cdc5 production. Strikingly, consistent with the kinetics of meiotic progression, expression of *GST-MEK1* in *zip1 dot1* cells restored a significant delay in Cdc5 induction. Furthermore, Cdc5 production was severely impaired in the arrested *zip1 GST-MEK1* strain. In summary, these observations indicate that artificial dimerization of Mek1 partially overcomes Dot1 requirement for Mek1 activation and further supports the conclusion that Dot1 function promotes Mek1 autophosphorylation.

Dot1 is required for localization and activation of the Hop1 meiotic checkpoint adaptor

It has been reported that activated Hop1 promotes Mek1 dimerization via a C-terminal domain (Niu et al. 2007; Niu et al. 2005); therefore, we investigated whether the effect of Dot1 on Mek1 phosphorylation was mediated by Hop1. First, we studied Hop1 localization on chromosome spreads of *ndt80*-arrested *zip1* and *zip1 dot1* strains. As previously described (Smith and Roeder 1997), Hop1 displayed a predominantly linear staining along the lateral elements of *zip1* chromosomes. In contrast, only short stretches of Hop1 could be detected in the *zip1 dot1* mutant, which showed a predominating Hop1 punctate pattern. Consistent with our observations in live cells, we also detected a marked reduction of Mek1 chromosomal foci in *zip1 dot1*, compared to the *zip1* single mutant. In addition, we also analyzed Hop1 localization in *zip1* and *zip1 dot1* live meiotic cells expressing *HOP1-GFP*. In line with the aberrant distribution on spreads, we observed that Hop1-GFP signal was weaker and less continuous in *zip1 dot1* cells. This discontinuous localization of Hop1 does not result from a pronounced alteration of overall chromosome structure, because the SC lateral component Red1 (Smith and Roeder 1997) displayed a linear distribution in both *zip1* and *zip1 dot1* strains. On the other hand, the *dot1* single mutant only showed a modest decrease of Hop1-GFP signal compared with the wild type. Thus, upon *zip1*-induced checkpoint activation, Dot1 enables proper loading or maintenance of Hop1 onto chromosomes.

Since Mec1/Tel1-dependent phosphorylation of Hop1 at defined S/T-Q motifs is required for Mek1 activation and localization (Carballo et al. 2008), we examined *zip1*-induced Hop1 phosphorylation in the absence of Dot1, by monitoring its gel mobility shift. The *zip1 dot1* mutant displayed a severe defect in Hop1 phosphorylation, similar to the *zip1 mec1* and *zip1 spo11* mutants also analyzed as controls. Even after long overexposure of the gels, only a barely visible phosphorylated form of Hop1 could be detected in the absence of Dot1.

These observations suggest that the defect in Mek1 autophosphorylation observed in the absence of Dot1 stems from impaired Hop1 function. To confirm this notion, we overexpressed *HOP1* from a high-copy plasmid in *zip1 dot1* cells. Whereas the *zip1 dot1* mutant transformed with empty vector showed defective

Mek1 localization and activation, *HOP1* overexpression in *zip1 dot1* restored Mek1 chromosomal foci, Mek1 phosphorylation, and reestablished a substantial meiotic delay. We found that Hop1 overproduction also conferred a slight reduction in the efficiency of meiotic progression in the wild type and further enhanced the *zip1* meiotic delay, as expected from the strong hyperphosphorylation of Mek1. Notably, in all cases (wild type, *zip1* or *zip1 dot1*), the further delay in meiotic progression imposed by high levels of Hop1 was suppressed by the absence of Mek1, proving that it was caused from amplified pachytene checkpoint signaling and not from an unrelated cause.

H3K79me is required for Mek1 and Hop1 phosphorylation and localization

We have shown that, like *dot1*, mutation of H3K79 to non-methylatable residues completely bypasses the checkpoint-induced meiotic delay of *zip1*. On the other hand, we have revealed that, in *zip1* cells, Dot1 orchestrates Hop1 and Mek1 activation and chromosomal distribution. To confirm that Hop1 and Mek1 checkpoint functions are also directly regulated by H3K79me, and not by another possible methyltransferase-independent function of Dot1, we examined their phosphorylation and localization in the *zip1 H3-K79R* and *zip1 H3-K79A* mutants. We found that, indeed, these histone point mutants phenocopy the *dot1* defects in Mek1 foci formation and Mek1 autophosphorylation. Likewise, the *zip1 H3-K79R* and *zip1 H3-K79A* mutants resemble *dot1* in the impaired Hop1 chromosomal distribution and checkpoint-induced phosphorylation.

Thus, taken together, our results indicate that, upon meiotic recombination checkpoint triggering, Dot1-dependent H3K79 methylation promotes proper chromosomal localization and activation of Hop1, which in turn, is required to sustain Mek1 autophosphorylation and the ensuing checkpoint response.

H3K79me partially controls Hop1 chromosomal localization via Pch2

Previous studies have shown that whereas in the *zip1* mutant the Pch2 meiotic checkpoint protein is detected only in the nucleolar (rDNA) region, in the *zip1 dot1* double mutant Pch2 is distributed throughout all chromatin (San-Segundo and Roeder 2000). To confirm that the regulation of Pch2 localization by Dot1 depends on the histone H3 methyltransferase activity, we analyzed Pch2 distribution on spread meiotic chromosomes of the *zip1 H3-K79R* and *zip1 H3-K79A* mutants. Although global Pch2 protein levels remained fairly invariable in the different mutants, we found that, like in *zip1 dot1*, Pch2 mislocalized to chromatin outside the rDNA in *zip1 H3-K79R* and *zip1 H3-K79A* strains, suggesting that H3K79me excludes Pch2 from chromosomes.

Several lines of evidence support a role for Pch2 in promoting the turnover of Hop1 from meiotic chromosomes, at least in unperturbed meiosis (Borner et al. 2008; Joshi et al. 2009; San-Segundo and Roeder 1999); therefore, it was possible that the reduced localization of Hop1 in the absence of Dot1 could stem from the action of the Pch2 protein aberrantly present at chromosomal locations removing Hop1 from

zip1 chromosomes. To investigate this possibility, we monitored Hop1 localization in *zip1 dot1 pch2* strains. Interestingly, we found that deletion of *PCH2* alleviated to some extent the defective Hop1 localization pattern of *zip1 dot1*, although it did not fully restore the high and continuous Hop1 levels present in *zip1*. To determine whether the increased abundance of Hop1 along chromosomes in *zip1 dot1 pch2* restores the checkpoint-induced delay we analyzed meiotic divisions and Mek1 phosphorylation. We found that the checkpoint was still impaired in the *zip1 dot1 pch2* triple mutant because, like the *zip1 dot1* and the *zip1 pch2* double mutants, it displayed wild-type kinetics of meiotic progression and defective Mek1 activation, implying a more complex contribution of Pch2's function to the pachytene checkpoint response.

In summary, these observations indicate that in the *zip1* mutant, methylation of H3K79 by Dot1 controls proper chromosomal distribution of Hop1 by maintaining Pch2 confined in the nucleolar region. The fact that Hop1 localization is still partially impaired in the *zip1 dot1 pch2* triple mutant suggests that Dot1 may also regulate Hop1 chromosomal recruitment by a Pch2-independent mechanism.

DISCUSSION

Previous studies have shown that Dot1 is important for the pachytene checkpoint, but the molecular mechanism underlying such function remained unclear. Here, we provide evidence that methylation of H3K79 by Dot1 contributes to the meiotic recombination checkpoint response by enabling proper Hop1 chromosomal recruitment, which, in turn is a requisite for Mek1 activation by autophosphorylation.

We demonstrate that the function of Dot1 in the meiotic recombination checkpoint specifically relies on the methylation of H3K79, since the non-methylatable *H3-K79A* and *H3-K79R* mutations confer essentially the same meiotic phenotypes as the lack of Dot1. Moreover, by modulating Dot1 catalytic activity, we found that high levels of the H3K79-me3 are required for full checkpoint activation raising the possibility that this methylation state is particularly critical for promoting the proper localization of the Hop1 meiotic checkpoint adaptor (see below).

In mitotic cells, methylated histones are well-known chromatin marks for recognition of DSBs by checkpoint adaptors. In *S. cerevisiae*, the Rad9 adaptor is recruited to DSB sites by H3K79me (Grenon et al. 2007; Wysocki et al. 2005), whereas in *S. pombe*, which lacks H3K79me, the recruitment of the Crb2 adaptor relies on H4K20me (Sanders et al. 2004). In mammalian cells, the Rad9 and Crb2 homolog 53BP1 appears to recognize both H3K79me and H4K20me (Botuyan et al. 2006; Huyen et al. 2004; Wakeman et al. 2012). All these DNA damage checkpoint adaptors (Rad9, Crb2 and 53BP1) contain tandem tudor domains that mediate the interaction with the methylated histones. Rad9, Crb2 and 53BP1 also possess BRCT motifs; in fact, the recognition of DSBs by Rad9 and Crb2 in *S. cerevisiae* and *S. pombe*, respectively, is also mediated by their binding to phosphorylated histone H2A (hereafter γH2AX) via the BRCT domains (Hammet et al. 2007;

Sanders et al. 2010). However, the Hop1 meiotic checkpoint adaptor lacks either tudor or BRCT motifs and contains a HORMA domain likely involved in protein-protein interactions (Hunter 2008), raising the possibility that its chromosomal recruitment can be mediated by different mechanisms.

As mentioned before, in DNA damaged vegetative cells, Rad9 function depends both on H3K79me and γH2AX (Conde et al. 2009; Hammet et al. 2007; Javaheri et al. 2006; Toh et al. 2006); however, the relevance of both histone modifications appears to be different in meiotic cells. Dot1-dependent H3K79me is crucial for checkpoint function, at least in Zip1-deficient cells, because deletion of *DOT1* (or mutation of H3K79) results in complete bypass of the *zip1* meiotic block. In contrast, an *H2A-S129** mutant, lacking the four C-terminal amino acids of histone H2A including the SQ phosphorylation site (Downs et al. 2000), has no defect in the *zip1*-induced checkpoint. Moreover, like in both single mutants, meiotic progression and spore viability are essentially normal in the *dot1 H2A-S129** double mutant.

We show here that Dot1 is required for Mek1 and Hop1 activation in meiotically-challenged cells, but in addition to the checkpoint function, Mek1 and Hop1 promote the repair of meiotic DSBs by Dmc1-dependent interhomolog recombination (Carballo et al. 2008; Niu et al. 2005; Niu et al. 2009; Wu et al. 2010). Consistent with this function, in the absence of Dmc1, Dot1 prevents the repair of DSBs by Rad54-dependent sister-chromatid recombination, which is controlled, at least in part, by inhibitory phosphorylation of Rad54 by Mek1 (Niu et al. 2009; San-Segundo and Roeder 2000). In principle, it could be possible that impaired Hop1/Mek1 function in the absence of Dot1 could induce an alternative intersister recombination pathway resulting in meiotic progression because of the disappearance of the meiotic defects initially triggering the checkpoint. However, deletion of *DOT1* alleviates the meiotic arrest of *zip1 rad54* and *dmc1 rad54* mutants, where intersister repair is impaired, strongly suggesting that Dot1 performs a bona-fide meiotic checkpoint function (San-Segundo and Roeder 2000). The fact that, unlike Mek1 and Hop1, the Dot1 protein is dispensable in otherwise unperturbed meiosis implies the H3K79me is mostly relevant to signal defects when meiotic chromosome metabolism is disturbed (i.e., *zip1* or *dmc1* mutants). Consistent with this notion, Hop1 localization on *zip1* chromosomes is dramatically altered in the absence of Dot1, but it is only slightly reduced in the *dot1* single mutant as compared with the wild type.

In other studies, activation of the Mek1 effector meiotic kinase has been monitored either by a slight electrophoretic mobility shift (Carballo et al. 2008; Cartagena-Lirola et al. 2006) or by using an anti-phospho-Ser/Thr Akt substrate antibody, which specifically recognizes phosphorylation of Mek1 at T327 (Ho and Burgess 2011; Niu et al. 2007; Wu et al. 2010). However, those assays do not permit one to delineate the different events contributing to Mek1 activation. Here, by using high-resolution Phos-tag gels, we identify several phosphorylated Mek1 forms and dissect the genetic requirements for sequential Mek1 activation. Our findings support a model in which the presence of unrepaired DSBs and/or unsynapsed chromosomes results in the initial phosphorylation of Mek1 by the redundant action of Mec1/Tel1. This priming phosphorylation is

followed by autophosphorylation of Mek1 at T327 and T331 leading to full Mek1 activation supporting the checkpoint response. We found that Dot1 is chiefly required for this last step, which is mediated by Mek1 dimerization promoted by the Hop1 C-terminal domain (Niu et al. 2005). Thus, the altered localization of Hop1 on *zip1 dot1* chromosomes likely explains the defect in Mek1 autophosphorylation. Interestingly, GST-mediated forced dimerization of Mek1 bypasses Dot1 requirement for its activation; however, this activation is only transient in the absence of Dot1, suggesting that proper chromosome axis architecture is required for maintenance of Mek1 activity.

We found that global levels of H3K79me do not significantly change in response to the meiotic defects of the *zip1* mutant, but this methylation is critical for the checkpoint response. The nature of the signal that triggers the meiotic checkpoint in *zip1* is still unclear. Like in mammals (Wojtasz et al. 2012), the existence of a synapsis checkpoint in yeast has also been proposed (Ho and Burgess 2011; Hochwagen and Amon 2006; MacQueen and Hochwagen 2011). Nevertheless, Dot1 is also required for the meiotic cell cycle arrest of the *dmc1* mutant that accumulates unrepaired DSBs (San-Segundo and Roeder 2000), indicating that H3K79me is also involved in the response to meiotic DSBs. It has been reported that, under certain conditions, DSBs are efficiently repaired in *zip1* mutants (Wu et al. 2010) implying that the signal triggering the checkpoint could be different. However, Ddc2 foci marking the presence of recombination intermediates are detected in *zip1* (Refolio et al. 2011), consistent with at least some DSBs remaining unrepaired in *zip1* mutants (Bishop 1994; Borner et al. 2004; Storlazzi et al. 1996) sufficient to induce the checkpoint. Alternatively, or in addition, Mec1-Ddc2 may also sense defects in structural aspects of interhomolog interactions resulting from the lack of the central region of the SC (Borner et al. 2008). In any case, independently of the nature of the signal triggering the meiotic checkpoint response(s), the question of how a constitutive histone mark, such as H3K79me, contributes to Hop1-mediated Mek1 activation specifically in challenged meiosis remains to be elucidated. In the DNA damage response in vegetative yeast cells or somatic mammalian cells it has been proposed, though never proven, that chromatin remodeling in the vicinity of DNA lesions may locally expose constitutive marks (i.e., H3K79me, H4K20me) supporting the recruitment of DNA damage checkpoint adaptors to activate the checkpoint (Botuyan et al. 2006; Huyen et al. 2004). In meiotic cells, the DSB metabolism is linked to the special architecture of the chromosome axis (Panizza et al. 2011). Therefore, we envision that unrepaired DSBs and/or defects in interhomolog connections may provoke chromatin conformational changes unmasking H3K79me capable to drive proper Hop1 distribution along the axes, enabling its activation by Mec1 to elicit the downstream checkpoint events including Mek1 full activation by autophosphorylation.

Although it is formally possible that H3K79me may directly facilitate Hop1 recruitment to some extent, we provide evidence indicating that the control of Hop1 chromosomal distribution by H3K79me is substantially driven by regulation of the Pch2 protein. Pch2 was initially discovered as a meiotic checkpoint protein required for the *zip1*-induced meiotic arrest (San-Segundo and Roeder 1999), but more recent studies have shown that

Pch2 impacts multiple aspects of meiotic chromosome dynamics (Farmer et al. 2012; Ho and Burgess 2011; Vader et al. 2011; Zanders and Alani 2009). In particular, Pch2 acts as a negative regulator of Hop1 chromosomal abundance (Borner et al. 2008; Joshi et al. 2009). In wild-type pachytene chromosomes, Pch2 localizes to the unsynapsed rDNA region (nucleolus) and also along synapsed chromosomes (Joshi et al. 2009; San-Segundo and Roeder 1999). In contrast, Pch2 is solely detectable at the nucleolar region in the *zip1* mutant (San-Segundo and Roeder 1999); remarkably, in the absence of H3K79me, Pch2 is redistributed throughout all chromatin of *zip1* nuclei. We hypothesize that, as a consequence of the synapsis defects of *zip1,* the H3K79me mark becomes exposed functioning as an anti-binding signal for Pch2, thus permitting the extensive Hop1 distribution found on *zip1* chromosomes. In the absence of Dot1 (or H3K79me), the presence of chromosomal Pch2 triggers the removal of Hop1 and the consequent defect in Mek1 activation. The reduced global levels of Hop1 detected in *zip1 dot1* are also consistent with a higher protein turnover.

Interestingly, like in *zip1 dot1*, the synapsis checkpoint is still completely defective in the *zip1 dot1 pch2* triple mutant, despite the partial restoration of Hop1 localization. Since the excess of Hop1 induced by other means, such as *HOP1* overexpression, but in the presence of Pch2, does confer a meiotic delay in *zip1 dot1* and restores Mek1 phosphorylation, it is conceivable that nucleolar Pch2 performs an additional downstream function in Mek1 activation and/or that the excess of Hop1 in the absence of Pch2 is not correctly assembled on chromosome axes to support checkpoint activation. In fact, the *zip1 pch2* mutant itself is also checkpoint deficient. Future studies will address these intriguing possibilities.

Dot1/DOT1L is structurally conserved throughout evolution from budding yeast to worms, flies, mice and humans; therefore, it is possible that members of the Dot1 family play similar roles in Metazoa. DOT1L is essential in mammals (Jones et al. 2008) functioning in embryogenesis, hematopoiesis and cardiac development (Nguyen and Zhang 2011); however, much less is known about the impact of mammalian DOT1L in the DNA damage response. It would be interesting to determine whether, like the yeast counterpart, Dot1 orthologs are involved in meiotic checkpoint control in higher eukaryotes.

ARTICLE 2

Dynamics of DOT1L localization and H3K79 methylation during meiotic prophase I in mouse spermatocytes

Here, we report the characterization of DOT1L localization and the chromatin distribution of the distinct H3K79 methylation states (me1, me2 and me3) during meiotic prophase I in spermatocytes of wild-type mice and various meiotic mutants. Our results reveal a progressive increment of DOT1L activity as prophase I advances, and the existence of differential spatio-temporal patterns for H3K79me2 and H3K79me3. Furthermore, the comparison of the distribution of these epigenetic marks with that of the H3.3, γH2AX, macroH2A and H2A.Z histone variants hints at a functional contribution of H3K79me2 and H3K79me3 to the characteristic transcriptional states of the different subnuclear territories in spermatocyte nuclei.

Spatial and temporal patterns of DOT1L and H3K79me distribution during meiotic prophase I

To investigate the localization of mammalian DOT1L and the associated mono-, di- and tri-methylation of histone H3 at lysine 79 (H3K79me1, me2, and me3, respectively) we performed immunofluorescence of surface-spread meiotic chromosomes from wild-type mouse spermatocytes. We tracked SYCP3, a component of the axial/lateral elements of the SC (Lammers et al. 1994), to define the stage of prophase I of each spermatocyte nucleus based on the degree of synapsis exhibited by the chromosomes. At the beginning of prophase I, short stretches of SYCP3 start to develop during leptonema. At zygonema, synapsis of homologs begins and thickened SYCP3 areas along the already synapsed regions are detected. At pachynema, synapsis between the autosomes is completed, resulting in a thick and uniform SYCP3 signal. A subnuclear domain formed by the sex chromosomes, the so-called "XY body" or "sex body", begins to emerge around the end of zygonema, and is fully formed in pachynema. This chromosome pair displays a short synapsed area on a limited distal region of homology, the pseudoautosomal region (PAR). The PAR exhibits thickened SYCP3 staining, whereas a thinner signal is visible along the unsynapsed non-homologous regions. At diplonema, homologs progressively desynapse revealing spaces between the SYCP3 axes, but they still remain joined at chiasmata sites where crossovers have occurred. In addition, from late pachynema, but more evident during diplonema, the chromosomes show thickenings at the ends, which correspond with their attachment to the inner nuclear membrane (Liebe et al. 2004). Meanwhile, in the sex body desynapsis also occurs, the X and Y chromosomes are joined end-to-end, and the X chromosome shows thickenings along its length. At diakinesis-metaphase I, SC disassembly is general, SYCP3 staining is mainly concentrated at the centromeric areas, and only remnants persist on chromosome arms. The X chromosome remnants are the last ones to disappear (Parra et al. 2004; Barchi et al. 2008).

First, we monitored DOT1L localization throughout meiotic prophase I. Interestingly, we found a progressive increment of the association of this histone methyltransferase with meiotic chromatin correlating with the progression through prophase I stages. DOT1L nuclear staining started at very low levels at leptonema, increased slightly in zygonema, followed by a dramatic increment in DOT1L levels at pachynema and, especially, during the diplonema and diakinesis stages. The sex body exhibited particularly dynamic patterns, detailed below.

Next, we analyzed the distribution of the three possible methylated states of H3K79 resulting from DOT1L action: H3K79me1, -me2 and -me3. Overall levels of H3K79me1 were uniformly weak at all stages. In contrast, H3K79me2 exhibited a progressive enrichment concurrent with prophase I progression, achieving relatively strong staining during pachynema, diplonema and diakinesis/metaphase I. H3K79me3 staining also intensified during meiotic prophase I, reaching the highest levels in diakinesis/metaphase I.

These observations indicate that overall levels of chromatin-associated DOT1L and H3K79 methylation undergo significant change during male mouse meiotic prophase I. The enrichment of DOT1L is accompanied by higher amounts of two particular methylation states, H3K79me2 and H3K79me3; however, their dynamics and subnuclear distribution were different.

We examined DOT1L and H3K79me in more detail starting from the stage when they became more abundant, pachynema, and focused on the distinctive chromatin regions that can be distinguished according with their intensity of DAPI staining and chromosome positioning, marked by SYCP3. In this way, we discriminated areas with weaker DAPI fluorescence signal, corresponding to euchromatin and encompassing most of the autosome domains. On the other hand, subnuclear territories with more intense DAPI staining were classified into two groups: the constitutive heterochromatin located at the centromeric regions surrounding one end of each mouse autosome (which are telocentric; Kalitsis et al. 2006), and the facultative heterochromatin of the sex body. We quantified the signal intensity of DOT1L and the different H3K79me states in the DAPI-bright regions relative to the remaining chromatin. Strikingly, we found that, as soon as the large centromeric regions became apparent after mid-zygonema, they exhibited strong accumulation (about 7-fold) of H3K79me3. These areas continued to be highly trimethylated at H3K79 through metaphase I, enclosing the centromere-proximal SYCP3 remnants (Parra et al. 2004). Furthermore, strong H3K79me3 staining could be still detected at the chromocenter in round spermatids. In contrast, neither DOT1L, H3K79me1, nor H3K79me2 showed this centromeric accumulation, with ratios relative to euchromatin regions close to 1, denoting a more uniform distribution between both types of subnuclear territories.

Sex body development involves massive chromatin remodeling events to establish a heterochromatin configuration that leads to a transcriptional inactivation program, the so-called "meiotic sex chromosome

inactivation" (MSCI) (Handel 2004; Turner 2007). Little is known about the contribution of DOT1L and H3K79me to MSCI, so we analyzed their distribution in the sex body from pachynema to metaphase I. At pachynema, the amount of DOT1L in the sex body was roughly at the average level of the rest of the nucleus, but during diplonema and at diakinesis-metaphase I it significantly increased (2- and 4-fold, respectively). H3K79me1 maintained a stable, relatively uniform pattern over the entire nucleus at all stages, while H3K79me2 was under-represented in the sex body from pachynema up to diakinesis/metaphase I. Finally, XY-associated H3K79me3 started at low amounts during pachynema, matched autosome levels at diplonema and reached a 2-fold higher level at diakinesis-metaphase. In more advanced stages of spermatogenesis, such as in round spermatids, the more intense DAPI-stained territory adjacent to the chromocenter contains the sex chromosome X or Y (Greaves et al. 2006). We found that H3K79me3 was also detected in this region, although at lower levels than in the chromocenter.

Thus, DOT1L and the ensuing H3K79me states exhibit characteristic spatio-temporal dynamics suggestive of possible differential roles during male mouse meiotic prophase I.

Impaired DOT1L localization and H3K79 methylation patterns in meiotic mutants

To determine whether DOT1L and H3K79 methylation patterns are functionally tied to meiotic progression and/or recombination, we examined mutants affected at different stages during meiosis: *Spo11β*-only, *Trip13*$^{mod/mod}$, *Spo11*$^{-/-}$ and *Dmc1*$^{-/-}$ (ordered from the one that reaches the furthest stage to the mutant with the least progression). These mutants exhibit defects in synapsis and/or recombination, with different degrees of severity that are incompatible with a successful meiosis program and lead to widespread checkpoint-induced arrest and apoptosis before the first meiotic division. The arrest point varies in the different male mouse mutants, but all are infertile (Barchi et al. 2005; Burgoyne et al. 2009; Handel and Schimenti 2010; Kauppi et al. 2011).

> *Spo11β*-only

The *Spo11*$^{-/-}$ *Tg(Xmr-Spo11β*$_B$*)*$^{+/+}$ transgenic mouse (hereafter, *Spo11β*-only) exclusively expresses the *Spo11β* splice variant, which is capable of supporting crossing-over, pairing, and synapsis normally in autosomes, but is defective in promoting late, efficient DSB formation specifically at the PAR (Kauppi et al. 2011). *Spo11β*-only spermatocytes frequently display X-Y association defects that trigger the spindle checkpoint causing apoptosis at metaphase I, so few spermatocytes reach later stages (Kauppi et al. 2011). We analyzed DOT1L localization and the H3K79me state in *Spo11β*-only from leptonema to diplonema. Consistent with prior results, although some sperm were seen, few spermatocytes at diakinesis or more advanced stages were found. Also as described previously, the X-Y chromosomes were unsynapsed in most sex bodies. *Spo11β*-only spermatocytes showed DOT1L staining similar to wild type: little or no signal at leptonema and zygonema, but significant signal during the pachytene and diplotene stages with

accumulation at the sex body especially in diplotene nuclei. H3K79me1 also showed no significant differences from control spermatocytes. In contrast, overall H3K79me2 levels were reduced in *Spo11β*-only diplotene nuclei relative to the wild type, although close to the control values for the remaining stages. As in the control, the H3K79me2 signal in the *Spo11β*-only sex body was lower than the average for the rest of the nucleus. Finally, although H3K79me3 staining in *Spo11β*-only displayed the characteristic increasing trend throughout prophase I progression, the levels were significantly reduced during pachynema and diplonema. Nevertheless, H3K79me3 was enriched at centromeric regions in the mutant.

> Trip13$^{mod/mod}$

We analyzed mice carrying a hypomorphic mutation of the yeast *PCH2* ortholog, *Trip13*, referred to as *Trip13$^{mod/mod}$* for "moderate" defect (Li et al. 2007; Roig et al. 2010). *Trip13$^{mod/mod}$* males show apparently fully synapsed chromosomes, but there is inefficient repair of meiotic DSBs, aberrant SC development and abnormal sex body formation, triggering a checkpoint response that leads to meiotic arrest and apoptosis at pachynema (Li et al. 2007; Wojtasz et al. 2009; Roig et al. 2010). We found no significant differences between wild type and *Trip13$^{mod/mod}$* spermatocytes with respect to either distribution or amount of DOT1L, H3K79me1, H3K79me2 or H3K79me3 in leptotene through pachytene spermatocytes (too few spermatocytes at diplonema or further are found in this mutant, precluding analysis of later stages). H3K79me3 localization in the sex body and centromeric regions was also unaltered.

> Spo11$^{-/-}$

This mutant lacks the evolutionary-conserved Spo11 transesterase that catalyzes meiotic DSBs, so it exhibits no meiotic recombination and fails in homolog pairing and synapsis. These defects trigger a DNA damage-independent checkpoint that leads to apoptosis at the zygotene-pachytene transition, a so-called zygotene-like stage (Baudat et al. 2000; Romanienko and Camerini-Otero 2000). We examined *Spo11$^{-/-}$* spermatocytes from leptotene to the zygotene-like stage, dividing the latter into two classes: early, with shorter SYCP3 stretches and low levels of axial association; and late, with full-length SYCP3 and extensive aberrant non-homologous synapsis. We found only very low levels of DOT1L and H3K79me1 staining throughout these stages in the *Spo11$^{-/-}$* mutant. H3K79me2 and H3K79me3 increased slightly at the zygotene-like stage, but in all cases, the signal intensity of DOT1L and all H3K79 methylation states was significantly reduced in the *Spo11$^{-/-}$* mutant.

> Dmc1$^{-/-}$

The *Dmc1$^{-/-}$* mutant fails to repair meiotic DSBs and exhibits impaired synapsis, leading to arrest and apoptosis in a zygotene-like stage similar to that of *Spo11$^{-/-}$* (Pittman et al. 1998; Yoshida et al. 1998). However, molecular markers have revealed differences between the arrests in these two mutants. Specifically, unlike *Spo11$^{-/-}$*, *Dmc1$^{-/-}$* spermatocytes maintain the TopBP1 and γH2AX DNA damage checkpoint factors associated with chromatin, lack the H1t histone variant, and do not establish pseudo-sex

bodies (Barchi et al. 2005). Therefore, although both mutants undergo apoptosis at a cytologically similar zygotene-like stage, molecular events indicate that *Dmc1*$^{-/-}$ spermatocytes are arrested earlier. We monitored DOT1L and H3K79me in *Dmc1*$^{-/-}$ from leptotene to zygotene-like stages, divided into early and late categories, as above. Similar to *Spo11*$^{-/-}$, we found that the levels of DOT1L and all the H3K79 methylation states were significantly lower than in the wild-type control, especially in late zygotene-like spermatocytes.

Sex body-specific dynamics of H3K79me3 and particular histone variants

To achieve MSCI, chromatin remodeling takes place in the sex body during pachynema. Histone H3 plays an important role in this process, via eviction of the canonical H3.1 and H3.2 forms and replacement by the H3.3 histone variant. As a consequence of this replacement, the PTMs carried by the H3.1/H3.2–H4 tetramers are removed; thus, the chance to establish new marks and/or the need to recover some of the lost ones emerges (van der Heijden et al. 2007). Other histone variants, such as H2A.Z, macroH2A and γH2AX, also exhibit remarkable changes during sex body development (Hoyer-Fender et al. 2000; Fernandez-Capetillo et al. 2003; Greaves et al. 2006). Therefore, we compared the spatio-temporal pattern of DOT1L-dependent H3K79me3 at the sex body with that of those specific histone variants.

In agreement with previous observations (van der Heijden et al. 2007), we found an approximately 4-fold enrichment for the H3.3 variant in the sex body during pachynema and diplonema. The incorporation of H3.3 appeared to be exclusive for the sex body, since the centromeric regions did not show any particular accumulation of this histone variant. Total histone H3 distribution at these stages remained more uniform.

We found that the progressive enrichment of DOT1L in the sex body from early diplonema correlated with a decrease in γH2AX. In addition, the strong accumulation of H3K79me3 in the sex body during diakinesis-metaphase coincided with the complete disappearance of detectable γH2AX signal. Therefore, these two histone PTMs (H3K79me3 and γH2AX) are largely mutually exclusive, at least in the sex body. During these stages, H3K79me2 remained low and the H3K79me1 was uniformly weak.

Finally, we analyzed the dynamics of the histone H2A variants macroH2A and H2A.Z in the sex body. The macroH2A variant defines heterochromatin areas, is enriched in the sex body from pachynema onward, participates in MSCI and disappears at later stages during diakinesis-metaphase I (Hoyer-Fender et al. 2000). In turn, it has been reported that the expression of H2A.Z begins in pachynema and peaks in round spermatids, supporting a role for H2A.Z in maintaining MSCI after disappearance of macroH2A and γH2AX (Greaves et al. 2006). We found H2A.Z all over the nucleus, except for strong exclusion from the sex body during pachynema and early-mid diplonema. Then, H2A.Z became progressively more abundant in the sex body starting in late diplonema, reaching the same overall levels as the rest of the chromatin during diakinesis-metaphase I.

Therefore, whereas H3K79me3 exhibits limited coexistence with macroH2A at the sex body, its accumulation at this region correlates with the deposition of H2A.Z during late prophase I.

DISCUSSION

In this report, we describe the localization of the histone methyltransferase DOT1L during male mouse meiotic prophase I. Since Dot1/DOT1L can mono-, di-, or tri-methylate H3K79, we also followed the dynamics of each individual methylation state resulting from DOT1L activity. Our cytological analyses show that the association of DOT1L with meiotic chromatin increases as prophase I progresses. Interestingly, although the H3K79me2 and H3K79me3 states, but not H3K79me1, also display a progressive increment, they show remarkable differences with respect to the subnuclear distribution, particularly in autosomal chromatin domains, centromeric chromatin, and the sex body. The findings suggest that each H3K79 methylation state may have a specific role during mammalian spermatogenesis. This highly dynamic scenario contrasts with the situation in yeast, where global levels of H3K79me do not significantly change during meiosis (Ontoso et al. 2013a). Although the precise chromosomal distribution of the different methylation states remains to be tested in yeast, it is likely that DOT1L activity during male mouse meiosis is subjected to a more complex regulation.

H3K79me3 in the sex body

Of the extensive chromatin remodeling that accompanies MSCI during early pachynema (Handel 2004; Turner 2007), one of the most dramatic changes is the replacement of histone H3.1/2 by the H3.3 variant, which implies the loss of most of the PTMs already established in the XY chromatin and the opportunity to introduce novel or additional marks (van der Heijden et al. 2007). Tri-methylation of histone H3 at other sites, such as H3K27, is among the repressive PTMs lost from the XY body during pachynema (van der Heijden et al. 2007). We find that the gradual increase of DOT1L all over the nucleus is especially evident in the sex body from diplonema onwards, coincident with the pronounced accumulation of H3.3. The H3.3 histone variant differs from H3.1 or H3.2 only in five or four amino acids, respectively, and the H3K79 position, as well as the structure of nucleosomes containing either one of these three H3 variants, is conserved (Tachiwana et al. 2011). Moreover, in somatic mammalian cells, the presence of K79me1 and K79me2 in H3.3 has been reported (Hake et al. 2006; Sweet et al. 2010; Zee et al. 2010). Therefore, since DOT1L is the only methyltransferase known for H3K79, it is conceivable that DOT1L is responsible for the extensive tri-methylation of the H3.3 variant at K79 in the sex body during the late stages of meiotic prophase I. We note that there is a temporal shift between the prominent localization of DOT1L in the sex body (at diplonema) and the strong accumulation of H3K79me3 (at diakinesis). The additional regulation of DOT1L activity and/or substrate accessibility by other histone PTMs (i.e., H2BK120 ubiquitylation; McGinty et al. 2008) may account for this displacement.

H3K79me3 has been related with transcriptional repression in mammalian somatic cells (Barski et al. 2007). The H3K79me3 enrichment at the XY pair takes place during the diplotene/diakinesis transition when the staining for γH2AX and the repressive macroH2A variant becomes weaker. Nevertheless, it is possible that, although undetectable with our spreading technique, at least a fraction of these histone variants remains associated with the sex chromosomes until later meiotic stages, as occurs in other mammalian species (de la Fuente et al. 2007, 2012; Namekawa et al. 2007). Conversely, H2A.Z, which is initially excluded from the sex body, arrives at this location at the same time as H3K79me3 accumulates. Most of the gene repression started with MSCI remains at postmeiotic stages, and may be linked with imprinted X-inactivation, although a subset of sex chromosome genes is upregulated postmeiotically (Namekawa et al. 2006; Mueller et al. 2008). As has been proposed for H2A.Z (Greaves et al. 2006) and other chromatin modifications, such as H3K9me2 and the recruitment of the heterochromatin proteins HP1β and HP1γ (Namekawa et al. 2006), our results are consistent with a role for DOT1L-mediated H3K79me3 in maintaining silencing of sex chromosomes from diplonema onwards. Curiously, in yeast, H2A.Z and H3K79 methylation also collaborate in the maintenance of differentiated chromatin domains contributing to the establishment of boundaries between the subtelomeric silenced chromatin and the active euchromatin (van Leeuwen et al. 2002; Ng et al. 2003; Meneghini et al. 2003). On the other hand, we demonstrate that the H3K79me2 mark, which is related with active transcription in somatic cells (Kouskouti and Talianidis 2005; Miao and Natarajan 2005; Zhou et al. 2011), remains largely excluded from the sex body with a faint signal only during late prophase I and metaphase I stages, presumably corresponding to the small fraction of X-linked genes expressed after MSCI (Mueller et al. 2008).

H3K79me3 at the centromeric heterochromatin

H3K79me3 also exhibits strong enrichment in the constitutive heterochromatin at centromeric regions during meiotic prophase I. This tendency was also reported in mouse somatic cells and oocytes, where H3K79me3 colocalizes with the heterochromatin protein HP1β (Ooga et al. 2008). Another histone PTM associated with transcriptional silencing, such as H3K9me3 (Cowell et al. 2002; Wu et al. 2005), similarly accumulates at centromeric regions during mid-prophase I (Page et al. 2012). However, this mark has a wider localization all over the nucleus until mid-pachynema and, unlike H3K79me3, displays a reduced signal in the sex chromosomes from mid-pachynema onwards (Page et al. 2012), coincident with the replacement of H3.1/2 by H3.3. These observations are consistent with a specific role for H3K9me3 in transcriptional repression of the autosomes during early prophase I, and together with H3K79me3 in the establishment of centromeric heterochromatin. However, whereas the H3.3 newly incorporated at the sex body appears to be a favorable substrate for DOT1L and becomes highly tri-methylated at K79 during diplonema/diakinesis, it does not seem to be a target for the Suv39h methyltransferases responsible for H3K9me. Additional histone PTMs at centromeric regions, such as H3K9me2, H4K5ac and H4K16ac (ac, acetylation) also undergo particular dynamics during

meiotic prophase I (Khalil and Driscoll 2010). Therefore, distinctive PTM combinations could set up spatial and temporal control of transcriptional repression or (re)activation during particular stages (Greaves et al. 2006; Namekawa et al. 2006; van der Heijden et al. 2007; Mueller et al. 2008; Khalil and Driscoll 2010; Page et al. 2012). Our results suggest that DOT1L-dependent H3K79me3 also impinges on this exquisite control. Consistent with a role for H3K79 methylation in heterochromatin formation it has been shown that DOT1L-deficient mouse embryonic stem cells possess reduced levels of constitutive heterochromatin marks, such as H4K20me3, at subtelomeric regions (Jones et al. 2008). Since DOT1L appears to be the only methyltransferase responsible for H3K79me in mouse (Jones et al. 2008), it is somehow surprising that the accumulation of H3K79me3 at centromeric domains does not correlate with stronger DOT1L staining in these regions. It is possible that the crosstalk with other(s) centromeric-specific histone PTMs may stimulate DOT1L activity specifically at these locations to reach higher levels of the maximum methylation state (i.e., H3K79me3). Alternatively, slower dynamics of histone H3 replacement at centromeres could also explain the accumulation of H3K79me3 (De Vos et al. 2011).

A potential role for H3K79me2 in autosomal transcriptional reactivation

In contrast to H3K79me3, we found a rather homogeneous distribution of H3K79me2 all over the nucleus, except for the exclusion from the sex body. Similar widespread localization has been described in mouse oocytes (Ooga et al. 2008). H3K79me2, like H3K4me3 and various H3 acetylation events, are characteristic marks of active genes in mammalian somatic cells (Kouskouti and Talianidis 2005; Miao and Natarajan 2005; Zhou et al. 2011). The H3K79me2 increase that we detect starting at pachynema and following DOT1L accumulation coincides temporally with the general transcriptional reactivation occurring on autosomes during the transition from mid to late pachynema and continuing in diplonema (Page et al. 2012). In addition, H3K79me2 distribution during prophase I exhibits a similar spatio-temporal pattern to that of H3K9ac and the active form of RNA polymerase II (RNAPII), both strongly associated with active transcription (Page et al. 2012). Furthermore, human DOT1L functionally interacts with actively transcribing RNAPII, which targets the methyltransferase to active genes (Kim et al. 2012a). Therefore, widespread DOT1L-dependent H3K79me2 from pachynema onwards could be an additional element contributing to the resumption of transcription in autosomes when recombination intermediates are resolved and characteristic marks, like γH2AX, and Dmc1/Rad51 foci, disappear. Alternatively, it could be also possible that accumulation of H3K79me2 is a consequence of transcriptional reactivation.

H3K79 methylation in challenged meiosis

Dot1/DOT1L-mediated H3K79me has multiple functions in a variety of biological processes from yeast to mammals (Nguyen and Zhang 2011); but the functional contribution of Dot1 to meiosis has been investigated mostly in budding yeast. Dot1 is not required in unperturbed meiosis, but is essential for the

checkpoint responses to the accumulation of unrepaired meiotic DSBs and synapsis defects that occur in yeast *dmc1* and *zip1* mutants, respectively (San-Segundo and Roeder 2000; Ontoso et al. 2013a). Unlike other chromatin marks, e.g., γH2AX, neither DOT1L nor H3K79me showed evidence for relocalization or redistribution in various mouse mutants defective at different steps in prophase I. The reduced levels of DOT1L, H3K79me2 and H3K79me3 at the latest stage of development reached in *Spo11*$^{-/-}$ and *Dmc1*$^{-/-}$ mutants are likely the consequence of the arrested meiosis that hampers the progressive accumulation of DOT1L observed in the wild type. Higher levels of H3K79me2/3 are present in the *Spo11β*-only mouse, which shows milder meiotic defects, compared to the severely affected and prematurely arrested *Spo11*$^{-/-}$ and *Dmc1*$^{-/-}$ mutants, which barely accumulate those marks. The fact that DOT1L-dependent H3K79 modifications do not relocalize to sites of unrepaired DSBs or unsynapsed chromosomes in these mutants does not preclude a role for DOT1L in the mammalian checkpoints responding to meiotic defects. Actually, in the synapsis-defective *zip1* mutant of budding yeast, global H3K79me levels do not change compared with the wild type, despite the essential role of Dot1-dependent H3K79me in the checkpoint response promoting the *zip1* meiotic delay (Ontoso et al. 2013a). Furthermore, in the DNA damage checkpoint triggered by unrepaired DSBs in somatic cells, a similar situation exists, because neither global nor local changes in H3K79 methylation occur, despite its role in the recruitment of mammalian 53BP1 or yeast Rad9 checkpoint adaptors (Huyen et al. 2004; Wysocki et al. 2005). Models involving chromatin remodeling events that locally expose methylated H3K79 residues under certain faulty circumstances have been invoked to explain these findings (Huyen et al. 2004; Wysocki et al. 2005; Ontoso et al. 2013a). In the yeast *zip1* mutant, Dot1 promotes the accumulation of the HORMAD1/2 homolog Hop1 on unsynapsed axes to enable activation of the Mek1 checkpoint effector kinase. H3K79me-dependent chromosonal exclusion of the Trip13-homolog Pch2 contributes in part to the regulation of Hop1 localization (Ontoso et al. 2013a). Although Pch2's checkpoint role is not restricted to yeast and it also exists in worms and flies (San-Segundo and Roeder 1999; Bhalla and Dernburg 2005; Joyce and McKim 2009), no evidence of the participation of Trip13 in mouse meiotic checkpoints has been found so far (Li et al. 2007; Roig et al. 2010). Therefore, if DOT1L also performs a meiotic checkpoint function in mouse it is unlikely to be exerted via Trip13 regulation.

Concluding remarks

Although functional interpretations from cytological analysis must be taken with caution, our results are consistent with a role for DOT1L and H3K79me at least in the special dynamics of chromatin repression/(re)activation that takes place during male mouse meiotic prophase I. Our observations open several intriguing questions, and more work needs to be done to expand our knowledge about DOT1L and H3K79me meiotic function(s) and regulation. For example, how is the same methyltransferase responsible for two methylated stages at the same target with such different roles? Undoubtedly, a fine regulation must

be involved, perhaps mediated through the crosstalk with neighboring PTMs and/or histone variants in each moment and location. Alternatively, or in addition, the several DOT1L splicing isoforms in mice (Zhang et al. 2004) may have different affinities and/or requirements for catalytic activity, or the regulation could be imposed by other components of the DotCom complex (Mohan et al. 2010). Since DOT1L-knockout mice are not viable and die by embryonic day 10.5 (Jones et al. 2008), the development of conditional testis-specific DOT1L-deficient mice would be an invaluable tool to address the functional contribution of H3K79me to various meiotic events.

ARTICLE 3

Regulation of tolerance to DNA alkylating damage by Dot1 and Rad53 in *Saccharomyces cerevisiae*

Here we investigate in more detail how Dot1 function contributes to the regulation of DNA damage tolerance. We find that Dot1 modulates the response to the alkylating agent MMS through its catalytic activity on H3K79. In fact, progressively reduced levels of H3K79 trimethylation result in gradually increased resistance to MMS. In addition, we examine the functional interaction between Dot1 and an HA-tagged version of the Rad53 checkpoint kinase that also promotes increased MMS resistance and mutagenesis (Cordon-Preciado et al., 2006). Our results indicate that there is a window of opportunity for TLS to act in the face of MMS lesions that is delineated by threshold levels of Rad53 activity. Moreover, we present evidence indicating that the contribution of Dot1 to DNA damage tolerance is exerted via Rad53 and controls the levels of Rev1 protein associated with chromosomes

Dot1-dependent histone H3K79 methylation regulates tolerance to alkylating DNA damage

Our group previously reported that the absence of Dot1 results in increased resistance to chronic MMS exposure as a consequence of enhanced TLS-mediated tolerance (Conde and San-Segundo 2008). The only known biochemical function of Dot1 is the mono-, di-, and trimethylation of lysine 79 in histone H3 (van Leeuwen et al. 2002). To determine whether regulation of MMS resistance by Dot1 relies on its methyltransferase activity, we analyzed a catalytically-inactive *dot1-G401V* mutant, in which the glycine at position 401 in the Dot1 active site has been substituted by a valine (Sawada et al. 2004). Like *dot1*Δ, the *dot1-G401V* mutant completely lacked detectable H3K79 methyltransferase activity and also displayed enhanced MMS resistance relative to the isogenic wild-type strain, indicating that the catalytic activity of Dot1 is required for its function in MMS tolerance. The only known substrate of Dot1 is H3K79; therefore, to confirm that the MMS resistance of *dot1*Δ is due to the lack of H3K79 methylation, we analyzed an *H3-K79A* mutant, in which the lysine 79 targeted by Dot1 has been replaced by an alanine and cannot be methylated (Fleming et al. 2008). Like *dot1*Δ, the *H3-K79A* allele conferred increased MMS resistance.

To investigate in more detail the regulation of DNA damage tolerance by H3K79 methylation, we examined MMS resistance in strains exhibiting gradually diminished Dot1 catalytic activity. We utilized the combination of two genetic tools to alter the levels of Dot1 activity: a) use of a *dot1-G401A* mutant, which produces a partially active protein (Frederiks et al. 2008), and b) expression of the gene under its own promoter, but from a single-copy plasmid (p[*DOT1*] or p[*dot1-G401A*]), which results in reduced amount of protein. Given the distributive mode of action of Dot1 (Frederiks et al. 2008), the wild-type strain expressing *DOT1* from its endogenous locus displayed the maximal activity with the highest levels of H3K79-me3 and the

lowest levels of H3K79-me1. The catalytic activity was then gradually reduced, as manifested by decreasing levels of H3K79-me3 and increasing levels of H3K79-me1, following this sequence: *DOT1* > p[*DOT1*] > *dot1-G401A* > p[*dot1-G401A*] > *dot1-G401V* ≈ *dot1*Δ. Interestingly, we found that the progressive reduction of Dot1 activity led to a gradually elevated MMS resistance. In particular, quantification of the relative levels of each methylation state revealed a clear correlation between the drop of H3K79-me3 and the enhanced resistance to MMS. Thus, tolerance to alkylating damage is finely modulated by H3K79 methylation levels.

The MMS resistance of *dot1D* depends on PCNA ubiquitylation at lysine 164

Our previous observations indicated that the increased MMS resistance and mutagenesis frequency of *dot1*Δ is as a consequence of enhanced tolerance mediated by the TLS pathway of DNA damage bypass, because it is abolished in the absence of Polz/Rev1 (Conde and San-Segundo 2008). DNA damage-induced PCNA ubiquitylation at lysine 164 is carried out by the Rad6/Rad18 (E2-E3) complex (Bergink and Jentsch 2009; Hoege et al. 2002; Ulrich 2005) and it is a key regulator of the tolerance to genotoxic insults (Gallego-Sanchez et al., 2010). Therefore, to determine whether the MMS resistance conferred by the absence of Dot1-promoted H3K79 methylation relies on this PCNA modification, we deleted *DOT1* in a PCNA ubiquitylation-deficient *pol30-K164R* mutant (Hishida et al. 2006). As expected, the *pol30-K164R* mutant was extremely sensitive even to low MMS concentrations, underscoring the importance of DNA damage tolerance pathways in promoting viability after alkylating damage (Hoege et al. 2002). However, although the absence of Dot1 suppresses the sensitivity of an ample range of mutants impaired in coping with MMS-induced lesions (Conde and San-Segundo 2008), deletion of *DOT1* failed to suppress the MMS sensitivity of *pol30-K164R*. Moreover, the *dot1*Δ *pol30-K164R* double mutant was more sensitive to MMS than *pol30-K164R*. Likewise, the *rev3*Δ *dot1*Δ or *rev1*Δ *dot1*Δ double mutants are also more sensitive to MMS than *rev3*Δ or *rev1*Δ (Conde and San-Segundo 2008). These observations unveil the additional role of Dot1 in another process, such as homologous recombination (Conde et al. 2009), which becomes more relevant to deal with MMS damage in the absence of TLS.

Threshold levels of Rad53 activity modulate DNA damage tolerance

Previous studies have shown that, like *dot1*Δ, cells expressing an HA-tagged version of the Rad53 checkpoint kinase display increased MMS resistance and increased MMS-induced mutagenesis frequency (Cordon-Preciado et al. 2006). Moreover, recent observations indicate that the enhanced MMS resistance of *rad53-HA* also requires PCNA-K164 ubiquitylation and TLS activity (Gallego-Sánchez et al. 2010).

Thus, the similar phenotypes of *dot1*Δ and *rad53-HA* prompted us to further explore the possible relationship between Dot1 and Rad53 in the regulation of MMS resistance, as we have previously proposed (Conde and San-Segundo 2008). Indeed, we found that the enhanced MMS resistance of *dot1*Δ was

abolished in the absence of Rad53 because a *rad53*Δ *dot1*Δ double mutant showed similar MMS sensitivity than *rad53*Δ; therefore, MMS resistance conferred by *dot1*Δ requires Rad53 function.

Activation of Rad53 can be monitored by a well-characterized phosphorylation-dependent electrophoretic mobility shift (Pellicioli et al. 1999). In the *dot1*Δ mutant, Rad53 is not fully activated in response to MMS (Giannattasio et al., 2005). In contrast, in the *rad53-HA* mutant, although the Rad53-HA protein can be activated to the same extent as the wild-type protein, it is produced in much lower amounts and, consequently, also renders reduced levels of Rad53 activity (Cordon-Preciado et al. 2006). These observations suggest that the sub-optimal levels of Rad53 activity present in *dot1*Δ or *rad53-HA* cells lead to increased MMS resistance. Therefore, we generated a *dot1*Δ *rad53-HA* double mutant to analyze the extent of Rad53-HA phosphorylation (activation) and MMS resistance. Using anti-Rad53 antibodies, the Rad53-HA protein was not detectable in *rad53-HA* and *dot1*Δ *rad53-HA* cells in the absence of DNA damage. Interestingly, in the *dot1*Δ *rad53-HA* double mutant, in addition to the low amount of Rad53-HA protein characteristic of this tagged version, the levels of MMS-induced phosphorylated (and therefore active) Rad53-HA were further reduced compared with the *rad53-HA* single mutant. Indeed, the phosphorylated species of Rad53-HA induced by MMS were only barely detectable after long exposure of the membranes. Using anti-HA antibodies, it was possible to detect a faint band corresponding to the basal form of Rad53-HA, which was not detectable with anti-Rad53. In addition, upon MMS treatment, only the phosphorylated species of Rad53-HA were detected, and the reduced levels of activated Rad53-HA in the *dot1*Δ *rad53-HA* double mutant compared with the *rad53-HA* single mutant were also manifested. Strinkingly, whereas both *dot1*Δ and *rad53-HA* single mutants display increased MMS resistance (Conde and San-Segundo 2008; Cordon-Preciado et al. 2006), the *dot1*Δ *rad53-HA* double mutant was extremely sensitive to MMS, resembling a *rad53*Δ mutant.

Moreover, if the increase in MMS resistance observed in *dot1*Δ results from the inability to fully activate Rad53, we reasoned that raising the levels of active Rad53 kinase in the *dot1*Δ mutant by overproducing the protein should bring the MMS resistance closer to wild-type levels. Indeed, we found that moderate overexpression of *RAD53* from a high-copy plasmid significantly restored the levels of MMS-activated Rad53 in a *dot1*Δ mutant and partially suppressed the increased MMS resistance of *dot1*Δ. Collectively, these results suggest that intermediate Rad53 activity (below wild-type levels) supports enhanced resistance to MMS, as occurs in *dot1*Δ or *rad53-HA* mutants. However, when Rad53 function drops below certain threshold level the cells become very sensitive to this genotoxic agent, which is the situation present in the *dot1D rad53-HA* double mutant and in *rad53*Δ.

Dot1 and Rad53 modulate binding of Rev1 to Chromatin

Current models for TLS propose that when the replication machinery stalls at a lesion, binding of the Rev1 protein to monoubiquitylated PCNA serves as scaffold for recruiting the Polζ polymerase to the stalled

fork by virtue of the interaction between Rev1 and the Rev7 accessory subunit of Polζ (Bienko et al. 2005; D'Souza et al. 2008; Guo et al. 2003). This would promote the switch of the replicative polymerase by the TLS polymerase to continue replication past the lesion (Acharya et al. 2006; Lehmann et al. 2007; Zhuang et al. 2008). However, compelling evidence supports that DNA damage tolerance mechanisms function during the G2/M phase acting on gaps behind replication forks (Daigaku et al. 2010; Karras and Jentsch 2010; Lopes et al. 2006; Waters and Walker 2006). In any case, Rev1 is a key regulator of Polζ activity (Waters et al. 2009), and it has been shown that forms chromosomal foci (Guo et al. 2006b; Sabbioneda et al. 2007); therefore, we examined MMS-induced Rev1 localization in nuclear spreads of wild-type, *dot1*Δ and *rad53-HA* strains.

Chromatin-associated Rev1 signal was observed both in untreated and MMS-treated cells. To analyze in more detail the binding of Rev1 to chromosomes, we quantified the number of Rev1 foci detected in the nuclear spreads and established three categories. In the absence of damage, all strains analyzed contained a high number of Rev1 foci on chromosomes; most nuclei corresponded to class III (i.e., more than 30 foci per nucleus). However, after MMS treatment, the number of Rev1 foci remarkably diminished in chromosome spreads from the wild-type strain, but remained high in the *dot1*Δ and *rad53-HA* mutants. Indeed, whereas most nuclei from the MMS-treated *dot1*Δ and *rad53-HA* mutants contained more than 30 Rev1 foci (79% and 61% of nuclei belonged to class III, respectively), only 34% of wild-type nuclei fell into this category.

In summary, these results suggest that full activation of Rad53 promotes Rev1 disassembly from chromosomes upon MMS treatment, but the reduced Rad53 activity present in *dot1*Δ and *rad53-HA* allows extended Rev1 binding to chromatin accounting for the increased MMS resistance of these mutants.

DISCUSSION

Our group previously described a role for the histone H3K79 methyltransferase Dot1 in the tolerance to alkylating DNA damage (Conde and San-Segundo 2008). Here, we have further characterized this function of Dot1 by first analyzing the impact of different methylation states of H3K79 in the response to continuous MMS exposure. We provide evidence indicating that the regulation of DNA damage tolerance by Dot1 depends on its catalytic activity on H3K79 and not on other possible unknown substrate(s) because, like *dot1*Δ, both a catalytically-defective *dot1-G401V* allele, and a non-methylatable *H3-K79A* version of histone H3 confer MMS hyper-resistance. To investigate how different degrees of H3K79 methylation affect MMS resistance, we have engineered and analyzed a set of strains with progressively crippled Dot1 activity, ranging between wild-type *DOT1* and *dot1*Δ as the maximal and minimal Dot1 catalytic activity, respectively. We find a striking correlation between the decline of Dot1 activity and the increase in MMS resistance. This correlation was particularly evident for the loss of H3K79me3, suggesting that this methylation state is the most relevant

for the MMS response. Similarly, different functional relevance for the different methylation states of H3K79 in the coordination of DNA repair and checkpoint activation in response to UV has been proposed (Evans et al. 2008). In contrast, it has been clearly demonstrated that chromatin silencing relies on global levels of H3K79 methylation, and not on specific methylation states (Frederiks et al. 2008). Importantly, the MMS resistance conferred by the absence of Dot1 is independent of the silencing SIR complex (Conde and San-Segundo 2008).

The role of Dot1 in multiple nuclear processes, such as transcriptional silencing, meiotic checkpoint, DNA damage checkpoint or DSB repair, relies on the regulated binding of various key factors to specific chromosomal regions (Conde et al. 2009; San-Segundo and Roeder 2000; van Leeuwen et al. 2002; Wysocki et al. 2005). In principle, the impact of Dot1 (i.e. H3K79 methylation) in MMS resistance and the higher number of MMS-induced chromosome-associated Rev1 foci in the *dot1*Δ mutant could emanate from a direct effect of a peculiar chromatin structure dictated by the H3K79 methylation status modulating the recruitment of the TLS machinery. However, our results support an alternative possibility implying that the effect of Dot1 in DNA damage tolerance is exerted indirectly through the regulation of the Rad53 checkpoint kinase. The fact that a *rad53-HA* mutant, characterized by reduced levels of the kinase, substantially phenocopies *dot1*Δ in the response to chronic MMS exposure (Conde and San-Segundo 2008; Cordon-Preciado et al. 2006) suggested a possible relationship between Dot1 and Rad53 in the regulation of tolerance to alkylating damage. Supporting this possibility, we find that the MMS resistance of both *dot1*Δ and *rad53-HA* depends on ubiquitylation of PCNA at K164, which is a crucial regulator of the TLS mechanism of DNA damage tolerance. Moreover, we show here that the increased MMS resistance of the *dot1*Δ mutant depends on Rad53.

Both *dot1*Δ and *rad53-HA* mutants display enhanced resistance to alkylating damage and increased TLS-dependent MMS-induced mutagenesis. Strinkingly, in both mutants, the levels of Rad53 activated by MMS treatment are reduced compared to the wild type, but for different reasons. In the case of *dot1*Δ, Rad53 is produced at normal levels, but the inability to properly recruit the Rad9 adaptor to DNA damage sites results in defective activation of Rad53 (Conde et al. 2009; Giannattasio et al. 2005; Wysocki et al. 2005). On the other hand, the *rad53-HA* allele gives rise to a functional protein, which can be fully activated; however, it is highly unstable, resulting in the production of low levels of MMS-induced active kinase (Cordon-Preciado et al., 2006). In the *dot1*Δ *rad53-HA* double mutant, the activation of the low amounts of kinase produced by the HA-tagged allele is further hampered by the absence of *DOT1* resulting in barely detectable levels of phosphorylated kinase. Remarkably, whereas the *dot1*Δ and *rad53-HA* single mutants show increased MMS resistance, the *dot1*Δ *rad53-HA* double mutant shows strong MMS sensitivity implying that threshold levels of Rad53 activity determine the outcome of the cellular response to alkylating damage. In the face of MMS challenge that prevents the advance of replication forks, the wild-type strain fully activates Rad53 and the

subsequent checkpoint responses controlled by this effector kinase, including cell cycle arrest, stabilization of replication forks and induction of DNA repair mechanisms (Branzei and Foiani 2010). In addition, high levels of Rad53 activity would negatively regulate the TLS mechanism of damage tolerance to prevent excessive mutagenesis. We propose that the sub-optimal levels of activated Rad53 present in *rad53-HA* mutants or in mutants that cripple H3K79 methylation (*dot1-G401A*, *dot1-G401V*, *dot1*Δ), while still preventing replication fork collapse, allow cell cycle progression and TLS-dependent replication across damage. Consistent with this idea, analysis of MMS-treated cells lacking the Rad53 phosphatases Pph3 an Ptc2 suggested that a graded response to the level of Rad53 phosphorylation occurs controlling replication fork restart (O'Neill et al. 2007; Szyjka et al. 2008). These authors propose that a cycle of Rad53 activation and deactivation coordinates DNA repair with TLS-dependent replication fork progression through damaged DNA by a mechanism involving the Cdc7-Dbf4 kinase activity (Szyjka et al. 2008). Indeed, the cooperation of a functional Rad53-dependent checkpoint response with multiple pathways involving base excision repair, recombination and DNA damage tolerance has been shown to be crucial for a proper cellular response to alkylated DNA (Segurado and Tercero 2009; Vazquez et al. 2008). Our analysis of the *dot1*Δ *rad53-HA* double mutant suggests that when Rad53 activity drops below a critical threshold level, damaged replication forks would irreversibly collapse, like in *rad53*Δ (Tercero and Diffley 2001; Tercero et al. 2003), resulting in cell death and pronounced MMS sensitivity. We note, however, that in contrast with *rad53*Δ, the low amounts of the Rad53-HA protein in the *dot1*Δ *rad53-HA* mutant must be sufficient to support viability in undamaged cells.

The Rev1 protein is a crucial regulator of TLS activity because of its structural function (Waters et al. 2009); therefore, we focused on Rev1 to investigate how Dot1/Rad53 function impinges on TLS-dependent mutagenic bypass of MMS-induced lesions. In particular, we examined Rev1 localization to chromatin by immunofluorescence of nuclear spreads. We found that Rev1 foci are present in most nuclei even in the absence of MMS damage, suggesting that there is a constitutive localization of Rev1 to chromosomes. Similar results have been reported for 4NQO-treated cells (Sabbioneda et al. 2007). Since PCNA ubiquitylation is triggered by DNA damage (Hoege et al., 2002), these observations imply that the basal formation of Rev1 foci does not depend on the interaction with ubiquitylated PCNA. Consistent with this possibility, we detect Rev1 foci in the ubiquitylation-deficient *pol30-K164R* mutant. In fact, studies of mouse and yeast Rev1 suggest that the BRCT domain of Rev1 is required for its constitutive recruitment to foci, whereas the ubiquitin-binding motifs specifically drive Rev1 to damaged replication forks (Bomar et al. 2010; Guo et al. 2006a; Guo et al. 2006b). Moreover, in DT40 chicken cells, Rev1 maintains progression of replication forks upon DNA damage independently of PCNA ubiquitylation (Edmunds et al. 2008).

Strikingly, although most nuclei maintain Rev1 signal, we observe a decrease in the number of Rev1 foci per nucleus in MMS-treated wild-type cells. Since mutagenic TLS is induced by alkylating damage (Conde

and San-Segundo 2008), this reduced number of Rev1 foci (or a significant fraction of them) must by actively engaged in TLS. In contrast, the number of chromatin-bound Rev1 foci remains elevated in the *dot1*Δ or *rad53-HA* mutants, providing the opportunity for more TLS-dependent mutagenic events once DNA damage-induced ubiquitylation of PCNA occurs. We propose that full activation of the Rad53 checkpoint kinase, which depends on Dot1, somehow restrains TLS activity by preventing promiscuous formation of Rev1 foci associated with chromosomes. Rev1 undergoes Mec1-dependent phosphorylation, which promotes Polζ activity only in NER-deficient cells (Pages et al. 2009; Sabbioneda et al. 2007). Phosphorylation of Rev1 also requires the checkpoint clamp '9-1-1' and the clamp loader Rad24; however, it is independent of Rad53 (Pages et al. 2009). Therefore, it is unlikely that this posttranslational modification of Rev1 controls the formation of TLS-active Rev1 foci. Perhaps, Rad53 acts on other regulators of TLS that mediate Rev1 chromosomal binding or stability. Future studies will be aimed to unveil these mechanisms.

In summary, our studies provide insight into how a chromatin modification, namely Dot1-dependent H3K79 methylation, regulates the tolerance to alkylating damage by TLS through modulation of Rad53 activity. TLS constitutes one important aspect of the coordinated global cellular response to DNA damage because of the ability to bypass lesions that impede replication progression, thus preventing fork collapse and eventual formation of DNA breaks potentially leading to chromosomal rearrangements. However, given the error-prone nature of TLS, this process must be kept under strict control to avoid excessive mutagenesis, which can also have deleterious consequences. Therefore, an appropriate balance between error-prone and error-free processes to face DNA damage is essential to avoid genomic instability, which is directly linked to cancer development. Our studies in yeast reveal that the conserved Rad53 checkpoint kinase contributes to finely tune this balance at least by regulating the levels of chromatin-bound Rev1. Recent studies using a mouse model point to the influence of correct Rev1 levels in reducing the incidence of carcinogen-induced lung cancer (Dumstorf et al. 2009), highlighting the importance of these mechanisms for the maintenance of genomic stability.

CONCLUSIONS

ARTICLE 1: Dot1-dependent histone H3K79 methylation promotes activation of the Mek1 meiotic checkpoint effector kinase by regulating the Hop1 adaptor

1. Global levels of H3K79me, exclusively catalyzed by Dot1, do not change in response to either meiosis induction or meiotic defects. However, this epigenetic modification is essential for proper meiotic recombination checkpoint response in *Saccharomyces cerevisiae*.

2. Dot1 function in this meiotic checkpoint relies solely on the methylation of H3K79, being H3K79me3 the most relevant form to sustain this function.

3. Full activation of the meiotic recombination checkpoint effector kinase, Mek1, is achieved in two sequential phosphorylation events: initial phosphorylation of Mek1 mediated by the sensor kinases Mec1/Tel1 is followed by *in trans* autophosphorylation of Mek1 itself.

4. Dot1-dependent H3K79me is required for both Mek1 recruitment to meiotic chromosomes and Mek1 autophosphorylation, thereby promoting its full activation and the ensuing checkpoint response.

5. Dot1-dependent H3K79me controls phosphorylation of the Hop1 adaptor and its localization along the chromosome axes of the *zip1* mutant, thus enabling Mek1 activation.

6. Regulation of H3K79me-mediated Hop1 localization is exerted, at least in part, by excluding the Pch2 meiotic checkpoint protein from the chromatin and its confinement in the ribosomal DNA region (nucleolus).

ARTICLE 2: Dynamics of DOT1L localization and H3K79 methylation during meiotic prophase I in mouse spermatocytes

1. The DOT1L methyltransferase and the different H3K79me states exhibit characteristic spatio-temporal dynamics during meiotic prophase I in mouse spermatocytes, suggesting differential roles for each methylation state.

2. H3K79me2 levels increase in autosomal regions from pachynema onwards, but H3K79me2 is excluded from the sex body, consistent with a role in the resumption of transcription in autosomes during late prophase I stages.

3. H3K79me3 shows a progressive enrichment at the sex body, which correlates with that of H2A.Z, with the replacement of H3.1/H3.2 by H3.3 and with the loss of γH2AX and macroH2A. Therefore, trimethylation of K79 in the H3.3 variant at the sex body, together with H2A.Z incorporation, supports a contribution in maintaining silencing of sex chromosomes from diplonema onward.

4. H3K79me3 is also enriched at pericentromeric heterochromatin areas, consistent with a role in silencing these regions.

5. The chromosomal distribution of DOT1L and the different H3K79me states is not altered in mutant mice with defects in synapsis and/or recombination, although the accumulation of H3K79me is blocked at the corresponding prophase I stage where each mutant analyzed undergoes meiotic arrest.

ARTICLE 3 : Regulation of tolerance to DNA alkylating damage by Dot1 and Rad53 in *Saccharomyces cerevisiae*

1. The regulation of MMS resistance by Dot1 relies on its H3K79 methyltransferase activity.

2. H3K79me levels finely modulate the degree of tolerance to alkylating DNA damage.

3. The MMS resistance of *dot1*Δ and *rad53-HA* depends on PCNA-K164 ubiquitylation

4. Threshold levels of Rad53 activity modulate DNA damage tolerance: whereas the sub-optimal levels of Rad53 activity present in *dot1*Δ or *rad53-HA* cells lead to increased MMS resistance, the low levels in the *dot1*Δ *rad53-HA* double mutant or the complete lack of activity in *rad53Δ* confer MMS sensitivity.

5. Dot1 and Rad53 regulate TLS, at least partially, by controlling Rev1 chromatin binding

BIBLIOGRAPHY

Acharya, N., Johnson, R.E., Prakash, S., and Prakash, L. (2006). Complex formation with Rev1 enhances the proficiency of Saccharomyces cerevisiae DNA polymerase zeta for mismatch extension and for extension opposite from DNA lesions. Mol Cell Biol 26, 9555-9563.

Acosta, I., Ontoso, D., and San-Segundo, P.A. (2011). The budding yeast polo-like kinase Cdc5 regulates the Ndt80 branch of the meiotic recombination checkpoint pathway. Mol Biol Cell 22, 3478-3490.

Anglin JL, Deng L, Yao Y, Cai G, Liu Z, Jiang H, Cheng G, Chen P, et al. (2012) Synthesis and structure-activity relationship investigation of adenosine-containing inhibitors of histone methyltransferase DOT1L. J Med Chem 55:8066–8074.

Bailis, J.M., and Roeder, G.S. (2000). Pachytene exit controlled by reversal of Mek1-dependent phosphorylation. Cell 101, 211-221.

Barchi M, Mahadevaiah S, Di Giacomo M, Baudat F, de Rooij DG, Burgoyne PS, Jasin M, Keeney S (2005) Surveillance of different recombination defects in mouse spermatocytes yields distinct responses despite elimination at an identical developmental stage. Mol Cell Biol 25:7203–7215.

Barchi M, Roig I, Di Giacomo M, de Rooij DG, Keeney S, Jasin M (2008) ATM promotes the obligate XY crossover and both crossover control and chromosome axis integrity on autosomes. PLoS Genet 4:e1000076.

Barry ER, Krueger W, Jakuba CM, Veilleux E, Ambrosi DJ, Nelson CE, Rasmussen TP (2009) ES cell cycle progression and differentiation require the action of the histone methyltransferase Dot1L. Stem Cells 27:1538–47.

Barski A, Cuddapah S, Cui K, Roh T-Y, Schones DE, Wang Z, Wei G, Chepelev I, et al. (2007) High-resolution profiling of histone methylations in the human genome. Cell 129:823–837.

Baudat F, Manova K, Yuen JP, Jasin M, Keeney S (2000) Chromosome synapsis defects and sexually dimorphic meiotic progression in mice lacking Spo11. Mol Cell 6:989–998.

Becker PB, Workman JL (2013) Nucleosome remodeling and epigenetics. Cold Spring Harb Perspect Biol. (Epub ahead of print).

Bergink, S., and Jentsch, S. (2009). Principles of ubiquitin and SUMO modifications in DNA repair. Nature 458, 461-467.

Bernt KM, Zhu N, Sinha AU, Vempati S, Faber J, Krivtsov A V, Feng Z, Punt N, et al. (2011) MLL-rearranged leukemia is dependent on aberrant H3K79 methylation by DOT1L. Cancer Cell 20:66–78.

Bhalla N, Dernburg AF (2005) A conserved checkpoint monitors meiotic chromosome synapsis in *Caenorhabditis elegans*. Science 310:1683–1686.

Bienko, M., Green, C.M., Crosetto, N., Rudolf, F., Zapart, G., Coull, B., Kannouche, P., Wider, G., Peter, M., Lehmann, A.R., et al. (2005). Ubiquitin-binding domains in Y-family polymerases regulate translesion synthesis. Science 310, 1821-1824.

Bishop, D.K. (1994). RecA homologs Dmc1 and Rad51 interact to form multiple nuclear complexes prior to meiotic chromosome synapsis. Cell 79, 1081-1092.

Bomar, M.G., D'Souza, S., Bienko, M., Dikic, I., Walker, G.C., and Zhou, P. (2010). Unconventional ubiquitin recognition by the ubiquitin-binding motif within the Y family DNA polymerases iota and Rev1. Mol Cell 37, 408-417.

Borde, V., Robine, N., Lin, W., Bonfils, S., Geli, V., and Nicolas, A. (2009). Histone H3 lysine 4 trimethylation marks meiotic recombination initiation sites. EMBO J 28, 99-111.

Borner, G.V., Barot, A., and Kleckner, N. (2008). Yeast Pch2 promotes domainal axis organization, timely recombination progression, and arrest of defective recombinosomes during meiosis. Proc Natl Acad Sci U S A 105, 3327-3332.

Borner, G.V., Kleckner, N., and Hunter, N. (2004). Crossover/noncrossover differentiation, synaptonemal complex formation, and regulatory surveillance at the leptotene/zygotene transition of meiosis. Cell 117, 29-45.

Bostelman LJ, Keller AM, Albrecht AM, Arat A, Thompson JS (2007) Methylation of histone H3 lysine-79 by Dot1p plays multiple roles in the response to UV damage in *Saccharomyces cerevisiae*. DNA Repair 6:383–395.

Botuyan, M.V., Lee, J., Ward, I.M., Kim, J.E., Thompson, J.R., Chen, J., and Mer, G. (2006). Structural basis for the methylation state-specific recognition of histone H4-K20 by 53BP1 and Crb2 in DNA repair. Cell 127, 1361-1373.

Branzei, D., and Foiani, M. (2010). Maintaining genome stability at the replication fork. Nat Rev Mol Cell Biol 11, 208-219.

Burgoyne PS, Mahadevaiah SK, Turner JMA (2009) The consequences of asynapsis for mammalian meiosis. Nat Rev Genet 10:207–216.

Carballo, J.A., Johnson, A.L., Sedgwick, S.G., and Cha, R.S. (2008). Phosphorylation of the axial element protein Hop1 by Mec1/Tel1 ensures meiotic interhomolog recombination. Cell 132, 758-770.

Cartagena-Lirola, H., Guerini, I., Viscardi, V., Lucchini, G., and Longhese, M.P. (2006). Budding Yeast Sae2 is an In Vivo Target of the Mec1 and Tel1 Checkpoint Kinases During Meiosis. Cell Cycle 5, 1549-1559.

Castaño Betancourt MC, Cailotto F, Kerkhof HJ, Cornelis FMF, Doherty SA, Hart DJ, Hofman A, Luyten FP, et al. (2012) Genome-wide association and functional studies identify the DOT1L gene to be involved in cartilage thickness and hip osteoarthritis. Proc Natl Acad Sci U S A 109:8218–23.

Cecere G, Hoersch S, Jensen MB, Dixit S, Grishok A (2013) The ZFP-1(AF10)/DOT-1 complex opposes H2B ubiquitination to reduce Pol II transcription. Mol Cell 50:894–907.

Cohen PE, Pollack SE, Pollard JW (2006) Genetic analysis of chromosome pairing, recombination, and cell cycle control during first meiotic prophase in mammals. Endocr Rev 27:398–426.

Conde, F., Ontoso, D., Acosta, I., Gallego-Sanchez, A., Bueno, A., and San-Segundo, P.A. (2010). Regulation of tolerance to DNA alkylating damage by Dot1 and Rad53 in *Saccharomyces cerevisiae*. DNA Repair 9, 1038-1049.

Conde, F., Refolio, E., Cordon-Preciado, V., Cortes-Ledesma, F., Aragon, L., Aguilera, A., and San-Segundo, P.A. (2009). The Dot1 histone methyltransferase and the Rad9 checkpoint adaptor contribute to cohesin-dependent double-strand break repair by sister chromatid recombination in Saccharomyces cerevisiae. Genetics 182, 437-446.

Conde, F. and San-Segundo, P.A. (2008) Role of Dot1 in the response to alkylating DNA damage in *Saccharomyces cerevisiae*: regulation of DNA damage tolerance by the error-prone polymerases Polζ/Rev1. Genetics 179:1197–1210.

Cordon-Preciado, V., Ufano, S., and Bueno, A. (2006). Limiting amounts of budding yeast Rad53 S-phase checkpoint activity results in increased resistance to DNA alkylation damage. Nucleic Acids Res 34, 5852-5862.

Cowell I, Aucott R, Mahadevaiah S, Huskisson N, Bongiorni S, Prantera G, Fanti L, Pimpinelli S, et al. (2002) Heterochromatin, HP1 and methylation at lysine 9 of histone H3 in animals. Chromosoma 111:22–36.

D'Souza, S., Waters, L.S., and Walker, G.C. (2008). Novel conserved motifs in Rev1 C-terminus are required for mutagenic DNA damage tolerance. DNA Repair 7, 1455-1470.

Daigaku, Y., Davies, A.A., and Ulrich, H.D. (2010). Ubiquitin-dependent DNA damage bypass is separable from genome replication. Nature 465, 951-955.

Daigle SR, Olhava EJ, Therkelsen C A, Majer CR, Sneeringer CJ, Song J, Johnston LD, Scott MP, et al. (2011) Selective killing of mixed lineage leukemia cells by a potent small-molecule DOT1L inhibitor. Cancer Cell 20:53–65.

de la Fuente R, Parra MT, Viera A, Calvente A, Gómez R, Suja JA, Rufas JS, Page J (2007) Meiotic pairing and segregation of achiasmate sex chromosomes in eutherian mammals: the role of SYCP3 protein. PLOS Genet 3: e198.

de la Fuente R, Sánchez A, Marchal JA, Viera A, Parra MT, Rufas JS, Page J (2012) A synaptonemal complex-derived mechanism for meiotic segregation precedes the evolutionary loss of homology between sex chromosomes in arvicolid mammals. Chromosoma 121: 433–446.

De Vos D, Frederiks F, Terweij M, van Welsem T, Verzijlbergen KF, Iachina E, de Graaf EL, Maarten Altelaar AF, et al. (2011) Progressive methylation of ageing histones by Dot1 functions as a timer. EMBO Rep 12:956–962.

Downs, J.A., Lowndes, N.F., and Jackson, S.P. (2000). A role for Saccharomyces cerevisiae histone H2A in DNA repair. Nature 408, 1001-1004.

Dumstorf, C.A., Mukhopadhyay, S., Krishnan, E., Haribabu, B., and McGregor, W.G. (2009). REV1 is implicated in the development of carcinogen-induced lung cancer. Mol Cancer Res 7, 247-254.

Edmunds, C.E., Simpson, L.J., and Sale, J.E. (2008). PCNA ubiquitination and REV1 define temporally distinct mechanisms for controlling translesion synthesis in the avian cell line DT40. Mol Cell 30, 519-529.

Evans, M.L., Bostelman, L.J., Albrecht, A.M., Keller, A.M., Strande, N.T., and Thompson, J.S. (2008). UV sensitive mutations in histone H3 in Saccharomyces cerevisiae that alter specific K79 methylation states genetically act through distinct DNA repair pathways. Curr Genet 53, 259-274.

Farmer, S., Hong, E.J., Leung, W.K., Argunhan, B., Terentyev, Y., Humphryes, N., Toyoizumi, H., and Tsubouchi, H. (2012). Budding yeast Pch2, a widely conserved meiotic protein, is involved in the initiation of meiotic recombination. PLOS ONE 7, e39724.

Feng Y, Yang Y, Ortega MM, Copeland JN, Zhang M, Jacob JB, Fields T A, Vivian JL, et al. (2010) Early mammalian erythropoiesis requires the Dot1L methyltransferase. Blood 116:4483–91.

Feng, Q., Wang, H., Ng, H.H., Erdjument-Bromage, H., Tempst, P., Struhl, K., and Zhang, Y. (2002). Methylation of H3-lysine 79 is mediated by a new family of HMTases without a SET domain. Curr Biol 12, 1052-1058.

Fernandez-Capetillo O, Mahadevaiah SK, Celeste A, Romanienko PJ, Camerini-Otero RD, Bonner WM, Manova K, Burgoyne P, et al. (2003) H2AX is required for chromatin remodeling and inactivation of sex chromosomes in male mouse meiosis. Dev Cell 4:497–508.

Fleming, A.B., Kao, C.F., Hillyer, C., Pikaart, M., and Osley, M.A. (2008). H2B ubiquitylation plays a role in nucleosome dynamics during transcription elongation. Mol Cell 31, 57-66.

Frederiks, F., Heynen, G.J., van Deventer, S.J., Janssen, H., and van Leeuwen, F. (2009). Two Dot1 isoforms in Saccharomyces cerevisiae as a result of leaky scanning by the ribosome. Nucleic Acids Res 37, 7047-7058.

Frederiks, F., Tzouros, M., Oudgenoeg, G., van Welsem, T., Fornerod, M., Krijgsveld, J., and van Leeuwen, F. (2008). Nonprocessive methylation by Dot1 leads to functional redundancy of histone H3K79 methylation states. Nat Struct Mol Biol 15, 550-557.

Gallego-Sanchez, A., Conde, F., San Segundo, P., and Bueno, A. (2010). Control of PCNA deubiquitylation in yeast. Biochem Soc Trans 38, 104-109.

Game JC, Williamson MS, Spicakova T, Brown JM (2006) The RAD6/BRE1 histone modification pathway in Saccharomyces confers radiation resistance through a RAD51-dependent process that is independent of RAD18. Genetics 173:1951–68.

Giannattasio, M., Lazzaro, F., Plevani, P., and Muzi-Falconi, M. (2005). The DNA damage checkpoint response requires histone H2B ubiquitination by Rad6-Bre1 and H3 methylation by Dot1. J Biol Chem 280, 9879-9886.

Greaves IK, Rangasamy D, Devoy M, Marshall Graves JA, Tremethick DJ (2006) The X and Y chromosomes assemble into H2A.Z, containing facultative heterochromatin, following meiosis. Mol Cell Biol 26:5394–5405.

Grenon, M., Costelloe, T., Jimeno, S., O'Shaughnessy, A., Fitzgerald, J., Zgheib, O., Degerth, L., and Lowndes, N.F. (2007). Docking onto chromatin via the *Saccharomyces cerevisiae* Rad9 Tudor domain. Yeast 24, 105-119.

Guo, C., Fischhaber, P.L., Luk-Paszyc, M.J., Masuda, Y., Zhou, J., Kamiya, K., Kisker, C., and Friedberg, E.C. (2003). Mouse Rev1 protein interacts with multiple DNA polymerases involved in translesion DNA synthesis. EMBO J 22, 6621-6630.

Guo, C., Sonoda, E., Tang, T.S., Parker, J.L., Bielen, A.B., Takeda, S., Ulrich, H.D., and Friedberg, E.C. (2006a). REV1 protein interacts with PCNA: significance of the REV1 BRCT domain in vitro and in vivo. Mol Cell 23, 265-271.

Guo, C., Tang, T.S., Bienko, M., Parker, J.L., Bielen, A.B., Sonoda, E., Takeda, S., Ulrich, H.D., Dikic, I., and Friedberg, E.C. (2006b). Ubiquitin-binding motifs in REV1 protein are required for its role in the tolerance of DNA damage. Mol Cell Biol 26, 8892-8900.

Hake SB, Garcia BA, Duncan EM, Kauer M, Dellaire G, Shabanowitz J, Bazett-Jones DP, Allis CD, et al. (2006) Expression patterns and post-translational modifications associated with mammalian histone H3 variants. J Biol Chem 281:559–568.

Hammet, A., Magill, C., Heierhorst, J., and Jackson, S.P. (2007). Rad9 BRCT domain interaction with phosphorylated H2AX regulates the G1 checkpoint in budding yeast. EMBO Rep 8, 851-857.

Handel MA (2004) The XY body: a specialized meiotic chromatin domain. Exp Cell Res 296:57–63.

Handel MA, Schimenti JC (2010) Genetics of mammalian meiosis: regulation, dynamics and impact on fertility. Nat Rev Genet 11:124–136.

Helin K, Dhanak D (2013) Chromatin proteins and modifications as drug targets. Nature 502:480–488.

Hishida, T., Ohya, T., Kubota, Y., Kamada, Y., and Shinagawa, H. (2006). Functional and physical interaction of yeast Mgs1 with PCNA: impact on RAD6-dependent DNA damage tolerance. Mol Cell Biol 26, 5509-5517.

Ho, H.C., and Burgess, S.M. (2011). Pch2 acts through Xrs2 and Tel1/ATM to modulate interhomolog bias and checkpoint function during meiosis. PLOS Genet 7, e1002351.

Hochwagen, A., and Amon, A. (2006). Checking your breaks: surveillance mechanisms of meiotic recombination. Curr Biol 16, R217-228.

Hoege, C., Pfander, B., Moldovan, G.L., Pyrowolakis, G., and Jentsch, S. (2002). RAD6-dependent DNA repair is linked to modification of PCNA by ubiquitin and SUMO. Nature 419, 135-141.

Hong, E.J., and Roeder, G.S. (2002). A role for Ddc1 in signaling meiotic double-strand breaks at the pachytene checkpoint. Genes Dev 16, 363-376.

Hoyer-Fender S, Costanzi C, Pehrson JR (2000) Histone macroH2A1.2 is concentrated in the XY-body by the early pachytene stage of spermatogenesis. Exp Cell Res 258:254–260.

Hunter, N. (2008). Hop1 and the meiotic DNA-damage response. Cell 132, 731-732.

Huyen, Y., Zgheib, O., Ditullio, R.A., Jr., Gorgoulis, V.G., Zacharatos, P., Petty, T.J., Sheston, E.A., Mellert, H.S., Stavridi, E.S., and Halazonetis, T.D. (2004). Methylated lysine 79 of histone H3 targets 53BP1 to DNA double-strand breaks. Nature 432, 406-411.

Javaheri, A., Wysocki, R., Jobin-Robitaille, O., Altaf, M., Cote, J., and Kron, S.J. (2006). Yeast G1 DNA damage checkpoint regulation by H2A phosphorylation is independent of chromatin remodeling. Proceedings of the National Academy of Sciences of the United States of America 103, 13771-13776.

Jo SY, Granowicz EM, Maillard I, Thomas D, Hess JL (2011) Requirement for Dot1l in murine postnatal hematopoiesis and leukemogenesis by MLL translocation. Blood 117:4759–68.

Jones, B., Su, H., Bhat, A., Lei, H., Bajko, J., Hevi, S., Baltus, G.A., Kadam, S., Zhai, H., Valdez, R., et al. (2008). The histone H3K79 methyltransferase Dot1L is essential for mammalian development and heterochromatin structure. PLOS Genet 4, e1000190.

Joshi, N., Barot, A., Jamison, C., and Borner, G.V. (2009). Pch2 links chromosome axis remodeling at future crossover sites and crossover distribution during yeast meiosis. PLoS Genet 5, e1000557.

Joyce EF, McKim KS (2009) Drosophila PCH2 is required for a pachytene checkpoint that monitors double-strand-break-independent events leading to meiotic crossover formation. Genetics 181:39–51.

Kalitsis P, Griffiths B, Choo KHA (2006) Mouse telocentric sequences reveal a high rate of homogenization and possible role in Robertsonian translocation. Proc Natl Acad Sci U S A 103:8786–8791.

Karras, G.I., and Jentsch, S. (2010). The RAD6 DNA damage tolerance pathway operates uncoupled from the replication fork and is functional beyond S phase. Cell 141, 255-267.

Kauppi L, Barchi M, Baudat F, Romanienko PJ, Keeney S, Jasin M (2011) Distinct properties of the XY pseudoautosomal region crucial for male meiosis. Science 331:916–920.

Keeney, S. (2001). Mechanism and control of meiotic recombination initiation. Current topics in developmental biology 52, 1-53.

Keeney, S., Giroux, C.N., and Kleckner, N. (1997). Meiosis-specific DNA double-strand breaks are catalyzed by Spo11, a member of a widely conserved protein family. Cell 88, 375-384.

Khalil AM, Driscoll DJ (2010) Epigenetic regulation of pericentromeric heterochromatin during mammalian meiosis. Cytogenet Genome Res 129:280–289.

Kim S-K, Jung I, Lee H, Kang K, Kim M, Jeong K, Kwon CS, Han Y-M, et al. (2012a) Human histone H3K79 methyltransferase DOT1L binds actively transcribing RNA polymerase II to regulate gene expression. J Biol Chem 287:39698–39709.

Kim W, Kim R, Park G, Park J-W, Kim J-E (2012b) Deficiency of H3K79 histone methyltransferase Dot1-like protein (DOT1L) inhibits cell proliferation. J Biol Chem 287:5588–5599.

Kornberg RD, Lorch Y (1999) Twenty-five years of the nucleosome, fundamental particle of the eukaryote chromosome. Cell 98:285–294.

Kouskouti A, Talianidis I (2005) Histone modifications defining active genes persist after transcriptional and mitotic inactivation. EMBO J 24:347–357.

Kouzarides T (2007) Chromatin modifications and their function. Cell 128:693–705.

Krivtsov A V, Feng Z, Lemieux ME, Faber J, Vempati S, Sinha AU, Xia X, Jesneck J, et al. (2008) H3K79 methylation profiles define murine and human MLL-AF4 leukemias. Cancer Cell 14:355–68.

Lacoste, N., Utley, R.T., Hunter, J.M., Poirier, G.G., and Cote, J. (2002). Disruptor of telomeric silencing-1 is a chromatin-specific histone H3 methyltransferase. J Biol Chem 277, 30421-30424.

Lammers JH, Offenberg HH, van Aalderen M, Vink AC, Dietrich AJ, Heyting C (1994) The gene encoding a major component of the lateral elements of synaptonemal complexes of the rat is related to X-linked lymphocyte-regulated genes. Mol Cell Biol 14:1137–1146.

Lehmann, A.R., Niimi, A., Ogi, T., Brown, S., Sabbioneda, S., Wing, J.F., Kannouche, P.L., and Green, C.M. (2007). Translesion synthesis: Y-family polymerases and the polymerase switch. DNA Repair 6, 891-899.

Li XC, Li X, Schimenti JC (2007) Mouse Pachytene Checkpoint 2 (Trip13) is required for completing meiotic recombination but not synapsis. PLOS Genet 3:e130.

Liebe B, Alsheimer M, Höög C, Benavente R, Scherthan H (2004) Telomere attachment, meiotic chromosome condensation, pairing, and bouquet stage duration are modified in spermatocytes lacking axial elements. Mol Biol Cell 15:827–837.

Lopes, M., Foiani, M., and Sogo, J.M. (2006). Multiple mechanisms control chromosome integrity after replication fork uncoupling and restart at irreparable UV lesions. Mol Cell 21, 15-27.

Luger K, Dechassa ML, Tremethick DJ (2012) New insights into nucleosome and chromatin structure: an ordered state or a disordered affair? Nat Rev Mol Cell Biol 13:436–447.

Lui, D.Y., Peoples-Holst, T.L., Mell, J.C., Wu, H.Y., Dean, E.W., and Burgess, S.M. (2006). Analysis of close stable homolog juxtaposition during meiosis in mutants of *Saccharomyces cerevisiae*. Genetics 173, 1207-1222.

Lydall, D., Nikolsky, Y., Bishop, D.K., and Weinert, T. (1996). A meiotic recombination checkpoint controlled by mitotic checkpoint genes. Nature 383, 840-843.

MacQueen, A.J., and Hochwagen, A. (2011). Checkpoint mechanisms: the puppet masters of meiotic prophase. Trends Cell Biol 21, 393-400.

McGinty RK, Kim J, Chatterjee C, Roeder RG, Muir TW (2008) Chemically ubiquitylated histone H2B stimulates hDot1L-mediated intranucleosomal methylation. Nature 453:812–816.

Meneghini MD, Wu M, Madhani HD (2003) Conserved histone variant H2A.Z protects euchromatin from the ectopic spread of silent heterochromatin. Cell 112:725–736.

Miao F, Natarajan R (2005) Mapping global histone methylation patterns in the coding regions of human genes. Mol Cell Biol 25:4650–4661.

Mohan M, Herz H, Takahashi Y, Lin C, Lai KC, Zhang Y, Washburn MP, Florens L, et al. (2010) Linking H3K79 trimethylation to Wnt signaling through a novel Dot1-containing complex (DotCom). Genes Dev 24:574–589.

Mueller JL, Mahadevaiah SK, Park PJ, Warburton PE, Page DC, Turner JMA (2008) The mouse X chromosome is enriched for multicopy testis genes showing postmeiotic expression. Nat Genet 40:794–799.

Müller-Taubenberger A, Bönisch C, Fürbringer M, Wittek F, Hake SB (2011) The histone methyltransferase Dot1 is required for DNA damage repair and proper development in *Dictyostelium*. Biochem Biophys Res Commun 404:1016–1022.

Namekawa SH, Park PJ, Zhang L-F, Shima JE, McCarrey JR, Griswold MD, Lee JT (2006) Postmeiotic sex chromatin in the male germline of mice. Curr Biol 16:660–667.

Namekawa SH, VandeBerg JL, McCarrey JR, Lee JT (2007) Sex chromosome silencing in the marsupial male germ line. Proc Natl Acad Sci U S A 104: 9730–9735.

Ng HH, Ciccone DN, Morshead KB, Oettinger MA, Struhl K (2003) Lysine-79 of histone H3 is hypomethylated at silenced loci in yeast and mammalian cells: a potential mechanism for position-effect variegation. Proc Natl Acad Sci U S A 100:1820–1825.

Ng, H.H., Feng, Q., Wang, H., Erdjument-Bromage, H., Tempst, P., Zhang, Y., and Struhl, K. (2002). Lysine methylation within the globular domain of histone H3 by Dot1 is important for telomeric silencing and Sir protein association. Genes Dev 16, 1518-1527.

Nguyen, A.T., and Zhang, Y. (2011). The diverse functions of Dot1 and H3K79 methylation. Genes Dev 25, 1345-1358.

Niu, H., Li, X., Job, E., Park, C., Moazed, D., Gygi, S.P., and Hollingsworth, N.M. (2007). Mek1 kinase is regulated to suppress double-strand break repair between sister chromatids during budding yeast meiosis. Mol Cell Biol 27, 5456-5467.

Niu, H., Wan, L., Baumgartner, B., Schaefer, D., Loidl, J., and Hollingsworth, N.M. (2005). Partner choice during meiosis is regulated by Hop1-promoted dimerization of Mek1. Mol Biol Cell 16, 5804-5818.

Niu, H., Wan, L., Busygina, V., Kwon, Y., Allen, J.A., Li, X., Kunz, R.C., Kubota, K., Wang, B., Sung, P., et al. (2009). Regulation of meiotic recombination via Mek1-mediated Rad54 phosphorylation. Mol Cell 36, 393-404.

O'Neill, B.M., Szyjka, S.J., Lis, E.T., Bailey, A.O., Yates, J.R., 3rd, Aparicio, O.M., and Romesberg, F.E. (2007). Pph3-Psy2 is a phosphatase complex required for Rad53 dephosphorylation and replication fork restart during recovery from DNA damage. Proc Natl Acad Sci U S A 104, 9290-9295.

Okada Y, Feng Q, Lin Y, Jiang Q, Li Y, Coffield VM, Su L, Xu G, et al. (2005) hDOT1L links histone methylation to leukemogenesis. Cell 121:167–78.

Ontoso D, Acosta I, van Leeuwen F, Freire R, San-Segundo PA (2013a) Dot1-dependent histone H3K79 methylation promotes activation of the Mek1 meiotic checkpoint effector kinase by regulating the Hop1 adaptor. PLOS Genet 9:e1003262.

Ontoso D, Kauppi L, Keeney S, San-Segundo PA (2013b) Dynamics of DOT1L localization and H3K79 methylation during meiotic prophase I in mouse spermatocytes. Chromosoma (Epub ahead of print).

Ooga M, Inoue A, Kageyama S, Akiyama T, Nagata M, Aoki F (2008) Changes in H3K79 methylation during preimplantation development in mice. Biol Reprod 78:413–424.

Page J, de la Fuente R, Manterola M, Parra MT, Viera A, Berríos S, Fernández-Donoso R, Rufas JS (2012) Inactivation or non-reactivation: what accounts better for the silence of sex chromosomes during mammalian male meiosis? Chromosoma 121:307–326.

Pages, V., Santa Maria, S.R., Prakash, L., and Prakash, S. (2009). Role of DNA damage-induced replication checkpoint in promoting lesion bypass by translesion synthesis in yeast. Genes Dev 23, 1438-1449.

Pak, J., and Segall, J. (2002). Role of Ndt80, Sum1, and Swe1 as targets of the meiotic recombination checkpoint that control exit from pachytene and spore formation in *Saccharomyces cerevisiae*. Mol Cell Biol 22, 6430-6440.

Panizza, S., Mendoza, M.A., Berlinger, M., Huang, L., Nicolas, A., Shirahige, K., and Klein, F. (2011). Spo11-accessory proteins link double-strand break sites to the chromosome axis in early meiotic recombination. Cell 146, 372-383.

Parra MT, Viera A, Gómez R, Page J, Benavente R, Santos JL, Rufas JS, Suja JA (2004) Involvement of the cohesin Rad21 and SCP3 in monopolar attachment of sister kinetochores during mouse meiosis I. J Cell Sci 117:1221–1234.

Pellicioli, A., Lucca, C., Liberi, G., Marini, F., Lopes, M., Plevani, P., Romano, A., Di Fiore, P.P., and Foiani, M. (1999). Activation of Rad53 kinase in response to DNA damage and its effect in modulating phosphorylation of the lagging strand DNA polymerase. EMBO J 18, 6561-6572.

Pittman DL, Cobb J, Schimenti KJ, Wilson LA, Cooper DM, Brignull E, Handel MA, Schimenti JC (1998) Meiotic prophase arrest with failure of chromosome synapsis in mice deficient for Dmc1, a germline-specific RecA homolog. Mol Cell 1:697–705.

Refolio, E., Cavero, S., Marcon, E., Freire, R., and San-Segundo, P.A. (2011). The Ddc2/ATRIP checkpoint protein monitors meiotic recombination intermediates J Cell Sci 124, 2488-2500.

Roeder, G.S. (1997). Meiotic chromosomes: it takes two to tango. Genes Dev 11, 2600-2621.

Roeder, G.S., and Bailis, J.M. (2000). The pachytene checkpoint. Trends Genet 16, 395-403.

Roig I, Dowdle JA, Toth A, de Rooij DG, Jasin M, Keeney S (2010) Mouse TRIP13/PCH2 is required for recombination and normal higher-order chromosome structure during meiosis. PLOS Genet 6:e1001062.

Romanienko PJ, Camerini-Otero RD (2000) The mouse Spo11 gene is required for meiotic chromosome synapsis. Mol Cell 6:975–987.

Sabbioneda, S., Bortolomai, I., Giannattasio, M., Plevani, P., and Muzi-Falconi, M. (2007). Yeast Rev1 is cell cycle regulated, phosphorylated in response to DNA damage and its binding to chromosomes is dependent upon MEC1. DNA Repair 6, 121-127.

San-Segundo, P.A., and Roeder, G.S. (2000). Role for the silencing protein Dot1 in meiotic checkpoint control. Mol Biol Cell 11, 3601-3615.

San-Segundo, P.A., and Roeder, G.S. (1999). Pch2 links chromatin silencing to meiotic checkpoint control. Cell 97, 313-324.

Sanders, S.L., Arida, A.R., and Phan, F.P. (2010). Requirement for the phospho-H2AX binding module of Crb2 in double-strand break targeting and checkpoint activation. Mol Cell Biol 30, 4722-4731.

Sanders, S.L., Portoso, M., Mata, J., Bahler, J., Allshire, R.C., and Kouzarides, T. (2004). Methylation of histone H4 lysine 20 controls recruitment of Crb2 to sites of DNA damage. Cell 119, 603-614.

Sawada, K., Yang, Z., Horton, J.R., Collins, R.E., Zhang, X., and Cheng, X. (2004). Structure of the conserved core of the yeast Dot1p, a nucleosomal histone H3 lysine 79 methyltransferase. J Biol Chem 279, 43296-43306.

Segurado, M., and Tercero, J.A. (2009). The S-phase checkpoint: targeting the replication fork. Biol Cell 101, 617-627.

Shanower G a, Muller M, Blanton JL, Honti V, Gyurkovics H, Schedl P (2005) Characterization of the grappa gene, the Drosophila histone H3 lysine 79 methyltransferase. Genetics 169:173–84.

Singer MS, Kahana A, Wolf AJ, Meisinger LL, Peterson SE, Goggin C, Mahowald M, Gottschling DE (1998) Identification of high-copy disruptors of telomeric silencing in *Saccharomyces cerevisiae*. Genetics 150:613–632.

Smith, A.V., and Roeder, G.S. (1997). The yeast Red1 protein localizes to the cores of meiotic chromosomes. J Cell Biol 136, 957-967.

Sourirajan, A., and Lichten, M. (2008). Polo-like kinase Cdc5 drives exit from pachytene during budding yeast meiosis. Genes Dev 22, 2627-2632.

Steger DJ, Lefterova MI, Ying L, Stonestrom AJ, Schupp M, Zhuo D, Vakoc AL, Kim J-E, et al. (2008) DOT1L/KMT4 recruitment and H3K79 methylation are ubiquitously coupled with gene transcription in mammalian cells. Mol Cell Biol 28:2825–39.

Storlazzi, A., Xu, L., Schwacha, A., and Kleckner, N. (1996). Synaptonemal complex (SC) component Zip1 plays a role in meiotic recombination independent of SC polymerization along the chromosomes. Proc Natl Acad Sci U S A 93, 9043-9048.

Sweet SMM, Li M, Thomas PM, Durbin KR, Kelleher NL (2010) Kinetics of re-establishing H3K79 methylation marks in global human chromatin. J Biol Chem 285:32778–32786.

Szyjka, S.J., Aparicio, J.G., Viggiani, C.J., Knott, S., Xu, W., Tavare, S., and Aparicio, O.M. (2008). Rad53 regulates replication fork restart after DNA damage in *Saccharomyces cerevisiae*. Genes Dev 22, 1906-1920.

Tachiwana H, Osakabe A, Shiga T, Miya Y, Kimura H, Kagawa W, Kurumizaka H (2011) Structures of human nucleosomes containing major histone H3 variants. Acta Crystallogr D Biol Crystallogr 67:578–583.

Tercero, J.A., and Diffley, J.F. (2001). Regulation of DNA replication fork progression through damaged DNA by the Mec1/Rad53 checkpoint. Nature 412, 553-557.

Tercero, J.A., Longhese, M.P., and Diffley, J.F. (2003). A central role for DNA replication forks in checkpoint activation and response. Mol Cell 11, 1323-1336.

Toh, G.W., O'Shaughnessy, A.M., Jimeno, S., Dobbie, I.M., Grenon, M., Maffini, S., O'Rorke, A., and Lowndes, N.F. (2006). Histone H2A phosphorylation and H3 methylation are required for a novel Rad9 DSB repair function following checkpoint activation. DNA Repair 5, 693-703.

Turner JMA (2007) Meiotic sex chromosome inactivation. Development 134:1823–1831.

Ulrich, H.D. (2005). The RAD6 pathway: control of DNA damage bypass and mutagenesis by ubiquitin and SUMO. Chembiochem 6, 1735-1743.

Vader, G., Blitzblau, H.G., Tame, M.A., Falk, J.E., Curtin, L., and Hochwagen, A. (2011). Protection of repetitive DNA borders from self-induced meiotic instability. Nature 477, 115-119.

van der Heijden GW, Derijck AAHA, Pósfai E, Giele M, Pelczar P, Ramos L, Wansink DG, van der Vlag J, et al. (2007) Chromosome-wide nucleosome replacement and H3.3 incorporation during mammalian meiotic sex chromosome inactivation. Nat Genet 39:251–258.

van Leeuwen, F., Gafken, P.R., and Gottschling, D.E. (2002). Dot1p modulates silencing in yeast by methylation of the nucleosome core. Cell 109, 745-756.

van Welsem T, Frederiks F, Verzijlbergen KF, Faber AW, Nelson ZW, Egan DA, Gottschling DE, van Leeuwen F (2008) Synthetic lethal screens identify gene silencing processes in yeast and implicate the acetylated amino terminus of Sir3 in recognition of the nucleosome core. Mol Cell Biol 28:3861–3872.

Vazquez, M.V., Rojas, V., and Tercero, J.A. (2008). Multiple pathways cooperate to facilitate DNA replication fork progression through alkylated DNA. DNA Repair 7, 1693-1704.

Wakeman, T.P., Wang, Q., Feng, J., and Wang, X.F. (2012). Bat3 facilitates H3K79 dimethylation by DOT1L and promotes DNA damage-induced 53BP1 foci at G1/G2 cell-cycle phases. EMBO J 31, 2169-2181.

Waters, L.S., and Walker, G.C. (2006). The critical mutagenic translesion DNA polymerase Rev1 is highly expressed during G(2)/M phase rather than S phase. Proc Natl Acad Sci U S A 103, 8971-8976.

Waters, L.S., Minesinger, B.K., Wiltrout, M.E., D'Souza, S., Woodruff, R.V., and Walker, G.C. (2009). Eukaryotic translesion polymerases and their roles and regulation in DNA damage tolerance. Microbiol Mol Biol Rev 73, 134-154.

Wojtasz L, Daniel K, Roig I, Bolcun-Filas E, Xu H, Boonsanay V, Eckmann CR, Cooke HJ, et al. (2009) Mouse HORMAD1 and HORMAD2, two conserved meiotic chromosomal proteins, are depleted from synapsed chromosome axes with the help of TRIP13 AAA-ATPase. PLOS Genet 5:e1000702.

Wojtasz, L., Cloutier, J.M., Baumann, M., Daniel, K., Varga, J., Fu, J., Anastassiadis, K., Stewart, A.F., Remenyi, A., Turner, J.M., et al. (2012). Meiotic DNA double-strand breaks and chromosome asynapsis in mice are monitored by distinct HORMAD2-independent and -dependent mechanisms. Genes Dev 26, 958-973.

Woltering, D., Baumgartner, B., Bagchi, S., Larkin, B., Loidl, J., de los Santos, T., and Hollingsworth, N.M. (2000). Meiotic segregation, synapsis, and recombination checkpoint functions require physical interaction between the chromosomal proteins Red1p and Hop1p. Mol Cell Biol 20, 6646-6658.

Wu R, Terry AV, Singh PB, Gilbert DM (2005) Differential subnuclear localization and replication timing of histone H3 lysine 9 methylation states. Mol Biol Cell 16:2872–2881.

Wu, H.Y., Ho, H.C., and Burgess, S.M. (2010). Mek1 kinase governs outcomes of meiotic recombination and the checkpoint response. Curr Biol 20, 1707-1716.

Wysocki, R., Javaheri, A., Allard, S., Sha, F., Cote, J., and Kron, S.J. (2005). Role of Dot1-dependent histone H3 methylation in G1 and S phase DNA damage checkpoint functions of Rad9. Mol Cell Biol 25, 8430-8443.

Yao Y, Chen P, Diao J, Cheng G, Deng L, Anglin JL, Prasad BVV, Song Y (2011) Selective inhibitors of histone methyltransferase DOT1L: design, synthesis, and crystallographic studies. J Am Chem Soc 133:16746–9.

Yoshida K, Kondoh G, Matsuda Y, Habu T, Nishimune Y, Morita T (1998) The mouse RecA-like gene Dmc1 is required for homologous chromosome synapsis during meiosis. Mol Cell 1:707–718.

Zanders, S., and Alani, E. (2009). The *pch2*Δ mutation in baker's yeast alters meiotic crossover levels and confers a defect in crossover interference. PLoS Genet 5, e1000571.

Zee BM, Levin RS, Dimaggio PA, Garcia BA (2010) Global turnover of histone post-translational modifications and variants in human cells. Epigenetics & Chromatin 3:22.

Zhang Q, Xue P, Li H, Bao Y, Wu L, Chang S, Niu B, Yang F, et al. (2013) Histone modification mapping in human brain reveals aberrant expression of histone H3 lysine 79 dimethylation in neural tube defects. Neurobiol Dis 54:404–413.

Zhang W, Hayashizaki Y, Kone BC (2004) Structure and regulation of the mDot1 gene, a mouse histone H3 methyltransferase. Biochem J 377:641–651.

Zhou VW, Goren A, Bernstein BE (2011) Charting histone modifications and the functional organization of mammalian genomes. Nat Rev Genet 12:7–18.

Zhuang, Z., Johnson, R.E., Haracska, L., Prakash, L., Prakash, S., and Benkovic, S.J. (2008). Regulation of polymerase exchange between Poleta and Poldelta by monoubiquitination of PCNA and the movement of DNA polymerase holoenzyme. Proc Natl Acad Sci U S A 105, 5361-5366.

ABBREVIATIONS

- ✓ **BRCT domains:** BRCA1 C-Terminus domains
- ✓ **CCD:** Charge-Coupled Device
- ✓ **DAPI:** 4',6-Diamidino-2-Phenylindole
- ✓ **DNA:** Deoxyribonucleic acid
- ✓ **DOI:** Digital Object Identifier
- ✓ **DSB:** Double-Strand Break
- ✓ **EC:** Enzyme Commission (number)
- ✓ **FHA domain:** Forkhead-Associated domain
- ✓ **GFP:** Green Fluorescent Protein
- ✓ **GST:** Glutathione S-Transferase
- ✓ **H3K79me:** methylation of histone H3 at lysine 79
- ✓ **H3K79me1:** monomethylation of histone H3 at lysine 79
- ✓ **H3K79me2:** dimethylation of histone H3 at lysine 79
- ✓ **H3K79me3:** trimethylation of histone H3 at lysine 79
- ✓ **HA:** Human influenza hemagglutinin
- ✓ **HORMA domain:** Hop1, Rev1 and Mad2 domain
- ✓ **HRP:** Horseradish Peroxidase
- ✓ **IR:** Ionizing Radiation
- ✓ **ISSN:** International Standard Serial Number
- ✓ **LE:** Lateral Element (of the synaptonemal complex)
- ✓ **MMS:** Methyl Methanesulfonate.
- ✓ **MSCI:** Meiotic Sex Chromosome Inactivation
- ✓ **PAR:** Pseudoautosomal Region
- ✓ **PCNA:** Proliferating Cell Nuclear Antigen
- ✓ **PCR:** Polymerase Chain Reaction
- ✓ **PGK:** Phosphoglycerate kinase
- ✓ **PTMs:** Posttranslational Modifications
- ✓ **PVDF:** Polyvinylidene Difluoride
- ✓ **rDNA:** ribosomal DNA
- ✓ **RNA:** Ribonucleic Acid
- ✓ **RNAPII:** RNA Polymerase II
- ✓ **SAH:** S-Adenosyl Homocysteine

- ✓ **SAM:** S-Adenosyl Methionine
- ✓ **SC:** Synaptonemal Complex
- ✓ **SDS:** Sodium dodecyl sulfate
- ✓ **SET domain:** Su(var)3- 9, Enhancer of Zeste [E(Z)], and Trithorax (trx) domain
- ✓ **SYCP3:** Synaptonemal Complex Protein 3
- ✓ **TCA:** Trichloroacetic Acid
- ✓ **TLS:** Translesion Synthesis
- ✓ **UV:** Ultraviolet
- ✓ **WCA:** Whole Cell Extracts
- ✓ **WT:** Wild type
- ✓ **YPDA:** Yeast extract, Peptone, Dextrose and Adenine medium
- ✓ **γH2A**: phosphorylated histone H2A

LIST OF MUTATED GENES

List of mutated or modified genes used in the thesis, grouped under the name of the gene and a brief description of the encoded protein, followed by all the mutated or modified versions used. Please note that the yeast genes/mutants are in black and mouse mutants are in dark red. Protein function description partially obtained and modified from The *Saccharomyces* Genome Database (http://www.yeastgenome.org/).

- ***DDC2*:** DNA damage sensor component, physically interacts with Mec1. Homolog of mammalian ATRIP.
  - ***DDC2-GFP*:** Ddc2 tagged with GFP at the C-terminus.
- ***DMC1*:** Meiosis-specific protein, promotes ATP-dependent DNA strand exchange required for repair of meiotic DSBs; homolog of the bacterial RecA protein and of mammalian *Dmc1*.
  - ***dmc1*:** deletion mutant.
  - ***Dmc1*$^{-/-}$:** mouse deletion mutant.
- ***DOT1*:** H3K79 methyltransferase; homolog of mammalian *DOT1L*.
  - ***dot1*:** deletion mutant.
  - ***dot1-G401A*:** partially-active catalytic mutant.
  - ***dot1-G401V*:** inactive catalytic mutant.
- ***HHF1* & *HHF2*:** core histone H4 copy 1 and copy 2.
  - ***hhf1* & *hhf2:*** deletion mutant.
- ***HHT1* & *HHT2*:** core histone H3 copy 1 and copy 2.
  - ***hht1* & *hht2:*** deletion mutant.
  - ***hht1-K79A* & *hht2-K79A:*** lysine 79 changed to alanine (non-methylatable non-polar amino acid).
  - ***hht2-K79R:*** lysine 79 changed to arginine (non-methylatable basic amino acid).
- ***HTA1* & *HTA2*:** core histone H2A copy 1 and copy 2.
  - ***hta1-S129** & *hta2-S129*:*** histone H2A lacking the four C-terminal amino acids, including the SQ phosphorylation site.
- ***HOP1*:** Meiosis-specific component of the axial/lateral elements of the synaptonemal complex; meiotic checkpoint adaptor.
  - ***hop1:*** deletion mutant.
  - ***HOP1-GFP:*** Hop1 tagged with GFP at the C-terminus (partially active).
- ***MEC1*:** DNA damage sensor kinase, interacts physically with Ddc2. Homolog of mammalian ATR.
  - ***mec1:*** deletion mutant.

- ***MEK1*:** Meiosis-specific checkpoint effector kinase.
  - ***mek1:*** deletion mutant.
  - ***mek1-K199R:*** kinase-dead mutant.
  - ***mek1-T327A:*** autophosphorylation-defective mutant.
  - ***mek1-T331A:*** autophosphorylation-defective mutant.
  - ***MEK1-GFP:*** Mek1 tagged with GFP at the C-terminus.
  - ***MEK1-13myc:*** Mek1 tagged with 13 myc copies at the C-terminus.
  - ***GST-MEK1:*** Mek1 tagged with GST at the N-terminus.
  - ***GST-mek1-K199R:*** autophosphorylation-defective Mek1 tagged with GST at the N-terminus.
  - ***GST-mek1-T327A:*** autophosphorylation-defective Mek1 tagged with GST at the N-terminus.
- ***NDT80*:** Meiosis-specific transcription factor that activates middle meiotic genes; required for exit from pachytene.
  - ***ndt80:*** deletion mutant.
- ***PCH2*:** Meiosis-specific checkpoint AAA^+ ATPase; ortholog of mammalian *Trip13*.
  - ***pch2:*** deletion mutant.
  - ***PCH2-3HA:*** Pch2 tagged with 3 HA copies at the N-terminus.
  - ***$Trip13^{mod/mod}$:*** hypomorphic mutation of *Trip13*.
- ***POL30*:** PCNA (Proliferating cell nuclear antigen), Sliding clamp for DNA polymerases and docking site for other proteins involved in DNA repair.
  - ***pol30-K164R:*** lysine 164 changed to arginine (cannot be modified by ubiquitilation or sumoylation).
- ***RAD24*:** Protein involved in the activation of the DNA damage and pachytene checkpoints.
  - ***rad24:*** deletion mutant.
- ***RAD53*:** DNA damage checkpoint effector kinase.
  - ***rad53:*** deletion mutant.
  - ***rad53-HA:*** Rad53 tagged with HA at the C-terminus, protein produced at reduced levels.
- ***REV1*:** Deoxycytidyl transferase. Functions in DNA damage tolerance by TLS
  - ***REV1-13myc:*** Rev1 tagged with 13 myc copies at the C-terminus.
- ***SML1***: Ribonucleotide reductase inhibitor,.
  - ***sml1:*** deletion mutant; suppressor of *mec1* or *ddc2* lethality
- ***SPO11***: Meiosis-specific topoisomerase-like protein that initiates meiotic recombination by catalyzing the formation of DSBs in DNA; homolog of mammalian *Spo11*.

· ***spo11:*** deletion mutant.

· ***Spo11$^{-/-}$*:** mouse deletion mutant.

· ***Spo11*β-only:** exclusively expresses the *Spo11*β splice variant mutant; defective in promoting late DSB formation, specifically at the PAR of X-Y chromosomes.

- ***TEL1***: DNA damage sensor kinase; homolog of mammalian ATM.

  · ***tel1:*** deletion mutant.

- ***ZIP1***: Meiosis-specific component of the central element of the synaptonemal complex.

  · ***zip1:*** deletion mutant.

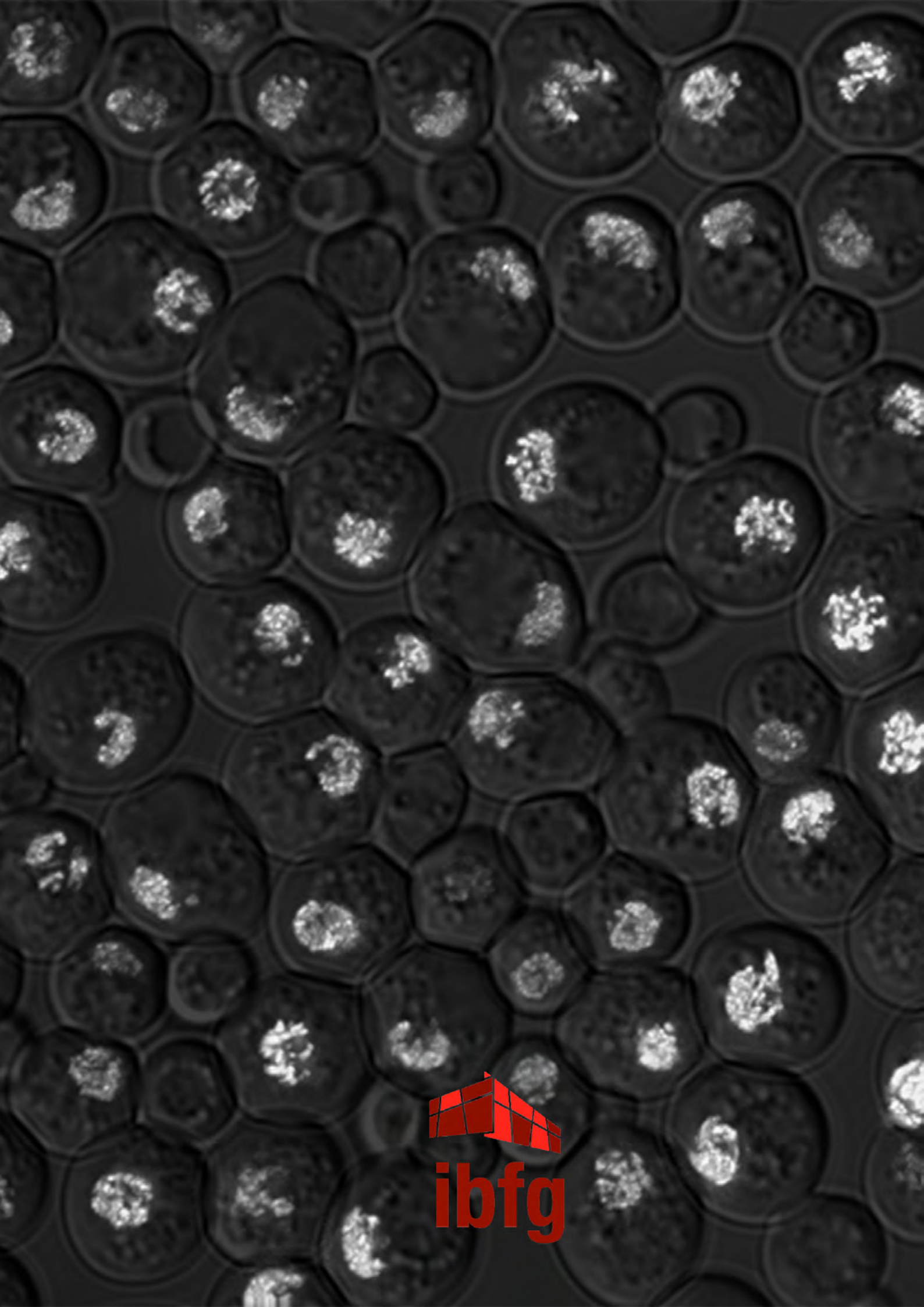
ibfg